New Electrical and Electronic Technologies and their Industrial Implementation

INTERNATIONAL SCIENTIFIC COMMITTEE

Paweł Zhukowski — Lublin University of Technology, Poland – **Chairman**
Vladimir Odzhaev — Belarussian State University, Belarus – **Co-Chairman**
Liudvikas Pranevicius — Vytautas Magnus University, Lithuania – **Co-Chairman**
Fiodor Romaniuk — Belarussian State Technical University, Belarus – **Co-Chairman**
Dmitro Freik — Precarpathian University, Ukraine – **Co-Chairmans**
Igor Tashlykov — Belarussian State Pedagogical University, Belarus – **Co-Chairman**
Janusz Partyka — Lublin University of Technology, Poland – **Scientific Secretary**

Viktor Anischik — Belarussian State University, Belarus
Guennadi Bondarenko — Moscow State Institute of Elektronics and Mathematics, Russia
Tomasz Boczar — Technical University of Opole, Poland
Kazimierz Cywiński — Bialystok Technical University, Poland
Zbigniew Gacek — Silesian University of Technology, Poland
Alfonsas Grigonis — Kanaus University of Technology, Lithuania
Jeon Han — Sung Kyun Kwan University, Korea
Czesław Karwat — Lublin University of Technology, Poland
Stas Kharin — Mathematic Institute of Kazakhstan Academy of Science, Kazakhstan
Sergei Kislitsin — Institute of Nuclear Physics, Kazakhstan
Fadiej Komarov — Belarussian State University, Belarus
Zbigniew W. Kowalski — Wroclaw University of Technology, Poland
Arturas Medvids — Riga Technical University, Latvia
Enn Mellikov — Tallinn University of Technology, Estonia
Bogdan Miedziński — Wroclaw University of Technology, Poland
Hassan Nouri — University of the West of England, United Kingdom
Aleksy Patryn — Technical University of Koszalin, Poland
Wiktor Pietrzyk — Lublin University of Technology, Poland
Vladimir Philipenko — RPC Integral, Minsk, Belarus
Alexander Pogrebnjak — Sumy Institute of Surface Modification, Ukraine
Ivo Rangelow — Ilmenau University of Technology, Germany
Jerzy Skubis — Technical University of Opole, Poland
Ryszard Smarzewski — Catholic University of Lublin, Poland
Jan Subocz — Technical University of Szczecin, Poland
Lech Subocz — Technical University of Szczecin, Poland
Aleksander Tadzhibaev — Petersburg Power Engineering Training Institute for Managers and Experts, Russia
Piotr Tarkowski — Lublin University of Technology, Poland
Roland Wiśniewski — Institute of Atomic Energy, Poland
Waldemar Wójcik — Lublin University of Technology, Poland
Jerzy Żuk — Maria Curie-Sklodowska University, Poland

LOCAL ORGANIZING COMMITTEE

Paweł Węgierek — Lublin University of Technology – **Chairman**
Piotr Billewicz — Lublin University of Technology
Mariusz Kolasik — Lublin University of Technology
Tomasz N. Kołtunowicz — Lublin University of Technology
Czesław Kozak — Lublin University of Technology
Zenon Pawełczak — Lublin University of Technology
Mirosław Pawłot — Lublin University of Technology
Wiktor Pyda — Lublin University of Technology

7th International Conference

NEET 2011

New Electrical and Electronic Technologies and their Industrial Implementation

Zakopane, Poland, June 28 – July 1, 2011

Edited by **Tomasz N. Kołtunowicz**

Cover design by **Mariusz Kolasik**

ISBN 978-83-62596-31-7

Contents

Dynamic X-ray diffractometry study of the defect structure of single crystal gadolinium gallium garnet

**Volodymyr M. Pylypiv, Tetyana P. Vladimirova , Yevgen M. Kyslovskyy,
Stepan I. Olikhovskii, Oksana Z. Garpul**
*Precarpathian National University named by Vasyl Stefanyk, Ivano-Frankivsk, Ukraine,
E-mail: ogorishna@ukr.net*

Optical and electron spectroscopy was used to demonstrate that garnet crystals grown by the liquid phase epitazy posess residual defects, such as inclusions, pores, dislocation loops and complexes. This qualitative information can be substantially supplemented by the quantitative study of micro defects using high-resolution X-ray diffractometry. In this technique a number of statistical characteristics of micro defects, such as their mean size and concentration can be determined from the analysis of x-ray diffraction rocking curves.

In this work, we developed a theoretical foundation for the modern crystallography of real crystals with a complex basis, which takes into account the presence of various structural defects and allows describing both coherent and diffusion components of x-ray rocking curves in a self-consistent way within the framework of statistical diffraction.

Complex structural factors and Fourier-components of polarizatbility have been calculated for gadolinium gallium garnet-$Gd_3Ga_5O_{12}$ (GGG) single crystals for a set of reflexes and two characteristic x-ray wavelengths. The dependences of these parameters and coherent diffractive components of x-ray rocking curves have been studied as a function of concentration of anti-structural defects and vacancies.

Quantitative characteristics of the defect structure of GGG single crystals have been determined from the analysis of experimental two-reflex rocking curves using formulas of statistical dynamic diffraction in imperfect crystals.

These findings lead us to conclude that a new methodology to diagnose the defect structure of real single crystalline materials has been developed. One area when this methodology can be especially valuable is quantitative study of deformations and defects in ion-implanted layers of garnet thin films, which are used in magnetic and magneto-optical devices.

References
[1] Massa W.: *Crystal structure determination*. Second edition, Berlin, Springer, 2004, p. 210.
[2] Datsenko L.I., Molodkin V.M., Osinovskii M.E.: *Dynamical scattering of X-rays by real crystals*, Nauk. Dumka, Kiev, 1998.

Influence of iron implantation of silicon at different energies of optical absorption of YIG-films

Oksana Garpul, Yaroslav Solovko

Precarpathian National University named by Vasyl Stefanyk, Ivano-Frankivsk, Ukraine,
E-mail: jaroslavsol@rambler.ru

Scientific interest in studying obtical absorption in epitaxial ferrite-garnet films is driven by both fundamental questions of light-matter interactions and the practical possibility to use nonlinear optical phenomena to process and transmit information and develop a variety of non-destructive evaluation and diagnostic techniques [1]. Implanted epitaxial $Y_3Fe_5O_{12}$ (YIG) films generally possess large number of defects on the surface and in the sub-surface area.

The objective of our work is to investigate additional absorption from defects generated by implanting YIG films with a fixed dose of implantation by ions Si^+ with energies in a range of 100 - 150 keV and with fixed dose $D = 5 \cdot 10^{13}$ sm^{-2}. Samples used in this investigation were single crystalline YIG films with the lattice constant a_f = 12.3697 Å and thickness h = 4.28 mm grown on (111) gadolinium-gallium grenade ($Gd_3Ga_5O_{12}$, a_s = 12.3820 Å) substrates using a liquid-phase epitaxy. Room temperature IR absorption spectra for wave vectors of 400 - 4000 sm^{-1} were recorded using a Thermo-Nicolet infrared Fourier spectrometer. In addition, the absorption spectra for the wave vectors of 10000 - 50000 sm^{-1} were recorded using a Percin-Elmer Lambda Bio-40 spectrophotometer.
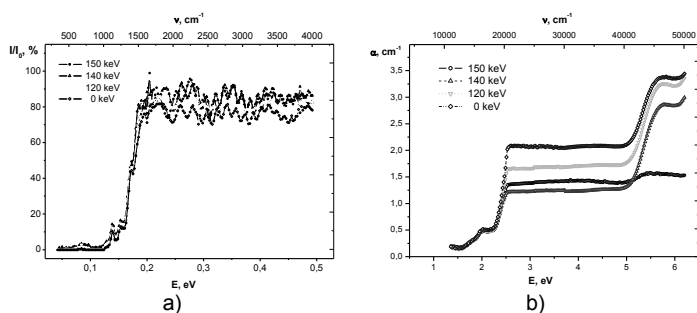
Fig. 1. The transmission (a) and absorption (b) spectra of single crystal $Y_3Fe_5O_{12}$ films implanted with Si^+ ions with various energies

The analysis of optical transmission and absorption spectra of YIG film has led to the following conclusions:
- grafting treatment does not alter vibration spectra of molecules, while the bandwidth at 0.2-0.5 eV increases for films implanted with 140 keV and 150 keV Si^+ ions;
- in case of implantation with 150 keV Si^+ ions, additional absorption at 5.0-6.0 eV and strong at $E < 2$ eV is caused by Fe^{2+} ions;
- the decrease if the absorption intensity at 5.0 - 6.0 eV for films implanted with 150 keV Si^+ ions is caused by oxygen vacancies; while the absorption at 2.5 - 5.0 eV for all samples is associated with intense interband transitions and transitions involving charge transfer.

References

[1] Павлов В.В., Писарев Р.В., Fiebig M., Frohlich D.: *Генерация оптических гармоник в эпитаксиальных пленках магнитных гранатов в области края фундаментальных поглощений*, ФТТ, Т. 45, вып. 4. 2003, с. 630-637.

Charge mobility measurements in dielectric liquids using the streaming electrification phenomenon

Maciej Zdanowski, Stefan Wolny, Józef Kędzia
Opole University of Technology, Faculty of Electrical Engineering, Automatic Control and Computer Science, Chair of Electrical Power Engineering, 76 B2 Prószkowska Str., 45-748 Opole, Poland, E-mail: m.zdanowski@po.opole.pl

In insulation liquids, despite the fact that they are dielectrics, there is an infinite number of charge carriers. Their behavior in the electric field is of significance in the description of the mechanism of conductivity, loss, breakdown mechanisms, charge injection from the electrodes, currents limited by a spatial charge, electroconvection phenomena. The parameter used for describing the behavior of charge carriers is their mobility. In practice, a lot of methods are used for investigating the charge carrier mobility in conductors, semi-conductors and insulators. Their application results from the usefulness of the particular methods. In insulation liquids, the research work in this scope was developed by Adamczewski [1]. The research was based on examining the phenomenon of conductivity induced by an external ionizing factor. An observation of the phenomenon of the currents limited by the spatial charge was carried out as well. Also the research work on the charge injections from the electrodes was of great significance. The methods based on the measurements of the Hall phenomenon, so widely used in the research on carrier mobility in semi-conductors, did not find their application in the research on charge mobility in dielectric liquids. However, the mobility measurement method, based on the observation of the electrokinetic phenomena, the so-called electrophoresis phenomenon, was found useful. This method is based on the measurement of electrokinetic potential δ. This potential can be determined through the observation of the solid particle movement in liquid affected by the electric field applied.

The paper presents the suggestion of determining the charge carrier mobility in liquid using for measurements a different electrokinetic phenomenon – the so-called flow potential.

References

[1] Adamczewski I.: *Jonizacja i przewodnictwo ciekłych dielektryków*, PWN, Warszawa, 1965.

The strain distribution measurement by the use
of the optoelectronic method based on the fibre bragg gratings

Waldemar Wójcik, Piotr Kisała, Sławomir Cięszczyk, Leszek Kobyliński
Lublin University of Technology, Department of Electronics, 38a Nadbystrzycka Str.,
20-618 Lublin, Poland, E-mail: p.kisala@pollub.pl

This paper outlines the analysis of the measurement and the method of the fibre bragg grating strain distribution recovery. To carry it out we used a grating spectra and the inverse problem was discussed. Analyzed parameters are grating period values which were distributed in a few points along the grating length. On the basis of the bragg grating period values its strain values are determined. The inverse analysis was used for calculations. First, the forward problem was defined, and then by the development and validation of the mathematical model of the Bragg grating sensor and the simulated annealing algorithm the inverse problem solution was presented. The inverse problem consist in the strain distribution of the grating recovery on the basis of its spectra.

Fibre Bragg gratings can be used in optical communications as wavelength filters in multi-wavelength fiber lasers [1], wavelength division multiplexing filters [2], and gain flattening of erbium-doped fiber amplifiers [3]. Recently, there has been considerable interest in developing HiBi-FLM sensors to measure strain [4], and other physical parameters [5]. Special attention has been paid to simultaneous measurement of temperature and strain [6]. We use the fiber Bragg gratings as a strain sensor, and we have carried out distributed strain measurements by using of optimization algorithms. There is a need to knowledge the strain distribution in large accuracy on small sections. The present methods of the strain state evaluation (which are confirmed even by the tensometers) allow us to obtain average information. Our proposal to solve this problem is Fiber Bragg gratings application. The problem of the strain profile recovery, on the base of grating spectra, is so-called inverse problem [7]. There are no analytical methods for the recovery of the grating strain distribution on the base of its spectra.

We put the direct problem in this article. We consider this as a an experience from the refractive index modulation to the grating spectra. After presenting the direct problem in this way, the inverse problem looks as fallows. The inverse problem for our grating is to pass from the grating spectra to the refractive index modulation.

The strain distribution may be recovered on the base of spectral characteristic of the fiber Bragg grating, which work as a sensor. Numerical methods for resolve the inverse problem are necessary to recover strain distribution, which was measured by using of FBG element. These methods will use next numerical algorithm of the global optimization. Selection of the algorithm for this kind of task is not indifferent for the accuracy of distribution recovery and time of the computation procedure.

References
[1] Dong X.P., Li S., Chiang K.S., Ng M.N., Chu B.C.B., Electron. Lett. 36, 2000, 1609.
[2] Kim S., Kang J. U., IEEE Photon. Technol. Lett. 16, 2004, 494.
[3] Li S., Chiang K.S., Gambling W.A., IEEE Photon. Technol. Lett. 13, 2001, 942.
[4] Campbell M., Zheng G., Smith A.S.H., Wallace P.A., Meas. Sci. Technol. 10, 1999, 218.
[5] Bo D., Qida Z., Feng L., Tuan G., Lifang X., Shuhong L., Hong G., Appl. Opt. 45, 2006, 7767.
[6] Sun G., Moon D.S., Chung Y., IEEE Photon. Technol. Lett. 19, 2007, 2027.
[7] Lebedev L.P., Vorovich I.L., Gladwell G.N.L.: *Functional Analysis: Applications in Mechanics and Inverse Problems,* Kluwer Academic Publishers, Dordrecht, 1996, VIII, 239 p.

Thermoelectric properties of nanostructures compounds IV-VI

D. Freik[1), W. Wojcik[2), M. Lopianko[1), I. Yurchyshyn[1)
[1) *Vasyl Stefanyk PreCarpathian National University, Ivano-Frankivsk, Ukraine,*
E-mail: freik@pu.if.ua
[2) *Lublin University of Technology, 38A Nadbystrzycka Str., 20-618 Lublin, Poland*

Condensed Matter Research found that it is possible significantly to increase the value of the material thermoelectric figure of merit Z in them [1]. The paper presents an analysis of new approaches to improve the thermoelectric parameters of nanostructures on the basis of compounds IV-VI.

Found that thermoelectric figure of merit for materials based on superlattices of quantum dots reaches a value ZT = 2 at 300 K by a sharp decrease lattice thermal conductivity of more than 4 times compared to the bulk material of the same composition [2].

The optimal parameters of the segment length and orientation for superlattice nanowires based on lead chalcogenides is evaluated [3].

Oscillation character for thickness dependence of kinetic parameters of quantum wells superlattices suggests that this behavior is caused by quantum size effects associated with movement confinement of the main carrier [f.e. 4]. Defining the period of oscillations has allowed to get energy parameters of appropriate nanostructures for future calculations of Z component and select the appropriate technological modes for obtaining materials with predicted properties.

We studied saples of p-PbTe on poliamide and p-SnTe on mica. Results of atomic force microscopy show a clear island structure for both p-PbTe and p-SnTe nanosturctures. It is due to Volmer-Weber growth mechanism on dielectric substrates for lead chalcogenides. The thickness dependencies of kinetic parameters in this structures have been explained by the quantum-size nature due to confinement of carrier movement in the quantum well, formed by the substrate and oxidative layer on the surface of structure.

Note, that calculations of Z and $S^2\zeta$ in systems with quantum wells and wires have shown that they are influenced by changes in the electronic density of states due to dimension decrease. Indeed, as shown in [5], using the density of states in low-dimensional systems, we can achieve a substantial increase in the asymmetry of the density of states and, consequently, the growth of thermopower by changing the position of Fermi level with respect to these features.

References
[1] Dresselhaus M.S., Chen G., Tang M.I., Yang R., Lee H.: *New directions for low-dimensional thermoelectric materials*, Adv. Mater 19, 1, 2007.
[2] Sur I., Casian A., Baladin A.: *Electronic thermal conductivity and thermoelectric figure of merit of n-type PbTe/PbEuTe quantum wells*, Phys. Rev. B. 69, 2004, 035306.
[3] Yu-Ming Lin, Dresselhaus M.S.: *Thermoelectric properties of superlattice nanowires*, Physical Review B 68, 2003, 075304.
[4] Rogacheva E.I., Nashchekina O.N., Vekhov Y.O., Dresselhaus M.S., Cronin S.B.: *Effect of thickness on the thermoelectric properties of PbS thin films*, Thin Solid Films 423, 2003, p. 115-118.
[5] Springholz G., Pinczolits M., Mayer P., Holy V., Bauer G., Kang H., Salamanca-Riba L.: *Tuning of lateral and vertical correlations in self-organized PbSe/PbEuTe quantum dot superlattices*, Phys. Rev. Lett. 84, 2000, 4669.

New areas of optimization of thermoelectric parameters of lead telluride and germanium telluride based solid solutions

D.M. Freik, V.V. Boryk, L.Yo. Mezhylovska, L.V. Turovska, L.D. Yurchyshyn
Vasyl Stefanyk PreCarpathian National University, Ivano-Frankivsk, Ukraine,
E-mail: freik@pu.if.ua

IV-VI semiconductor compounds and their solid solutions are basic materials for thermoelectric energy converters that operate in the medium temperature area [1 - 2]. Point defects and their complexes largely responsible for the physical and chemical properties of the material. At present there is no consensus about the nature of these defects and their charge states. Lead telluride has n-type conductivity in metal excess presence relative to stehiometry and p-type conductivity in chalcogen excess presence. and germanium telluride has only hole conductivity [1].

The basis of the method of crystalquasichemical analysis is superposition of doping cluster formed on the basis of lead telluride antistructure, and the crystal formula of stoichiometric compound. Crystalquasichemical model of nonstoichiometric PbTe with a complex range of Frenkel defects (V_{Pb}^{2-}, V_{Pb}^{-}, V_{Te}^{2+}, Pb_i^{2+}, Te_i^{0}), and p-GeTe (V_{Ge}^{2-}, V_{Ge}^{4-}), and based on them ternary systems have been offered. Dependences of concentration of point defects, electrons and holes, and the Hall concentration of current carriers on the size and nature of deviation from stoichiometry of n-and p-PbTe and solid solution composition have been calculated on the basis of the first developed crystalquasichemical formulas and equations of full electroneutrality. Thus hole conduction of lead telluride relates to a vacancy in cation sublattices V_{Pb}^{2-}, V_{Pb}^{-}, and electronic – in anion sublattices V_{Te}^{2+} of lead telluride crystal structure.

The influence of chemical composition and the deviation from stoichiometry on the side of tellurium on the ratio between two- (V_i^{2-}) and fourfold charged (V_i^{4-}) cationic vacancies (dominant defects in this case) and thermoelectric properties of PbTe-SnTe solid solution have been specified. Complicated dependence of the spectrum of metal vacancies of $Pb_{1-x}Sn_xTe$ solid solutions on the composition and size of deviation from stoichiometry on the side of tellurium significantly affects the entire range of thermoelectric properties of the material. In particular, considerable conductivity (ζ) is provided by high electrical activity of defects, which in our case associated with fourfold charged cationic vacancies V_i^{4-}.

A similar analysis has been done for germanium telluride and germanium telluride based solid solutions. Thus that the main areas of optimization of thermoelectric parameters of PbTe, GeTe based materials are decrease of the thermal conductivity (PbTe-SnTe, PbTe-Sb$_2$Te$_3$), and increase of electric conduction and activity of point defects (PbTe-SnTe, PbTe-GeTe), and the incorporation of noncentral dopant ions in solid solutions (Pb-Te-Se-S).

Introduced crystalquasichemical approaches extend possibilities of scientific analysis of the defect subsystem in semiconductor crystals, and determine the technological aspects of managing their properties.

References
[1] Abrykosov N.Kh., Shelimova L.E.: *Semiconductors Materials on the basis of combinations of $A^{IV}B^{VI}$*, M. Science, 1975, 196 p.
[2] Ioffe A.F.: *Semicondusctor thermoelements*. M.-H. Publishing House of USSR Academy of Sciences, 1960, 346 p.

Defective subsystem and modification of crystals' properties of compounds A^{2}B^6

V. Prokopiv, I. Gorichok, G. Gurgula, N. Freik
Vasyl Stefanyk Precarpathian National University, Ivano-Frankivsk, Ukraine,
E-mail: freik@pu.if.ua

Metal chalcogenides of the second subgroup of the periodic table are perspective materials in electronic engineering for making detectors for γ - and x-rays, photo receiving and radiating structures of visible and infrared light spectrum. These materials are characterized by high quantum yield of photo-luminescence and cathode excitement. However, the largest quantum yield can be obtained only in homo-n-p-transition, which requires the ability to grow material of hole and electron conductivity type.

It is known that the basic electrical and photovoltaic properties of semiconductors are determined by their own defects and impurities, which are almost always present in the crystal. The concentration of point defects, among other parameters, (defect of energy formation, its ionization energy and changes of the oscillation frequency of atoms in the vicinity of the defect), also depend on technological conditions and high temperature after growth treatment of the material in vacuum or pair of components. According to the results of the experimental studies, in particular PL, CL, EPR, defective crystals' structure of A^{2}B^2 compounds is extremely difficult, and only in rare case it becomes possible to interpret the experimental data using the approximation of one dominant effect. The concentrations of different types of defects depend on each other, and therefore, the development of the model of point defects that would enable, on one hand, to identify the relationships that exist between the concentrations of defects and on the other – to establish qualitative and quantitative dependency of the physical crystals' properties of compounds A^{2}B^6 on the concentration of defects.

In this work, the crystalquasichemical formulas of non-steikiometric metal chalcogenides of the second subgroup of n- and p-type conductivity have been proposed provided the existence of the complex defect subsystem after the scheme of Schottky-Frenkel. On their basis, the concentration dependencies of the prevailing defects have been calculated, as well as major current carriers and Hall concentration which would depend on the degree of deviation from the stoichiometric disproportion of the charge state of point defects.

By using the obtained crystalquasichemical formulas one can determine not only the prevailing types of point defects, but also their concentration depending on chemical composition, in particular, the magnitude of deviation from stoichiometry (α, β) and content of alloying elements (Me, X) respectively. Based on quasi-chemical equations of the formation of point defects, the annealing processes of double temperature treatment of MeX crystals have been described and the dominant defects have been determined. Crystalquasichemical formulas of the non-stoichiometric n- and p-MeX (Me – Zn, Cd;X – Te, Se, S) have been proposed provided the realization of the complex spectrum of point defects. Besides, the analysis of the principal models of point defects in ZnX crystals with the concomitant process of self alloying by p-MeX and chacolgenide –n-MeX has been performed when interacting with oxygen, and also the mechanisms of defect formation in solid solution on the basis of metal chalcogenides.

The obtained two-dimensional diagrams of concentration of defects (charge carriers) – the chemical composition is determined by the technological factors (conditions of annealing), that provide obtaining of the crystals with already preset properties.

Features domains of homogeneity binary compounds CdTe, SnTe, PbTe and their physical and chemical properties

I. Gorichok, V. Prokopiv (Yn), A. Tkachyk
[1] *Vasyl Stefanyk PreCarpathian National University, Ivano-Frankivsk, Ukraine*
E-mail: goritchok@rambler.ru

Semiconductors $A^{II}B^{VI}$ $A^{IV}B^{VI}$ are basic materials for broad class of optoelectronic device structures. Among this materials attract special attention cadmium telluride, tin and lead, is caused by the peculiarities of their physical and chemical properties and relatively straightforward and sufficiently researched the technology of their synthesis. In recent years, promising research activities of the above mentioned materials are quantum heterostructures in the system $A^{II}B^{VI}$ $A^{IV}B^{VI}$, and thermoelectric materials based on solid solutions A^{II}–A^{IV}–B^{VI}.

Despite the significant progress made in this direction, a number of problems relating to each material particular, require further study. First of all it concerns the influence of technological parameters two-temperature annealing on the formation defect structures and the effect of point defects on the physical and chemical properties the telluride of cadmium, lead and tin. Among these issues crucial study of the defect structure of the material beyond the homogeneity of compounds, since it is under such conditions can receive the maximum concentration of free charge carriers.

Using method based on minimizing the thermodynamic potential of "crystal-pair" as a function defects concentration in the designed area of homogeneity telluride of cadmium, lead and tin from the surplus metal and chalcogen, and also the electrical properties of single crystals at the boundary of the existence compounds with to clarify the ensemble of intrinsic point defects. At the calculation used model that takes into account practically all possible types of intrinsic point defects: V_A, V_B, A_i, B_i, A_B, B_A, each of which may be in three charge states (neutral, one or twofold charged). Concentration of point defects was determined directly from the system of equations describing the equilibrium in two-phase two-component system crystal - pair:

$$\pm\mu_{D_i}^s = \mu_i^g$$

where: $\mu_{D_i}^s$ – chemical potential of the defect i-th component (i = A, B), μ_i^g – chemical potential i-th component in the pair. Defect chemical potential determined by differentiation crystal Gibbs energy concentrations of defects.

The comparative analysis identified the dominant types of defects in material or metal with excess chalcogen. Theoretically calculated concentration of free carriers and the degree of deviation from stoichiometry CdTe satisfactory agreement with experimental data in a wide range of vapor pressure components and annealing temperature T.

Mechanisms of oxygen adsorbtion on a surface of PbTe films

Ya. Saliy[1)], W. Wojcik[2)], N. Stefaniv[1)], Ya. Yavorskiy[1)]
[1)] *Vasyl Stefanyk Precarpathian National University, Ivano-Frankivsk, Ukraine,*
E-mail: freik@pu.if.ua
[2)] *Lublin University of Technology, Department of Electronics, 38a Nadbystrzycka Str.,*
20-618 Lublin, Poland

At studying of adsorbtion the most informative are researches of kinetics of process and form of isotherm. Kinetics of adsorbtion was determined by the change of concentration of carriers in films during an exposition in oxygen at a room temperature. Research made for pressure in a range 10^{-7} - 10^{-4} Pa, filling with specially cleared oxygen. At this pressures the concentration of electrons decreases with characteristic time, which depend from external pressure of oxygen. This decreasing continues until the concentration becomes close to own, independently of concentration of electrons in initial samples. The process of change is irreversible. The process come to the end with reaching of own conductivity in samples with saving high values of mobility, that testify to absence of noticeable charge localization on surface, which cause bending of zones.

Alloying influence of oxygen in this range of pressure best describes by the model of mobile defects, according to which donor interstitial atoms of lead locking from bulk of a film by oxygen atoms on a surface. When all excess of oxygen will be locked by surface, concentration of defects will be low. Electron concentration decreases with decreasing concentration of donors as

$$n = N_D(t) + p \qquad N_D(t) = N_{D\max} \cdot e^{-\frac{\tau}{t}}$$

$$np = n_i^2$$

that respond process of locking donors from bulk on surface unsaturated traps created by oxygen with characteristic time η, which is determined by external pressure of oxygen.

Adsorbtion of oxygen depend from defects concentration on surface and decreases sharply with time. All interstitial atoms of lead binding on surface with oxygen atoms in oxide form, which is stable compound. The process of adsorbtion of oxygen at low pressures is irreversible.

Fundamentally different phenomena occur on surface at high pressures of oxygen in system. Already at pressure 1 Pa samples get p-type of conductivity with concentration 10^{17} cm^{-3}, and their mobility decreases. It is typical for all samples independently from concentration and whether they pre-doped with oxygen at low pressures. With increasing of pressure to atmospheric, concentration of acceptors increases to $3 \cdot 10^{18}$ cm^{-3} and it can be reduced by exposure under the pressure 10^{-5} Pa, but only to value $p = 10^{17}$ cm^{-3}, i.e. the concentration that occurs at pressure 1 Pa. Occurrence p-type conductivity with concentration $\sim 10^{18}$ cm^{-3} is explained by the appearance of acceptor near-surface states in the process of oxidation at high pressures. Described process is reversible.

The oxygen actively adsorbed on grain boundaries of a film, creating potential barriers that greatly limit the mobility of carriers. This mechanism is less reversible. At this pressures electron concentration decreases not saturating as logarithm

$$\Delta n(t) = \Delta n_0 \ln(\frac{t}{\tau} + 1)$$

which is typical for chemical reactions.

Technological aspects of formation thin films of compounds $A^{II}B^{IV}$ vapor methods

D. Freik, I. Gorichok, A. Sokolov, V. Potyak

Physical-chemical institute of Vasyl Stefanyk Precarpathian National University, Ivano-Frankivsk, Ukraine

Thin films based on cadmium telluride are widely used in various fields of semiconductor instrumentation: detectors for producing infrared radiation, solar cells, also as protective coatings for semiconductor structures, such as infrared radiation detectors based on $Hg_{1-x}Cd_xTe$. In recent years, considerable interest CdTe films due to the possibility of building on the basis of quantum dots for spin and quantum information systems with a characteristic spin relaxation time of 100 ps [1].

This paper presents the results of investigation of the condensation of cadmium telluride on the substrate mica-muscovite under different technological parameters (temperature substrate, temperature evaporator, time deposition).

CdTe films obtained by hot-wall [2] at 10^{-2} Pa vacuum. As the substrates used mica-muscovite. The temperature of deposition (substrate) varied within T_s = (100 - 350)°C. Temperature evaporator of the synthesized compounds CdTe advance variation within the T_e = (400 - 500)°C. Wall temperature maintained at 50°C higher temperature evaporator. Thickness of condensate asked the time of deposition.

The main feature of hot-wall method is growing films to as close as possible to equilibrium. Such conditions are provided quasi-locked space in which the condensate is derived, and the selection of three temperature settings (T_w, T_e, T_s) providing a constant temperature gradient of grows reactor. The value of these parameters were selected and optimized to experimental data.

Dependences of the condensation rate of technological parameters are set pattern: with increasing substrate temperature T_s at constant temperature evaporator T_e condensation rate decreases, with increasing temperature evaporator T_e with constant substrate temperature T_s condensation rate increases.

In the studied range of technological parameters of film thickness was obtained 0.1-20.0 microns. The regularities of structural formation tapes CdTe films investigated changing technological factors.

References

[1] Tomashik V.M., Bylevych E.O., Tomashik V.N.: *Interaction with soluble cadmium telluride systems HNO3-HCl (HBr)- tartaric acid*, Condensed matter and interface boundaries 3 (33), 2002, p. 237-241.
[2] Freik D.M., Galuschak M.A., Mezhylovska L.Yo.: *Physics and Technology semiconductor films*, High School, Lviv, 1988, 152 p.

Computer simulation of temperature distribution in depth from the surface of metals under e-beam and plasma jet irradiation

D.L. Alontseva[1), G.Z. Ganeev[2), A.M. Pavlov[3), S.J. Rakhmetullina[1)
[1) *East-Kazakhstan State Technical University, Ust-Kamenogorsk, Kazakhstan,*
E-mail: dalontseva@mail.ru
[2) *Instutute of Nuclear Physics NNC RK, Almaty, Kazakhstan*
[3) *East-Kazakhstan State University, Ust-Kamenogorsk, Kazakhstan*

Modification of surfaces of metals and alloys or coatings by electron beam or plasma jet is of current concern [1, 2]. However despite the considerable practical interest, the mechanisms of formation of surface structures in the treated materials caused basically by thermal and thermomechanical effects remain insufficiently investigated. Mainly it is caused by that the processes going on in materials under electronic irradiation and pulse plasma influence, occur very quickly, and the temperatures reached are considerable. Temperature measurement in such conditions is complicated and is unreliable.

The decision of the problem of creating a mathematical model of temperature distribution in a material depending on irradiation parametres makes it possible to expect certain structures and phases to be generated in the given material at irradiation (on the basis of the received temperature values). On the basis of such a model it is possible to select irradiation parametres so that to receive predetermined structure-phase states with specified physical and chemical properties. A number of works devoted to development of a similar model [3, 4] confirm the timely character of the given problem, but they do not give a comprehensive decision.

Taking into account the urgency of industrial use of plasma and electron beam exposure technologies, as well as for decision of concrete questions of selecting irradiation modes, we set the following objectives in the given work:

- estimation of temperature distribution in a two-layer metal sample exposed to a pulse plasma jet, depending on irradiation rate intensity and duration of an impulse, using analytical method and ‚Diffpack Encounter' licenced application;
- development of software application for the automated calculation of distribution of temperature profiles in two-layer metal absorbers under continuous electronic irradiation depending on the energy and intensity of e-beam current.

References
[1] Pote J., Foti G., Jackobson D.: *Modification and Alloying of the Surface by the* Laser, Ion and Electron Beams, Mashinostroyenie, Moscow, Russia, 1987, 424 p.
[2] Kadyrzhanov K.K., Komarov F.F., Pogrebnyak A.D. et al.: *Ion-beam and Ion-plasma Modification of Materials*, Moscow: MGU, 2005, 640 p.
[3] Ganeev G.Z, Kislitsin S.B.: *Calculation of temperature fields, thermopressure, thermal erosion at a pulse irradiation by e-beam*, Abstract Book of 7th International Conference Nuclear and Radiaion Physics, Almaty, Kazakhstan, 2009, p. 133.
[4] Pischasov N.I., Nikolaev A.V.: *Modification of structure and properties of firm alloys of system WC-Co by high-current charged particles beams*, The Bulletin of Omsk University 2, 1996, p. 39-43.

Scattering mechanisms in PbTe:Bi

D.M. Freik, L.I. Nukuruy, R.O. Dzumedzey, V.M. Chobanyuk
Vasyl Stefanyk PreCarpathian National University, Ivano-Frankivsk, Ukraine,
E-mail: kepa@nashemisto.if.ua

Semiconductors IV-VI have proved as reliable material for building on the basis of active infrared devices, elements and techniques of thermoelectric energy converters. It is known that PbTe is efficient thermoelectric material for a middle temperature range (500 - 850) K. Doping significantly affects the electronic states and properties of semiconductor materials and nanostructures based on them. We are considering changing the properties of lead chalcogenides doped elements V group (Sb, Bi) of the periodic table of elements.

It is known that impurity V group of the periodic table have different affect on the energy spectrum of electrons in PbX (X = S, Se, Te), which is associated with amphoteric properties. Thus, when changing the stoichiometric PbTe bismuth atoms moving from sublattice of Pb in tellurium sublattice. Bismuth, replacing lead in its sublattice, is donor and gives one electron into the conduction band to one impurity atom.

In this work are the theoretical calculations, held variational method, of the kinetic parameters PbTe doped with bismuth (0.25, 0.5 and 1 at%.). Charge carrier mobility was calculated using the formula:

$$\mu = A(\varepsilon_F, n, T) \sum_i (B_i F_i)^{-1},$$

were $A(\varepsilon_F, n, T)$ has mobility dimension, and dimensionless B_i and F_i depends on the type of carrier scattering mechanism.

In the table are contributions of different scattering mechanisms, including impurity scattering, scattering by optical phonons, short-range potential vacancies, acoustic phonons, total mobility value and experimental values.

T, K	B_i, at.%	μ_{imp}, cm^2/Ws	μ_{opt}, cm^2/Ws	μ_{sh-r}, cm^2/Ws	μ_{acoust}, cm^2/Ws	μ_{total}, cm^2/Ws	μ_{exp}, cm^2/Ws
300		1950	1898	210006	10087	874	818
200	0,25	2551	3790	142762	17384	1388	1292
77		6022	25719	57740	127310	4345	4227
300		449	709	5363	2202	233	181
200	1	796	2002	5150	5362	468	333
77		1542	8875	3187	30411	902	773

As the result set the dominant scattering mechanism in the temperature range 77 - 300 K. The influence of impurity content on the semiconductor kinetic parameters are analyzed. Set the mobility change in across the studied temperature range of dopant content.

Modification of the thermoelectric parameters of IV-VI thin films during their holding in air

W. Wojcik[1), B.S. Dzundza[2), Ya.S. Yavorsky[2), V.V. Bachuk[2), H.D. Mateik[3)
[1) Lublin University of Technology, Lublin, Poland
[2) Vasyl Stefanyk PreCarpathian National University, Ivano-Frankivsk, Ukraine,
E-mail: freik@pu.if.ua
[3) Ivano-Frankivsk National Technical University of Oil and Gas, Ivano-Frankivsk, Ukraine

Lead chalcogenides thin films – promising materials for creating detectors and radiation sources in the infrared light spectrum [1] as well as thermoelectric materials in high temperatures (500 - 700 K). It was found that their properties are defined by the technological factors of the growing process, and conditions of their subsequent operation [2].

In the research the changes in kinetic parameters of lead telluride films of different thickness at long holding time in the air are examined.

Films for research were received from the vapor phase by open evaporation in vacuum on polyamide tape substrates. Measurements of electrical parameters of films was in air at room temperature in stationary magnetic fields. For each sample series of measurements over time for about one year were carried out.

The received dependences of conductivity and the Hall coefficient for PbTe film on the thickness show that while increasing of film thickness regardless of time of air exposure conductivity increases with access to the full when thickness of about 0.8 microns. For aged in air for several days' films while thickness reducing the Hall coefficient also decreases, the concentration of p-type carriers increases, due to the acceptor influence of adsorbed oxygen and formation of concentrated of p-type carriers layer on the surface. At long holding time in air (about 1 year) with decreasing of film thickness R_H increases and concentration of current carriers decreases respectively, which indicates a small rate of diffusion of oxygen deep into the surface and subsequent diffusion of lead to surface which compensates the acceptor influence of oxygen.

For the quantitative assessment of the conductivity of the near-surface layer of the films its appropriate to analyze electrical properties by Petrits' two-layer model [3], which allowed to determine the dependence of the surface layer thickness on the air exposure time and average speed of oxidation at each stage.

In the initial stages of exposure oxidation rate is significant, but in the sequel it sharply decreases, and during the first day it becomes negligible. This fact also indicates the difference of oxidation mechanisms at an early stage and during prolonged exposure in the air.

References
[1] Zemel J.N.: *Recent developments in epitaxial IV-VI films*, J. Luminescence 7, 1973, p. 524-541.
[2] Freik D.M., Halushchak M.O., Mezhylovska L.Yo.: *Physics and technology of thin films*, High School, Lviv, 1988, 182 p.
[3] Petritz R.L.: *Theory of an experiment for measuring the mobility and density of carriers in the space-charge region of a semiconductor surface*, Phis. Rev. 110, 1958, p. 1254

Evaluation of reliability of gate dielectric of submicron microcircuits by value of breakdown charge

A.S. Turtsevich, S.V. Shvedov, V.S. Tsymbal, R.R. Chyhir
Open Joint Stock Society "INTEGRAL", Minsk, Belarus, E-mail: office@bms.by

The modern tendency of transition to the submicron technologies imposes the high demands to the gate dielectric, whose thickness under the contemporary technologies constitutes less than 10 nm. The thin gate oxide in many respects determines reliability of the integrated microcircuits. Availability of defects substantially reduces reliability of dielectric, and the express-control of reliability is most actual. The procedure is intended for control of the breakdown charge value and is applied for the express control of defectiveness and reliability of the gate dielectrics with the thickness of 4 - 100 nm. The procedure complies with the Standards JESD35-A, JESD35-1, JESD35-2.

Evaluation of Reliability is based on the statistic measurement of the breakdown charge value of the diectric layer on selection of the test structures (MOS-capacitors). After measurements the number of the test structures is determined, possessing the breakdown charge value smaller, than the stipulated criterion. Such structures are rejected, as they are prone to breakdown by the small-value charge and. Due to this cause, possess the low level of reliability. The rejection criterion of the test structure by the breakdown charge value is stipulated for each type of the microcircuits. It is considered, that the rejected test structure contains the defect in the gate dielectric. The procedure stipulates the reliability criterion of the gate dielectric by the permissible number of the rejected test structures in the measured selection. The given criterion is stipulated on the basis of the Poisson distribution law when presetting the required level of the veritable probability, for instance, with the value of 0.95. If in the measured selection the number of the rejected structures is more than the permissible number, then the gate dielectric is considered unreliable. In the procedure the breakdown charge value measurements are performed when passing through test structure the step-wise increasing current (I-sweep). Selection of the I-sweep nsures the possibility of conducting the express-analysis on the test structures of the small area (about 100×100 μm^2), which are accommodated on the scribe paths of the wafers as goods. The method is statistical. In order to obtain the veritable result on the wafer it is necessary to perform control of 50 - 80 test MOS-structures. The measurement results are formulated in the form of the Weibull distribution, showing the dependence of the accumulated number of failures on the breakdown charge value. If in the process of formation of the gate oxide the factor was of influence, deteriorating its quality, then on the Weibull distribution the section emerges with another slope of the characteristic, and the chracteristic charge value drops [1]. This factor can be accounted to the deviations of the technological process, caused by the silicon surface irregularities, polluted materials, etc. The procedure makes it possible to establish the fact of the quality deterioration, as well as to clarify the supposed cause.

Thus, the control method of the breakdown charge value of the gate dielectric ensures the wafer detection with the evident defects and is effective in ensuring reliability of the microcircuits.

References
[1] Belous A.I., Emelyanov V.A., Syakersky V.S., Chyhir R.R.: *Analysis of Microheterogeneities of the Gate Dielectric of the Submicron Microcircuits*, Zakopane, Poland, June 12-15, 2007, p. 22.

Informative analysis of defectiveness of technological processes and forecasting of good microcircuit yield

A.S. Turtsevich, S.V. Shvedov, A.N. Petlitsky, R.R. Chyhir
Open Joint Stock Society "INTEGRAL", Minsk, Belarus, E-mail: office@bms.by

The enhancement of the functional complexity of the integrated microcircuits (ICs), their degree of integration becomes impossible without application of the high informative test control methods. The designed automated system for the test quality control of the technological processes is based on application of the test structures (TS), reflecting all main structural IC elements with consideration of the actual sizes and gaps between them, the real relief of the layers. The peculiarity of the given control system is, that selection of the number of the analyzed elements in composition of the test structures was performed with consideration of the number of the appropriate elements on the IC chip. The test modules (TM), designed for the automated control system, contain the specialized TS, making it possible to receive the expanded information on the electric, physical and geometric parameters, refelecting the quality of the technological process. TM is accomodated on the scribe paths, covering several working chips of the integrated microcircuits and contains up to 64 contact pads. Such TM design ensures the possibility of the technological processes control in the system of the chips layout projection transfer on the wafers.

TM consists of the test structures of two types: parameteric TS (transistors, transistor cells, resistors, etc.) and the statistic test structures (chains of contacts to the various areas, TS for control of ruptures of the extended buses, drains and short circuits between the various layers). The parameteric TSs are intended for control of the physical and electric parameters of the single elements, used in ICs. The next statistic processing of the results makes it possible to determine the reproducibility of the controlled parameters on the wafer, lot. The correlational analysis makes it possible to stipulate the ranges of the parameter optimum values. The statistic TSs are intended for the defectiveness control of the individual technological operations, which is attained by application in TS of a large number of the similar type elements, in serial or parallel combination depending on the type of the controlled element. The correct selection of the test module composition makes it possible to perform the post-operation reject selection in the technological processes of the ICs creation, ensuring forecasting the microcircuit chips good yield [1]. Control of the parameters of the test structures in the TM composition was performed on the automated test system ‚AIK Test-2‘ as per the program, ensuring measurements, the intermediary processing (computation of the parameters) and the finishing data processing (statistic processing, histograms plotting). This ensures acqusition of the more voluminous statistic information under the conditions of the mass production on the individual operations and on the IC technological process as a whole, to perform the post-operational reject selection, to determine the factors of relevance to the good yield.

Thus, the test control automated system provides informative analysis of defectiveness of technological processes and forecasting of good microcircuit yield.

References
[1] Belous A.I., Emelyanov V.A., Syakersky V.S., Chyhir R.R.: *Model for Forecasting Good Yield of Microcircuit Chips by Results of Test Control*, Electrical Review 3/2008, 2008, p. 20-23.

Formation peculiarities of ohmic contacts of metal-semiconductor for the submicron microcircuits

V.A. Pilipenko, V.V. Ponaryadov, V.A. Gorushko, S.V. Shvedau,
T.V. Petlitskaya, A.S. Turtsevich

Open Joint Stock Society "INTEGRAL", Minsk, Belarus, E-mail: office@bms.by

Resistance of contacts with the ultra-small dimensions to a great extent is determined by the edge effects, due to the phenomenon, that with the submicron dimensions the area of bulk charge goes beyond the geometrical margins of the electron at application of the potential to it. At actual contacts with the charge unavailable in the passivating dielectric the shape of areas of the voluminous bulk charge deviates from the ideal one. In this in the contact there emerge the additional current constituents, resulting in leakages and deviations of the IV-parameters from the ideal ones. The greater the ratio of the overlapped area with the metal electrode of the passivating dielectric along the perimeter of the contact to the contact area, the more substantial is influence of the peripheral currents on the total contact current with the direct shift.

With the small shifts (at $\theta_s > |\theta_e|$) and availability of the positive charge in dielectric the peripheral current constituents make a considerable contribution into the common contact current at the direct shift. With increase of the direct shift the peripheral areas of the contact may go beyond the voluminous bulk charge and not participate in the current transfer processes through the contact. The reverse branch of IV-parameters (i.e. during the reverse shift) is little influenced by the shape of the voluminous bulk charge.

In case of the negative charge in dielectric with small shifts (i.e. with $\theta_s > |\theta_e|$) the peripheral current constituents make a considerable contribution into the IV-parameters reverse branch of the contact. With the increase of the reverse shift the contribution of the peripheral current into the common reverse current of the contact diminishes. The direct branch of the IV-parameters is little influenced by the shape of the voluminous bulk charge in this case.

The full current through the contact may be determined by the total of the currents, passing through the definite areas of the contact: 1 – the central one, where the current is determined by the thermal electron emission and recombination in the depleted area; 2 – the peripheral one, where the current is determined by the same constituents, but with the other values of the barrier height θ_h, the thickness of the depleted layer W and the life time of electrons η, 3 – the overlapped area by the dielectric electrode, where the current recombination constituent exist.

In this case the resistivity of the contact R_C, Ohm·cm can be written as:

$$R_C = [k/(qA^*T)]\exp\{2(\varepsilon_0\varepsilon_{Si}m_e^*)^{1/2}[\hbar\,(N_D)^{1/2}]^{-1}\{q\varphi_B - kT\ln\{\alpha[\exp(q\Delta\varphi/kT) - 1] + 1\}\}\} +$$
$$+ 2\tau_e(\beta - 1)(qn_i)^{-1}[2qn_0(\varepsilon_0\varepsilon_{Si})^{-1}]^{1/2}[qN_{SS}(\beta - 1)S_0(\varepsilon_0\varepsilon_{SiO_2}d)^{-1} - V]^{1/2}$$

where: k – Boltzmann constant, J/K, A^* – Richardson constant, A·m⁻²·K⁻²; T – absolute temperature, K; ε_0 – electric constant, F·m⁻¹, ε_{Si} – permittivity Si; m_e^* – effective mass of electron, kg; N_D – concentration of donors in n-layer, m⁻³; q – electron charge, Coulomb; θ_h – height of metal-silicon barrier, eV; $\alpha = S_1/S_0$; S_0 – area of contact window, m²; S_1 – area of the peripheral area of the contact window, m²; $\Delta\theta_h$ – barrier reduction due to the Schottki effect, eV; τ_e – life time of electrons, sec; $\beta = S_E/S_0$; S_E – area of metal electrode, m²; n_i – intrinsic concentration of carriers, m⁻³; n_0 – concentration of carriers in the volume of Si, m⁻²; N_{SS} – charge density at the separation margin of SiO₂ – Si in the overlapped area by the dielectric metal along the periphery of the contact window, m⁻²; ε_{SiO2} – permittivity SiO₂; d – thickness of SiO₂, m; V – voltage at the contact metal-Si, V.

Thus, it is shown, that with the design rules less than 1 μm, the value of the contact resistance is determined both by the contact area and mechanism of the charge carriers transfer and by the area of the voluminous bulk charge, resulting in emergence of the peripheral currents, making a considerable contribution into the total contact current with the direct and reverse shift.

Superparamagnetic behavior of cobalt nanoparticles formed into polyimide by ion implantation

**A.A. Kharchenko[1), M.G. Lukashevich[1), V.F. Valeev[2), O. Petracic[3),
R.I. Khaibullin[2), V.B. Odzhaev[1), P. Zhukowski[4), T.N. Koltunowicz[4)**

[1) *Belarussian State University, 4 Nezavisimosti Ave., 220030 Minsk, Belarus*
[2) *Kazan Physical-Technical Institute, 10/7 Sibirsky Tract, 420029 Kazan, Russia*
[3) *Ruchr University Bochum, 150 University Str., D 44780 Bochum, Germany*
[4) *Lublin University of Technology, 38a Nadbystrzycka Str., 20-618 Lublin, Poland*

Magnetic properties of the assembles of magnetic nanoparticles are a subject of extensive investigations because of their promising potential industrial applications in magnetic recording media, magnetosensor electronic, magnetooptical devices, etc. High-fluence implantation of transition metal ions into polymers is an effective method to form magnetic nanoparticles in the near-surface region of the implanted polymers.

Thin (40 µm) polyimide $(C_{22}H_{10}O_5N_2)_n$ films were implanted with 40 keV Co$^+$ ions to fluencies of $(2.5 - 7.5) \times 10^{16}$ cm^{-2} at ion current density of 4.0 µA/cm^2. Magnetic properties of the implanted polymer films were investigated in-plane of film by using SQUID magnetometer in the temperature range of 4.5 - 300 K. Thermo-magnetic curves were taken for both ZFC and FC regimes under low (1 mT) applied magnetic fields.

Polyimide film implanted with the smallest fluence reveals the negligible paramagnetic response due to small value of metal filling factor of polymer matrix. Starting with the fluency of 5×10^{16} cm^{-2} the samples show superparamagnetic behaviour that is typical for an assembly of magnetic nanoparticles. ZFC curve for the sample implanted up to the fluency of 5×10^{16} cm^{-2} show narrow peak at blocking temperature of T_b = 10 K indicating the formation of small cobalt nanoparticles into polyimide matrix. Further increase of fluency to 7.5×10^{16} cm^{-2} leads to the broadening of ZFC peak and ones shifts to the higher temperature of T_b = 30 K.

We use well-known relation $K_{eff}V = 25\,k_B T_b$, where K_{eff} – constant of magnetic anisotropy and V is the volume of nanoparticles, to calculate the mean sizes of a cobalt nanoparticles. The mean diameters of nanoparticles are found to be about 2 or 6 nm for hexagonal or cubic crystalline modification of cobalt. These sizes are in agreement with our previous results of TEM and FMR studies [1] of cobalt nanoparticles implanted in polyimide films.

For both above mentioned high fluencies the temperatures of magnetic irreversibility, when ZFC and FC curves split, are $T_{ir} \approx$ 12 K and $T_{ir} \approx$ 37 K, respectively, that is close to blocking temperatures. This observation indicates that system of cobalt nanoparticles have narrow distribution of energy barriers.

For the sample implanted to fluency of 5.0×10^1 cm^{-2} the magnetization decreases with the increasing of temperature in according to the Langevin equation at the temperature above the blocking temperature. However, for the sample implanted to the higher fluency of 7.5×10^{16} cm^{-2} the magnetization decreases faster in the superparamagnetic regime due to interparticle interactions or, perhaps, the formation of heterogeneous magnetic media.

References

[1] Rameev B., Okay C., Yildiz F., Khaibullin R.I., Popok V.N., Aktas B.: *Ferromagnetic resonance investigation of cobalt-implanted polyimides*, Journal of Magnetism and Magnetic Materials 278, 2004, p. 164-171.

Pressure-assisted generation of thermal donors in doped Cz-Si

Andrzej Misiuk[1)], Jadwiga Bak-Misiuk[2)], Marek Prujszczyk[1)]
[1)] *Institute of Electron Technology, 46 Al. Lotnikow, 02-668 Warsaw, Poland,*
E-mail: misiuk@ite.waw.pl
[2)] *Institute of Physics, PAS, 32/46 Al. Lotnikow, 02-668 Warsaw, Poland*

In spite of extended investigations [1], some aspects of thermal donors (TDs) generation in oxygen-containing Czochralski grown silicon (Cz-Si) remain to be mysterious, hydrostatic pressure (HP)-induced enhancement of the TDs formation [2] among them. The effect of HP on TDs generation in Cz-Si doped with B, N, P and Ge and processed at 700 - 750 K (HT) under HP ≤ 1.4 GPa is now investigated by four points probe; the sample structure has been controlled by X-ray diffractometry.

HP-stimulated (for up to an order of magnitude) generation of TDs has been confirmed for all investigated samples; it increases with interstitial oxygen concentration (c_o) and, sometimes, with HT (Fig. 1) while is less dependent on the concentration of investigated dopants (compare [3]).

The presence of local clouds of oxygen interstitials [4] seems to be at least in part responsible for the HP-induced increase of TDs concentration.
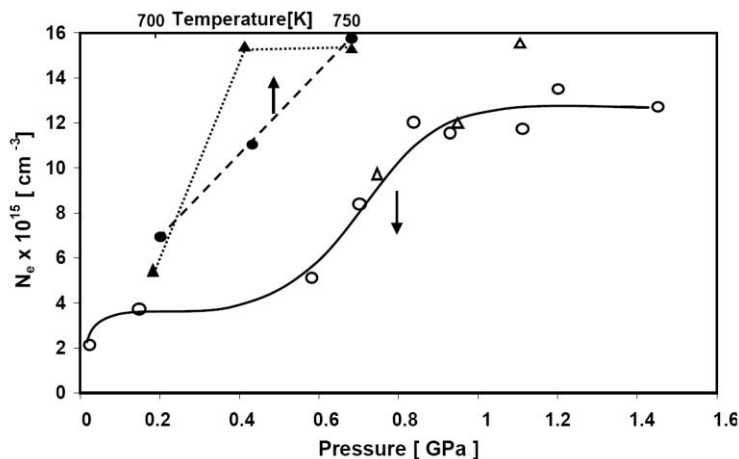
Fig. 1. Electron concentration, N_e, versus pressure and temperature for P-doped (circles: N_e=1.2×10^{15} cm^{-3}, c_O=9.1×10^{17}cm^{-3}) and B-doped (triangles: N_p=7×10^{14} cm^{-3}, c_O=1×10^{18}cm^{-3}) Cz-Si processed for 10 h at HT-HP. ○, Δ – processing at 723 K under HP; ●, ▲ – processing at HT under 1.2 GPa

References

[1] Voronkov V.V., Voronkova G.I., Batunina A.V., Golovina V.N., Falster R., Cornara M., Tiurina N.B., Guliaeva A.S.: *Properties of fast-diffusing oxygen species in silicon deduced from the generation kinetics of thermal donors*, Solid State Phen. 156-158, 2010, p. 115-122.
[2] Misiuk A., Jung W., Surma B., Jun J., Rozental M.: *Effect of stress induced defects on electrical properties of Czochralski grown silicon*, Solid State Phen. 57-58, 1997, p. 393-398.
[3] Misiuk A., Surma B., Deren Yang, Prujszczyk M.: *Stress dependent structure of annealed nitrogen-doped Cz-Si*, Materials Sci. Engng B 134, 2006, p. 218-221.
[4] Kraitchinkii A., Kras'ko M., Neimash V., Shpinar L., Tishchenko V., Voitovich V., Goushcha A.O., Metzler R.A.: *Small angle light scattering and clusters of thermal donors in Si*, J. Appl. Phys. 96, 2004, p. 7235-7238.

Encoding apparatus for Variable Low Density Parity Check Codes

N.V. Patsei

Belarusian State Technological University, Minsk, Belarus, E-mail: pat_dim@rambler.ru

Reliable data transfer is ensured by using channel detecting and correcting errors coding schemes. Low Density Parity Check (LDPC) codes are being suggested for use in a variety of transmission system, such as satellite communications, wireless transmissions, fiber optics, and a variety of storage media. To reduce the errors probabilities and increase the channel bandwidth optimized mechanisms in coding system are used. For example, by dynamically changing the parameters of codes.

The present method and apparatus provides LDPC encoder that can support multiple code block lengths and code rates by supporting a variable parity check matrixes. Let call presented codes VLDPC (variable LDPC).

Functionally encoding data processing apparatus have blocks for control, analyze, generating, storing memory, registers and adder. The input coder parameters: information block length (k) and bit error rate (*BER*) can be changed during the information transfer due to quality of the channel, giving a wide range of codes with different correction capability.

The code word can be represented by a vector: $c = [v \mid p]$, where v – input vector of length k (information bits that must be encoded), and p – a check bits vector of length $(N - k)$. Structural parity check matrix H of VLDPC code will be divided into two submatricxes: $H = [H_d \mid H_p]$. According to $c^T H = 0$ obtain $[H_d \mid H_p] \ [v \mid p]^T = 0$, then $p = ((inv(H_p)H_d)v$, where $inv(H_p)$ is the inversion of the matrix. Parity matrix H is an orthogonal to the code word, generated by generator matrix G. So, code word can obtain directly from H, without the use of G.

Square base matrix P_0 is generated in the first phase of encoder process [1, 2]. The size m of the matrix P_0 affects to the structure of verification matrix H_d. It is possible to manage the code corrective ability by increasing or decreasing the *m* value. Then permutation matrixes of P_0 must be determined by using cyclic shift right/left operation of the rows/columns. The operation is repeated *m - 1* times, giving a $P_1, \ldots, P_{m-1}$ shifted matrixes. The next step – placing shift matrices in H_d [2]. To control the code rate R it can be used the schemes of parity matrixes H transformation (lengthening, shortening, puncturing).

A VLDPC parity check matrix is said to be sparse. In other words, there are a small number of non-zero entries in the matrix relative to the size of the matrix. For efficient memory storing and accelerating encoder matrix H can be organized through two arrays size *z* (called ‚string' and ‚end'), where *z* is total number of entries in the matrix H. The ‚string' and ‚end' arrays determine the bits involved in multiplication and their locations in the code vector c.

Thus, the described solution will increase the encoder functionality and flexibility.

References
[1] Kou Y., Lin S., Fossorier R. M.P.C.: *Low Density Parity Check Codes based on Finite Geometries: A Rediscovery*, IEEE Trans. Inform. Theory. 47, 2001, p. 2711-2736.
[2] Tanner R.M., Sridhara D., Sridharan A., Costello D.J., Fuja T.E.: *LDPC block and convolutional codes based on circulant matrices*, IEEE Trans. on Inform. Theory 50 № 12, 2004, p. 2966-2984.

Interactive Intellectual Web Quiz "Polymath"

A.U. Kokhan, E.E. Chupakhina
*East Kazakhstan State University after S. Amanzholov, Ust-Kamenogorsk,
Kazakstan, E-mail: alexandrkohan@mail.ru*

All educational institutions nowadays need such organization of their maintenance to provide individual skills and creativity of every student by implementing different educational programmes realizing the principle of humane studying.

Recently computer games are becoming important educational tools. There are research groups investigating educational potential of such games and their role in educating and creating pedagogical model of their implementation.

Not only formal education can be the sphere of implementation of such computer games, but also stimulating games for military, trade, health care, or any other informal education.

Despite the versatile educational potential, computer games should be used carefully. It means full understanding is necessary to help computer games be effective.

Analysing the theory of computer games usage, web application realization and research of how different web applications interact inside one local web allow to identify the software which provides the work of net application and create the Interactive Intellectual Web Quiz —Polymath", which is aimed to improve cognitive activities of students.

The software was created in object oriented programming Delphi.

To exchange data on record of proceedings TCP/IP we will use three indy-components:

- TIdTCP Server;
- TIdTCPClient;
- TIdThreadMgrDefault.

The game process consists of three tours.

In the first round the participants have to answer the succession of questions. Every question is displayed along with time limit.

If the participants do not manage to meet the time limit, they don't get scores and the question fails to be answered.

The information of whether the answer is correct or not, the programme gets through the local net.

After all the questions are answered, the information about the correct answers is displayed onto the screen. The results of the first round show the list of participants of the second round.

In the second round the captains of the teams need to answer the maximum number of questions during one-minute time.

In the third round the participants get the opportunity to choose the topics and complexity of questions.

Questions are ranged according to difficulty. Each correct answer brings the team 10 to 50 scores.

The results of the third round lead to winning prizes.

This software can be effectively used for checking, revision and consolidation of material, for activities with big number of participants.

Zigzag diode-pumped lasers based on crystals and glasses doped with rare earth ions

M.S. Leanenia[1), I.S. Manak[1)], W. Wojcik[2)]
[1) Belarusian Staty University, 4 Prosp. Nezavisimosti, 220030, Minsk, Belarus,
E-mail: manak@bsu.by
[2) Lublin University of Technology, 38A Nadbystrzycka Str., 20618, Lublin, Poland,
E-mail: waldemar.wojcik@pollub.pl

Meeting the challenges to achieve compactness and efficiency of solid-state laser systems can be successfully solved in diode-pumped lasers with active element (AE) in the form of a flat truncated prism and a zigzag course of the beam propagation in three-mirror optical cavity (zigzag lasers). The radiation during a single pass in the zigzag laser cavity undergoes multiple reflections from the highly reflecting mirrors arranged at a small angle α realizing energy transfer with minor losses while reflecting on these mirrors to the output mirror. The radiation emerges from the cavity through the small size output mirror located at angle φ to one of the highly reflecting mirrors. The size of the optical beam cross section is much smaller than the longitudinal and transverse dimensions of the AE which allows generating radiation of high power density on the output mirror. One of the plane-parallel faces of the AE is used for pumping from the matrix of laser diode or LED emitters. Another face is made with high-reflectivity coating at pump wavelength that enhances efficiency and uniformity throughout the volume of the AE.

The active mediums doped with rare-earth ions such as Nd^{3+}, Er^{3+}, Yb^{3+} embedded in crystalline matrix or glass are the most promising active elements of solid-state zigzag lasers. Laser diodes or LEDs are used as pump sources providing high efficiency, low power consumption and high durability of solid-state lasers. Particularly promising in this case are matrices based on GaAlAs, InGaAsP and InGaAs whose spectrum can be effectively controlled by varying the component composition of the semiconductor. Such pump sources cover the spectrum from ~0.75 to ~1.1 µm. The absorption spectrum of neodymium has a broad band at a wavelength of ~0.8 µm and the ideal matching of absorption spectrum of Nd^{3+} ions and $Ga_{1-x}Al_xAs$-matrix radiation can be achieved because the matrix radiation spectrum lies in the range from ~0.75 µm to ~0.88 µm. The absorption spectrum of Er^{3+} ions lies at ~ 0.97 µm. In erbium-doped glasses the energy accumulation in the upper laser level is carried out mainly through the channel of sensitization. For Er^{3+} effective sensitizers are Yb^{3+} ions which have a single but strong absorption band in the range 0.9 - 1.02 µm. Intense absorption lines of Yb^{3+} are well suited for laser diode pumping near 0.98 µm by InGaAs-matrix with a spectral range from ~0.9 µm to ~ 1.1 µm. Perfect matching of the active substance absorption spectrum and matrices emission spectrum is obtained by varying the heat temperature of the latter, which also leads to the pumping efficiency increasing.

Analysis of energy losses in the zigzag lasers based on a flat truncated prism

M.S. Leanenia[1), I.S. Manak[1), W. Wojcik[2)
[1) *Belarusian Staty University, 4 Prosp. Nezavisimosti, 220030, Minsk, Belarus,*
E-mail: manak@bsu.by
[2) *Lublin University of Technology, 38A Nadbystrzycka Str., 20-618, Lublin, Poland,*
E-mail: waldemar.wojcik@pollub.pl

In the zigzag laser with an active element (AE) in the form of a flat truncated prism compared to lasers with Fabry-Perot resonator in addition to harmful losses ρ according to absorption and scattering in the matrix of the active substance and utility losses of the generated radiation through the output mirror with reflectivity r_3 characterized by the value $k_r = \dfrac{1}{2l}\ln\dfrac{1}{r_3}$, where l is the trajectory length of zigzag propagating radiation in the cavity, there are additional harmful losses caused by radiation reflection from the mirrors located at a small angle α to each other with reflection coefficients r_1 and r_2. In case of coefficients r_1 and r_2 equality denote them by r. Then the total harmful losses coefficient is determined by the formula:

$$\rho^* = \frac{2N-1}{2l}\ln\frac{1}{r} + \rho, \tag{1}$$

where N is the number of reflections. When $0{,}1° \le \alpha < 5°$ and the angle $0{,}1° \le \theta < 25°$ between the output mirror and a mirror with reflectivity r trajectory length can be delivered by $l \approx N \cdot h$, where h – the height of the AE. Then the dependence (1) is transformed to:

$$\rho^* = \frac{2N-1}{2Nh}\ln\frac{1}{r} + \rho. \tag{2}$$

when $N - 1$ equation (2) is simplified to the form:

$$\rho^* = \frac{1}{h}\ln\frac{1}{r} + \rho. \tag{3}$$

At angles $0.1° \le \alpha \le 5°$ the mirrors that provide a zigzag course of the beam in the cavity in first approximation can be assumed parallel to each other and form a Fabry-Perot resonator with the loss coefficient on the mirrors determined exactly by the formula (3). The accuracy of determination ρ^* from the approximate formulas (2) and (3) with respect to the expression (1) is 95% and 87.5% respectively at $r = 0.998$.

Analysis of expressions (1)–(3) shows that to reduce the harmful losses coefficient ρ^* in the cavity is necessary to use mirrors between which the radiation propagates by zigzag course with the highest value of the reflection coefficient $r \approx 0{,}998$. With the increasing number of reflections N with variation of angles α and φ the loss coefficient ρ^* increases only by 7% with respect to the value of ρ^* for $N = 2$ (for $h = 1$ cm and $r = 0{,}998$). As follows from dependence (3) the height h of the active element can be increased to minimize ρ^* but this leads to the growth of the laser size.

For a neodymium glass laser with a coefficient of material losses $\rho = 0.01$ cm^{-1} for $h = 1$ cm and $r = 0.998$ $\rho^* = 0.012$ cm^{-1} and only 20% higher than the value of ρ.

Hydrated nanodispersed anatase as cathode material for lithium power sources

V.O. Kotsyubynsky, V.L. Chelyadyn, I.F. Myronyuk, V.V. Moklyak
Precarpathion National University named after Vasyl Stefanyk, Ivano-Frankivsk, Ukraine,
E-mail: v_kotsuybynsky@mail.ru

Lithium power sources (LPS) are considered the one of the most promising energy storage technologies. Using of nanodispersed metal oxides as the cathode material is one of the most advanced ways of improving its specific capacity.

Nanoparticles of titanium dioxide with various hydratation degrees were obtained by controlled hydrolysis of $TiCl_4$ by hydrochloric acid. It was found out that the synthesis conditions (pH and temperature of reaction medium, content of additional precursors) affect on the nucleation rate and determine the phase state and morphology of TiO_2 nanoparticles. The obtained materials were tested as a base component of cathode composition of model LPS. Comparative analysis of specific capacity of LPS model with cathodes based on titanium oxide and titanium hydroxide was carried out. Discharge of model LPS were realized in galvanostatic conditions at current density of C/200. Maximal specific capacity (up to 900 mA·h/g) is fixed for LPS with cathodes on the base of X-ray amorphous oxide-hydroxide titanium $TiO_2 \cdot 1.2\,H_2O$, for which mass loss at annealing up to $500^{o}C$ is 21%. Multistage character of LPS discharge process is observed by the methods of potentiometry and impedance spectroscopy. Obtained data reflect the process of lithium ions intercalation in the particles of titania and the course of by-reactions on the surface of cathode material. The presence of surface hydroxyl and carboxyl groups and bounded in the pores of the material H_2O molecules is fixed by the method of infrared spectroscopy. Presence of the hydroxyl groups and protons in the electrolyte causes the formation of Li_2CO_3, LiOH and Li_2O phases islands on the cathode material surface on the initial stage of discharge process. Simultaneously the diffusion of Li^+ ions in crystal regions of the matrix material $TiO_2 \cdot 1.2\,H_2O$ takes place. Water in the electrolyte initiates the destruction of BF_4^- complexes. Molecules of HF are forming in the reaction of fluoride ions with protons. Nucleus of LiF is formed as the result of HF interaction with lithium-containing phases on the surface of the cathode. Thus, part of the Li^+ ions which are transferred through the electrolyte takes part in the formation of passivate layer on the cathode surface.

Similar mechanism of current formation is implemented for the cathode material on the base of anatase with the water and hydroxyl groups content about 10 mass.% synthesized by analogical way with the using of the $NaHCO_3$ as pH regulator agent. Accordingly to the XRD data the particles of this material had the ellipse-like form with the average size of 5×3 nm. This result is consistent with the data of electron microscopy investigations. In this case the value of the specific capacity of material about 540 mAh/g is reached. Annealing of this materials at 600°C results in the formation of agglomerates with the sizes of 100 - 300 nm, consisting of weakly bounded spherical particles with individual linear dimensions about 10 - 15 nm. After dehydration of this material, confirmed by IR-spectroscopy data, specific capacity about 360 mAh/g is fixed which corresponds to the intercalation compound $LiTiO_2$ formation.

So, the specific capacity linearly increases with hydratation degree of TiO_2 which together with morphological and phase parameters affects on the specific energy characteristics of model LPS.

The analysis of the influence of voltage electricity power transformer on the parameters of recorded vibration

Sebastian Borucki

Opole University of Technology, Institute of Electric Power Engineering,
76 B2 Prószkowska Str, 45-758 Opole, Poland; E-mail: s.borucki@po.opole.pl

In order to eliminate the occurrence of catastrophic failure of power transformers developed and implemented a number of methods of measurement [1 - 2], which more or less great extent, allow for early detection of damage occurring in them. One of the elements of a comprehensive diagnosis of transformer units is to assess the condition of their core, which is carried out primarily on the basis of: measurement of magnetising currents, measuring sound pressure at variable load and the direct-inspection facility, which is complicated and time-consuming procedure [2]. Currently, more and more widely used, and what is to emphasize non-invasive diagnostic method in the cores of power transformers is the vibroacoustic method [3], which relies on the measurement and analysis of mechanical vibrations of the test object. Conducted at the Institute of Electric Power Engineering of the Opole University of Technology research, the results presented in this article, focus on the development of vibro-acoustic method used to assess the condition of the mechanical design of magnetic circuit units operating in the country transformer.

The paper presents the results of laboratory measurements and analysis of mechanical vibrations in the transformer core according to the variable supply voltage of the test unit (Fig. 1). The aim of this work was to evaluate the effective value of voltage diagnosed object on the recorded energy and parameters of vibroacoustic signals, which are used in the diagnosis of power transformers, magnetic circuits.
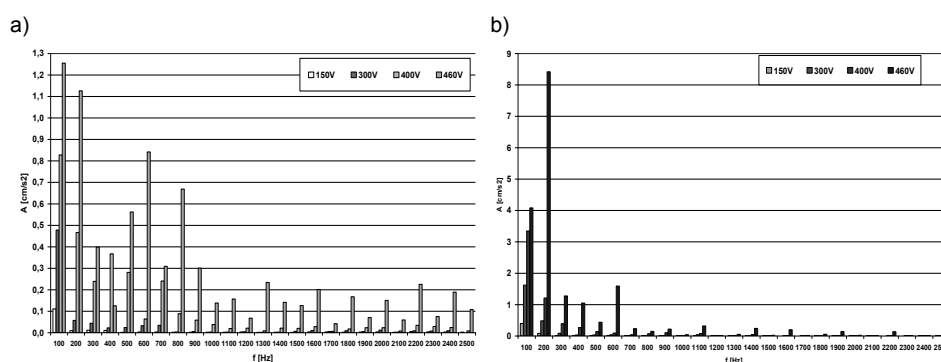
Fig. 1. Frequency of vibration of the core components of the test transformer recorded at the measuring point P1 according to changes in supply voltage: a) twisted core, b) loose core

References
[1] Duval M.: *Calculation of DGA limit values and sampling intervals in transformers in service*, IEEE Electrical Insulation Magazine, 24, 2008, p. 7-13.
[2] Praca zbiorowa pod red. J. Subocza: *Transformatory w eksploatacji*, Energo-Complex, Piekary Śląskie, 2007.
[3] Garcia B., Burgos J.C., Alonso A.: *Transformer tank vibration modeling as a method of detecting winding deformation, part I: Theoretical foundation*, IEEE Trans. on Power Delivery, 50, 2006, n.1, p. 157-163.

A way of recording-reading of the digital information

Oleg Svistunov
Belarusian State University, Minsk, Belarus, E-mail: svistunov@bsu.by

Computing systems with natural parallelism of calculations aren't always more effective than the classical by solving majority practical problems.

Considering huge cost quantum or neuron computers the gain received often doesn't correspond to expenses.

Our usual personal computers will successfully compete to expensive systems of quantum or neuron structure if to find a simple way for technical realisation allowing without the big financial expenses:

- considerably to increase computing possibilities (information capacity and speed of information processing) classical computers;
- to protect the information from decoding by systems with natural parallelism of calculations.

The way based on the reorganisation of a computer language allows to solve these problems.

By means of the way realisation in a computer language of three symbols of the digital alphabet, that leads to substantial growth of calculating possibilities of the computer.

Use technological processes of manufacturing of integrated microcircuits existing nowadays and other elements of circuitry for technical realisation of the way.

Use the trit trigger for a data recording on a computer language. The trit trigger - a cell of memory with one target condition from three possible: 0 or 1 or 2.

This way gives the chance to pass from information operating in bits to operating trits information, from information operating in bytes to operating trytes information instead of use of 3 categories for definition of the address of bit in byte to occupy only 2 categories for trits address definition in tryte, and also to represent one tryte 19 683 numbers instead of 256 numbers in one byte, that raises information capacity in 76.9 times increasing time of a data recording-reading for 12.5 %.

In two bytes united positionally in group represent 65 536 numbers.

United positionally to group two trytes represent 387 420 489 numbers at the expense of what raise information capacity in 5 911.5 times increasing time of record-reading of the information only on the same of 12.5 %.

The basic technical result consists:

- in substantial increase of information capacity of the computer at the expense of use in a computer language of three symbols of the digital alphabet for information record-reading;
- in increase in speed of processing of the information in comparison with use in a computer language of two symbols of the digital alphabet.

The basic advantages of the way are:

- rather small complexity for circuit and hardware implementation;
- indiscriminateness to change of technological process of manufacturing of integrated microcircuits and other elements of circuitry.

Such computer system is steady against hindrances at data transmission on communication lines and is inaccessible to decoding by systems with natural parallelism of the calculations the binary data operating only.

Dependencies of grain structure formation in dielectric materials based on solid state solutions $Ba_xSr_{1-x}(R_{0.5}Nb_{0.5})O_3$ with R = Ho, Er, Tm, Yb and Lu

L.A. Bliznyuk[1), A.A. Klimza[1), V.V. Fedotova[1), C. Karwat[2)

[1) *State Scientific and Production Association „Scientific-Practical Materials Research Center of NAS of Belarus', 19 P. Brovka Str., 220072 Minsk, Belarus,*
E-mail: klimal@physics.by
[2) *Lublin University of Technology, 38a Nadbystrzycka Str., 20-618 Lublin, Poland*

The knowledge of correlations between technological parameters of ceramic materials, their crystalline structure, microstructure and properties are of the great importance for their properties prediction as well as the estimation of their applications prospectives.

Present study is focused on the analysis of correlations between grain structure formation in ceramic materials like $Ba_xSr_{1-x}(R_{0.5}Nb_{0.5})O_3$ doped with are rare-earth elements R = Ho, Er, Tm, Yb and Lu, and their dielectric properties.

Basic problem to be solved was the synthesis of high-qualty complex ceramic perovskites $A(B'_yB''_{1-y})O_3$ (A = Ba, Sr, Ca; B' – rare earth elements, B'' = Nb and Ta) [1] with desired properties at low temperatures of sintering. This is particularly important because high sintering temperatures (about 1550 - 1700°C) in these ceramics is strongly inhibits their industrial application

We tried to solve this problem using method of mechanical activation of powders containing sintered solid solutions.

The changes in grain structure as a function of activation time have been studied in this work. The effects of mechanical activation of the studied ceramic materials on phase composition, sintering temperature, microstructure, porosity and temperature dependencies of dielectric parameters (relative dielectric permeability, dielectric loss tangent) were also investigated.

These measurements allowed to develop new technological approach to the synthesis of high-density ceramic materials based on the above-mentioned systems with low sintering temperatures (about 1200 - 1350°C that is lower on 250 - 400°C as compared to previously applied technology) with desired combination of properties [2].

References
[1] Sebastian M.T: *Dielectric materials for wireless communication*, Elsevier Science and Technology Publishers, Oxford, 2008.
[2] Patent №13589 by application № a20090628 from 30.04.2009, Blizniyuk L.A., Ges A.P., Klimza A.A.: *Method of the sysnthesis of dielectric ceramic material for microwave devices*.

Dynamics of fusion and crystallization processes induced by nanosecond emission of ruby crystal laser in gallium arsenide and gallium antimonide

A.I. Urbanovich[1), S.P. Zhvavyi[2)
[1) *Belarusian State University, Minsk, Belarus, Email: urbanovich@bsu.by*
[2) *Institute of Physics, National Academy of Science, Minsk, Belarus,*
E-mail: Zhvavyi@inel.bas-net.by

Diversity of $A^{III}B^{V}$ semiconductors properties preconditions their expansive application in the instruments and devices. $A^{III}B^{V}$ semiconductors based injection lasers feature good efficiency of electrical power to electromagnetic conversion. GaAs is potentially one of the best photosensitive materials. For successful application of laser methods in modern technological processes of semiconductor materials treatment the data on the physical phenomena occurring if these semiconductors are subject to the laser emission. Some works covered modification regularities of GaAs top layers when subjected to laser pulses. However numerical simulation of fusion and crystallization was performed ignoring surface evaporation processes and diffusion of the components in the melt. Here there are provided the results of the numerical simulation fusion and crystallization processes in GaAs and GaSb induced by nano-second emission of ruby laser (λ = 694 nm, η =80 ns) with account of surface evaporation and diffusion of the components in the melt). Waveform of laser pulse was set by function $\sin^2(\pi t/2\eta)$. The thickness of semiconductor wafer was assumed to considerably exceed the larger length of heat diffusion for the time of laser pulse and was taken equal to 38 µm. Numerical simulation was performed on the base of mathematical model provided in [1]. At the result of the simulation of laser-induced gallium arsenide surface modification with account of surface evaporation processes and diffusion of the components in the melt it is demonstrated that the process of arsenic atoms evaporation affects the dynamics of the phase transition at near – surface area. At the result of arsenic atoms evaporation and diffusion of gallium arsenide components in the melt there occur the gallium enrichment of the near-surface area. Using at simulation the dependences of crystallization temperature and latent heat of phase transition upon the components concentration in the melt allowed to obtain satisfactory conformity to the experimental data on the dependence of the maximum temperature of melt surface and life time of liquid phase upon the energy density. Simultaneously the process of the components evaporation in gallium antimonide under the impact produced by nano-pulse emission of ruby laser does not significantly affect the dynamics of the phase transitions in the near-surface area.

References

[1] Zhvavyi S.P., Urbanovich A.I., Zykiv G.L., Bulletin of Belarussian State University, Series 1, Issue1, 2010, p. 36.

The analysis of the paper-oil insulation aging process using the X-Y type diagram and the Cole-Cole model

Stefan Wolny, Maciej Zdanowski

Opole University of Technology, Institute of Electrical Power Engineering, Opole, Poland
E-mail: s.wolny@po.opole.pl

The paper presents research results simulating the influence of the paper-oil insulation aging degree of power transformers on the time constant values of the return voltage decay. According to authors, this value may be well used as a parameter describing the thermal degradation degree of the insulation to ground of oil power transformers during diagnostic tests using the Recovery Voltage Method (RVM) [1, 2]. The insulation aging degree was simulated by proper selection of parameter α of the Cole-Cole model, which is closely connected with the relaxation time distribution function of cellulose macromolecules. The values of the equivalent circuit diagram elements were determined using the author's discrete approximation method of characteristic operator impedance of the Cole-Cole model [1, 3]. The insulation to ground of the oil power transformer was simulated applying a commonly-used in literature cumulative X-Y type equivalent circuit diagram [1, 4]. Figure shows the diagram used in the research.
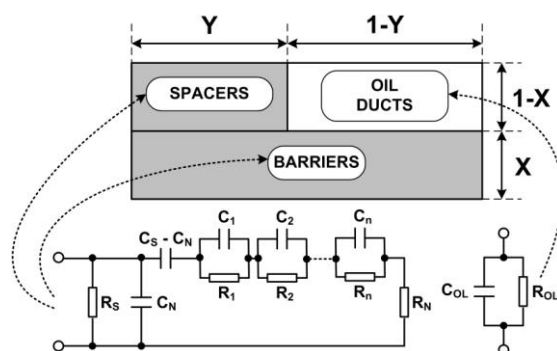
Fig. A cumulative X-Y type equivalent circuit diagram of the insulation to ground of oil power transformer based on the Cole-Cole model: R_S - direct-current resistance, R_N - resistance for $f = \infty$, f - frequency, C_S - direct-current capacity, C_N - capacity for $f = \infty$, R_1, R_2, R_n, C_1, C_2, C_n - elements simulating consecutive insulation relaxation processes, C_{OL} - oil ducts capacity, R_{OL} - creepage resistance of oil ducts

References
[1] Wolny S.: *Diagnostyka stanu izolacji papierowo-olejowej z wykorzystaniem metod polaryzacyjnych*, Oficyna Wydawnicza Politechniki Opolskiej, Studia i Monografie, 2008, Opole, s. 222.
[2] Wolny S., Zdanowski M.: *Analysis of Recovery Voltages Parameters of Paper-Oil Insulation Obtained from Simulation Investigations Using the Cole-Cole Model*, IEEE Transactions on Dielectrics and Electrical Insulation 16 No.6, 2009, p. 1676-1680.
[3] Wolny S.: *The Application of the Cole-Cole Model in Diagnostics of the Paper-Oil Insulation Condition Using the RVM Method*, 37th International Conference Defektoskopie 2007, Praque, 7-9 November 2007, Czech Republic, p. 279-286.
[4] Graczkowski A., Szymański J.: *Analiza wpływu parametrów geometrycznych i materiałowych na spektrum napięcia powrotnego w oparciu o schemat zastępczy izolacji papierowo-olejowej*, Przegląd Elektrotechniczny – Konferencje 3, 1/2005, 2005, p. 116-119.

Determination of short circuit type on distribution networks lines

F.A. Romaniuk, E.V. Buloichyk

Belarusian National Technical University, Minsk, Belarus, E-mail: ev_pst@list.ru

One of the improvement directions of the lines microprocessor current protections is based on an efficient change of the steps current settings depending on the occurred short circuit type.

Asymmetrical fault mode detection can be carried out through the checking of the relative asymmetry of the currents in the line phases. Under these conditions only the load current $\dot{I}_L$ flows in the unfaulted phase of the line, and in the faulted phases load current is superimposed on the fault current $\dot{I}_{SC}$ increasing current of one phase and decreasing another one. Load currents in the faulted phases two times less in the value and opposite in sign to the load current in the unfaulted phase.

Under two-phase fault conditions the smallest of the line phases' currents I_{min} is the load current in the unfaulted phase, and the largest of the mentioned currents I_{max} is equal to vector sum of short-circuit current $\dot{I}_{SC}$ and load current in the faulted phase which is equal to $0.5 \cdot \dot{I}_L$.

In this connection the difference between I_{max} and I_{min} (1) has significant value which indicates asymmetrical fault on the line

$$(I_{max} - I_{min}) = (|\dot{I}_{SC} + 0.5 \cdot \dot{I}_L| - |\dot{I}_L|). \tag{1}$$

In the case of the identical fault occurrence in the one of the parallel distribution network lines only load currents which are distinguished by the value and the phase angle flow in all phases of the controlled line.

In this case the difference between I_{max} and I_{min} of phase currents of controlled line does not exceed half of the load current

$$(I_{max} - I_{min}) \le 0.5 \cdot I_L. \tag{2}$$

Hence the asymmetrical mode in the controlled line will take place at

$$(I_{max} - I_{min})/I_L > 0.5. \tag{3}$$

Taking into consideration that during asymmetrical faults $I_L = I_{min}$, the condition of their existence on the line under control is given by

$$(I_{max} - I_{min})/I_{min} > 0.5. \tag{4}$$

With non-fulfillment (4) the fault is symmetrical.

For two-phase short-circuit I_{max} is the current of the faulted phases and I_{min} is the load current. After introducing fault current to load current multiplicity concept $k = I_{max}/I_L$ and taking into account (4) it is possible to write down

$$(k \cdot I_L - I_L)/I_L > 0.5. \tag{5}$$

After solving (5) relative to k we will have that $k > 1.5$. This indicates that the method considered makes it possible to clearly establish two-phase short-circuit mode when fault currents not less than 1.5 times exceed under-load operation currents. Application of this method in the microprocessor-based line current protection will ensure an improvement of their sensitivity to remote asymmetrical short-circuits.

References

[1] Romaniuk F.A., Tishechkin A.A., Kovalevsky A.V.: *Principles of implementation of adaptive microprocessor current protection from the phase-to-phase short circuits*, Energetika – Proceedings of CIS Higher Educational Institutions and Power Engineering Associations 3, 2005, p. 11-14.

Morphotropic phase boundary in $Bi_{1-x}Ca_xFe_{1-x/2}Nb_{x/2}O_3$ multiferroics

I.O. Troyanchuk[1], N.V. Tereshko[1], D.V. Karpinsky[1], V.V. Fedotova[1], C. Kozak[2]

[1] *SSPA, Scientific-Practical Materials Research Center of NAS of Belarus,*
19 P. Brovka Str., 220072 Minsk, Belarus, E-mail: tereshko@physics.by
[2] *Lublin University of Technology, 38a Nadbystrzycka Str., 20-618 Lublin, Poland*

$BiFeO_3$ is a very rare example of the single phase material, in which ferroelectricity, antiferromagnetism and ferroelasticity coexist in a broad temperature range. High transition temperatures and a large spontaneous polarization take this compound a good candidate for various device applications [1, 2]. Recently, the examples of solid solutions of $Bi_{1-x}Ca_xFe_{1-x/2}Nb_{x/2}O_3$ have been studied [3]. It was shown that the compound with the composition $x = 0.3$ exhibits spontaneous magnetization of about 0.3 emu/g. This effect has been attributed to nonpolar orthorhombic structure (space group P_{nma}) which allows weak ferromagnetism. However, the magnetic properties of the compounds with the lightly doped compositions still revealing the ferroelectric properties have not been studied.

In this work, investigation of the crystal structure, magnetic and piezoelectric properties of polycrystalline $Bi_{1-x}Ca_xFe_{1-x/2}Nb_{x/2}O_3$ system was performed by *X*-ray diffraction, Mössbauer spectroscopy, Vibrating Sample Magnetometry (VSM), and Piezoresponse Force Microscopy (PFM). It is shown that increasing niobium content induces a polar-to-nonpolar morphotropic boundary near the $x = 0.19$. Within the polar region ($0.15 \leq x \leq 0.18$) the solid solutions are the homogeneous weak ferromagnets. It is assumed that the chemical substitutions lead to decrease of the initial volume of the unit cell and favor stabilization of weak ferromagnetic state within rhombohedral ferroelectric phase. The piezoresponse is significantly enhanced near the morphotropic boundary. The piezoelectric properties of parent antiferromagnet $BiFeO_3$ with a cycloidal spatially spin-modulated structure and polar weak ferromagnet $Bi_{0.82}Ca_{0.18}Fe_{0.91}Nb_{0.09}O_3$ are compared and analyzed.

References

[1] Fiebig M.: *Revival of the magnetoelectric effect,* Journal of Physics D: Applied Physics, 38, 2005, p. R123-R152.
[2] Catalan G., Scott J.K.: *Physics and application of bismuth ferrite*, Advanced Materials, 21, 2009, p. 2463-225.
[3] Troyanchuk I.O., Bushinsky M.V., Chobot A.N., Mantytskaya O.S., Pushkarev N.V., Szymczak R.: *Crystal-structure and magnetic phase transformations in solid solutions of BiFeO3-AFe0.5Nb0.5O3 (A = Ca, Sr, Ba, Pb),* Journal of Experimental and Theoretical Physics, 107, 2008, p. 245-250.

Issues concerning single phase earth faults in lines connecting high-power units to the electric power system

Piotr Kacejko, Marek Wancerz
Lublin University of Technology, 38a Nadbystrzycka Str., 20-618 Lublin, Poland

Among the actual trends within the national electric power system development there is a construction of new generating units in already operating power plants. Their design includes partial use of the existing infrastructure but the new units are meant to be totally separate independently operating entities. Such a unit can be located at some distance from the existing generators. In that case the length of a special line connecting the new unit to a power plant substation can be considerable. Such operation conditions occur e.g. in the case of a 800 MW unit constructed for the Belchatow power plant. The special 400 kV line that connects the unit to the Trebaczew substation is almost 50 km long. With such line lengths fault hazard gets very real and, as it is in the case of all overhead lines, 80 % of faults are single phase earth faults that vanish when a line gets cut off the power supply. The question is what should be the reaction of the unit protection system to such faults. The two following approaches can be considered:

- a traditional approach that consists in the fault clearance by means of a simultaneous opening of WG and WB breakers (Fig. 1a) which makes the unit pass to its auxiliary operation mode or causes its cutout;
- an alternative approach that consists in the action of WB1 and WB2 breakers (Fig. 1b) according to the rules accepted for ―common" lines i.e. related to the operation of an auto-reclosing (one-phase) equipment and an attempt (in the case of a successful fault clearance) of maintaining the generator in the mode of its synchronic operation in the system.

Although for a number of reasons a decision of implementing a WB1 breaker at the HV side of a unit transformer has been taken, the alternative approach has many opponents despite its obvious attractiveness from the viewpoint of maintaining power balance in the power system. The opponents point to the hazards for a generator shaft, high-power turbine and other elements of its design that follow from the realization of a single-phase auto-reclosing cycle at such a close distance to it. The paper reports on detailed simulation testing applied to the problem. Modeling of transient electromechanical processes for asymmetric fault conditions and a single-phase supply interruption has made it possible to objectively assess the potential of implementing single-phase auto-reclosing equipment to the special unit line and to evaluate real-time hazards for the TG set.

a)
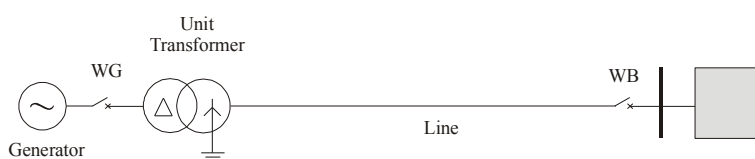
b)
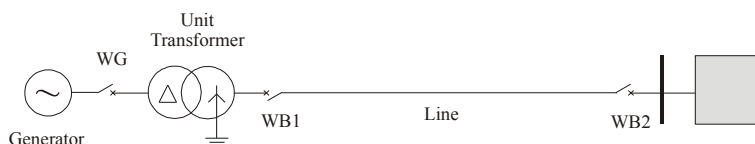
Fig. 1. Variant operation modes of a line for power evacuation from a power plant

Use of prediction methods to diagnose aging of composite insulators

Jan Purczyński
West Pomeranian University of Technology, Szczecin, Poland,
E-mail: janpurczynski@ps.pl

Diagnostic tests of composite insulators aging are characterized by relatively long observation time period, e.g. in [1] measurement results were provided for 13 weeks. The question put forward in this paper is whether the testing time can be shortened by determining the values of the last observations based on a determined trend, which is the subject of prediction theory. Applicability of the following trends was tested: linear, parabolic, power, exponential, logarithmic and hyperbolic [3, 4]. Prediction was made using the trend that yielded the smallest value of forecast ex ante error.

Drawing on the data presented in [2], the approximation of current pulse quantity using a power trend was considered. Assuming that the last measurement is omitted and its value is determined on the basis of the trend, the following relative error was obtained: -0.93 % in range (20, 30) mA and 0.31 % in range(30, 40) mA.

Paper [1] presents, among others, the values of dielectric loss coefficients obtained during aging tests lasting 11 weeks for two composites (A, B) intended to be used to make an insulator. In the case of A composite, logarithmic trend parameters were determined, and the trend was based on 7 observations. By omitting the measurements for the last 5 weeks, the obtained error was 5.14 %. For B composite, the values of dielectric loss coefficients were modeled using a hyperbolic trend determined on the basis of 4 observations. The omission of measurements for the last 8 weeks leads to the mean error equal 2.69 %. It means that the measurement period is limited to 3 weeks instead of 11 weeks. Due to small values of ex post error, we can propose the method that limits the number of measurements by determining the values of the last observations based on a determined trend, which shortens testing period.

References
[1] Banaszak Sz.: *Diagnostic method for composite insulators ageing level estimation,* Proceedings of the XVth International Symposium on High Voltage Engineering – ISH 2007, Ljubljana, Slovenia, 27-31 August 2007, p. 193 + CD.
[2] Banaszak Sz.: *Badanie stopnia zestarzenia izolatorów kompozytowych,* Przegląd Elektrotechniczny Konferencje 3/2007, 2007, s. 17-20.
[3] Purczyński J.: *Metody prognozowania z wykorzystaniem trendu potęgowego*, Przegląd Statystyczny 56 2, 2009, s. 52-66.
[4] Purczyński J.: *Estimation of exponential function parameters*, Przegląd Elektrotechniczny 86 7/2010, 2010.

Improvement of the MSW spectrum temperature stability in the iron-yittrium garnet films

G.G. Bondarenko, V.V. Shagaev
Research Institute of Advanced Materials and Technology, Moscow, Russia,
E-mail: niipmt@cea.ru

Now a large number of devices is available for the functional electronics in the microwave range based on the ferrite-garnet films. The processing of the signals in these devices is carried out using magnetostatic spin waves (MSW), excited in the film element. It is well known that the ferrites characterised by weak attenuation are more suitable for the construction of MSW devices, have also a distinctive temperature dependence of the saturation magnetization. The latter circumstance results in the temperature instability of the spectrum of the MSW and this impairs the frequency selection characteristic of the devices. The currently available methods of improving thermal stability may be divided into two groups. The first group uses thermostats, the electronic circuits for self-adjustment of frequency, and other additional sections. This complicates the design of the devices, increases the dimensions, and also the energy consumption. The second group of the methods is based on the use of the properties of the film elements and, therefore, is most efficient. The interesting properties may be described as follows. Firstly, there is a strong dependence of the temperature coefficient of the frequency of the MSW on the angle between the film and the vector of static magnetization. This dependence forms as a result of the effect of the demagnetizing field. Secondly, the temperature characteristics depends strongly also on the orientation of the vector of magnetization in relation to the crystal lattice. In previous investigations, only one of these factors was usually taken into account. For example, the temperature characteristics of the films with inclined magnetization were analysed on the basis of the isotropic model of ferrite, and in the examination of the effect of the field of magnetic anisotropy, investigators used the geometry of tangential magnetization. The combined effect of the two factors on the temperature characteristics has not been examined in great detail. The aim of the present work is the experimental and theoretical examination of the temperature characteristics of the MSW in the films of the cubic anisotropic ferrites in the conditions of inclined magnetization. In this work investigations were carried out into the temperature characteristics of the magnetostatic waves in single crystal iron-yittrium garnet ferrite films. The results, obtained in the geometric of inclined and tangential magnetization, are compared. Special attention is devoted to the explanation of the special features, associated with the effect of the field of magnetic anisotropy of the ferrite on the drift of frequencies. It has obtained an improvement of the temperature characteristics due the selection of the optimum crystallographic orientation of the film.

The comparison of potential use of electric filters with bifilar winding and discharging filters

Andrzej Sumorek

*Faculty of Electrical Engineering and Computer Science, Lublin University
of Technology, Lublin, Poland, E-mail: a.sumorek@pollub.pl*

The fabric filter represents the contamination removal technology with theoretically warranted contamination removal efficiency of 100%. The problem consists in the necessity of periodical elimination of contaminations from the filtering "fabric" [3]. The problem consisting in the periodical shutdown of filters has been eliminated in case of electrofilters. There are two types of electrostatic separation/filtration. The dielectrophoresis is based upon the assumption that the particles will be not pre-charged. The presence of charged particles is required in case of electrophoresis. There are three methods of particles charging i.e. contact charging, corona charging and inductive charging [2]. The electrophoresis with corona discharging found application in powder coating technique (Fig. 1b) and in electric filters (Fig. 1a). The electrophoresis with contact charging (Fig. 1c) is the basis of the operating principle of electroseparators.
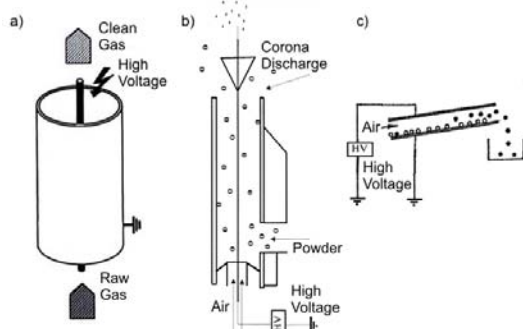
Fig.1. a) Electrofilter [3]; b) Tribo gun (for powder coating) [1]; c) Electroseparator

The continuous occurrence of an electric discharge or its possibility is assumed in course of the operation of typical electrofilters. Furthermore the non-uniform electric field around the winding is utilized in the "bifilar" filter. The winding is supplied with a voltage not causing any hazard of an corona discharging and consequently the dust explosion. The experiments carried out by the author of the present study make it possible to present the comparison of the functioning aspects for the bifilar and discharge filters. The results obtained from the tests demonstrated it is possible to achieve the dedusting efficiency above 98% in case of bifilar filters power supply in the form of DC voltage of $13 \cdot 10^3$ V [4]. Therefore the bifilar filter can be considered as a solution competing against the standard discharging filter.

References
[1] Bailey A.G.: *The science and technology of electrostatic powder spraying, transport and coating*, Journal of Electrostatics 45, 1998, pp. 85-120.
[2] Butcher D.A., Rowson N.A.: *Electrostatic separation of pyrite from coal*, Magnetic and Electrical Separation 6, 1994, pp. 19-30.
[3] Parker K.R. (red.): *Applied electrostatic precipitation*, Blackie Academic & Professional, 1997
[4] Pietrzyk W. (red.): *Elektrofiltr bifilarny do usuwania pyłów pochodzenia roślinnego*, Wydawnictwo Naukowe FRNA, ISBN-13: 978-83-60489-10-9, Lublin, 2008.

The application of dispersed processing networks in order to optimize the energy consumption in contemporary buildings

Marek Horyński

Department of Computer and Electrical Engineering, Lublin University of Technology, Lublin, Poland, E-mail: m.horynski@pollub.pl

The energy saving contributes to the reduction of negative impact on the natural environment caused by the systems used in human activity. Except of power supply continuity to be assured for the electric equipment in the contemporary buildings, their energy-saving operation is extremely important.

Owing to the presence of electric energy in many fields of modern human life as well as to increasing prices of energy raw materials and their limited resources, the introduction of energy-saving systems is extraordinarily important. The scope of energy-saving systems encompasses the dispersed processing systems applied in the building management systems; among others KNX/EIB. The efforts are made in all phases of the building construction and of its operation in order to find potential energy savings. An economical utilization of electric energy is commenced as early as in the building design phase. The following measures are essential for the achievement of energy savings:

- monitoring and automatic control over energy consumption as well as the consideration of heat emitted by the equipment and human organisms in the heat balance;
- application of modern energy-saving technologies in the scope of the heating, cooling, air – conditioning and ventilation of the building;
- use of alternative renewable energy sources i.e. sun radiation, wind, sea waves, geothermal heat and hot waters;
- application of hybrid systems in HVAC installations.

The optimisation of energy consumption in the buildings should be based upon the following assumptions:

- energy is used in case of necessity only, i.e. shutdown of the devices which are not used at the moment;
- the amount of energy needed for use should be maintained on a reasonably low level;
- energy is used with an efficiency as high as possible.

This article presents the use of KNX/EIB system for the optimisation of energy consumption in the buildings and the description of the issues associated with their programming by means of the last version of ETS4 utility. The design basis for the laboratory stand enabling KNX/EIB system energy-saving test has been also specified. An important advantage of the prepared design of laboratory stand is the possibility to design and to arrange various configurations of bus devices connections, because the stand is not provided with permanent connections between modules.

References

[1] Horyński M.: *Heating system control in an intelligent building*, Teka Komisji Motoryzacji I Energetyki Rolnictwa 8, 2008, p. 83-88.

[2] Mikulik J.: *Europejska Magistrala Instalacyjna EIB – rozproszony system sterowania bezpieczeństwem i komfortem [European Installation Bus – safety and comfort dispersed control system]*, Warszawa, 2008 (in Polish).

Electron Paramagnetic Resonance of $(CoFeZr)_x(Al_2O_3)_{100-x}$ nanocomposites produced in the atmosphere of oxygen and argon

Pawel Zhukowski[1)], Tomasz N. Kołtunowicz[1)], Julia V. Sidorenko[2)],
Julia A. Fedotova[3)], Vera V. Fedotova[4)]
[1)] *Lublin University of Technology, Department of Electrical Devices*
and H.V. Technology, 38a Nadbystrzycka Str., 20-618 Lublin, Poland,
E-mail: t.koltunowicz@pollub.pl
[2)] *Belarusian State University, 4 Nezavisimosti Str., 220040 Minsk, Belarus*
[3)] *National Scientific and Educational Centre of Particle and High Energy Physics*
of the Belarusian State University, 153 M. Bogdanovich Str., Minsk, Belarus
[4)] *State Scientific and Production Association „Scientific-Practical Materials Research*
Center of NAS of Belarus', 19 P. Brovka Str., 220072 Minsk, Belarus

Within the presented research project the method of electron paramagnetic resonance (EPR) has been applied to test magnetic properties of $(CoFeZr)_x(Al_2O_3)_{100-x}$ nanocomposites produced in the atmosphere of oxygen and argon. The obtained data have been compared to equivalent characteristics of nanocomposites produced in the atmosphere of pure argon [1]. Figure 1a presents angular dependence of the EPR line maximum (H_{max}) position for various values of the metallic phase content x. When a layer is positioned perpendicular to magnetic field lines inside the sample demagnetizing field forms and the real internal field H is weaker than the external field $H\perp$

$$H = H_\perp - 2\pi NJ \ . \tag{1}$$

In the case of a parallel position:

$$H = H_\parallel , \qquad (2) \quad \text{hence:} \quad H_\parallel = H_\perp - 2\pi NJ \qquad (3)$$

where: N – demagnetizing factor, (in our case N = 1)

Figure 1b presents dependences of $H_{max}(90°)$ on the temperature of 15-minute annealing for various metallic-phase contents x. Along with the increasing value of x the $H_{max}(90°)$ value decreases and annealing contributes to additional reduction of the value.
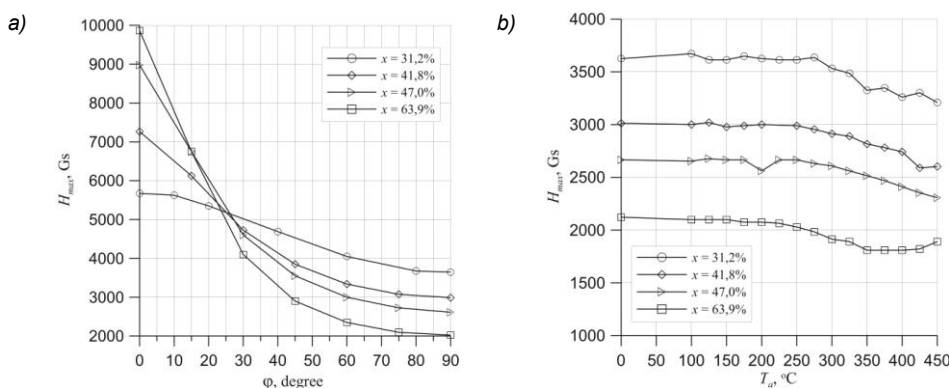
Fig. 1. Angular dependence $H_{max}(\theta)$ (a) and the dependence of $H_{max}(90°)$ on annealing temperature T_a for various content values x (b)

References

[1] Zhukowski P., Sidorenko J., Kołtunowicz T.N., Fedotova J.A., Larkin A.V., Przegląd Elektrotechniczny 86 7/2010, 2010, p. 296-298.

Low temperature formation of platinum silicide
for Schottky high-power diodes

F. Komarov[1], O. Milchanin[1], T. Kovaleva[1], J. Solovjov[2], A. Turtsevich[2]
[1] *Institute of Applied Physics Problems, 7 Kurchatov Str., 220108 Minsk, Belarus,*
E-mail: KomarovF@bsu.by
[2] *Unitary enterprise "Transistor Plant", 220108, Minsk, Belarus*

Platinum silicide films are widely used in silicon devices. The crystallography, morphology and kinetics of formation of PtSi films has been the subject of much research due to the ability of these films to form near-ideal n- and p-type ohmic contacts and also Schottky contacts on substrates of silicon in the manufacture of various semiconductor devices. In particular, application of PtSi contact layer in Schottky high-power diodes allows to lower leakage current, to raise break-down voltage and also to increase temperature operating modes of devices.

In our work structural and electrical properties of contact platinum silicide layers for Schottky high-power diodes formed on silicon wafers by deposition of thin platinum layers (20 - 40 nm) and low temperature annealing (100 - 360°C, 30 - 480 min) were investigated. The depth distributions of Pt into the silicon matrix were analysed using RBS. In all cases the RBS measurements were performed in identical conditions with 1.4 MeV He$^+$. The structural-phase modifications of Pt/Si system after annealing have been studied by means of transmission electron microscopy in "plan-view" and "cross-section" geometries using a Hitachi H-800 instrument operating at 200 keV.

It is shown that process of silicide formation in Pt/Si system begins at temperatures of about 180°C. During heat treatment at 180 - 240°C only Pt_2Si phase is revealed. However, when the annealing of a 40 nm Pt layer occurs at 200 - 220°C, the Pt_2Si silicidation reaction is not fully completed even after 480 min. It is found that PtSi silicides are formed at the temperature above 240°C. There is no any influence of Si wafer doping on process of silicide formation. Thin layers of silicides, generated at lower temperatures (< 260°C), are more perfect in depth, and also are characterized by more homogeneous grain sizes.

Nanoporous SiO$_2$ and Si$_3$N$_4$ layers on silicon wafers created by swift ion irradiation followed by chemical etching

L. Vlasukova[1], F. Komarov[1], O. Milchanin[1], A. Didyk[2], V. Skuratov[2], S. Kislitsin[3]

[1] *Belarusian State University, 4 Nezavisimosti Ave., 220030 Minsk, Belarus,*
E-mail: KomarovF@bsu.by
[2] *Joint Institute for Nuclear Research, 141980 Dubna, Russia*
[3] *Nuclear Physics Institute, NNC, Almaty, Kazakhstan*

We examined pore formation in SiO$_2$ and Si$_3$N$_4$ layers on Si wafers by means of swift ion irradiation followed by etching of latent tracks. The samples were irradiated with ions energy of 710 – 40 MeV up to the fluence from 1x10^8 to 5x10^{10} cm^{-2} and then etched in the dilute solutions or in the HF vapours. SEM and TEM were used to probe the processed samples. From the geometric parameters of the pores the etch rate of the tracks and the etch rate of undamaged material for SiO$_2$ and Si$_3$N$_4$ were estimated. For SiO$_2$ layers with pore size from 15 to 500 nm varying by the etching duration were created. The etching in HF solutions results in the formation in SiO$_2$ conical channels. The treatment in HF vapours forms nearly cylindrical ones with the length/diameter ratios up to 15. The TEM investigation confirms that latent tracks in thermal SiO$_2$ are not annealed after the thermal treatment at 900°C for 30 minutes. The morphology of etched tracks does not change after the annealing at 900°C during 30 min, too. In Si$_3$N$_4$, tracks were etched only after exposure to W ions (180 MeV) with S_e = 20.4 keV/nm being maximal for our experiment in the case of silicon nitride. The low track etching efficiency and the considerable size spread of pores allow assuming the formation of discontinuous tracks. The results of computer simulation in terms of thermal spike of the track formation in SiO$_2$ and Si$_3$N$_4$ are also presented. The comparison of the calculation results with the etching data has been made.

Nickel-platinum compound silicide formation on silicon by IBAD

F. Komarov[1], O. Milchanin[1], T. Kovaleva[1], I. Konopljanik[1], J. Solovjov[2],
K. Kiszczak[3], P. Zhukowski[4], C. Karwat[4], C. Kozak[4]

[1] *Institute of Applied Physics Problems, 7 Kurchatov Str., 220108 Minsk, Belarus,*
E-mail: KomarovF@bsu.by
[2] *Unitary enterprise "Transistor Plant", 220108, Minsk, Belarus*
[3] *Maria Curie-Sklodowska University, 1 Pl. M. Curie-Sklodowskiej,*
20-031 Lublin, Poland
[4] *Lublin University of Technology, 38a Nadbystrzycka Str., 20-618 Lublin, Poland*

Nickel silicide is now widely used in advanced devices thanks to its low formation temperature, low resistivity and low Si consumption. The stability of the sheet and contact resistance on nickel-silicide is an important issue. The main NiSi integration concern is its instability at high temperature. Ni (Pt) alloys introduction may considerably improve NiSi films thermal stability against agglomeration. Initial studies have shown that Pt addition could improve the thermal stability of NiSi films against transformation to $NiSi_2$, also. An amount of alloying element dissolved in NiSi determines structural and electrophysical properties of the formed layers. The one-beam ion mixing method using the truncated cones coated with layers of different materials makes it possible to modify near-surface metal or semiconductor layers by simultaneous deposition of one or several materials [1].

The truncated cones coated with Ni and Pt of different areas have been irradiated by 60 keV Ar^+ ions to the fluences of $2x10^{16}$ cm^{-2} and $5x10^{16}$ cm^{-2} at a beam current density of 10 μA/cm^2. The post-deposition furnace annealing as well as RTA in an inert ambient have been used to form or modify silicide layers. Auger electron spectroscopy and RBS with 1.5 MeV He^+ beam have been used for depth profiling over the whole modified structure.

The as-deposited and annealed samples were characterized by TEM and XTEM. Silicide layer resistance was measured with four-point probe method.

The structural and electrophysical properties of prepared samples are discussed as a function of Pt concentration and regimes of the layer deposition and thermal treatments.

References

[1] Zukowski P., Komarov F.F., Karwat Cz., Kiszczak K., Kozak Cz., Kamyshan A.S., Vacuum 83, 2009, p. 204-207.

Numerical simulation of low-energy ion implantation and diffusion of donor or acceptor atoms under RTA for IC design

A. Komarov[1], A. Mironov[1], G. Zayats[2], Y. Makarevich[1], S. Miskevich[1]

[1] *Institute of Applied Physics Problems, 220108 Minsk, Belarus, E-mail: elionics@bsu.by*
[2] *Institute of Mathematics, Academy of Sciences of Belarus, 11 Surganov Str., 220072 Minsk, Belarus*

One of the possible ways of achieving the necessary characteristics in ULSI field-effect transistors is the forming of shallow p-n-junctions in low-doped substrates. The basic method of creating such shallow junctions in silicon-based integrated circuits is a low-energy ion implantation and subsequent rapid thermal annealing (RTA). Such approach permits the fabrication of the devices with ultra-small transitions [1, 2]. The usage of such kind of technologies, however, leads to complex dopant profiles in the wafer. Experimental evaluation of proper technological modes is a costly and time-consuming process, which makes numerical modeling such a necessary tool. But, even latest versions of the ULSI process-simulation software do not allow predicting the resulting dopant distributions precise enough. The well-known rapid thermal annealing models very often lead to the results, which disagree with the experimental data [3].

Here we present physical and mathematical models and numerical algorithms that allow us to accurately simulate advanced technological processes of the creation of ULSI, namely low-energy ion implantation and rapid thermal annealing. Some of these models were earlier discussed in [4-6]. Recently, we have developed a software package based on these models that works in conjunction with the Silvaco ATHENA Process Simulation Framework. The developed software allows applying models and calculation methods that are alternative ones to the implemented in TCAD software products developed by Silvaco or Synopsis, mainly in solving problems with shallow depth of the impurity. The various processes including implantation of B, BF_2, P, As, Sb ions and subsequent rapid thermal annealing in silicon-based structures corresponding to the typical highly doped shallow active areas of ULSI elements were simulated using the developed software. The simulation results agree well with the experimental data obtained by secondary ion mass spectroscopy and Rutherford backscattering and display the prediction of observable experimentally anomalous phenomena.

References

[1] Ihaddadene-Le Coq L., Marcon J., Dush-Nicolini A., Masmoudi K., Ketata K.: *Diffusion simulations of boron implanted at low energy (500 eV) in crystalline silicon,* Nucl. Instrum. Meth. Phys. Res. B. 216, 2004, p. 303.

[2] Boucard F., Roger F., Chakarov I., Zhuk V., Temkin M., Montagner X., Guichard E., Mathiot D.: *A comprehensive solution for simulating ultra-shallow junctions: From high dose/low energy implant to diffusion annealing,* Mat. Sci. Eng. B 124-125, 2005, p. 409-414.

[3] Girginoudi D., Georguolas N., Thanailakis A., Polycroniadis E. A.: *Studies of ultra shallow p-n junctions formed by low-energy As-implantation,* Mat. Sci. Eng. B 114-115, 2004, p. 381-385.

[4] Komarov F.F., Mironov A.M., Zayats G.M., Tsurko V.A., Velicko O.I., Komarov A.F., Belous A.I.: *2D modelling of the diffusion of low-energy implanted arsenic in silicon at rapid thermal annealing,* Vacuum, 81, 2007, p. 1184-1187.

[5] Komarov F.F., Komarov A.F., Mironov A.M., Zayats G.M., Tsurko V.A., Velichko O.I.: *Simulation of Rapid Thermal Annealing of Low-Energy Implanted Arsenic in Silicon,* Physics and Chemistry of Solid State 8 N3, 2007, p. 494-499.

[6] Mironov A.M., Komarov F.F., Komarov A.F., Tsurko V.A., Zayats G.M., Velichko O.I.: *Modelling of low-energy-implanted phosphorus diffusion during rapid thermal processing of the semiconductor structures,* Vacuum 83, 2009, p. 127-130.

Photoluminescence induced from (As+In) implantation into crystalline Si

F. Komarov[1), L. Vlasukova[1), O. Milchanin[1), J. Zuk[2), A. Mudryi[3), K. Pyszniak[2)

[1) *Belarusian State University, 4 Nezavisimosti Ave., 220030 Minsk, Belarus*
[2) *Maria Curie-Sklodowska University, 1 Pl. M. Curie-Sklodowskiej,*
20-031 Lublin, Poland
[3) *Scientific and Practical Materials Research Center, National Academy of Sciences*
of Belarus, 17 P. Brovki Str., 220072 Minsk, Belarus

A silicon based optoelectronics progress is restrained because of the absence of effective light source. The main problem is the indirect band gap nature of silicon, resulting in inefficient light emission. A number of approaches to overcome this problem were reported including the synthesis of A^3B^5 quantum dots, or the intentional formation of structural defects in Si matrix. In this work, we report the results of structural and optical characterizations of Si layers with InAs nanocrystals ion-beam synthesized in Si. (100) and (111) Si wafers were implanted at 25 and 500°C subsequently with As (245 keV, 4.1×10^{16} cm^{-2}) and In ions (350 keV, 3.7×10^{16} cm^{-2}). Afterwards, the samples were annealed at 600, 900 and 1050°C using RTA. The depth distributions of embedded impurities and the structure-phase transformations were evaluated by means of RBS/C and TEM/TED technique. The optical properties of samples have been characterized using low-temperature photoluminescence (PL). It has been shown that an annealing of samples at 950°C results in PI spectra with dominant dislocation-related lines. An increase of annealing temperature up to 1050°C results in the appearance of a broad band in an energy range of 0.75 - 1.1 eV. This feature is ascribed to the InAs nanocrystals formation. Ion-implantation induced formation and evolution of nanocrystals and crystal defects in silicon as a function of annealing parameters are discussed.

Structure, mechanical and tribological properties of nanostructured compound coatings deposited by IBAD

F.F. Komarov[1], V.V. Pil'ko[1], A.D. Pogrebnjak[2], V.V. Pilko[1], P.V. Zhukowski[3], C. Karwat[3], K. Kiszczak[4]

[1] *Institute of Applied Physics Problems, Belarusian State University, 7 Kurchatov Str., 220108 Minsk, Belarus, E-mail: Elionics@bsu.by*
[2] *Sumy Institute for Surface Modification, POB 163, 40030, 160 Kirova Str., Sumy Ukraine*
[3] *Lublin University of Technology, 38a Nadbystrzycka Str., 20-618 Lublin, Poland*
[4] *Institute of Physics, Maria Curie-Sklodowska University, 20-031 Lublin, Poland*

Multicomponent nanostuctured coatings of TiCrN, TiSiN and TiAlN were deposited on different substrates by the method of ion-beam assisted deposition (IBAD). Atomic species sputtered from the inner surface of hollow truncated cones of different compositions were deposited on these substrates. Nitrogen and argon ions were used as a sputter source. The nitrogen ion implantation was also used to control nitrogen contents in deposited layers. AES and RBS were used to determine depth distributions of deposited elements. The structural properties were studied by means of transmission electron microscopy in both plan-view and cross-section geometry, and transmission electron diffraction. Nano- and microhardness measurements and wear tests under the scheme of the cylinder-on-plane showed that these coatings possess high physical-mechanical protective properties as well as high thermal stability. Effects of composition and regimes of deposition and nitrogen implantation on the nanostructuring and the properties of created compound coatings are discussed.

Transmission and focusing of ion beam in micro- and nanocapillaries made of insulating materials

F.F. Komarov, A.S. Kamyshan, P.A. Grishin, V.V. Pilko
Institute of Applied Physics Problems, 7 Kurchatov Str., 220108 Minsk, Belarus,
E-mail: KomarovF@bsu.by

A study of the (150 - 320) keV proton beam transmission through glass (borosilicate) tapered capillaries with different diameters of the input and output of the capillary was performed. The focusing effect was observed. The areal density of the transmitted beam is enhanced by approximately 20 times. It was shown that changing a taper angle from 0.5 deg to 1.7 deg evidences increase of the transmission coefficient more than by 300 times keeping the initial energy spectrum of ions. Charging up a face part of the capillary causes the transformation of continues ion beams to oscillating ones. The most of protons (94 - 95)% in the energy range of 150 to 320 keV transmit the capillary without energy loss.

Anodic alumina wafers with thickness of 42 µm and capillary entrance holes in a range of 60 - 70 nm and density of holes 1.2×10^{10} cm^{-2} were used, also. It was shown that FWHM of angular distributions of transmitted protons was considerably narrower than the width of the initial beam. Proton beam intensities were measured behind the sample with a thickness of 42 µm that considerable (more than one order of magnitude) exceeds range of protons in Al_2O_3. This is an evidence of an anomalous motion of protons like the hyperchanneling of charged particles in along the low-index directions of crystal lattices. The transmission coefficient in this system achieved a few percent if the face part of the sample was covered with a thin Au layer. Compared with the conventional micro-beam facilities, the usage of tapered capillaries is certainly simple and low-cost, thus providing an interesting technique of submicron RBS or PIXE elemental analyses.

Influence of supply voltage quality on harmonics generated by AC adjustable speed drives

Stanislav Kocman, Petr Orság, Pavel Svoboda

VŠB-Technical University of Ostrava, FEECS, Dept. of Electrical Engineering
15 17. Listopadu Str., 708 33 Ostrava-Poruba, Czech Republic,
E-mail: stanislav.kocman@vsb.cz

Semiconductor converters in structures of such devices as adjustable speed drives, UPS or data processing and electronics devices used in various technical applications represent sources of harmonic currents generated into the network to which they are connected. Standard AC adjustable speed drives utilize the input three phase six-pulse diode rectifier for the AC-DC conversion, so the drawn current is not harmonic, but non-harmonic with harmonics in its spectrum, and with a high level of distortion if no harmonic mitigation technique is used. Harmonic currents can have a negative impact on the network and devices connected into it. Their consequences are linked to the increase in RMS and peak values and to the frequency spectrum of voltages and currents, which can cause failures in some protective devices operations, accuracy loss of some measurement instruments, negative influences on operating of sensitive devices or their failure, current overload producing excessive overheating and leading to premature ageing or a destruction of equipment, and a degradation of network voltage. The levels of harmonics are affected by short-circuit ratio at the point of the drive coupling to the network, the used converter type and its loading, used technique for harmonics mitigation and quality of supply voltage.

The paper presents results from computer simulations and experimental measurements for several topologies of AC adjustable speed drives fitted with AC input reactor, broad-band harmonic filter and active front end rectifier (AFE) used for harmonics mitigation. Simulation models of the drive topologies have been developed using the program EMTP-ATP and tested under chosen levels of supply voltage distortion represented by the total harmonic distortion THD_v. Its influence on levels of the drive input current distortion can be seen in Fig. 1 for output frequency adjusted to 50 Hz on the frequency converter. As seen, the generated levels of harmonics are considerably reduced, especially when using broad-band filter and active front end rectifier, resulting in low levels of the total harmonic distortion THD_i of the drawn current from the network.
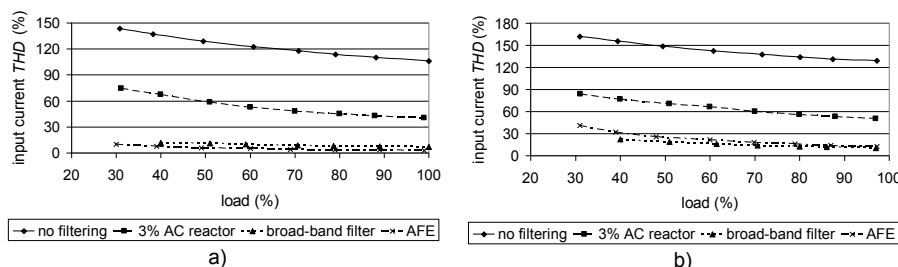
Fig. 1. Input current THD versus load: a) THD_v = 0%, b) THD_v = 4% (f_{out} = 50 Hz, simulation)

References
[1] Fuchs E.F., Masoum M.A.S.: *Power quality in power systems and electrical machines*, 2008, 638 p.
[2] Wakileh G.J.: *Power systems harmonics*, 2001, 506 p.

Co-implantation of stibium and phosphorus into silicon

P.K. Sadovski[1)], A.R. Chelyadinskii[1)], V.B. Odzaev[1)], P. Węgiereki[2)]
[1)] *Belorussian State University, Minsk, Belarus, E-mail: sadovski@bsu.by*
[2)] *Lublin University of Technology, Lublin, Poland*

The ion implantation of phosphorus is used for the formation of highly doped n-type silicon layers. Because of the mismatch of the covalent radii R of Si and P atoms (0.1175 nm and 0.11 nm, respectively) elastic tension appears at the interface between a heavily-doped layer and bulk silicon, which leads to the generation of misfit dislocations [1]. This phenomenon worsens electric characteristics of discrete semiconductor devices and integrated circuits and results in lower production efficiency [2]. The ion co-implantation of P$^+$ and Sb$^+$ (R = 0.135 nm) is expected to compensate the mismatch elastic tension in heavily-doped n-type Si layers due to their opposite influence on the silicon lattice. But the problems of impurity solubility and the crystal structure damage emerge when high implantation doses are used.

The presented work was aimed at performing the structural and electrical studies of heavily-doped silicon layers co-implanted with P$^+$ and Sb$^+$ ions at high doses. P-type silicon wafers doped with P and Sb impurities were studied with the transmission electron microscopy (TEM), the x-ray diffraction method, Hall effect measurements and the secondary ion mass-spectrometry (SIMS) method.

TEM images of silicon layers implanted with Sb$^+$ ions at E = 60 keV with the dose of 1.3·10^{15} cm^{-2} and annealed at T = 1000°C showed that Sb precipitates of 10-20 nm diameter were formed. In the case of co-implantation of P$^+$ (E = 30 keV, D = 3.1·10^{15} cm^{-2}) and Sb$^+$ (E = 60 keV, D = 1.3·10^{15} cm^{-2}), together with the precipitates of 10 - 20 nm, TEM images revealed a large number of small precipitates 3 - 5 nm in diameter. In the case of co-implantation of P and Sb atoms sheet carrier concentration appeared to be lower than that in the case of implantation of only P atoms. Analyzing the results of electrical measurements and TEM images we can conclude that the P atoms are the precipitation centers of the Sb atoms in silicon.

The absence of precipitates and complete electrical activation of implanted Sb were achieved after thermal treatment at 1200°C for 8 hours. When the electrical activation of the implanted Sb was complete there was a clear diffraction peak from the ion-doped layer indicating the increase in the lattice spacing parameter. When the Sb precipitates were formed, no significant increase in the lattice parameter of the doped layer was detected. This means that Sb precipitates contract the silicon lattice and compensate the increase of the lattice parameter due to Sb atoms at lattice sites. Silicon layers co-implanted with P and Sb were free from dislocation loops. This was due to amorphization of the layer implanted with the high dose of heavy Sb atoms.

References
[1] Khalinin V.V., Gherasimenko V.V., Stenin S.I.: *The formation of misfit dislocations during annealing of boron implanted silicon layers*, Physics of the Solid State, 18 No9, 1976, p. 2803-2805.
[2] Bonm A.J., Bernewitz L., Bohm W.R., Kopl R.: *Megaelectronvolt phosphorus implantation for bipolar devices*, IEEE Trans. Electron Dev 35, 1998, p. 1616-1619.

The evaluation of alternator technical condition on the basis of thermovision tests

Sebastian Styła
Lublin University of Technology, Department of Computer and Electrical Engineering,
Lublin, Poland, E-mail: s.styla@pollub.pl

The alternator (alternating current generator) is the basic source ensuring the electric energy supply to the battery and electric system of the car. Its power generated in course of low speed operation is sufficiently high which is important during motor vehicle operation in idling mode constituting about 40% [1] in urban traffic. The application of alternators is favourable owing to their maintenance - free operation. The scope of maintenance encompasses the following periodical checks only: fastening, cleanness and quality of cables as well as V-belt tension. Furthermore the alternators are characterized by small sizes, wide scope of speed and favourable value of power - to - weight ratio. Despite many years of their use, design and operational parameters of the alternators are continuously optimised in order to reduce their sizes and weight, to optimise the excitation and cooling circuit and to reduce the noise level [2].

The symptoms of incorrect operation in the alternators can be observed on the basis of indications of control light located on the dashboard of motor vehicle. It is the first diagnostic message informing about an inefficiency of this device. In order to enable an accurate diagnosis the following parameters should be checked: current efficiency, rectifying diodes, regulated voltage and leakage current [3]. Such tests are often carried out by means of universal meters or oscilloscope. The majority of above mentioned tests is possible without removing the alternator from the vehicle but particular care should be taken to avoid any damages of the alternator and rectifying diodes as a result of incidental short – circuit or interchange of pole terminals of the cables.

This article presents an innovatory method of testing for technical condition of an alternator consisting in the use of infrared radiation emitted by the structural elements of the generator. The tests have been performed by means of ThermaCAM E45 thermovision camera manufactured by FLIR and obtained results have been processed by means of specialized software. This diagnostic procedure is a fast and non-invasive method. Therefore an accurate analysis of the alternator condition is possible without its removal from the vehicle. Moreover it is the non-contact method eliminating the risk of generator damage in course of its tests.

The measurements accuracy was the basic criterion taken in consideration. The impact of emissivity factor [4] on this accuracy is essential in case of thermovision test. The method of determination of this impact has been presented in this article and contributed to the obtainment of reliable and repeatable results from performed tests.

References
[1] Dziubiński M., Ocioszyński J., Walusiak S.: *Elektrotechnika i Elektronika Samochodowa*, WUPL, Lublin 1999.
[2] Sęk A., Bogusz R.: *Kryteria projektowania alternatorów samochodowych*, Przegląd Elektrotechniczny 3/2011, 2011, p. 243-248.
[3] Trzeciak K.: *Diagnostyka samochodów osobowych*, WKŁ, Warszawa 2010.
[4] Wesołowski M., Niedbała R., Kucharski D.: *Wiarygodność termowizyjnych technik pomiaru temperatury*, Przegląd Elektrotechniczny 12/2009, 2009, p. 208-211.

Sensitivity of FRA measurements to various failure modes

Szymon Banaszak
West Pomeranian University of Technology, Szczecin, Poland,
E-mail: szymon.banaszak@zut.edu.pl

Frequency Response Analysis (FRA) is one of diagnostic methods of power transformers. It is based on measurements of transfer function of windings in various connection setups and allows detection of changes in mechanic or electric structure of transformer's active part. The FRA is a comparative method, therefore it is important to know how various types of defects influence changes in measured curves. Such impact of different failure modes on FRA sensitivity depends on the type of defect, its location and scale. This paper presents results of detailed experimental study performed on real transformer and based on controlled deformations of windings and simulating electric faults. Over 600 measurements were taken with different failure modes present and in various connection setups. One of directions in analysis of gathered data is finding sensitivity of FRA method in detecting given defects and finding possible information on their scale and location. At present analysis of FRA curves is clear only in the cases of healthy transformers, but when some changes appear in FRA results it is difficult to state what and where has happened. Therefore presented experiment may be helpful in further analysis of real cases of transformers.
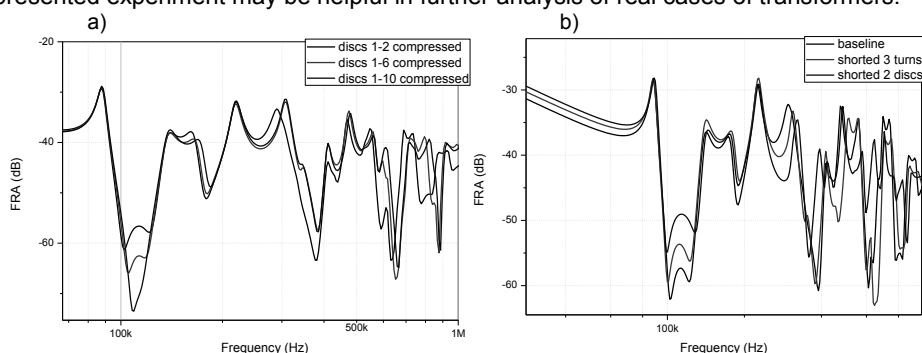
Fig. 1. Changes of FRA curves shape due to increasing deformation of HV winding in the case of two different failure modes: (a) compression of the top of the winding and (b) short circuits

The example of FRA results with different scale of the same deformation are given in Fig. 1a. Differences are clearly visible – below 500 kHz there is a change in damping and above also frequency shifts of resonances. Also in the second case (Fig. 1b) changes are clearly visible. Further analysis leads to conclusions that each type of failure mode has its specific influence on FRA results. For example at 300 kHz in the case of winding compression the curve is shifted up and also into higher frequency, while in the case of short circuits in the same region (250 kHz) change is quite contrary – curve is shifted down. The analysis of such differences may help FRA to become more valuable diagnostic tool for power transformers.

References

[1] Banaszak Sz.: *Detekcja deformacji uzwojeń transformatorów metodą analizy odpowiedzi częstotliwościowej FRA*, X Sympozjum Inżynieria Wysokich Napięć IW-2010, Będlewo, czerwiec 2010, Przegląd Elektrotechniczny 11b'2010, s. 174-177.

A contactless power supply system with bidirectional energy transfer

Cezary Worek

AGH University of Science and Technology in Krakow, Department of Electronics, Krakow, Poland, E-mail: worek@agh.edu.pl

The contactless inductive energy transmission technology has been intensively studied within the last few years [1-3]. The safety and reliability of an energy supply improve as a result of abandoning any mechanical contact, maintenance effort can also be reduced. Other advantages are: no wear and tear on the electrical contacts, no contact resistance, no spark formation and no unprotected voltage-carrying contacts [2, 3]. These features are very important in environments where gas or dust ignition hazard occurs, such as mines, fuel stations and chemical laboratories, as well as those applications where the use of direct connections is impractical, such as moving components or underwater devices. The article presents results of a project conducted at the AGH University of Science and Technology in Krakow, which aimed at creating a battery power supply with bidirectional wireless energy transfer, that is able to operate in a potentially explosive atmosphere [4]. The designed device is cost effective and allows to construct highly efficient power supply systems. In the presented solution energy is delivered from a battery in a wireless way and the battery is also charged contactlessly. This eliminates contacts both between the battery and powered device and between the battery and charger, increasing usability of the equipment, because battery can be safely exchanged in a harsh environment. The presented version is based on a series-parallel resonant converter working with medium frequency (typically 50 - 80 kHz), which consist of two inductances L1, L2 and two capacitive elements C1, C2 in main resonant circuits. To optimize the number of elements all inductive elements in power converter are realized as an integrated reactance module, and only one standard P ferromagnetic core is used. The reactance element L1, in parallel connection with the reactance element C1 constitutes the main resonant circuit in which the main portion of the whole circuit energy is stored. The integrated magnetic element concentrates the magnetic flux and transfers energy to load circuits by an insulating spacer. The air gap between the primary and the secondary coil can be in the range of several millimetres. With power supply voltage of about 7 V total energy efficiency obtained is over 70%. Control loop and data transfer between modules are also wireless. This provides reliable communication and voltage output stabilization with good dynamic characteristic under changing load parameters. The expected deployment of the designed wireless energy transfer methods, contactless batteries and chargers, capable of working in harsh underground environment will allow to develop new and innovative, highly efficient power supply solutions for the mining industry and possibly other areas of application.

References

[1] Kurs A., Moffatt R., Soljačić M.: *Simultaneous mid-range power transfer to multiple device,* Applied Physics Letters 96, 2010, 044102.

[2] Miśkiewicz R., Moradewicz A.: *Bezstykowe zasilanie komputerów przenośnych*, Przegląd Elektrotechniczny 85 3/2009, 2009, p. 8-14.

[3] Mecke R., Rathge C., Ecklebe A., Lindemann A.: *Bidirectional switches for matrix converter in contactless energy transmission systems*. EPE 2005, IJCSNS 7 No.5, 2007, p. P1-P10.

[4] Worek C., Krzak Ł., Rzepka D.*: Bezprzewodowy układ zasilania z systemem dwukierunkowego przesyłu energii przystosowany do pracy w przestrzeniach zagrożonych wybuchem,* Materiały konferencyjne XX Szkoły Eksploatacji Podziemnej, 21–25 II 2011, p. 580-588.

Using transient of pulse ionization to high vacuum measurement

Leszek Szczepaniak

Department of Automatic and Metrology, Lublin University of Technology,
38a Nadbystrzycka Str., 20-618 Lublin, Poland, E-mail: l.szczepaniak@poczta.pollub.pl

High vacuum pressure measurements are an important issue in the measurement volume for non-electric methods. One of the method is the ionization which uses thermionic emission. Unfortunately, such a vacuum gauge has many flaws and the most important is the impact of its work on pressure in measured object. Over the years, efforts were made to reduce this effect through design and materials to build more advanced ionization warheads [1]. From the electrical side is also possible to reduce adverse impact by shortening of the cathode heating time..This was the reason for the development of impulse method of measuring the pressure of high vacuum [2]. Pressure measurement was performed after reaching steady state impulse induced ion current.

During the study a new method on a properly equipped bench it turned out that it allows significant reduction of error method through reducing the impact of work of vacuum gauge on the pressure in the test chamber. Unfortunately, shortening of the cathode heating in this method reduced by the need to achieve steady-state ,in which the measurement was performed right. Further shortening the measurement time is required by its performance in transition. The first approach assumed the use of ion current intensity increment ΔI_j in time t and reference of this increase to the corresponding increase in the intensity of electron emission current ΔI_e. Then the pressure can be to try to determine from the dependence :

$$p = c_1 \frac{\Delta I_j}{\Delta I_e}$$

The problem is to adopt a current issue in transition. It could be register both the volume and then determine the appropriate gains. Unfortunately, the ion current need to register at a high potential to ground which can cause temporary displacement and a problem with the synchronous measurement of both volume. With a suitable controller parameters of the ionizing beam, which provides a stable time-value of the ion current it may be preferable from the calculations using a constant set of electron emission current. Increase the intensity of ion current in the proposed method was introduced to determine the slope of the tangent line to the course of ion current. Left designation of constant vacuum gauge operating in such conditions and to examine whether or not the change depending on the conditions of measurement.

$$p = c_p \frac{a_{lj}}{I_{\text{eust}}}$$

Appointment of a constant value c_p and verification if it does not affect the measurement conditions was conducted experimentally. The new method has allowed further shortening of the time pressure measurement of high vacuum using a ionization pulse. This gave the reduction of the impact of vacuum gauge work on pressure value in a test object which reduces the error of the method. An interesting issue is the math to determine the coefficient c_p. This requires creating a working model of pulse ionization vacuum gauge. This may be a basis for further research.

References
[1] Watanabe F.: *Bent belt-beam gauge: Extending low-pressure measurement limits in a hot-cathode ionization vacuum gauge by combining multiple methods*, J. Vac. Sci. Technol. A 28, 2010, p. 486.
[2] Szczepaniak L.: *Pomiar ciśnienia wysokiej próżni z wykorzystaniem impulsowej jonizacji gazu strumieniem elektronów*, Przegląd Elektrotechniczny 4/2009, 2009.

Configuration of electrodes in the setup for nanosecond discharges

Jerzy Pomianowski

West Pomeranian University of Technology, Department of Electrotechnology and Diagnostics, Szczecin, Poland, E-mail: jpomianowski@zut.edu.pl

The setup has been constructed for nanosecond discharges between flat electrodes 7.5 cm long. When the energy of discharge exceeded threshold value the emission of coherent light appeared having wave length 337.1 nm. The distance between electrodes has been changed to acquire dependency of threshold voltage from spark gap size. It was found that threshold voltage of laser action grew with longer gap. On the other side, increasing capacitances of capacitors in power supply resulted in lowering the value of voltage necessary to initiate the emission.

Fig. 1 shows dependency of threshold voltage of coherent light emission from the width of gap between electrodes in the case of using capacitors 4.4 nF.

in tested nitrogen laser type TEA
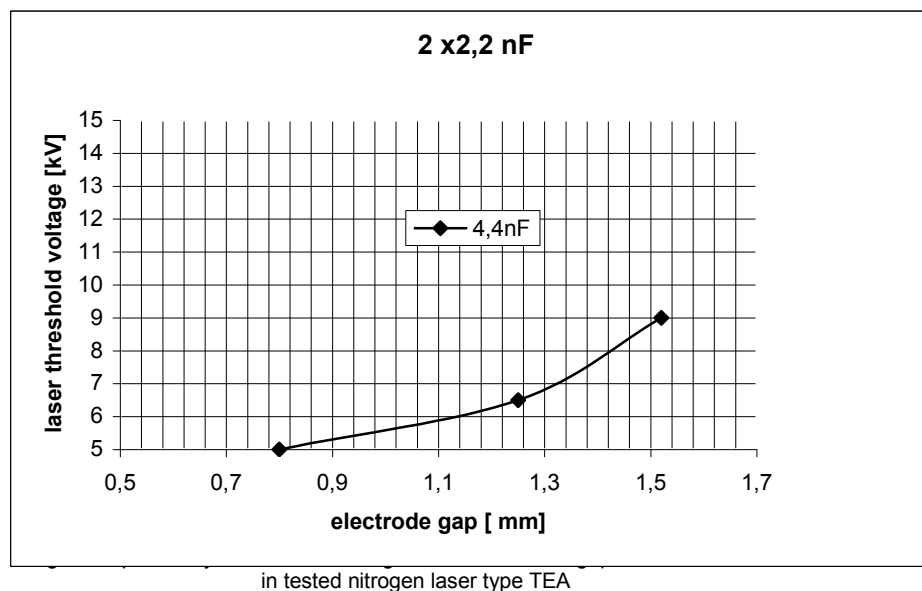
Modified chemically-hardened resins in electrical engineering

Jan Bursa, Jerzy Pomianowski
*West Pomeranian University of Technology, Department of Electrotechnology
|and Diagnostics, Szczecin, Poland, E-mail: bursa@zut.edu.pl*

Introduction

Epoxy resins hardened in room temperature are still often used in electrical insulation, regardless significant disadvantages such as: low mechanical strength of products without fillers, highly exothermic hardening process which makes difficult to prepare amounts of material larger than 200 g, high viscosity making difficult mixing with filler and necessity of degassing. The aim of this research was to check the possibility of replacing in electroinsulating products epoxy resin with polyurethane resin. The resin used for experiment was Topcast 60 L, having low viscosity and ability to self degassing.

Experiment

The first stage was to prepare test casts of both types of resins and measure their basic electrical parameters. Table 1 shows results of preliminary tests.

Table 1. Properties of non-modified resins

Tested property	Epidian 6D	Topcast 60 L
Mass change, %; after 22 days of WGS	1,8	2,5
Volume resistivity, Ωm	$4,48 \cdot 10^{12}$	$4,79 \cdot 10^{12}$
Permittivity	8,1718	4,32
Dielectric losses coefficient	0,0045	0,0028
Dielectric strength, kV/mm	27,1	19,5
PTI, V	500	500
Resistance to electric arc, s	155	123

In the following research the technology of preparing electroinsulating material was elaborated and described. The material is based on polyurethane or epoxy resin with fillers such as alumina and glass microgranules. The influence of fillers on the structure and properties of tested materials have been presented. Prepared samples were aged for seven weeks. In the experimental part there were presented properties changes of tested material with influence of climate conditions and electric parameters measurements. The last part of thesis contains conclusions and analysis of applicability of both resins in the field of high voltage insulation.

Measuring methods and an analysis of electrical measurements performed at cathode protection stations with the application of modern telemetric systems

**Janusz Partyka[1), Mirosław Mazur[2)

[1) *Faculty of Electrical Engineering and Computer Science, Lublin University of Technology, 38A Nadbystrzycka Str., Lublin, Poland*
[2) *Carpathian Gas Company in Tarnow, Branch Gas Plant in Lublin, 15 Diamentowa Str., Lublin, Poland, E-mail: mirekpolon@gmail.com*

The presented corrosion protection method consists in shifting the potential of corroding steel to considerably lower values when it exhibits corrosion-resistant properties. The potential change can be obtained by implementing an electrode to the system. In our case it has been a carbon electrode but it can also be made of lead, platinum or nickel. External polarization of such a cell by electric current of adequate intensity causes polarization of the steel electrode up to its protective potential. In that case it is cathode protection as the protected metal is a cathode. Apart from a few noble metals such as gold or platinum most of useful metals in their natural state occur in the form of minerals or oxides that have to be processed (decomposition, reduction), which destroys their natural equilibrium. A system for monitoring cathode protection station parameters has been developed with the application of dedicated measuring apparatus, industrial modems operating within the GSM/GPRS network and a computer (PC or a laptop). Additionally, the system can be supervised with the use of a PC equipped with a specialized software that real-time records measuring data and stores them in its memory. When performing measurements at cathode protection stations it is important for correct evaluation of the measurement data to constantly control electric parameters. They are essential especially in the case when the controlled system is of a dissipated character and includes a considerable number of devices that are located far away from one another. Cyclical checking of objects by qualified employees entails high costs and delays in detecting possible damages or malfunctions of the controlled devices. Installation of an efficient system for remote control and monitoring of individual stations reduces the costs and makes possible to currently obtain data that are important from the viewpoint of correct and efficient operation of the whole corrosion-protection system for steel pipelines and underground containers. Until only a few years ago radio communication has been used as a medium for remote transmission of information within such control systems. Presently, it is a modern GSM/GPRS platform that has been applied for that purpose because of its developed infrastructure and less expensive modems. Correct interpretation of the received measuring data is very important. The presented article focuses on measurements performed on operating devices where the cathode protection has been applied. It has been found that the application of cathode protection contributes to the corrosion rate reduction by over 25 times.

References
[1] Budnik K., Czarnywojtek P., Kozłowski J., Machczyński W.: *Komputerowa rejestracja i analiza sygnałów w technice korelacyjnej badania prądów błądzących*, VII Krajowa Konferencja Pomiary korozyjne w ochronie elektrochemicznej, Jurata, 18-20.09. 2002.
[2] http://automatykab2b.pl/katalog-produktow/produkt/1813-mt-101-sterownik-plc-z-integralnym-modemem-gsm-ghrs.
[3] Michałowski S.W.: *Rurociągi dalekiego zasięgu*, Odysseum, Warszawa, 2005.

Practical applications of electrical and computer technologies to the intelligent building control

Janusz Partyka[1)], Mirosław Mazur[2)]

[1)] *Faculty of Electrical Engineering and Computer Science, Lublin University of Technology, 38A Nadbystrzycka Str., Lublin, Poland*
[2)] *University of Economics and Innovation in Lublin, 7/9 Mełgiewska Str., Lublin, Poland,*
E-mail: mirekpolon@gmail.com

Automatic control systems in intelligent buildings aside with offering its inhabitants a sense of optimal comfort and safety also minimize consumption of electric and thermal energy and make possible to real-time control and monitor all electrical devices as well as individual systems in the building. Within the presented project a simple alarm control panel (specifically – a Satel Integra 128 panel) has been implemented for automatic and remote control of electrical equipment in the building. Household automatic control systems are rather expensive and therefore not widely available. Their cost follows from the application of adequate systems dedicated by their manufacturers. Our solution consists in implementing a variety of devices made by various manufacturers to perform tasks programmed or remotely programmable with the use of widely available components made by all the manufacturers. A cell phone and a mobile device with an access to a LAN or WLAN network have been applied to demonstrate a communication method used to control the panel. It is meant to be an open system i.e. a system whose automatic control installation can be developed and new equipment made by independent manufacturers can be connected to it as well as new operator stations and communication interfaces of determined standards. Usually the term ―intelligent building‖ is associated with an image of modern office buildings, which narrows the usage range of that terminology. It has been statistically shown that only 14% of ―intelligent‖ objects are office buildings and malls, while over 29% of the objects are industrial establishments like production plants, steel works or power stations. Industrial objects are of specific character. They often are located over a large area and include buildings used for various purposes. It has been observed that private persons get ever more interested in intelligent building systems. Considering a development rate of the useful electronics sector and the quantity of household appliances together with their energy consumption determined based on the realized investments it can be stated that the term ―intelligent building‖ enters every household nook. The article presents profitability calculations that demonstrate on real-time examples how a system of an intelligent building influences running costs of a building and show advantages that follow from automation of the processes. Profits obtained owing to the application of relatively simple and inexpensive systems to automate functions of electric and thermal energy loads of a standard household have been shown based on the calculation results

References
[1] Hołubowicz W., Płóciennik P.: *GSM – Cyfrowy system telefonii komórkowej*, Poznańska Drukarnia Naukowa, 1997.
[2] Niezabitowska E.: *Budynek inteligentny – Tom I Potrzeby użytkownika a standard budynku inteligentnego*, Gliwice, PWŚ, 2005.
[3] Niestępski S.: *Instalacje elektryczne: budowa projektowanie i eksploatacja*, Warszawa, OWPW, 2005.
[4] Sroczan E.: *Nowoczesne wyposażenie techniczne domu jednorodzinnego*, PKT, 2006.
[5] http//www.satel.pl.

Solar energy applied to feed electrical appliances in a standard household

Janusz Partyka[1), Mirosław Mazur[2)
[1) *Faculty of Electrical Engineering and Computer Science, Lublin University of Technology, 38A Nadbystrzycka Str., Lublin, Poland*
[2) *University of Economics and Innovation in Lublin, 7/9 Mełgiewska Str., Lublin, Poland,*
E-mail: mirekpolon@gmail.com

The sun makes an inexhaustible source of pure energy that can be taken advantage of by the application of photovoltaic modules. Photovoltaic systems can operate independently of power networks or expensive energy carriers. They can generate electric energy at varied weather conditions, also on cloudy days. Solar energy is free and makes an unlimited widely occurring source of energy available at various values of radiation intensity. In Poland, intensity of solar radiation varies depending on a region and ranges from 1 to 1.20 kWh/m^2. Owing to recently elaborated new technologies the amount of silicon required to produce a module of a determined power value is by 7-10 times smaller than that of a few years ago. Additionally, cells produced that way exhibit higher efficiency that can reach 22% and it seems that even higher values can be obtained with the application of high-quality monocrystals of silicon and refined processing. Owing to the mentioned developments the expense of battery purchase can get recouped in 2 years and not in 5 years as it was in the case of previously produced cells. The presented paper focuses on practical applications of photovoltaic cells and the related equipment with the purpose of meeting energy needs of a standard household by a helioelectric method that consists in a direct conversion of solar radiation energy to electric energy. Calculations of installation costs and depreciation time have been presented as well as advantages of photovoltaic cell application as compared to similar alternative energy sources. Efficiency of selected cells and methods for the generated energy conversion together with the conversion-related costs have been assessed from the viewpoint of reaching the highest watt-hour efficiency. Testing has been performed in a standard household in order to obtain reliable results. Solar energy finds ever greater number of applications, which at the time of growing prices for fossil fuels and wide-spread public apprehension for nuclear power plants, places it among important alternative and ecological sources of energy.

References
[1] Smoliński S.: *Fotowoltaiczne źródła energii i ich zastosowania*, Wyd. SGGW, Warszawa 1998.
[2] Pluta Z.: *Słoneczne instalacje energetyczne*, PW Warszawa 2003.
[3] Lewandowski W.M.: *Proekologiczne źródła energii odnawialnej*, WNT, Warszawa 2002.
[4] Centrum Fotowoltaiki Politechniki Warszawskiej, www.pv.pl.
[5] http://odnawialna.w.interia.pl.
[6] http://www.univ.rzeszow.pl/studenci/KNF/dokumenty/fotowoltaika.pdf.

The technological scheme of firm and superfirm materials workpieces sawing by transferring periodic circular movement to a workpiece

Darya A. Yamnaya, Michail G. Kiselyov
Belarusian National Technical University, Minsk, Belarus, E-mail: darya_echo@mail.ru

The technological operation of mechanical sawing of workpieces from firm and superfirm nonmetallic materials, including diamond monocrystals, finds wide application in many industries: in optic and electronic instrument-making, in tool and jewelry manufacture.

Despite the development of some new methods of diamond monocrystals separating (such as laser, electroerosive, electronic beam separating), due to maintenance of high percentage of yield, the method of mechanical sawing still finds wide application. However, it has certain drawbacks connected with low productivity of the process and insufficiently high quality of table surfaces of sawn workpieces. Therefore the attention of scientists and experts is directed to improvement of mechanical sawing of diamond monocrystals for the purpose of eliminating specified drawbacks.

In our research the industrial sawing unit of the machine tool SHP-2 applied to separate diamond monocrystals into parts (semifinished products) is used. This unit is equipped with special vibrotransmission which transfers periodic circular two-dimensional movement to a workpiece (Fig. 1).
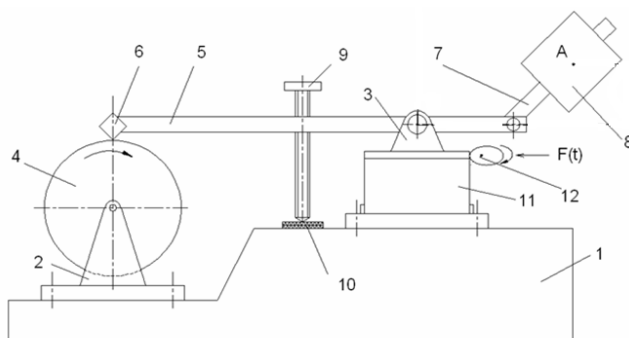
Fig. 1. The diagram of sawing unit providing periodic circular movement to the workpiece
1 – massive cast-iron plate; 2, 3 – front and back racks; 4 – sawing disk; 5 – lever (arrow); 6 – workpiece; 7 – rotary lever; 8 – weight; 9 – adjusting screw; 10 – rubber lining; 11 – flat springs; 12 – mechanical vibrator

The basic difference between the given sawing unit and the traditional one is in the fact that the arrow swing block (a pair of racks 3) is mounted on flat springs 11 forming the parallelogram suspension, which allows for the arrow swing axis movement along the horizontal direction.

It is experimentally proved that it is possible to significantly (from 2.5 to 3.5 times) raise intensity of sawing of the workpiece and to provide significant decrease (from 1.9 to 3 times) in roughness values of the parameter R_a of the processed surface in comparison with the values received in traditional operating conditions by transferring periodic two-dimensional circular movement to the workpiece with a trajectory similar to an ellipse. Thus with an increase in hardness of the processed material, the efficiency of influence of this movement on increase in sawing intensity and quality of the table surface of sawn workpieces is increased, which is a manifestation of promising use of the suggested method of processing to intensify diamond monocrystals sawing.

The reliability of aircraft propulsion unit control systems

Mariusz Duk, Katarzyna Sobańska
Lublin University of Technology, 38a Nadbystrzycka Str., 20-618 Lublin, Poland,
E-mail: m.duk@pollub.pl

The paper focuses on the special features of the construction requirements towards an aircraft engine control system and describes two examples of the developed control systems.

The first example deals with a fuel injection installation in a powerful aircraft engine K9-E, and the second one shows an all-function control system (injection, ignition) in an multifuel aircraft engine of 200 kW.

Efficiency determination of inverter-fed induction motor for low power applications

Petr Orság, Stanislav Kocman, Jan Unger

VŠB-Technical University of Ostrava, FEECS, Dept. of Electrical Engineering
15 17. Listopadu Str., 708 33 Ostrava-Poruba, Czech Republic,
E-mail: petr.orsag@vsb.cz

More and more public attention is now being focused on reducing energy consumption. New energy efficiency legislation has been drawn up in the EU in recent years to protect our environment with an impact on the design of new induction motors as well. It established mandatory minimum efficiency levels of induction motors for low power applications, which are going to come into force this year. The legislative changes have also caused modification of IEC standard methods for determining electrical machine efficiency to be consistent with the majority of the standards of the world. Energy savings make variable-frequency drives equipped by an inverter-fed induction motor possible as well. The efficiency testing methods for these types of drives are not standardized.

The paper presents the measurement results of the efficiency of a squirrel cage induction motor with the rated motor power of 4 kW in the new high efficiency class IE2 based on the direct measurement of the electrical input power and the mechanical output power. The motor was fed by both a programmable three-phase AC power source and a frequency converter. For comparison, different levels of the harmonic voltage distortion at the rated 50 Hz supply frequency and next chosen frequencies corresponding with the same output converter frequencies were adjusted by the AC source. The influence of harmonics on the drive efficiency was assessed on the base decomposing non-sinusoidal voltage and current waveforms into the fundamental and harmonic components. The measured results of motor efficiency were compared to results from computer simulations using T-model of the induction motor. The example is in Fig. 1.
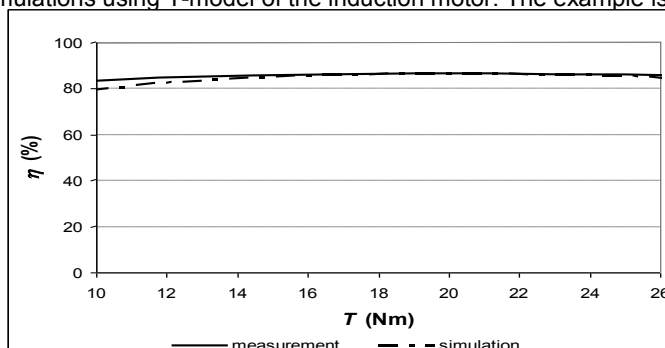
Fig. 1. Comparison of measured and simulated efficiencies versus load (THD_v = 0%, f_{out} = 50 Hz)

References
[1] How do you take the first step towards to an energy efficient future?, Siemens AG 2010.
[2] IEC 60034-2-1:2007, Rotating electrical machines – Part 2-1: Standard methods for determining losses and efficiency from tests (excluding machines for traction vehicles).
[3] Boglietti A., Bojoi R., Cavagnino A., Tenconi A.: *Efficiency Analysis of PWM Inverter Fed Three-Phase and Dual Three-Phase High Frequency Induction Machines for Low-Medium Power Applications*, IEEE Transactions on Industrial Electronics 50 No.5, 2008.

Neurocomputing of Inverse Problem approximated by Boundary Element Method

Krzysztof Król[1), Jan Sikora[1), 2)
[1) *Department of Electronics, Lublin University of Technology, Lublin, Poland,*
E-mail: k.krol@pollub.pl
[2) *Electrotechnical Institute, Warsaw, Poland*

This paper aims to develop methods to resolve the inverse problem in two-dimensional impedance tomography-based on neural approach. For this purpose, a model was created. From this model we obtained data which were used for neural network learning. The network is designed to detect change the size of the inner area, and its location.

Detection of the size and position of one area inner another is very important. The identification of this type is used to detect cases of various types of tumors, a stroke in infants. Identifying whether a tumor or a stroke does not increase, or not move.

For the solutions we created a model of the child's head, with the additional area simulating a stroke. Based on the model are calculated data, which were used for neural network learning.

References

[1] Filipowicz St.F., Rymarczyk T.: *Tomografia impedancyjna – pomiary, konstrukcje i metody tworzenia obrazu*, BEL Studio, Warszawa, 2004.
[2] Sikora J.: *Boundary Elelent Method for Impedance and Optical Tomography*, Wydawnictwa Politechniki Warszawskiej, 2007.
[3] Jabłoński P.: *Metoda elementów brzegowych w analizie pola elektromagnetycznego*, Wydawnictwo Politechniki Częstochowskiej, 2003.
[4] Brebbia C.A., Walker S.: *Boundary element techniques in engineering*, London-Boston, Newnes-Butterworth, 1980.
[5] Aliabadi M.H.: *The Boundary Element Method: Vol. 2 Applications in Solids and Structures*, WileyBlackwell, 2002.
[6] Osowski S.: Sieci neuronowe w ujęciu algorytmicznym, WNT, Warszawa, 1996.

NEET 2011

Analysis of biomass and pulverized coal co-combustion using curvelet transform

Waldemar Wójcik, Andrzej Kotyra, Tomasz Ławicki
Lublin University of Technology, Department of Electronics, Lublin, Poland,
E-mail: t.lawicki@pollub.pl

In Poland, coal combustion is the main source of energy. According to the current EU regulations, polish commercial energy producers are obliged to reduce pollutants' emissions such as nitride and sulfur oxides (NO_x, SO_x) to appropriate levels. Moreover, the regulations also impose that specific amounts of energy should be obtained from renewable fuels. Biomass co-combustion, among others means, plays an important role the more the existing combustion installation could be utilized.

Low-emission coal combustion techniques as well as coal and biomass co-combustion belong to primary methods of narrowing emission of harmful substances [1]. However, adding biomass to pulverized coal may lead to unstable state of the combustion process. For the flame is original and the fastest possible source of combustion process information, a number of image processing techniques can be utilized in detection of such a state [2].

The article describes application of curvelet transform of flame images that were captured during several combustion tests at Institute of Power Engineering, Warsaw. As opposed to Fourier or wavelet transforms, curvelet transform provides information of edge orientation within image being analyzed [3]. The combustion testes were made for different amounts of biomass that were added to pulverized coal. Flame images were obtained by a dedicated visual system.

References
[1] Wójcik W., Kotyra A., Golec T., Gromaszek K.: *Vision based monitoring of coal flames,* Przegląd Elektrotechniczny 3, 2008, p. 241-244.
[2] Yan Y., Lu G., Colechin M.: *Monitoring and characterization of pulverized coal flames using digital imaging techniques,* Fuel 81, 2002, p. 647-655.
[3] Candès E.J., Demanet L., Donoho D.L., Ying L.: *Fast discrete curvelet transforms*, Multiscale Model. Simul. 5, 2005, p. 861-899.

The principles of thermal optimization of carbon materials for electrochemical capacitors

I.M. Bydzulyak, B.I. Rachiy, R.I. Merena
Vasyl Stefanyk PreCarpathian National University, Ivano-Frankivsk, Ukraine,
E-mail: bogdan_rachiy@ukr.net

Interaction of carbon-containing raw materials with different oxidizing agents (carbon dioxide, water steam, etc.) at high temperatures (1000 - 1300 K) allows obtaining activated carbon with a porous structure and large specific surface area. The control of the thermo-chemical processes during carbon activation is very important, which becomes especially significant in the activated carbon obtaining for the electrodes of electrochemical capacitors (EC).

Researched porous carbon materials (PCM) was obtained in several stages, which consisted in the carbonization of raw materials in the reactor in an atmosphere of water steam, chemical washing from mineral additives and sol in concentrated hydrochloric acid, flushing in distilled water to neutral pH, washing in 30% nitric acid and flushing in distilled water to neutral pH [1]. Washed thus activated carbon has been dried and heat treatment has been performed in the temperature range of 573 - 873 K for disclosure of internal porosity and formation of new pores. Due to a thermal activation there are change and development of carbon porous structure: increasing of the pores size, fusion of two or more pores into one, part of micropores due to the growth becomes mesopores, changing of pore surface and volume, which is connected with the burning of organic material and removing of the resin.

It was found that the maximal specific capacity of EC is reached at the use of carbonized carbon obtained at 1173 K, which has been thermally modified at the temperature of 673 K.

Analysis of adsorption isotherms of these materials makes it possible to identify specific surface area, total pore volume and pore size distribution for porous carbon materials (Table 1). These data suggest that high-temperature treatment can serve as an effective tool for modifying the porosity of carbon.

Table 1. Structural-adsorption characteristics of PCM

Sample	Time of thermal treatment, min	Specific surface area, m^2/g	The square of micropores, cm^2/g	Total pore volume, cm^3/g	Micropore volume, cm^3/g
PCM	0	318	265	0.168	0.103
PCM 1	90	681	616	0.332	0.247
PCM 2	120	696	619	0.351	0.252
PCM 3	150	725	655	0.362	0.266
PCM 4	180	799	722	0.418	0.297

References
[1] Ostafiychuk B.K., Budzulyak I.M., Merena R.I., Rachiy B.I., Magometa O.D.: *Influencing of chemical treatment is on property of the activated carbon materials*, Physics and chemistry of solid state 9 №3, 2008, p. 609-612.

Influence of medium heterogeneity on measurement accuracy in absorption spectroscopy

Paweł Komada, Sławomir Cięszczyk, Waldemar Wójcik
Lublin University of Technology, Department of Electronics, Lublin, Poland,
E-mail: p.komada@pollub.pl

Correct leading of combustion process in a power boiler needs many diagnostic information [1, 6]. One of them is composition of gas mixture on different places on power boiler [4, 5]. Such a measurements could often be done using various optical methods [2, 3]. Among others, absorption spectroscopy is one of the commonly used method. It is characterized by high measurement rate and no interference with environment to be measured.

Absorption spectroscopy measurements assume that laser radiation goes along the measurement path across homogeneous environment. It's assumed that gas concentration as well as pressure and temperature have constant values within the measurement path. This assumption can be correct, but only in laboratory measurements when a sample was prepared in a proper way and the measurement path is short. On the other hand, testing a gas mixture in a power boiler involves use of long measurement path, for example running a cross boiler. A number of research, such as for instance [4] point out that distribution of temperature and gas concentration is not homogeneous. Therefore, concentration measurements done by absorption spectroscopy method are averaged. Question arises how results of such a measurement and real values differ from each other.

In this article, some results of simulations were presented, that permit assessing the influence of environment non-homogeneity on results of spectroscopy measurements. A number of cases were examined for which temperature distribution in the measurement path will be like within a real power boiler.

References

[1] Ebert V., Fernholz T., Giesemann C., Pitz H., Teichert H., Wolfrum J., Jaritz H.: *Simultaneous Diode-Laser-Based In-situ-Detection of Multiple Species and Temperature in a Gas-fired Power-Plant*, 28th Int. Symposium on Combustion, University of Edinburgh, Edinburgh, Scotland, 2000.

[2] Hanson R. K., Jeffries J. B., Zhou Xin, Liu Xiang, Li Hejie, Mattison D., Klingbeil A.: GCEP Technical Report: Smart Sensors for Advanced Combustion Systems, 2005.

[3] Jenkins T.P., Bergmans J.L., DeBarber P.A., Coffey M.R., Starnes G.M.C.: *In Situ Measurements of Temperature in a Coal-Fired Power Plant Using Tunable Diode Laser Absorption Spectroscopy*, AFRC/JFRC 2004 Joint International Symposium, Maui, 2004.

[4] Kruczek H.: *Przydatność pomiaru warstwy przyściennej do oceny stopnia zagrożenia korozją wysokotemperaturową (niskotlenową)*, Energetyka 7/2002, 2002, s. 419-427.

[5] Wójcik W., Cięszczyk S., Komada P.: *Wyznaczanie informacji z pomiarów spektralnych jako zagadnienie odwrotne*, Przegląd Elektrotechniczny 10/2010, 2010, s. 13-16.

[6] Wójcik W., Komada P., Firago V., Manak I.: *Pomiar stężenia CO z wykorzystaniem metod TDLAS w bliskiej podczerwieni*, Przegląd Elektrotechniczny 3/2008, 2008, s. 238-240.

Remote measurements of selected vital functions

Wojciech Surtel
Lublin University of Technology, Department of Electronics, Lublin, Poland,
E-mail: w.surtel@pollub.pl

Huge technology development especially evident in electronics, computer science, telecommunication, as well as medicine have initiated a new field of knowledge called telemedicine. Availability of modern nano-sensors and low-power highly effective microprocessors allows new approach to patients' tele-diagnostics and tele-monitoring. It assumes integration of sensors allowing non-invasive remote mobile measurements |of vital functions.

Mobile recorder is a device for patient monitoring, containing a pre-processing unit that allows mating sensors allowing measurements of vital signals as: pulse, blood pressure, temperature as well as other, adjusted to the actual disease entity e.g. blood glucose level in hypoglycaemia. The primary purpose of the device is signal processing and further data analysis. Additionally, the recorder should be compatible with data transmission system for the sake of sending patient's data to the Patient Monitoring Station. Moreover, it should provide bidirectional communication between doctor and patient. The device may also be equipped with a GPS module providing patients localization together with a set of additional sensors e.g. acceleration or location sensors, allowing tracking the patients behaviour for determining his state of consciousness. The figure below shows the simplified model of teleinformatic system indicating the placement of patient wireless recorder within the system. Patient data may be archived in the flash memory card or in the Home Station. Defining threshold indicators and values allows sending information about alarming patient status. In the opposite case only daily report of a patient status is sent to the Patient Monitoring Station.

The proposed solution is designed for medical diagnostics of persons who do not require hospitalisation. The developed recorder model together with proposed design of telemedicine system allow elaboration of electronic remote patient monitoring procedures.

References
[1] Gazit E.: *Self-assembled peptide nanostructures: the design of molecular building blocks and their technological utilization*, Chem Soc Rev. 36 (8), 2007, p. 1263-1269.
[2] Grossman P.: *The LifeShirt: a multi-function ambulatory system monitoring health, disease, and medical intervention in the real world*, Stud Health Technol Inform. 108, 2004, p. 133-141.
[3] Łoziak K., Sikora M., Dańda J., Watza R.: *Access techniques to the telemedical multimedia resources*, Workshop on Multimedia Communications and Services MCS'03, Proceedings of the international conference : Kielce, 23–25 April 2003, p. 77-80.
[4] Hasko R.T., Hotra O.: *Modelling and macromodelling of biomedical dynamical systems in ELCAB envoronment using ELBASIC build-in language interprefer*, 6. Proceedings of the International Conference TCSET'2006 "Modern problems of Radio engineering Telecommunication and Computer Science", Lviv-Slavske, 28 Febr.-4 March, 2006, p. 651-652.

Rapid heat treatment of TiN/Ti/Si system

P. Zhukowski[1], C. Karwat[1], V.V. Kolos[2], M.I. Markevich[3],
V.F. Stelmah[4], A.M. Chaplanov[3]

[1] *Lublin University of Technology, Department of Electrical Devices and H.V. Technology, 38a Nadbystrzycka Str., 20-618 Lublin, Poland,*
E-mail: pawel@elektron.pol.lublin.pl
[2] *Research-and-Production Association "Integral", 1 Kazinets Square, Minsk, Belarus*
[3] *Physical-Technical Institute of National Academy of Sciences of Belarus, 10 Kuprevich Str., 220141, Minsk, Belarus*
[4] *Belarussian State University, 5 Bobruyskaya Str., Minsk, Belarus*

The progress of microelectronics requires further development of stable and high-grade layers of titanium disilicide and of some other silicides for use in conductive lines and contacts of large-scale integrated circuits (LSIC).

One of the important research guidelines of solid-state physics is the development of new methods intended to synthesize advanced materials with desired structure-sensitive properties. The rapid heat treatment (RHT) appears to be a promising method for performing researches in the area of up-to-date materials science.

The establishment of material properties as well as of the effect of RHT parameters on the process of structure formation can make some technological processes easier and result in a substantial increase in quality of synthesized materials.

The investigation of the effect of dopant impurities on course of titanium silicide formation and revealing the distinctive features of titanium disilicide synthesizing under the layer of a specially grown titanium nitride layer is of interest for microelectronics as a significant and actual problem from both academic and industrial viewpoints.

The heat treatment of heterostructures in diffusion furnaces has found a limited use for fabrication of LSIC. As regards the fabrication of bipolar circuits only the method of rapid heat treatment ensures obtaining the high electric conductivity of doped layers and formation of shallow p-n junctions.

The work is aimed at elaboration of physical principles underlying the technology of formation of photosensitive $TiSi_2$(C49)/Si systems with controllable parameters on the basis of regularities established in the process of rapid heat treatment of the TiN/Ti/Si heterostructure.

The wafers of single-crystal KDB-12 silicon of (001) orientation were used as initial substrates. The wafers were implanted with $5 \cdot 10^{15}$ cm^{-2} doze of arsenic at the implantation energy of 80 keV.

The successive deposition of titanium and titanium nitride films was carried out on the Varian m2i system using the method of magnetron sputtering during a single vacuum cycle with subsequent rapid heat treatment that has been conducted on the Heat Pulse 8108 setup by means of halogen lamps.

In this work the investigation was made of the treatment temperature effect on surface resistance of formed structures after rapid heat treatment of the TiN/Ti/Si system in which silicon was doped by arsenic ions.

The analysis of experimental data indicates that temperature of heat treatment of the TiN/Ti/Si system in the range of 580°C to 600°C affects the titanium silicide formation and decreases the surface resistance to the value of 27.2 Ω/□. The decrease of surface resistance to this value is associated with lowering the concentration of crystal structure defects as well as with recrystallization processes and formation of silicide phases.

Tuning characteristics of coaxial microwave plasma generator operated with argon, nitrogen and methane at atmospheric pressure

Bartosz Hrycak[1), Dariusz Czylkowski[1), Mariusz Jasiński[1), Jerzy Mizeraczyk[1), 2)
[1) *Centre for Plasma and Laser Engineering, The Szewalski Institute of Fluid-Flow Machinery, Polish Academy of Sciences, 14 Fiszera Str., 80-952 Gdańsk, Poland, E-mail: bhrycak@imp.gda.pl*
[2) *Dept. of Marine Electronics, Gdynia Maritime University, 81-87 Morska Str., 81-225 Gdynia, Poland*

Recently, microwave plasma sources (MPSs) operated at atmospheric pressure have been developed. Such devices were used in spectroscopy, technological processes like surface treatment, carbon nanotubes synthesis and sterilization. They also found applications in the processing of various gases. Destruction of Freon HFC-134a [1] and production of hydrogen via methane conversion [2] in atmospheric pressure microwave plasmas were reported lately. We present results of experimental investigations with a new, coaxial-type, 2.45 GHz microwave plasma source (MPS) operated at atmospheric pressure gases at high gas flow rates.

The main parts of the experimental setup were: microwave generator (2.45 GHz and maximal power 6 kW), rectangular waveguide (WR-430) as a feeding line, directional coupler equipped with heads and double channel power meter, coaxial-type MPS terminated with movable plunger, gas supplying and measuring system. The microwave power P_A absorbed by the plasma was determined from (P_I - P_R), where P_I and P_R are the incident and reflected microwave powers, respectively.

The generator was based on a standard WR-430 rectangular waveguide with a section of reduced-height, preceded and followed by tapered sections. The plasma in a form of a flame was generated on the end of a cylindrical electrode which penetrated microwave plasma generator through circular gaps on the axis of the waveguide wide wall and protruded below bottom waveguide wall. The flame was enclosed in a quartz tube surrounded by cylindrical metal shield with gap for visualization. Nitrogen swirl flow (50 l/min) was used as a additional for cooling the quartz tube. The working gas was flowing through the internal electrode with the flow rates between 50 l/min and 200 l/min for argon and nitrogen and 87.5 l/min and 175 l/min for methane. The microwave power level was from 600 W up to 5600 W.

At optimal positions of movable plunger, the use of argon, nitrogen and methane as the working gases caused, that 1 - 2 %, 1 - 4 % and 5 - 18 % of the incident power was reflected, respectively according to discharge conditions. The length of the plasmas were 50 - 150 mm, 30 - 130 mm and 20 - 90 mm for argon, nitrogen and methane as the working gases, respectively.

The investigated waveguide-based coaxial-type MPS works very stable with various working gases. That makes it attractive tool for different gas processing at high flow rates.

References
[1] Jasiński M., Dors M., Mizeraczyk J.: *Destruction of Freon HFC-134a Using a Nozzleless Microwave Plasma Source*, Plasma Chemistry and Plasma Processing 29, 2009, pp. 363-372.
[2] Jasiński M., Dors M., Mizeraczyk J.: *Applications of Atmospheric Pressure Microwave Plasma Source for Production of Hydrogen via Methane Reforming*, The European Physical Journal D 54, 2009, p. 179-183.

Spark discharge in water for bacteria inactivation

Tomasz Izdebski, Mirosław Dors, Jerzy Mizeraczyk
The Szewalski Institute of Fluid-Flow Machinery, Polish Academy of Sciences,
14 Fiszera Str., 80-952 Gdańsk, Poland, E-mail: tizdebski@imp.gda.pl

In this paper an investigation of spark plasma discharge in water for bacteria inactivation is presented The water samples was taken from Strzyża river, which is a type IV-sanitary class in Poland, and has a very high concentration of bacteria and microorganisms (10^5 cfu/ml for microorganisms, 10^4 cfu/ml for *Coli* bacteria).

Water samples were being pumped once through the reactor tube at different flow rates and discharge voltages. A pulsed positive discharge was generated between a high voltage stainless steel hollow needle electrode and a grounded stainless steel rod electrode, both immersed in the water. The optimal spark discharge was found at the needle-rod spacing of 4 mm. The reactor configuration and power supply is shown in Fig. 1.

To optimize the river water treatment with our reactor, we first found the best parameters of the discharge. This was done through methylene blue dye decoloration. The concentration of the dye was 5 mg/l and the highest achieved removal of methylene blue was about 25% at a water flow of 30 ml/min. This was due to the fact that spark discharge produces high concentration of oxidizing radicals (H_2O_2, OH, O_3), and UV radiation that cause the degradation of dye, and also can inactivate the bacteria and other microorganisms.

The energy efficiency of the bacteria inactivation was also estimated. The averaged energy of single spark discharge pulse was about 0.41 J. At the pulse repetition rate of 50 Hz and water flow rate of 30 ml/min the energy efficiency of inactivating microorganisms were as following: for microorganisms growing at 36°C – 8,6 cfu/J, for microorganisms growing at 22°C – 21 cfu/J, for total *Coli* bacteria – 3.4 cfu/J, for *E. Coli* bacteria – 0.08 cfu/J.
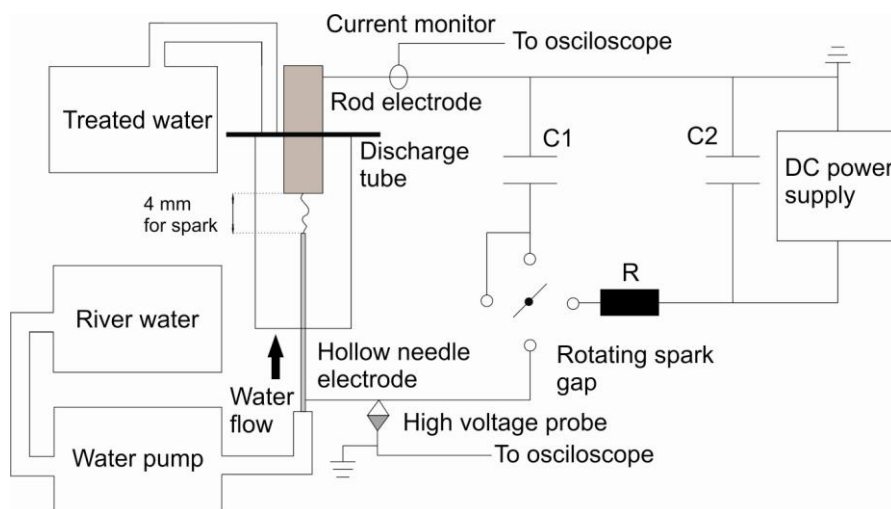
Fig. 1. Reactor configuration and power supply scheme

On the role of the design and discharge conditions on the Surfaguide tuning characteristics

Dariusz Czylkowski, Mariusz Jasiński, Jerzy Mizeraczyk
Centre for Plasma and Laser Engineering, The Szewalski Institute of Fluid-Flow Machinery, Polish Academy of Sciences, 14 Fiszera Str., 80-952 Gdańsk, Poland
E-mail: dczylkowski@imp.gda.pl

Since seventies of the twentieth century when the surface wave sustained discharges were discovered as a new plasma source [1], they find practical applications in various fields. Today they are still of high interest. One of the promising application is the hydrogen production [2]. Wide range of applications demands appropriate surface wave launchers suitable to operate under different discharge conditions. Stable and repeatable operation of such launcher with a high efficiency of power transfer to the plasma needs to take into account their geometry as well as discharge conditions [3].

In our experimental study we investigated the influence both of them on the tuning characteristics of the Surfaguide [4], waveguide based launcher operated at atmospheric pressure. The Surfaguide was based on a standard WR 430 rectangular waveguide with a section of reduced height and two tapered sections. Tapered sections ensure a smooth transition from standard waveguide to waveguide of reduced height. The discharge was sustained in a quartz tube with the inner r_i and outer r_o diameters of 1 mm and 5 mm, respectively, which penetrated the reduced height section through circular coupling gaps on the axis of the waveguide wide wall. The discharge tube inner diameter was chosen to prevent breaking the plasma column into separate filaments. The argon at total flow rate up to 6 l/min was introduced from one end of the tube. We used the experimental setup as that previously described in [5]. The microwave power was supplied to the Surfaguide via rectangular waveguide from a 2.45 GHz magnetron generator with maximum value of incident power of 500 W. The Surfaguide was terminated with a movable plunger playing a role of impedance matching element.

We took into account the influence of the following factors: height of the reduced height section, coupling gap diameter, input microwave power, gas flow rate, discharge tube cooling and metal enclosure on the tuning characteristics. The tuning characteristics of the Surfaguide was defined as the dependence of P_R/P_I, the fraction of the incident microwave power reflected at the applicator input, on the position l_s of the movable plunger, where l_s is the distance from the plunger to the axis of the discharge.

References
[1] Schluter H, Shivarova A.: *Travelling-wave-sustained discharges,* Physics Reports 443, 2007, p. 121-255.
[2] Henriques J., Bundaleska N., Tatarova E., Dias F.M., Ferreira C. M.: *Microwave plasma torches driven by surface wave applied for hydrogen production*, International Journal of Hydrogen Production XXX, 2010, p. 1-10.
[3] Fleisch T., Kabouzi Y., Moisan M., Pollak J., Castaños-Martínez E., Nowakowska H., Zakrzewski Z.: *Designing an efficient microwave-plasma source, independent of operating conditions, at atmospheric pressure*, Plasma Sources Sci. Technol. 16, 2007, pp. 173-182.
[4] Moisan M., Zakrzewski Z., Pantel R., Leprince P.: *A waveguide-based launcher to sustain long plasma columns through the propagation of an electromagnetic surface wave*, IEEE Trans. Plasma Sci. PS-12, 1984, p. 203-214.
[5] Czylkowski D., Jasiński M., Mizeraczyk J., Zakrzewski Z.: *Argon and neon plasma columns in continuous surface wave microwave discharge at atmospheric pressure,* Czech. J. Phys, 56 Suppl. B, 2006, p. 684-689.

Equivalent circuits for FeCoZr-Al$_2$O$_3$ nanocomposite films deposited in argon and oxygen atmospheres

A.V. Larkin[1), J.A. Fedotova[2), P. Zhukowski[3), T.N. Kołtunowicz[3), A.K. Fedotov[1)

[1) *Belarusian State University, 4 Independence av., 220030 Minsk, Belarus,*
E-mail: fedotov@bsu.by

[2) *National Center of Particles and High Energy Physics of BSU, 153 Bogdanovich Str.,*
220040 Minsk, Belarus

[3) *Lublin University of Technology, 38a Nadbystrzycka Str., 20-618 Lublin, Poland*

Nowadays the particular attention is given to the synthesis and investigation of the nanocomposites in which granules of soft ferromagnetic alloys with sizes about some nanometres are randomly distributed in dielectric matrix. The interest to such systems is mainly due to the possibilities for their application (e.g. for engineering of protecting screens against the HF electromagnetic radiation, in highly-Ohmic resistors and for other purposes) [1]. The fact that some nanocomposites possess the semiconductor properties but their manufacturing is usually cheaper, determines the possibility to use them as active and reactive elements in electrical circuits [2]. As was noted in [5], some of the metal-dielectric nanocomposites can be recommended as non-coil inductive elements.

The main goal of this paper is to investigate the equivalent circuits for granular nanocomposite films according to the method of the impedance spectroscopy [4]. The films, consisted of the Fe$_{0.45}$Co$_{0.45}$Zr$_{0.10}$ ferromagnetic alloy nanoparticles embedded into amorphous dielectric alumina matrix [3], were deposited in pure argon or argon and oxygen atmospheres.

The temperature dependences of active and reactive components in the equivalent circuits for the (Fe$_{0.45}$Co$_{0.45}$Zr$_{0.10}$)$_x$(Al$_2$O$_3$)$_{1-x}$ nanocomposite films are compared and analyzed. It is revealed that the equivalent circuits of the (Fe$_{0.45}$Co$_{0.45}$Zr$_{0.10}$)$_x$(Al$_2$O$_3$)$_{1-x}$ nanocomposites produced in argon + oxygen gas mixture show more strong inductive contribution than ones sputtered in pure argon.

References

[1] Bader S.D.: *Magnetism in Low Dimensionality*, Surface Science 500, 2002, p. 172-188.
[2] MacDonald J.R.: *Impedance Spectroscopy: Models, Data Fitting, and Analysis*. Solid State Ionics 176, 2005, p. 1961-1969.
[3] Kalinin Yu.E., Ponomarenko A.T., Sitnikov A.V., Stogney O.V.: *Granular Nanocomposites Metal-Dielectric with Amorphous Structure*, Physics and Chemistry of Materials Treatment 5, 2001, p. 14-20.
[4] Poklonskiy N.A., Gorbachuk N.I.: *Basis of the Impedance Spectroscopy of the Composites*, Minsk, BSU, 2005,130 p.
[5] Zhukowski P., Kołtunowicz T.N., Węgierek P., Fedotova J.A., Fedotov A.K., Larkin A.V.: *Formation of Noncoil-like Inductance in Film Nanocomposites (Fe$_{0.45}$Co$_{0.45}$Zr$_{0.10}$)$_x$(Al$_2$O$_3$)$_{(1-x)}$ Deposited in Ar+O$_2$ Atmosphere*, Acta Physica Polonica A 120 No1, 2011 (in press).

Detection of biomass-coal unstable combustion using frequency analysis of image series

**Andrzej Kotyra[1), Waldemar Wójcik[1), Konrad Gromaszek[1), Tomasz Ławicki[1),
Piotr Popiel[1), Krzysztof Jagiełło[2)**

[1) *Department of Electronics, Lublin University of Technology, Lublin, Poland,
E-mail: a.kotyra@pollub.pl*
[2) *Thermal Process Department, Institute of Power Engineering, Warsaw, Poland*

Biomass co-combustion with coal is one of the means of utilizing renewable energy. One of its main advantage is possibility of using existing combustion facilities after appropriate adaptations. Combustion of biomass-coal mixture can occur in unstable way, especially due to variable properties of biomass components and different weight density than that of the coal. Additionally, problems arise optimizing the operation of an individual burner for there are no methods of direct measurement of amount the coal dust supplied to the burner, as well as primary air. Usually, these parameters evaluated through indirect measurements of e.g. load of the mill and fan delivery, so the precision of such measurements is low [1].

The mentioned above reasons impose using of a proper monitoring system [2]. As the radiation emitted by flame is vital source of information for pending combustion process, optical-based systems are commonly used [3]. Most of them utilize frequency analysis of flame flickering that are obtained via optical probe. It should be mounted near burner being monitored. In practice, the probe installation may encounter difficulties for the boiler construction limitations. On the other hand, a care should be taken with optical probe mounting for it should provide signals as sensitive as possible to changing state of the combustion process. In order to simplify choosing flame the most sensitive area, a system consisting of high speed digital camera can be utilized.

The article presents experimental set-up and frequency analysis that was done for the captured image series. Every image was splitted into parts that were analyzed separately. The most sensitive flame area to possible combustion instabilities is pointed out on the basis of frequency analysis of times series obtained from each part of flame image series.

References
[1] Wójcik W.: *Światłowodowy układ do monitorowania procesu spalania*, Pomiary Automatyka Kontrola 53 11/2007, 2007, p. 24-28.
[2] Marques J.S., Jorge M.P.: *Visual inspection of a combustion process in a thermoelectric plant*, Signal Processing 80, 2000, p.1577-1589.
[3] Wójcik W., Kotyra A., Golec T., Gromaszek K.: *Vision based monitoring of coal flame*, Przegląd Elektrotechniczny 3/2008, 2008, p. 241-245.

Femtosecond laser micromachining system

**Katarzyna Garasz[1), Robert Barbucha[1), Michał Nejbauer[2),
Jerzy Mizeraczyk[1), Czesław Radzewicz[2)**
[1) *Centre for Plasma and Laser Engineering, The Szewalski Institute of Fluid-Flow
Machinery, Polish Academy of Sciences, Gdańsk, Poland, E-mail: kgarasz@imp.gda.pl*
[2) *Laser Centre, Institute of Physical Chemistry, Polish Academy of Sciences,
Warsaw, Poland*

We present a prototype design of the femtosecond laser micromachining system and the possible application of this system in fabrication of solar cells and industrial materials processing.

Within the research project supported by the European Commission, a femtosecond solid-state Yb:KYW laser with a fibre ytterbium amplifier has been developed. The ytterbium-doped active medium is pumped directly by a laser diode and a saturable absorber Bragg mirror is used for passive mode-locking. 350-fs output pulses are generated from the oscillator at the repetition rate of 94,7 MHz and centre wavelength of 1033 nm. Femtosecond pulses are amplified to a desired energy level using the technique of chirped-pulse amplification (CPA).

In parallel to the laser development, a micromachining system has been designed to meet the requirements of precision machining processes.

Femtosecond laser micromachining device presented here includes synchronized motion control and a galvoscanner system that provides the speed and precision needed for both, industrial and scientific applications. It is equipped with 2 μm precision linear positioning stages, high-performance galvanometer mirror scanner with a telecentric scan lens, six-axis robot arm and a versatile micromachining software.

Femtosecond laser materials processing offers many advantages over the long pulse (i.e. nanosecond) laser micromachining. Ultra-short laser pulses have a unique capacity to interact with different materials without transferring heat to the area surrounding the target. Due to the very short time scales involved in the ablation with femtosecond laser pulses the ablation process can be considered as a direct solid-vapor (or solid-plasma) transition [1]. This allows very precise and pure laser-processing, clean cuts, strong welds and sharp edges.

Furthermore, the advantages of femtosecond lasers are very promising for their applications in the photovoltaic industry. Efficiency loss due to regions of low shunt resistance is one of the major challenges currently facing PV manufacturers. It is well established that laser scribing can reduce the impact of shunted regions in thin-film solar cells [2]. Short-pulsed, fast and precise femtosecond laser makes it possible to achieve the exact depth and outline of the laser groove to improve efficiency of the solar cells.

References
[1] Chichkov B.N., Momma C., Nolte S., van Alvensleben F., Tunnerman A.: *Femtosecond, picosecond and nanosecond laser ablation of solids,* Applied Physics A 63, 1996, p. 109-115.
[2] Abbott M.D., Trupke T., Hartmann H.P., Gupta R., Breitenstein O.: *Laser Isolation of Shunted Regions in Industrial Solar Cells*, Progress in Photovoltaics: Research and Applications, Wiley InterScience, 2007.

Investigation of electrical characteristics of the carbon electrodes

Zydrūnas Kavaliauskas[1), 3)], Liutauras Marcinauskas[1), 2)], Vitas Valincius[1)]
[1)] *Lithuanian Energy Institute, 3 Breslaujos Str., LT-44403 Kaunas, Lithuania,*
E-mail: zydrunas@mail.lei.lt
[2)] *Kaunas University of Technology, 50 Studentu Str., LT-51368 Kaunas, Lithuania*
[3)] *Kaunas College, 20 Pramonės Str., LT-50468, Kaunas, Lithuania*

Recently developed low inertial high-power uninterruptable power supply systems start using new kinds of power sources: hybrid of battery-capacitor and supercapacitor (also known as ‚ultracapacitor'). Supercapacitors offer a promising alternative approach to meeting the increasing power demands of energy storage systems in general and of portable (digital) electronic devices in particular [1]. The power and energy-storage capabilities of these devices are closely linked to the physical and chemical properties of the carbon electrodes. The vast increases in capacitance achieved by supercapacitors are due to the combination of an extremely small distance that separates the opposite charges, as defined by the electric double-layer; and highly porous electrodes that embody very high surface area. A variety of porous forms of carbon are currently preferred as the electrode materials because they have exceptionally high surface areas, relatively high electronic conductivity, and acceptable cost [2].

In the present work, the atmospheric pressure plasma jet and magnetron sputtering deposition technology was used for fabrication of supercapacitor electrodes. The thick carbon layer was deposited using an atmospheric pressure plasma torch. Argon was used as plasma creating gas and acetylene as precursor. The ratio of Ar/C_2H_2 was 55, power of plasma torch – 840 W, deposition time – 150 s, and the distance between plasma torch outlet and sample – 0.005 m. The secondary layer of carbon was deposited by magnetron sputtering method. Carbon deposition time was 40, 60 and 80 min. Oxygen pressure in the vacuum chamber, varied in the rage of 1.4 - 1.8 Pa.

Surface morphology was characterized by scanning electron microscopy (SEM) model JEOL JSM–5600. Bonding structure of carbon coatings were characterized using X-ray diffraction (XRD) measurements and Raman scattering (RS) spectroscopy. The relative oxygen quantity contained in the carbon electrodes was measured by energy dispersive X-ray (EDX) method. Electrical characteristics (capacity, stability voltage, charging-discharging cycles) of fabricated supercapacitors were measured.

It was shown that the parameters of supercapacitors strongly depend on the secondary carbon layer deposition time. It was registered that the surface topography of fabricated electrodes and surface effective area depends on carbon deposition time. SEM analysis results indicated that the surface roughness increases with the deposition time of secondary carbon layer. XRD and RS spectroscopy demonstrated the amorphous carbon structure. The EDX results indicated that the increase of carbon deposition time from 40 to 80 min, decreases the relative oxygen quantity from 8 to 3.5%, meanwhile the supercapacitor capacity increases from 7 to 14 mF.

References

[1] Pandolfo A., Hollenkamp A.: *Carbon Properties and their Role in Supercapacitors*, Journal of Power Sources 157, 2006, p. 11-27.
[2] Kotz R., Carlen M.: *Principles and Applications of Electrochemical Capacitors*. Electrochimica Acta 45, 2000, p. 2483-2498.

N$^{EE}_{2011}$T

The preparation of input data in digital image processing

Jakub Pęksiński, Grzegorz Mikołajczak

*West Pomeranian University of Technology, Faculty of Electrical Engineering,
10 26 Kwietnia Str., 71-126 Szczecin, Poland, E-mail: jakub.peksinski@zut.edu.pl*

Introduction

The aim of the article is presenting what kind of influence an appropriate preparation of entry data in digital image processing has got upon the final results. The authors have presented it on the basis of lack of synchronization between entry data and its influence on the quality criterion Universal Image Quality Index "Q" (1) as well as the process of neuron network learning.

$$Q = \frac{\sigma_{f,f'}}{\sigma_f \cdot \sigma_{f'}} \cdot \frac{2 \cdot \bar{f} \cdot \bar{f'}}{(\bar{f})^2 + (\bar{f'})^2} \cdot \frac{2 \cdot \sigma_f \cdot \sigma_{f'}}{\sigma_f^2 + \sigma_{f'}^2} \tag{1}$$

where: $\bar{f} = \frac{1}{N} \cdot \sum_{i=1}^{N} f_i$; $\bar{f'} = \frac{1}{N} \cdot \sum_{i=1}^{N} f'_i$; $\sigma_f = \frac{1}{(N-1)} \cdot \sum_{i=1}^{N} (f_i - \bar{f})^2$; $\sigma_{f'} = \frac{1}{(N-1)} \cdot \sum_{i=1}^{N} (f_i - \bar{f'})^2$;

$\sigma_{ff'} = \frac{1}{(N-1)} \cdot \sum_{i=1}^{N} (f_i - \bar{f}) \cdot (f_i - \bar{f'})$

In the article an algorithm based on correlation has been proposed. Its function is to eliminate the lack of synchronization between entry images in such a way so that the final result is burdened by the smallest possible mistake, resulting from lack of adequate fitting.

Algorithm of the adjustment of the images in X and Y plane

As a criterion of the adjustment of both images, authors suggest using the algorithm which is based on the mutual correlation (2) between images.

$$r = \frac{\sum_i \sum_j (f_{i,j} - \bar{f}) \cdot (f'_{i,j} - \bar{f'})}{\sqrt{\left(\sum_i \sum_j (f_{i,j} - \bar{f})^2 \right) \cdot \left(\sum_i \sum_j (f'_{i,j} - \bar{f'})^2 \right)}} \tag{2}$$

where: f – orginal image; f' – result image; $\bar{f}$, $\bar{f'}$ – mean value
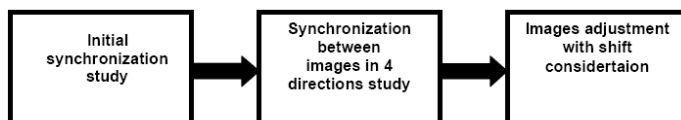
Fig. 1. Block diagram of the algorithm of the both images adjustment

Conclusions

Using this adjusting algorithm before issues of digital image processing, many errors caused by this can be eliminated. Therefore, the algorithm elaborated by the author has a practical value, because due to its simplicity and high efficiency, it can be applied in all fields requiring synchronization of the images.

References

[1] Wang Z., Alan C., Bovik A.: *Universal Image Quality Index*, IEEE Signal Processing Letters 9 no.3, 2002, p. 81-84.
[2] Pęksiński J, Mikołajczak G.: *Generation of a FIR filter by means of a neural network for improvement of the digital images obtained using the acquisition equipment based on the low quality CCD structure*, Lecture Notes in Artificial Intelligence 5990, p. 190-199.

Impedance of reverse biased diodes irradiated with krypton ions with energy of 250 MeV

**N.A. Poklonski[1), N.I. Gorbachuk[1), A.V. Ermakova[1), M.I. Tarasik[1),
S.V. Shpakovski[2), V.A. Filipenia[2), V.A. Skuratov[3), A. Wieck[4), T.N. Kołtunowicz[5)**

[1) *Belarusian State University, Minsk, Belarus, E-mail:* gorbachuk@bsu.by
[2) *JSK Integral, Minsk Belarus*
[3) *Joint Institute for Nuclear Research, Minsk, Belarus*
[4) *Ruhr-Universiteat, Bochum, Germany*
[5) *Lublin University of Technology, Lublin, Poland*

High energy ion implantation can be used for optimization of the parameters of fast recovery diodes, which implies an additional study of the frequency dependences of their parameters [1]. The diodes manufactured on the *n*-type float-zone Si wafers were investigated. The phosphorus concentration is 5×10^{13} cm^{-3}. The p^+-type region with area of 4.41 mm^2 was created by boron ion implantation. The diodes were irradiated from the side of the p^+-type region with krypton ions with energy of 250 MeV and fluencies within range from 10^8 to 10^9 cm^{-2}. The distance between the metallurgical border of p^+n-junction and the maximum of the primary vacancies distribution was about 26.4 μm. Static current-voltage characteristics (Fig. 1a) were measured by HP 4156B. The AC-measurements of the diodes were carried out using Agilent E4980A and Agilent 4285A LCR-meters at room temperature in the frequency range $f = \omega/2\pi$ from 20 Hz to 30 MHz.
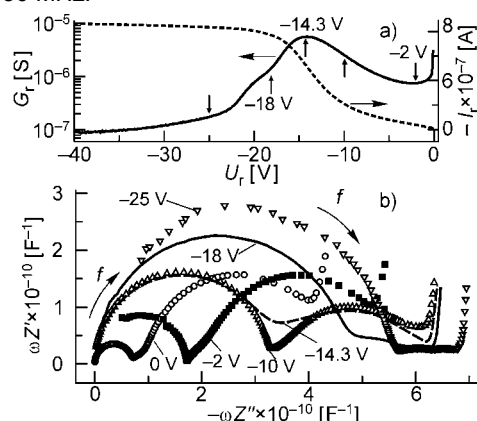
Fig. 1. Current-voltage characteristic of the diode irradiated with krypton ions with the fluency of 10^9 cm^{-2}, and the dependence of its differential conductivity $G_r = dI_r/dU_r$ on the reverse bias voltage U_r (a); plot of complex electrical modulus M/C_0 (b). Voltage values at which frequency dependences of the impedance were measured are marked with arrows in Fig. 1a

It was found that the observed in Fig. 1b at the increase of reverse bias voltage U_r transformations of the plot of complex electrical modulus $M/C_0 = \omega(-Z'' + iZ')$ of the irradiated diodes (C_0 is the geometric capacity, Z' and Z'' are real and imaginary parts of impedance) occur as a result of the change of: 1) the ratio Z_L/Z_J of impedances of the irradiation damaged layer Z_L and the space charge area Z_J; 2) the electron population of the energy levels of irradiation-induced defects.

References

[1] Poklonski N.A., Gorbachuk N.I., Shpakovski S.V., Filipenia V.A., Skuratov V.A., Wieck A.: *Kinetics of reverse resistance recovery of silicon diodes: the role of the distance the metallurgical p^+n-junction-defect layer formed by 250 MeV krypton implantation*, Physica B 404 No 23-24, 2009, p. 4667-4670.

The elemental composition, topography and wettability of $Pb_{0.25}Sn_{1.75}S_2$ thin films

I.S. Tashlykov[1], A.I. Turavets[1], V.F. Gremenok[2], P. Zhukowski[3]

[1] *Belarusian State Pedagogical University, Minsk, Belarus, E-mail: tashl@bspu.unibel.by*
[2] *State Scientific and Production Association "Scientific-Practical Materials Research Centre of the National Academy of Sciences of Belarus", Minsk, Belarus, E-mail: gremenok@ifttp.bas-net.by*
[3] *Lublin University of Technology, Lublin, Poland*

A systematic study of the potential of compounds derived from PbS, SnS and $PbSnS_2$ minerals indicated that many sulfides exhibit suitable optical band gaps for optoelectronic applications.

In this study, the $Pb_{0.25}Sn_{1.75}S_2$ thin films were prepared by hot wall vacuum evaporation of bulk material onto glass substrates. The deposition conditions were kept constant, while the substrate temperature was varied from 268ºC to 361ºC. Comparisons were drawn in terms of the structure, the elemental composition, the surface morphology and the surface wettability of the semiconductor films.

Rutherford backscattering spectroscopy in composition with computer code RUMP for the evaluation of RBS spectra is powerful method for the quantitative analysis of thin films and depth profiling of the near-surface layers of solids. The surface morphology and crystalline structure of thin films were investigated and analyzed using atomic force microscopy (AFM). Hydrophilicity was measured by means of the contact angle measurement technique.

According to experimental data, the $Pb_{0.25}Sn_{1.75}S_2$ films are 0.83 - 1.68 microns in the thickness (at different temperatures). With the increase of the substrate temperature, the thickness of film increases too. They are consisting of 6.8 - 10.4 at.% lead, 36.6 - 44 at.% tin and 48 - 53 at.% sulphur. Profiles of distribution of elements show that the obtained films are homogeneous. As appears from spectra, the substrate includes silicon, oxygen and calcium. Mutual diffusion of elements of a substrate (Si, O, Ca) and a put covering (Pb, Sn, S) has been found out. The thickness of an intermediate layer also increases from 0.48 microns to from above 1.65 microns with the increase of the substrate temperature.

The AFM studies showed that the increase in temperature of a substrate was accompanied by cardinal change of structure of a surface (Fig. 1) and growth of the average surface roughness of $Pb_{0,25}Sn_{1,75}S_2$ films (from 10.1 nm to 48.4 nm).
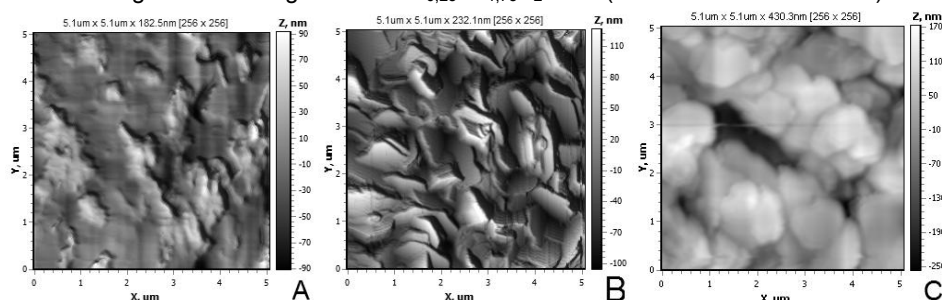
Fig.1. AFM-images of the surface of three different samples:
(A) T_{sub} = 268ºC, (B) T_{sub} = 330ºC, (C) T_{sub} = 361ºC

As it is seen from the wettability test results surfaces reveal hydrophobic behavior.

Pulverized coal combustion boiler efficient control

Waldemar Wójcik, Konrad Gromaszek, Andrzej Kotyra, Tomasz Ławicki
Lublin University of Technology, Department of Electronics, Lublin, Poland,
E-mail: k.gromaszek@pollub.pl

Combustion process is very complex, nonlinear and traditional modelling theory of thermodynamics based is very difficult. To overcome potential difficulties in modelling industrial scale combustion processes the intelligent control algorithms (e.g. artificial neural networks, fuzzy logic or genetic algorithms) implemented to the control result in acceptable results.

Due to consequences for the energy industry – both directives Integrated Pollution Prevention and Control (IPPC) and Large Combustion Plants (LCP) connected with air pollution have very significant influence on combustion process. They ought to be mentioned in control process.

Until recent years only the largest boilers could justify sophisticated controls of combustion process. Recently, higher costs and emission rigors make it necessary for users to improve boiler efficiency regarding to both economic and ecological criteria.

The paper presents stages of modelling methods to pulverized coal and biomass co-combustion of the single tangential burner.

References

[1] Azid I.A., Ripin Z.M., Aris M.S., Ahmad A.L., Seetharamu K.N., Yusoff R.M.: *Predicting combined-cycle natural gas power plant emissions by using artificial neural networks*, in Proc. IEEE TENCON: Intelligent Systems Technologies New Millennium, Kuala Lumpur, Malaysia, 2000, p. 512-517.

[2] Burns A., Kusiak A., Letsche T.: *Mining transformed data sets, in Knowledge-Based Intelligent Information and Engineering Systems*, R. Khosla, R. J. Howlett, and L. C. Jain, Eds. Heidelberg, Germany: Springer, 2004, vol. I, LNAI 3213, p. 148-154.

[3] Buche D., Stoll P., Dornberger R., Koumoutsakos P.: *Multiobjective evolutionary algorithm for the optimization of noisy combustion processes*, IEEE Trans. Syst., Man, Cybern. C 32 no.4, 2002, p. 460-473.

[4] Cass R., Radl B.: *Adaptive process optimization using functional-link networks and evolutionary optimization*, Control Eng. Practice 4 no.11, 1997, p. 1579-1584.

[5] Chu J.Z., Shieh S.S., Jang S.S., Chien C.I., Wan H.P., Ko H.H.: *Constrained optimization of combustion in a simulated coal-fired boiler using artificial neural network model and information analysis*, FUEL 82 no.6, 2003, p. 693-703.

[6] Espinosa J., Vandewalle J., Wertz V.: *Fuzzy Logic, Identification and Predictive Control*, London, U.K.: Springer-Verlag, 2005.

[7] Hangos K.M., Lakner R., Gerzson M.: *Intelligent Control Systems: An Introduction with Examples*, Amsterdam, The Netherlands: Kluwer, 2001.

[8] Kalogirou S. A.: *Artificial intelligence for the modeling and control of combustion processes: a review*, Progress Energy Combust. Sci. 29 no.6, 2003, p. 515-566.

[9] Miyayama T., Tanaka S., Miyatake T., Umeki T., Miyamoto Y., Nishino K., Harada E.: *A combustion control support expert system for a coal-fired boiler*, Proc. IEEE Industrial Electronics, Control, Instrumentation, Kobe, Japan, 1991, p. 1513-1516.

[10] Ogilvie T., Swidenbank E., Hogg B.W.: *Use of data mining techniques in the performance monitoring and optimization of a thermal power plant*, Proc. Inst. Elect. Eng. Colloq. Knowledge Discovery Data Mining, 1998, p. 7/1-7/4.

[11] Tascillo A., Gearhart C., Fridrich J.: *Nonlinear forecasting with wavelet neural networks*, Proc. IEEE Int. Conf. Systems, Man, Cybernetics, Orlando, FL, 1997, p. 1111-1116.

[12] Song Z., Kusiak A.: *Constraint-based control of boiler efficiency: A data-mining approach*, IEEE Transactions on Industrial Informatics 3 no.1, 2007, p 73-83.

Modern light sources in automotive engineering

Artur Boguta

Lublin University of Technology, Department of Computer and Electrical Engineering,
38D, Nadbystrzycka Str., 20-618 Lublin, Poland, E-mail: a.boguta@pollub.pl

The light emitting diodes are known as the light sources which have been initially used as signalling elements. Actually their application for lighting purposes is possible owing to significant improvement of their luminous efficiency. The light emitting diodes are characterized by small size, long term service life and high efficiency. Therefore they are more and more often used as the light sources in industry and household applications. LEDs are more and more often applied in signal and lighting lamps in motor vehicles.

The paper presents the construction of daytime running lights, using the composite reflector, which are mounted LEDs. Reflector has been tested to show evidence that it complies with current regulations.
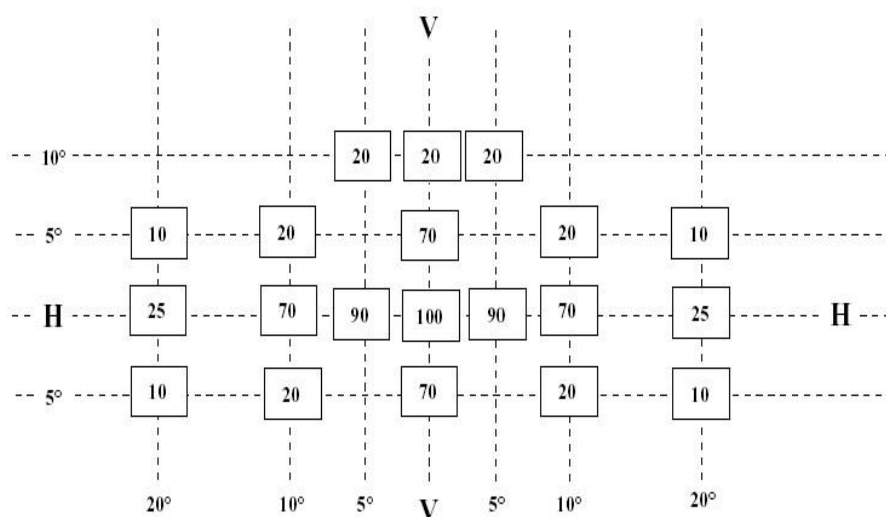
Fig. 1. Percentage distribution of light intensity for daytime running lights

References
[1] Żagan W.: *Podstawy techniki świetlnej*, Oficyna Wydawnicza Politechniki Warszawskiej 2005.
[2] PN-91/S-73034.: Światła pozycyjne i obrysowe –wymagania świetlne i metody badań.
[3] Economic Commission for Europe (ECE) Inland Transport Committee: TRANS/WP.29/GRE/2005/40,41,42.
[4] ECE Regulation No. 87 EKG ONZ48 z dnia: 7.08.2007 r.

The miniature cold plasma source for research and technological applications

Jerzy Janiszewski

Institute of Electric Power Engineering, Poznan University of Technology,
3A Piotrowo Str., 60–965 Poznań, Poland, E-mail: jerzy.janiszewski@put.poznan.pl

For many years we have been observing a dynamic increase of interest in plasma technique in technological and scientific use. Plasma techniques are applied for many aims including modifying materials' surfaces, coating with thin coverings, producing new materials, cleansing and treatment of surfaces, decomposing toxic chemical compounds and gases, sterilizing medical instruments or modifying textile fibres [1-3].

In technological uses the most popular is the low temperature plasma which is produced in atmospheric pressure or in the reduced one [4]. The sources of such plasma are usually arch, crown, barrier and microwave discharges. Plasma gained that way has a temperature between a few hundred and a few thousand Kelvins. Cold plasma with a temperature similar to ambient temperature is usually obtained in glow discharges. The discharges are generated in vacuum tanks between electrodes which are powered by sources of alternating current (AC) with radio or microwave frequency or direct current (DC).

The glow discharges can be produced in the whole volume of vacuum chamber or only locally. From an economical point of view, for technological uses one searches for a simple set, relatively cheap in exploitation. Plasma sources with gliding discharges have such features. Small volume of ionized gas enables to get comparatively high electrical efficiency of source while there is great homogeneity of plasma and easy regulation of its parameters.

Researches of DC gliding glow discharges [5, 6] has pointed at potential capability of executing a simple plasma micro reactor powered by AC with power-system frequency. The article presents the essence of construction of such a device and exemplary results of investigations on it. The reactor's work temperature and voltage in dependency to working current and pressure are shown. Low temperature of gained plasma is particularly profitable for etching polymers and membrane and textile fibres treatment.

References
[1] Kickuth R.: *Lasting surface magic, Plasma technology – Process diversity + sustainability*, BMBF Public, Germany November 2001, p. 17-20.
[2] Rakowski W.: *Plasma in textile industry – technology for XXI century?*, Advances in plasma chemistry, Acta Agrophysica 80, 2002, p. 349-358.
[3] Grün R.: *Economic and ecological aspects of plasma surface engineering*, Proc. 3rd Intern. Conference on Plasma Surface Engineering - PSE _92 Garmisch-Partenkirchen, Germany 1992, p.613-618.
[4] Friedrich J.F., Rohrer P., Saur W., Gross Th., Lippitz A., Unger W.: *Improvement in polymer adhesivity by low and normal pressure plasma surface modification*, Proc. 3rd Intern. Conference on Plasma Surface Engineering - PSE _92 Garmisch-Partenkirchen, Germany 1992, p.371-378.
[5] Janiszewski J, Kamińska A.: *Experimental investigation of magnetically gliding discharge*, Advances in plasma chemistry, Acta Agrophysica 80, 2002, p. 55-61.
[6] Kamińska A., Janiszewki J., Leys Ch.: *Study of non-equilibrium gliding discharges in air*, Czechoslovak Journal of Physics, vol.52, Suppl. A, 2002, p. 549-555.

N$_{2011}^{EE}$T

The influence of metal impurities to a-C:H films

Z. Rutkuniene, A. Grigonis, L. Vigricaite
*Kaunas University of Technology, Physics Department, 50 Studentu Str.,
LT 51368, Kaunas, Lithuania, E-mail: zivile.rutkuniene@ktu.lt*

Amorphous carbon thin films are the widely used materials for industrial applications due to their superior optical, physical, and chemical properties: the stability in aggressive chemical environments, high hardness, high optical transparence and hydrophobicity et all. Variation of these properties depends on quantity of sp^3 bonds in amorphous carbon matrix and hydrogen concentration. Inclusion of metal impurities and their concentration also conditioned structural changes determining properties of carbon films. For example, optical band gap can be decreased to zero during variation of metal concentration in film; hydrophobicity depends on the kind of the metal; film hardness changes several times by changing metal concentration. The size of metal particles affects film stress. Samples containing smaller inclusions become less stressed [1-3]. Metal impurities also can be catalyst for nanotube growing.

The carbon coatings on the silicon substrate by chemical vapour phase precipitated as the insertion of platinum and copper impurities were observed in this paper. Coatings were investigated by ellipsometry, Raman spectroscopy, and scanning electron microscopy. It was obtained that growing films are more polymeric like. The refractive index of all films are similar and varies from 1.6 to 1.7 and do not depend on nature of metal. Extinction coefficient is about 0.02. Analysis of Raman spectra showed that typical G peaks for amorphous carbon become dominant and move to the higher means (from 1560 cm^{-1} to approximately 1590 cm^{-1}) then metal impurities are introduced to the film. Also a new peak (about 1800 cm^{-1}) was obtained there. It can associate with single walled nanotubes [4] because of this peak moved to the lower values when temperature of substrate increased during films formation and graphitization became predominant. Typical D peak in films with platinum impurities is less intensive. D peak in Raman spectra disappears when Cu impurities are involved in film.

References
[1] Kukielka S., Gulbiński W., Pauleau Y., Dub S.N., Grob J.J.: *Nikel/Hydrogenated amorphous carbon composite films deposited in acetylene/argon microwave plasma discharge*, Reviews on advanced materials science 15, 2007, p. 127-133.
[2] Corbella C., Vives M., Pinyol A., Bertran E., Canal C., Polo M.C., Andújar J.L.: *Preparation of metal (W, Mo, Nb, Ti) containing a – C:H films by reactive magnetron sputtering*, Surface and Coatings Technology 177-178, 2004, p. 409-414.
[3] Guangan Zhang, Pengxun Yuan, Peng Wang, Youming Chen, Junyan Zhang: *The preaparation and mechanical properties of Al – containing a – C:H thin films*, Journal of Physics D: Applied Physics 40, 2007, p. 6748-6753.
[4] Pineta M.A, Maruci A., Empedocles S.A., Bawendi M.G. et al.: *Raman modes of metallic carbon nanotubes*, Physcal Rev. B 58, 1998, p. 16016-16019.

Selection of a measuring transducer for registration of acoustic emission signals generated by On Load Tap Changers

Andrzej Cichoń, Paweł Frącz

Opole University of Technology, Institute of Electric Power Engineering,
2 B76 Prószkowska Str.,45-758 Opole, Poland;
E-mail: a.cichon@po.opole.pl, p.fracz@po.opole.pl

Results of scientific research works considering selection of measuring transducer applied for registration of acoustic emission (AE) signals generated by on load tap changers (OLTC) are presented in the paper. During the coupling process AE signals are generated by: the mechanical setup of tap changer, contacts operation and partial discharges. For the most OLTC types, the working medium is insulation oil in which the created acoustic wave propagates to the steal tank. There exists a possibility for registration of AE signals with a piezoelectric transducer mounted on the outer tank surface or with a hydrophone immersed in the oil. In such way obtained AE signal contains information which describes operation of the power tap changer and the selector. A comparative analysis of AE signals generated by OLTC working under laboratory conditions in three setups, each applying measuring transducers with different transmittance, is presented in the paper. In measurements three kinds of transducers were applied: wide band transducer type WD AH-17 from Physical Acoustics Corporation, hydrophone type TC4038 from Reson and accelerometer type 4514–B–001 from Brüel & Kjær. The comparative analysis was performed in order to determine their suitability for OLTC technical condition diagnosis. Based on the results achieved one transducer which enables for registration of acoustic events generated by the mechanical setup as well as by electric phenomena occurring during OLTC operation was selected.
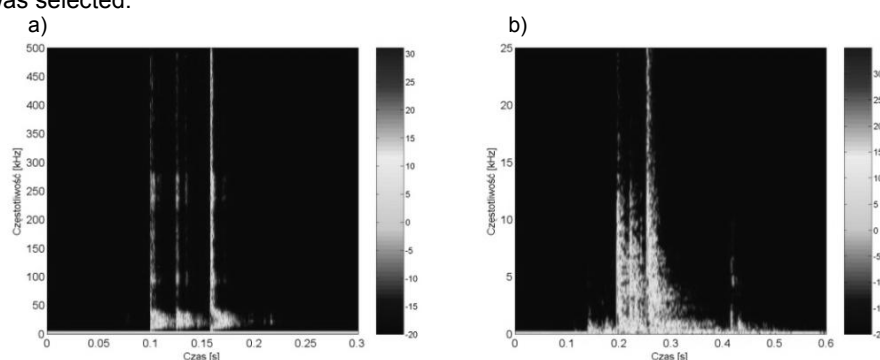
Fig. 1. Power spectrum density of the acoustic signals generated by OLTC registered by:
a) wide band transducer type WD AH-17, b) accelerometer type 4514 – B – 001

References
[1] Kang P.: *Characterisation of Vibration Signals Using Continuous Wavelet Transform for Condition Assessment of On- Load Tap - Changers*, Mechanical Systems and Signal Processing 17 (3), 2003, p. 561-577.
[2] Simas E.F., De Almeida L.A.L., De Lima A.C.: *Vibration Monitoring of On-Load Tap Changers Using a Genetic Algorithm*, Proceedings of the IEEE Instrumentation and Measurement Technology Conference, Ottawa, Ontario, Canada 16-19 May 2005, p. 2288-2293.

A low computationally video based algorithms for control of personal safety in industrial zone

Piotr Lech
West Pomeranian University of Technology, Szczecin, Poland
E-mail: piotr.lech@zut.edu.pl

Ensuring safety in the industrial zones is realised on the basis of specialised expert systems dedicated to specific industry. It is particularly important to define the safety zones at the interface between the human and machine related to the risk of health damage and threat to personal safety. Some of these systems are based on video processing and analysis [1, 2].

A fast algorithm for detecting changes in images (or frames from video sequence) is based on the Monte Carlo method [3]. As a result of the algorithm estimated value of field of the area described by a logical condition is obtained. The comparison of estimated values for individual video frames allows the detection of changes. Major studies have been done to remove undesirable properties of the algorithm and practical implementation for control over specific protected area for single or multi-camera systems. Unfortunately the area estimation based on the Monte Carlo method has an integrating character. The values of the area for all elementary square elements in the square grid for each analysed frame are estimated to remove the integrating character of presented method. All the calculated values are stored in memory for future comparison. As a consequence, a series of area values assigned to specific video frames is obtained. Comparing these values we are able to determine the number of moving objects, their direction and speed.

The studies carried out the algorithm with a uniform square grid is not optimal for the case when security zones of varying importance are defined. It was shown that the transition from a uniform grid for the matched (through the grid compaction) to the protected area provides better and more accurate detection of changes in the image. The density of a grid of squares is associated with predefined risk parameters for safety zones. Any changes in the image in these zones are classified [4] and indicated depending on the degree of risk. A controlled area can be defined statically or dynamically change during the observation. Dynamically defined safety zones can be used to control the phenomena occurring periodically, such as transport, machine movement etc.

The studies have shown: high-speed calculations resulting from the reduction of the analysed data, resistance to low noise and high efficiency of detection of changes in the safety zones.

References
[1] Collins R., Lipton A., Kanade T., Fujiyoshi H., Duggins D., Tsin Y., Tolliver D., Enomoto N., Hasegawa O.: *A system for video surveillance and monitoring: VSAM final report*, Robotics Inst.,CMU-RI-TR-00-12, 2000.
[2] O'Malley M.K.: *Principles of Human-machine Interfaces and Interactions*, In Life Science Automation: Fundamentals and Applications, Mingjun Zhang, Bradley Nelson and Robin A. Felder (Eds.) Artech House Publishers, 2007, p. 101-125.
[3] Okarma K., Lech P.: *Monte Carlo Based Algorithm for Fast Preliminary Video Analysis*, Lecture Notes in Computer Science 5101, Springer-Verlag, Heidelberg, 2009, p. 790-799.
[4] Okarma K., Lech P.: *Application of the Monte Carlo preliminary image analysis and classification method for the automatic reservation of parking space*, Machine Graphics and Vision 18 no 4, 2009, p. 439-452.

Influence of the reactionary charge composition
on the paramagnetic properties of the cubic boron nitride

I.I. Azarko[1), O.V. Ignatenko[2), E.I. Kozlova[1), N.A. Shempel[2), O.N. Yankovski[1)

[1) *Belarussian State University, Minsk, Belarus, E-mail: azarko@bsu.by*
[2) *SO _ScPC NAS of Belarus on Materials Science', E-mail: lgnatenko@ifttp.bas-net.by*

The topicality of the present paper is conditioned by the priority of the super hard materials synthesis perspective for the needs of nano- and optoelectronic elements formation in a stable matrix. Cubic boron nitride significantly supersedes toughness, endurance, abrasive ability, thermal conductivity and chemical stability of standard abrasive materials (electrocorundum, SiC), i.e. all parameters determining the quality and efficiency of the instrumental abrasive materials [1]. In the present research there were several regimes of the cubic boron nitride crystallization kinetics developed. The influence of a complex metal oxide composition introduction to the charge was also estimated. The studies of the structural perfectness of the synthesized samples over their paramagnetic properties were conducted at three different temperatures – liquid nitrogen temperature (77 K), room temperature (293 K) and 423 K.
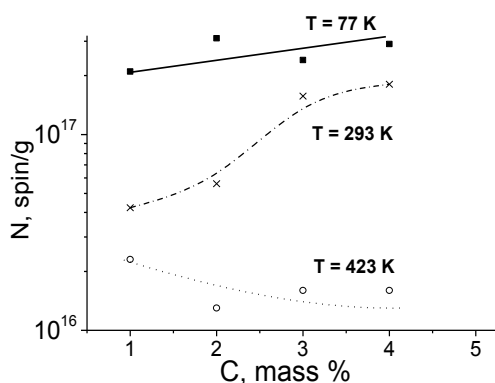
Fig. 1. The PC concentration dependence on the concentration of metal oxide compositon in the charge at different temperatures

The cubic boron nitride micro powders synthesized with minimum level of Ca-Mg-Fe-Si-Al-O composition introduced to the charge showed a single rather broad (23 - 28 Oe) signal with g-factor in the range of 2.0035 - 2.0044 on the ESR spectra at 77 K. This signal was independent on the synthesis duration and the formed crystals' structural perfection. The ESR-line became twice as narrow and the g-factor value declined to 2.0023 at room temperature measurements. A narrow signal (ΔH < 1.5 Oe) with g-value of 2.0015 dominated at 423 K.

This time the paramagnetic centers (PC) concentration showed a monotone decrease as the synthesis duration increased from 1 to 15 s. The studies of different sample groups synthesized in the containers with structural variations (i.e. several details or elements differed) were conducted. There was no some systematic matching determined of the paramagnetic signals' characteristics to the synthesis conditions.

The measurements of the samples synthesized at different levels of Ca-Mg-Fe-Si-Al-O composition (from 1 to 5% of the charge content) showed a significant increase of the paramagnetic centers concentration at 293 and 77 K, while the concentration of the high temperature defects amount decreases (see Fig.1.).

References

[1] http://www.harisdiamond.com

Integrated magnetic element for improving efficiency of resonant power converter

Cezary Worek[1), Sławomir Ligenza[2)
[1) *AGH University of Science and Technology, Krakow, Poland,*
E-mail: worek@agh.edu.pl
[2) *Fideltronik Imel Sp. z o.o., Sucha Beskidzka, Poland*

This paper presents a new winding design and construction of an integrated magnetic element (IME) to achieve high efficiency and high power density in class DE resonant power converter [1, 2]. Future applications of the proposed concept are demonstrated by an IME design for a 1MHz, 400V-input 100V-output 300-W half-bridge DC–DC series-parallel LCLC converter, dedicated for LED lighting application and other current source power supplies. Detailed SPICE simulation results are presented to evaluate the performance of the designed converter under varying load conditions. The results obtained from the theory, SPICE simulation, and the experimental integrated magnetic element are compared. The proposed converter has high efficiency from light to full load. The LCLC-type tank is a combination of one series and one parallel resonant circuits. The parallel circuit is inductively coupled to load, which results in a four-element series-parallel LCLC (SP-LCLC) converter [3, 4]. Thanks to such configuration, high output power dynamism requires only little switching frequency variation. The proposed IME can be modeled as a drilled toroidal core. The inner windings constitute the output transformer, with leakage inductance being the inductor of a parallel resonant circuit. On the outside, the windings of a series resonant circuit inductor are placed, perpendicular to the inner windings. By using orthogonal magnetic fields the coupling between series and parallel resonant inductors are negligible. Superposition of two magnetic inductions oriented orthogonally with respect to each other in the combined magnetic circuit allows to double the energy peak values in the selected portion of a magnetic circuit. Additionally, if the magnetic induction vectors are shifted in phase by 90° we obtain:

$$\left|B_{Axy}(t)\right| = \sqrt{B_A^2 \cdot \sin^2 \omega t + B_A^2 \cdot \cos^2 \omega t} = B_A \cdot \sqrt{\sin^2 \omega t + \cos^2 \omega t} = B_A$$

In this case two inductive elements are constructed utilising the same portion of the magnetic circuit, each of them having capability to operate at the maximum magnetic induction value B_{MAX}, close to the saturation induction. Thus, utilising the same portion of the magnetic circuit for two windings, the amount of stored energy is increased. The sum of peak energy values is increased while maintaining the same amplitude of the magnetic induction vector. Thanks to reduced magnetic core dimensions and high switching frequency resulting in smaller reactance elements the proposed IME allows to minimize the size and weight of a power supply, which is crucial in mass market applications.

References
[1] Worek C., Ligenza S.: *Parallel operation of MOSFET and IGBT transistors in resonant mode converter.* Przegląd Elektrotechniczny 86 7/2010, 2010, p. 317-319.
[2] Sun J., Mehrotra V.: *Orthogonal Winding Structures and Design for Planar Integrated Magnetics.* IEEE Transactions On Industrial Electronics 55 no.3, 2008, p.1463-1469.
[3] Yanjun Z., Dehong X., Kazuaki M., Kiyoaki S.: *1MHz-1kW LLC Resonant Converter with Integrated Magnetics.* Applied Power Electronics Conference, APEC 2007, 2007, p. 955–961.
[4] Gao X., Ayyanar R., Kazuaki M., Kiyoaki S.: *Integrated magnetics scheme for ZVS hybrid converter with improved performance.* Power Electronics Specialists Conference, 2004. PESC 04. 2004 IEEE 35th Annual 5, 2004, p. 3681-3687.

Magnetic component design and switching technique in high efficiency flyback SMPS

Rafał Widórek[1),] Sławomir Ligenza[1),] Cezary Worek[2)]
[1)]*Fideltronik Imel Sp. z o.o., Sucha Beskidzka, Poland,*
E-mail: rafal.widorek@fideltronik.com.pl, slawomir.ligenza@fideltronik.com.pl
[2)]*AGH University of Science and Technology, Krakow, Poland,*
E-mail: worek@agh.edu.pl

The LED lighting market is growing rapidly, so there is a demand for high efficient, not expensive power supplies. The power requirements are usually between 30 W-200 W. The flyback SMPS converter offers a low component count design while still being able to deliver power in the aforementioned range. The reduced component count, in comparison with e.g. forward converter, allows for a lower cost, high efficiency and small-sized design of the power supply.

This paper will focus on improving the design of the flyback transformer and will present a modification to the switching scheme. In the article an analysis of energy losses in the flyback converter as function of transformer design and operating frequency will be presented. The analysis includes transformer winding losses resulting from current conduction, air gap influence, core losses, transistor switching losses and conduction losses, as well as losses in other components (e.g. rectifier diode). This analysis will be concluded with a search of a point of operation, i.e. primary winding turn number and operating frequency, at which the overall energy losses in the converter are minimal, thus achieving high efficiency. The paper will contain both calculation and measurement results presentation and comparison.

A modification of the flyback circuit, which improves both efficiency and lowers electromagnetic interference will be presented. An introduction of a resnonant snubber circuit on the secondary side of the flyback transformer, combined with controlled switching time of the transistor will be discussed. The quasi-resonant switching takes advantage of the shape of the transistor V_{DS} voltage and I_D current, so switching losses can be largely reduced. The paper will present a description of the circuit that implements this technique as well as a description of the switching cycle of semiconductor elements.

References
[1] Shiroyama H., Matsuo H., Ishizuka Y.: *Quasi-resonant converter with divided resonant capacitor on primary and secondary side*, Telecomunications Energy Conference - INTELEC 2009.
[2] Ki-Bum Park, Chong-Eun Kim, Gun-Woo Moon, Myung-Joong Youn.: *PWM Resonant Single-Switch Isolated Converter,* IEEE Transactions on power electronics 24 no.8, 2009.
[3] Feng Tian, Chen Frank, Rustom Khalid, Batarseh Issa.: *Pulse Frequency Modulation with Soft-switching Flyback Single-stage Inverter*. Telecommunications Energy Conference, INTELEC 2010.
[4] Van den Bossche A., Valchev V.C..: *Improved calculation of winding losses in gapped inductors.* Journal of applied physics, 2005.
[5] Nan Xi, Sullivan C.R..: *An Improved Calculation of Proximity-Effect Loss in High-Frequency Windings of Round Conductors,* IEEE Power Electronics Specialists Conference, June 2003, pp. 853-860.
[6] *Design of Planar Power Transformers.* Ferroxcube Application Note.

Evolutionary design of polymorphic digital circuits

Adam Słowik

Koszalin University of Technology, Department of Electronics and Computer Science,
2 Śniadeckich Str., 75-453 Koszalin, Poland, E-mail: aslowik@ie.tu.koszalin.pl

In the paper an application of evolutionary algorithm to design polymorphic combinational digital circuits is presented. Polymorphic electronics is a relatively new research area. In this area digital polymorphic gates have been developed [1]. The main advantage of these gates is that a single polymorphic gate can realize several different logical functions. These functions can be switched depending on the change of the value of the power voltage supply, for example; therefore, we have a possibility of circuit reconfiguration in extremely short time. To design typical combinational digital circuits one of several methods (like Map Karnaugh method, Quine-McCluskey method) or one of software developed and dedicated to optimization of digital circuits (like SIS, MVSIS, ESPRESSO) [2] can be used. However, the design process of polymorphic combinational digital circuits is more complicated. Therefore, in last time, the evolutionary algorithms [3, 4] were used to design polymorphic combinational digital circuits. Among papers dedicated for application of evolutionary algorithms to design polymorphic combinational digital circuits we can mention papers: Liang [5], Gajda [6] and Sekanina [7]. In general, in the papers [5-7], the one-dimensional pattern of gates and single-layer chromosomes have been used for design polymorphic combinational digital circuits. However in the paper [8] it has been shown that application of multi-layer chromosomes can increase the efficiency of evolutionary design of combinational digital circuits. Therefore, in this paper, the application of evolutionary algorithm with multi-layer chromosomes to design polymorphic combinational digital circuits is presented. Due to multi-layer chromosomes during the cross-over operation, the whole gates are replaced by other gates in the circuit without change of their inputs structures. In this paper, several polymorphic combinational digital circuits have been designed using proposed method. The results obtained using presented method are compared with the results taken from literature.

References

[1] Stoica A., Zebulum R., Keymeulen D.: *Polymorphic Electronics*, LNCS, Volume 2210/2001, Springer Berlin / Heidelberg, 2001, p. 291-302.
[2] De Micheli G.: *Synthesis and Optimization of Digital Circuits*, McGraw-Hill, New York, 1994
[3] Michalewicz Z.: *Genetic Algorithms + Data Structures = Evolution Programs*, Springer, Heidelberg, 1992.
[4] Goldberg D.E.: *Genetic algorithms in search, optimization, and machine learning*, Addison-Wesley Publishing Company Inc., New York, 1989.
[5] Houjun Liang, Wenjian Luo, and Xufa Wang: *Designing polymorphic circuits with evolutionary algorithm based on weighted sum method*, In Proceedings of the 7th international conference on Evolvable systems: from biology to hardware (ICES'07), Lishan Kang, Yong Liu, and Sanyou Zeng (Eds.). Springer-Verlag, Berlin, Heidelberg, p. 331-342.
[6] Gajda Z., Sekanina L.: *Gate-level optimization of polymorphic circuits using Cartesian genetic programming*, In Proceedings of the Eleventh conference on Congress on Evolutionary Computation (CEC'09). IEEE Press, Piscataway, NJ, USA, 2009, p. 1599-1604.
[7] Sekanina L.: *Evolutionary design of gate-level polymorphic digital circuits*, LNCS, Volume 3449/2005, 2005, p. 185-194.
[8] Słowik A.: *Wpływ reprezentacji rozwiązań na zwiększenie efektywności ewolucyjnego projektowania kombinacyjnych układów cyfrowych*, Przegląd Elektrotechniczny 7/2010, 2010, s. 172-174.

Signal processing of sensors with cross-sensitivity and influence of interfering variables

Sławomir Cięszczyk, Piotr Kisała
*Lublin University of Technology, Department of Electronics, 38a Nadbystrzycka Str.,
20-618 Lublin, Poland, E-mail: s.cieszczyk@pollub.pl*

Monitoring of industrial process and devices requires appropriate measurement techniques. Direct influence of industrial or environmental condition means that transducer is under influence of miscellaneous disturbing variables. The cross sensitivity problem is eliminated mainly by maintaining constant value of the interfering variable. Unfortunately this may be done only in laboratory condition.

The influence of environmental condition may be decreased or eliminated by applying various methods. Main division proceeds in sensor construction and signal processing in calibration and measurand reconstruction. Application of optical fiber insensitive to electromagnetic filed in monitoring of energetic transformers it the example of the first method. Environmental (mainly temperature) robust calibration in transformer oil monitoring can be mention as the example of second method.

Temperature is most frequent disturbing variable in industrial and environmental condition [1-3]. In one-dimensional signals from sensors it must be additional variable in calibration. During measurement process temperature should be additionally measured and it serves as a correction in measurand reconstruction.

As a alternative to dedicated sensor with one dimensional output signal a system of sensors (multi sensors) without high selectivity to observed variable is proposed. Sensitivity to particular kind of environmental influence of individual sensor in system must differ. This system is similar both to multidimensional signal in virtual sensor and to spectroscopic transducer measurement [3].

Multidimensional data (multiple sensor or multivariable output transducer) is suitable for determining relationship between sensors signals and measurand even with disturbing environmental condition. This method may require additional temperature measurement. Without temperature data temperature insensitive signals are required. Other methods include global algorithms with excess signals and temperature robust calibration (calibration data set embracing range of temperatures).

In process analysis influence of environmental condition is eliminated with the use of the following signal processing methods:

- finding temperature insensitive signals from sensors,
- adjusting signals to environmental conditions: a) sensor signals correction (before measurand reconstruction process), b) measurand correction (after measurand reconstruction process), c) measurand reconstruction algorithm correction,
- temperature robust calibration (temperature resistance measurand reconstruction).

This article will show applying of signal processing method for multidimensional data both simulated and measured under the influence of environmental condition (temperature changes).

References
[1] Nowoceń S., Mroczka J.: *Influence of temperature on accuracy of pulse oximetry measurements,* Electrical Review 10/2010, 2010, p. 289-292.
[2] Wolny S., Kędzia J.: *The assessment of the influence of temperature of selected parameters of the approximation method of depolarization current analysis of paper-oil insulation*, Journal of Non-Crystalline Solids 356, 2010, p. 809-814.
[3] Wójcik W., Cięszczyk S.: *OP-FTIR spectrometer virtual calibration for biomass combustion process diagnostics*, Electrical Review 7/2010, 2010, p. 250-252.

Equivalent circuit and electrodynamic characteristics
of waveguide-based coaxial-type microwave plasma source

M. Sobański[1), T. Izdebski[1)], M. Lubański[1)], M. Jasiński[1)], J. Mizeraczyk[1, 2)]

[1)] *Centre for Plasma and Laser Engineering, The Szewalski Institute of Fluid-Flow Machinery, Polish Academy of Sciences, 14 Fiszera Str., 80-952 Gdańsk, Poland,*
E-mail: msobanski@imp.gda.pl
[2)] *Dept. of Marine Electronics, Gdynia Maritime University, Gdynia, Poland*

We present equivalent circuit of existing waveguide-based coaxial-type microwave plasma source (MPS). The waveguide-based coaxial-type MPS was used to hydrogen production via methane reforming [1]. This MPS is operating at frequency of 2.45 GHz, in gases at atmospheric pressure. The discussed coaxial-type MPS is based on rectangular waveguide WR 430. Equivalent circuit presented in this paper cannot describe all electrical properties of the real MPS accurately, due to some structural elements, which electrical lumped equivalents are difficult to find or are unknown. We used Comsol Multiphysics software to numerical investigate of the unknown lumped input impedance of some structural elements.

The equivalent circuit includes formula which allows to calculate tuning characteristics which are one of essential indicator of power transfer from the feeding line to the MPS. The MPS is terminated with movable plunger which plays the role of the tuning element. Tuning characteristics are defined as the dependence of the P_R/P_i, the fraction of the incident microwave power reflected at the MPS input as a function of the position l_s of the movable plunger, where P_R and P_I are power reflected and power incident, respectively [2]. The powers P_R and P_I are measured in input plane of MPS setup. We present tuning characteristics calculated for different unknown values of electrical quantities. One of those quantities is lumped plasma impedance Z_p. The formula describing tuning characteristic is:

$$\frac{P_R}{P_I}\left(\frac{l_s}{\lambda_g}\right) = \left|\frac{y_{in}-1}{y_{in}+1}\right|^2 ,$$

where: l_s is the movable plunger position, λ_g is the wavelength in WR 430 waveguide, and y_{in} is the normalized input admittance of the MPS. The calculated and measured characteristics are compared. When the lumped impedances calculated by Comsol Multiphysics were included, the calculated results and results achieved in experiment were very similar for plasma impedance Z_p = 35 Ω.

Despite of the fact that the equivalent circuit describes specific MPS, it can be helpful to examine theoretically any similar waveguide-based coaxial-type MPSs.

References

[1] Jasiński M., Dors M., Nowakowska H., Mizeraczyk J.: *Hydrogen production via methane reforming using various microwave plasma sources,* Chem. Listy 102, 2008, p. 1332-1337.
[2] Nowakowska H., Jasiński M., Mizeraczyk J.: *Optimization of energy transfer in waveguide-based microwave plasma source,* 6th International Conference: New Electrical and Electronic Technologies and their Industrial Implementation NEET 2009, Zakopane, Poland, June 23-26, 2009.

Temperature and pressure properties of the resistance ZERANIN30 alloy implanted by middle energy and high dose C+ ions

T. Wilczyńska[1)], R. Wiśniewski[1)], P. Konarski[2)]
[1)] *Institute of Nuclear Energy POLATOM, 04-500 Otwock-Świerk, Poland*
[2)] *Tele and Radio Research Institute, 11 Ratuszowa Str., 03-450 Warszawa, Poland*

The main application of zeranin 30 (Cu91Mn7Sn2), like as manganin (86Cu12Mn2Ni) resistance alloy, is construction of standard resistors. From the beginning of passed age manganin and a little later zeranin are successfully used also in high pressure measurement techniques. Dependence of relative resistance on pressure of zeranin 30 pressure sensor is almost linear up to 2 GPa and changes with the pressure at the rate of about 1.5×10^{-5} MPa^{-1} (the sensor constant). Its main advantage in comparison to other metallic pressure sensors is its almost zero-sensitivity to temperature, at room temperature and at normal pressure.

The increase the value of manganin pressure sensitivity and conserve its low sensitivity to temperature after the Kr and Bi implantation on manganin properties was a subject of more complete investigations described in [1]. Investigated in this work zeranin 30 specimens were of the foil type, 20 µm thick, and of relatively large planar dimensions (1x50 mm). C+ ions of the energy 100,150 and 250 keV were implanted on one side of specimen, with doses of 3×10^{16} ionC/cm^2. Specimens before implantation and after implantations were low-thermal (130°C) long time (100 h) treated. Resistance – temperature characteristic from 4.2 K to 420 K were investigated. Wide plateau in the temperature range from -20 to +80°C was observed. That means some improvement of those characteristics. The measurement of thermo power of C implanted zeranin 30 against copper gave its markedly decrease, almost 4 times. It must be underline that thermo power of zeranin alloys is small and equal to about 2 mV/^{o}C in room temperature. Using manganin as a secondary standard and transfer pressure sensor it was, possible to compare theirs R-p characteristics. Simple calculation give information that at pressure up to 5000 bar sensitivity of zeranin sensor increases about four times and became greater then sensitivity to pressure of non implanted manganin pressure sensor, see Fig. 1. Using SIMS method of determination of concentration of metals component of zeranin, carbon and oxygen (not technological predicted component) we can treated our specimens as two layers system with carbon layer thickness about 1 µm and second layer with not changed chemical content. Using developed earlier [2] method for more accurate interpretation of implanted flat specimens it was possible to determined properties of those layer which appeared to be interesting.
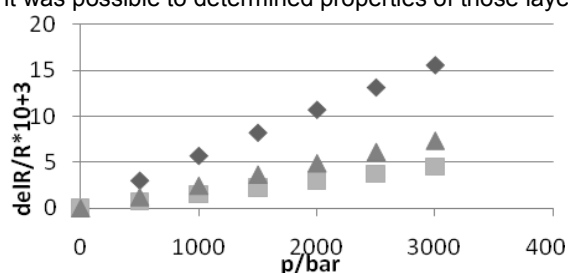
Fig.1 Relative resistance vs. pressure for (from top): Zeranin – implanted, Manganin - un implanted, Zeranin - un implanted.

References
[1] Wiśniewski R, et al, High Pres. Research 27 Nr1, p. 193-199.
[2] Wiśniewski R, et al, Electrical Review 7/2010, 2010, p. 32-35.

Equivalent circuit and electrodynamic characteristics of waveguide-based nozzleless cylinder-type microwave plasma source

M. Sobański[1], M. Lubański[1], M. Jasiński[1], J. Mizeraczyk[1, 2]

[1] *Centre for Plasma and Laser Engineering, The Szewalski Institute of Fluid-Flow Machinery, Polish Academy of Sciences, 14 Fiszera Str., 80-952 Gdańsk, Poland, E-mail: msobanski@imp.gda.pl*
[2] *Dept. of Marine Electronics, Gdynia Maritime University, Gdynia, Poland*

We present equivalent circuit of existing waveguide-based nozzleless cylinder-type microwave plasma source (MPS). The waveguide-based cylinder-type MPS was used to convert methane into hydrogen [1, 2]. This MPS operates at atmospheric pressure and frequency of 2.45 GHz. The discussed cylinder-type MPS is based on rectangular waveguide WR-430. Equivalent circuit presented in this paper cannot describe all electrical properties of the real MPS accurately, due to some structural elements, which electrical lumped equivalents are difficult to find or are unknown. We used Comsol Muliphysics software to calculate some of them.

The plasma column plunges partially into cylinders (non-symmetrically) creating two lossy coaxial lines. The central —conductor" of this lossy coaxial lines is a plasma column. Plasma is strongly non-linear element of the circuit because plasma impedance Z_p depends on incident microwave power.

One of essential characteristics of any MPS is power transfer from the feeding line to the plasma. It can be expressed as ratio P_R/P_I, where P_I and P_R are the power of the incident and reflected waves, respectively. The ratio is equal to the square of the module of the wave reflection coefficient. Tuning characteristics of the MPS is a dependence of P_R/P_I on the position of the movable short l_s normalized to the wavelength λ_g. It is easy to obtain experimentally and give an important information about the plasma source efficiency and stability.

The equivalent circuit includes formulation which allows to calculate tuning characteristics of discussed MPS. The MPS is terminated by movable short which is a tuning element. The formula describing the tuning characteristic can be written as

$$\frac{P_R}{P_I}\left(\frac{l_s}{\lambda_g}\right) = \left|\frac{y_{in}-1}{y_{in}+1}\right|^2 ,$$

where: l_s is the movable plunger position, λ_g is the wavelength in WR-430 waveguide, and y_{in} is the normalized input admittance of the MPS. We compare the calculated characteristics with the tuning characteristic of discussed MPS obtained in experiment. Despite of the fact that the equivalent circuit describes specific MPS, it can be helpful to examine theoretically any similar waveguide-based cylinder-type MPSs.

References

[1] Jasiński M., Dors M., Mizeraczyk J.: *Production of hydrogen via methane conversion using atmospheric pressure microwave plasma source with CH4 swirl,* HAKONE XI, Oleron Island, September 7-12, 2008.
[2] Jasiński M., Dors M., Mizeraczyk J.: *Production of hydrogen via methane reforming using atmospheric pressure microwave plasma,* Journal of Power Sources 181, 2008, p. 41-45.

Trust based authentication scheme for latency reduction in vehicular ad-hoc networks (VANETs)

Arūnas Andziulis, Mindaugas Kurmis, Jonas Vaupšas, Sergej Jakovlev, Valdemaras Pareigis

Klaipeda University, Informatics Engineering Department, 17 Bijunu Str., LT-91225, Klaipeda, Lithuania, E-mail: arunas.iik.ku@gmail.com

VANETs are getting more and more industry relevance, because they offer new vehicle communication services [1]. On the other hand, security of services is a major problem as typical security mechanisms are not suitable for VANETs: velocity of vehicles is higher than the normal wireless networks response time. That is why the handoff latency is crucial. In this paper, a new trust based authentication scheme is proposed which reduces the handoff latency time. The proposed systems authentication process (*AP*) is based on trust mechanism and is divided into two parts: *V2I* (vehicle to infrastructure) and *V2V* (vehicle to vehicle) communications. In the *V2V* scheme *AP* is initiated only when the vehicle connects to a new road side unit (*RSU*). All vehicles and *RSU*s are divided into different trust groups where every vehicle has assigned trust value and *ID*. In a trust group, the *RSU* thinks that vehicles within this trust group are trustable based on their services provided operations history and grants access to the network resources for them. When the vehicle wants to join the *RSU* from a different trust group, it must complete a whole authentication procedure. The authentication server constantly passes through a regularly updated table with connected nodes trust values, nodes *ID*s and information about successfully authenticated or blacklisted nodes. When the vehicle connects to other *RSU* it can use the group session key and information to generate the pair wise transient key (*PTK*). The hash functions are used to express the overall authentication process in time for *V2I* vehicle (1):

$$T_{ID_{vehicle}} = \left(t_1\left(hash\left(R_{vehicle}\right)\right) \cap t_1\left(hash\left(R_{trustRSU}\right)\right)\right) \cap$$
$$t_3\left(hash\left(PTK\left(ID_{trust}, ID_{vehicle}, GSK_{vehicle}, R_{vehicle}, R_{trustRSU}\right)\right)\right). \tag{1}$$

Here when the vehicle wants to join the *RSU* in its trust group, it generates a random number $R_{vehicle}$ and sends the authentication request packet to the *RSU*. The *RSU* first checks the trust table to find out if the vehicle is in its trust group. The *RSU* responds by sending an authentication response packet (*ASP*) with a generated random number $R_{trustAP}$. When the vehicle receives the *ARP*, both the vehicle and the *RSU* know the random generated numbers. Then both nodes can generate the *PTK* using the group session key (*GSK*), vehicle *ID*, *ID* of the *RSU* and two generated random numbers based on hash functions. The trust value plays the key role in the reduction of the handoff latency time; because vehicles that are connecting to the same trust group *RSU*s do not have to repeat the full authentication procedure. Vehicle trust based authentication (*RTV*) for *V2V* is expressed as (2):

$$T_{ID_{vehicle}} = t_1\left(RTV\left(mean\left(R_e, O_{sc}, ID_{vehicle}\right)\right)\right) \cap t_2\left(hash\left(PTK\left(ID_{trust}, ID_{vehicle}, GSK_{vehicle}\right)\right)\right). \tag{2}$$

Here R_e are the used resources by the ($ID_{vehicle}$) device and O_{sc} are the successfully completed services provided operations (based on history). The proposed authentication scheme can significantly reduce the time of the handoff procedure and thus be more efficient compared to general VANET authentication systems.

References

[1] Zhang Z., Boukerche A., Ramadan H.: *Design of a lightweight authentication scheme for IEEE 802.11p vehicular networks*, Ad Hoc Networks, 2010, In Press.

Strength of irradiated single-crystal silicon

**D.I. Brinkevich[1), V.S. Prosolovich[1), Y.N. Yankovski[1), N.V. Vabishchevich[2),
S.A. Vabishchevich[2)**

[1) *Belarussian State University, Minsk, Belarus, E-mail: prosolovich@bsu.by*
[2) *Polotsk State University, Novopolotsk, Belarus*

The irradiation in the cardinal image changes a condition of a subsystem of structural defects and, accordingly, influences physico-mechanical properties of monocrystal silicon. Influence of an irradiation on microhardness of semiconductor materials is investigated in detail enough [1, 2]. However the influence isovalent impurity on mechanical characteristics of irradiated silicon monocrystal was not investigated.

In the present work it was investigated influences of an electron (4 MeV, $\Phi = 5 \cdot 10^{12}$-$1 \cdot 10^{15}$ sm^2) and neutrons ($\Phi = 5 \cdot 10^{16}$ - $5 \cdot 10^{18}$ sm^2) irradiation on strengthing properties of the silicon single crystal doped by germanium at cultivation from melt by Czochralski method. The germanium concentration (N_{Ge}) was determined by neutron activation analysis and was varied in a range $3 \cdot 10^{18}$ - $1,7 \cdot 10^{20}$ sm^3. The interstitial oxygen concentration was measured on IR absorption spectra and was $9 \cdot 10^{17}$ sm^3 in all investigated samples. Single crystals had nominal resistivity of ~10 Ω·cm. The strength of the single crystal was assessed using microindentation method. Microhardness (H) was measured by a standard technique using a PMT-3 tester. The measurements results were analyzed using statistical methods. The microhardness data were found to follow a normal (Gaussian) distribution. Microfragility was determined by a standard technique. Factor of viscosity of destruction (K_{IC}) paid off the length of a radial crack at a print.

It is established, that Ge doping was reduced microhardness both initial and the irradiated crystals of silicon. The most strongly given effect is expressed in the neutron-irradiated samples. The Ge doping was suppresses effect of radiating hardening in silicon. The effect of radiating hardening was observed only in not Ge alloyed samples. At $N_{Ge} > 3 \cdot 10^{19}$ cm^{-2} the electron irradiation did not change microhardness. In the samples irradiated with neutrons width of casual distribution of microhardness was increased. That testifies to heterogeneity of a material and presence in silicon of defect congestion with the sizes ~1-5 microns, comparable with a size of a print at small loadings.

It is revealed, that isovalent Ge impurity reduces crack stability of silicon crystals. The Ge doping leads to increase in microfragility of silicon. Experimental results are explained in view of influence of fields of the elastic pressure created by Ge atoms in single crystals of silicon. It is shown, that the spatial charge, which formed at neutrons irradiation, increase microfragility of single crystals of silicon. Isovalent Ge impurity was suppresses the specified effect.

References
[1] Golovin Yu.I., Dmitrievskii A.A., Suchkova N.Yu: *Structure of complexes responsible for radiation-induced degradation of silicon,* Fizika tverogo tela (S.-Peterburgh) 48 No2, 2006, p. 262-265.
[2] Vabishchevich S.A., Vabishchevich N.V., Brinkevich D.I., Prosolovich V.S., Yankovskii Yu.N.: *Defect formation in silicon implanted with ~ 1 MeV/nucleon ions*, Inorganic materials 46 No12, 2010, p. 1281-1284.

Temperature and frequency dependences of impedance real part in the FeCoZr-doped PZT nanogranular composites

A.V. Larkin[1), J.A. Fedotova[2), A.K. Fedotov[1), P. Zhukowski[3), T.N. Kołtunowicz[3)
[1) *Belarusian State University, 4 Independence av., 220030, Minsk, Belarus,*
E-mail: fedotov@bsu.by
[2) *National Center of Particles and High Energy Physics of BSU, 153 Bogdanovich Str.,*
220040 Minsk, Belarus
[3) *Lublin University of Technology, 38a Nadbystrzycka Str., 20-618 Lublin, Poland*

Today the synthesis and investigation of the materials, usually called the granular nanocomposites with soft magnetic properies, are of a great interest for the material engineers [1]. Particular attention is given to the nanocomposites containing mixture of randomly distributed conductive (metallic) and nonconductive (dielectric) nanogranules Extremal values of physical parameters in such systems are usually observed while some critical concentration of metallic phase x_C is reached (when continuous conducting percolating cluster is formed from the contacting metallic particles). In accordance with percolation theory [2] the mentioned critical concentration is called the percolation threshold.

The main goal of this paper is to investigate the carrier transport mechanisms in granular nanocomposites consisting of the amorphous ferromagnetic $Fe_{0.45}Co_{0.45}Zr_{0.10}$ alloy nanoparticles embedded into low-conductive piezoelectric $Pb_{0.81}Sr_{0.04}(Na_{0.5}Bi_{0.5})_{0.15}(Zr_{0.575}Ti_{0.425})O_3$ (doped PZT) matrix according to the impedance spectroscopy method [3]. This study is based on the analysis of the temperature and frequency dependences of the nanocomposites impedance real part for the $(FeCoZr)_x(PZT)_{100-x}$ $(25 \leq x \leq 65$ at. %) samples deposited by ion-beam sputtering of complex target on glass-ceramic in argon + oxygen mixture with oxygen pressure $P_{O2} = 3.2 \cdot 10^{-5}$ and $3.8 \cdot 10^{-5}$ Torr during deposition.

It is shown that x_C value shifted to the region of higher FeCoZr concentrations with the P_{O2} increase. It is revealed that the nanocomposites transition from high-ohmic state (below the percolation threshold x_C), when samples impedance real part is weakly depending on temperature, to the low-ohmic state (beyond the x_C), when samples impedance real part temperature dependence possess exponential character (due to formation of oxide —core" around FeCoZr nanoparticles), takes place at $x_C \approx 42$ at.%. The analysis of the frequency dependences of impedance real part in the $(FeCoZr)_x(PZT)_{100-x}$ nanocomposites also confirms this conclusion.

References

[1] Skomski R.: *Nanomagnetics*, Condensed Matter 15, 2003, p. R841−R896.
[2] Stauffer D., Aharony A.: *Introduction to percolation theory*, Taylor & Francis, 2003, London, 181 p.
[3] Poklonskiy N.A., Gorbachuk N.I.: *Basis of the Impedance Spectroscopy of the Composites*, Minsk, BSU, 2005,130 p.

Defect formation processes in the monocrystal silicon plates subjected to various gettering heat treatment

**D.I. Brinkevich[1), V.I. Plebanovich[2), V.S. Prosolovich[1), A.I. Prostomolonov[3),
A.N. Pyatlitski[2), Yu.B. Vasiliev[2), N.A. Verezub[3), Yu.N. Yankovski[1)**

[1) *Belarussian State University, Minsk, Belarus, E-mail: prosolovich@bsu.by*
[2) *Open Joint-Stock Company "INTEGRAL", Minsk, Belarus*
[3) *Institute of Problem of Mechanics RAS, Moscow, Russia*

Last years the tendency to increase in duration and temperatures of thermal cycles in manufacturing techniques of modern integrated circuits was outlined. It reduces oxygen precipitates growth at the initial stage of manufacturing that can affect border at which gettering process is completely activated. In this connection it is rather important the knowledge about the thermal stage of manufacturing IC process when oxygen precipitates will begin gettering the fast diffusing transitive metals. Full gettering of Cu and Ni impurity, which specially entered in very high concentration, is reached at density oxygen преципитатов $(1.5\text{-}9) \cdot 10^9$ def./sm^3 with radiuses smaller 10 nanometers. Germs oxygen преципитатов, which created on technology MDZ or by long thermal отжигов in the furnace, can already grow till the sizes of 5 - 10 nanometers at initial stages техпроцесса manufacturing CMOS devices and to be effective геттерами. Conditions of heat treatment in manufacturing techniques modern IC can appear such, that growth oxygen precipitates will be essentially limited. The plates generated on method MDZ [1] essentially simplify the given problem as the precipitates density is set precisely by introduction of the set amount of vacancies and oxygen precipitation at vacancy defects.

In the present work processes of oxygen precipitate and other structural defects formation in plates of monocrystal silicon during the heat treatments used at manufacturing of microcircuits was studied. In parallel with control plates the plates subjected by additional stages of gettering oxygen precipitates formation by means of rapid thermal annealing (RTA) at 1190°C by duration 30 s in an atmosphere of oxygen or argon were investigated. In other set of samples, the oxygen precipitates formation oxygen преципитатов was carried out with use as the first operation of high-temperature heat treatment at 1000°C with the purpose of evaporation of oxygen.

It was established, that bulk stacking faults are by prevailing defects at the heat treatments, which not including gettering annealing. It was a formation as bulk stacking faults, and oxygen precipitates at carrying out RTA. Oxygen precipitation process was prevailed at carrying out high-temperature heat treatment for evaporation of oxygen impurity. The results was discussed a talk with the account quasichemical reactions of defect – impurity interaction between fast diffusing impurity, vacancies and oxygen precipitates.

References

[1] Voronkov V.V., Falster R.: *Effect of vacancies on nucleation of oxide precipitates in silicon*, Materials science in semiconductor processing 5, 2003, p. 387-390.

Submicron n-p-n-transistor parameters: dependence on the mode of the base region formation

**V.A. Belous[1), D.I. Brinkevich[2), V.B. Odzhaev[2), V.S. Prosolovich[2),
Yu.N. Yankovski[2)**
[1) Open Joint-Stock Company "INTEGRAL", Minsk, Belarus
[2) Belarussian State University, Minsk, Belarus, E-mail: prosolovich@bsu.by

In order to decrease the depth of the base-emitter it is necessary to increase the concentration of charge carriers in the active base during scaling in rapid thermal annealing (RTA). On the other hand, to keep the value U_{kb} we have to reduce ion implantation energy of the base at decrease the thickness of the epitaxial film [1, 2]. However, this case sharply increases nominal load resistance, which is formed under the base insulator.

We investigated the dependence of the gain n-p-n-transistor (β_N) and the nominal value load resistor on the ion implantation regimes (dose and energy) of the base region doping. The implantation regime of the base region was chosen on the basis of the following request: carriers concentration in the active base is maximum, direct current gain (at least 80) and breakdown voltage collector-base must be ≥ 9 V. Surface resistance in the base region must be within 850 ± 50 Ω/□ to ensure nominal value load resistor.

It was established that the decrease energy and dose of the base region doping can increase the β_N of n-p-n-transistor and reduce the number of RTA processes. For example, for β_N = 90 at a dose of 6.5 mkKl/sm^2, reduction energy implantation from 80 keV to 60 keV lead to decrease of number processes RTA from 5 to 3. Reducing the doses of doping (for β_N = 100) from 10 to 5 mkKl/sm^2 leads to decrease of number processes RTA from 7 to 2. The decrease of number RTA is because of carrier concentration in the base region and its width decreasing. This effect is caused the increase of the emitter efficiency and base transfer factor.

It is shown that the base doping of boron ions with energy above 50 keV and dose less 5 mkKl/sm^2 leads to the significant increase in the size of the depleted layer p-n-junction. The consequence of this is a "puncture" of the base. It is shown that the load resistor resistance increases with decreasing the dose and energy of doping and required value is reached at a dose of 10 mkKl/sm^2 and energy of 50 keV.

References

[1] Belous A.I., Emelianov V.A., Syakerski V.S.: *Proektirovanie integralnyh microshem s ponizennym energopotrebleniem*, Minsk, Interpoligraf, 2009, 320 p. *(in Russian).*
[2] Anischik V.M., Pilipenko V.A.: *Fizicheskie osnovy bystroi termoobrabotki. Getterirovanie, otzig ionnolegirovannyh sloev, BTO v tehnologii SBIS. Minsk, BGU, 2001, 149 p. (in Russian).*

Simulation analysis of variable current angle vector control and direct torque and flux vector control of synchronous reluctance motor

Radosław Machlarz

*Department of Electrical Machines and Drives, Lublin University of Technology,
Lublin, Poland, E-mail: r.machlarz@pollub.pl*

The paper deals with comparison analysis of two control strategies of synchronous reluctance motor with axially laminated anisotropic rotor: variable current angle vector control and direct torque and flux vector control (DTC). Within the first strategy two further options of control method were discussed: constant d-axis current component control and constant flux linkage control. DTC control strategy, with hysteresis regulators in torque and flux control loop and simplified circuit equations based estimators with rotor speed and position sensors, was considered. Both control strategies were analyzed on the basis of their simulation models, derived in Matlab-Simulink environment. The mathematical model of synchronous reluctance machine in d-q rotor coordinates was used in the simulations, with d-axis magnetic circuit saturation taken into account. Dynamic states of the motor were investigated, including starting, rapid changing of load torque and speed command, and braking.

Simulation results show, that although both analyzed control strategies offer good dynamic response of the motor, below base speed constant d-axis current component strategy, which is numerically less complex, appears to be a better solution for applications with low speed and high dynamic demand, whilst the DTC control, which also features good load disturbance response and speed tracking facility, has the drawbacks of high content of torque and flux pulsations and highly non-sinusoidal current waveforms.

In the conclusion, advantages and drawbacks, special features and perspectives of analyzed control strategies were thoroughly discussed, some improvements and future works were also proposed.

Literatura
[1] Boldea I.: *Synchronous reluctance machines and drives*, Clarendon Press, Oxford, 1996
[2] Kaźmierkowski M. P., Krishnan R., Blaabjerg F.: *Control in power electronics. Selected problems*. Elsevier Science, 2002.
[3] Machlarz R.: *Analiza symulacyjna metod sterowania wektorowego synchronicznego silnika reluktancyjnego przy zmiennym kącie wymuszenia*, Zeszyty problemowe – Maszyny Elektryczne 86/2010, BOBRME Komel, p. 101-104.
[4] Boldea I., Janosi L., Blaabjerg F: *A modified direct torque control (DTC) of reluctance synchronous motor sensorless drive*, Electric Machines and Power systems 28/2000, p. 115-128.

Needle type GMR sensor in biomedical applications

Adam Kurnicki

Automation and Metrology Department, Lublin University of Technology, Lublin, Poland,
E-mail: a.kurnicki@pollub.pl

This paper presents two biomedical applications in which a needle-type GMR sensor was proposed to estimate magnetic fluid weight density inside large tumors and to detect magnetic field generated by low current signals in medicine.

First application is hyperthermia therapy [1], a form of cancer treatment. Hyperthermia therapy utilizes the magnetic losses due to magnetization of magnetic nanoparticles by external alternating current magnetic fields. These magnetic losses can be dissipated in the form of heat depending on the thermal conductivity and heat capacity of the surrounding medium. The overall effect is an increase in temperature of the surrounding. This principle is applied to heat and destroy tumors since they are more sensitive to heat than normal healthy cells. Generally all parameters except the magnetic fluid weight density are known in the specific heat equation which governs the heat given in hyperthermia therapy to destroy cancer cells. Hence, accurate estimation of magnetic fluid weight density is critical for successful treatment. Special methodology to estimate magnetic fluid weight density inside the body with use needle-type giant magnetoresistive (GMR) sensor was worked out.

In second application GMR needle-type sensor was used for measurement of magnetic field generated by nervous systems [2]. A simplified nerve model was used as a source of such a magnetic field. The measurement performed by probe with a needle consisting of a sensing GMR element at the tip, showed that magnetic field generated by current signals as small as few µA can be detected as well as through layers covering the nerve. Presented experiments with nerve model is one example of a low magnetic field application, in which minimal invasive measurement is required or operations with using large size magnetometers are difficult. Small size and specific construction of needle type sensor indicates that it is a superior tool in such cases.

The needle-type GMR sensor has a good potential to be used in other medical applications such as targeted drug delivery where the needle-sensor can be used to confirm if the magnetic particles and drugs are present at a given site by detection as well as estimation of the content density for supplying heat to initiate a chemical reaction. Due considerations should also be given to improve some aspects of the proposed methods for successful implementation in clinical applications.

References

[1] Gooneratne C.P., Kurnicki A., Iwahara M., Kakikawa M., Mukhopadhyay S.C., Yamada S.: *A GMR Needle Probe to Estimate Magnetic Fluid Weight Density inside Large Tumors*, Recent Advances in Sensing Technology – Lecture Notes in Electrical Engineering, Springer-Verlag, Vol. 49, 2009, p. 1-14.

[2] Kurnicki A., Haraszczuk R., Yamada S., Kakikawa M., Stryczewska H., Wójcik W., *Detection of Magnetic Field Generated by Low Current Signals Using Novel Needle Type GMR Sensor*, W: Recent Advances In Numerical Modelling, J. Sikora, W. Wójcik, S. Wójtowicz (red.), 2009, p. 148-152.

Measurement techniques concerning droplet size distribution of electrosprayed water

Jacek Majewski

Lublin University of Technology, Chair of Automation and Metrology, Lublin, Poland,
E-mail: majewski@pollub.pl

Although the phenomenon of electrostatic spraying was discovered about the middle of the eighteenth century, its industrial applications emerged only during World War II. In the course of the electrospraying process, some electric potential difference between a capillary and a grounded surface causes the break-up of a liquid jet which emerges from a conical meniscus formed at the tip of the capillary. There are several modes of electrospraying of water, and each mode produces different droplet size distribution (DSD). The parameters of the distribution are of great importance in many applications. For example, in respirable water-based electroaerosols the droplet size distribution should be narrow, within the size range from 3 to 10 µm; droplets smaller than 3 µm are ejected during inhalations and larger than 10 µm are trapped in upper parts of the respiratory system. Knowledge of the droplet size distribution is necessary for controlling the effectiveness of the dose inhaled.

The measurement techniques used for estimation of electrosprayed droplet size distribution are similar to the techniques developed for measurements of sprays, mainly in combustion installations. There are several measurement methods suited to the measurement of liquid droplets, and the most promising are the laser-based ones. However, the instrumentation on which these methods are implemented as well as the measurement procedures are rather sophisticated. The instruments need calibration using a monodispersed droplet generator which makes the techniques even more complicated. Because of this, the analysis of accuracy of obtained DSD needs much skill and attention.

In this paper, the accuracy of DSD measurements with various types of instruments, which operating principle is based on different methods, has been discussed. Main factors influencing the measurements have been characterized, and ways of obtaining more accurate DSD measurements have been proposed.

References

[1] Babinsky E., Sojka P.E.: *Modeling drop size distribution,* Progress in Energy and Combustion Science 28, 2002, p. 303-329.
[2] Stachiewicz U. et al.: *Single event electrospraying of water*, Journal of Aerosol Science 41, 2010, p. 963-973.
[3] Hess C.F., L'Esperance D.: *Droplet imaging velocimeter and sizer: a two-dimensional technique to measure droplet size*, Experiments in Fluids 47, 2009, p. 171-182.
[4] Gajewski A.: *Procesy i technologie elektrostatyczne*, PWN Warszawa-Kraków 2000.

New method of determining electric and thermal characteristicsof Peltier device

Viktor Lozbin[1), Piotr Bylicki[1), Vitali Cuba[2)

[1) *Lublin University of Technology, Faculty of Electrical Engineering and Computer
Science, 20-618 Lublin, Poland, E-mail: v.lozbin@pollub.pl, piotrbylicki@wp.pl*
[2) *National University of Water Management and Nature Resources Use,
33028 Rivne, Ukraine*

In this article the authors propose a new method for experimental research of electric and thermal characteristics of Peltier device. Presented method differs from commonly as summary Seebeck coefficient, internal resistance (R), thermal conductivity coefficient of thermoelectric material and summarized thermal resistance of copper connections, join surfaces with structure of a heating system are simultaneously determined. The main assumption of the method is the comparison of the heat fluxes (Q_0 and Q_z) flowing through the tested thermoelectric element in open and short circuits. From theoretical deliberations for Seebeck coefficient the following equation was obtain

$$A = \left(\frac{Q_z}{I_z} - \frac{Q_0}{E_0/R} \right) \frac{1}{T_z}$$

where I_z – current in short circuit, E_0 - electromotive force in open circuit, T_z – average temperature of Peltier device in short circuit state.

To confirm that proposed method is right, prototype research set-up has been built, which can be used in temperatures from -20°C to 50°C. To achieve low temperatures, two stage cooling method with liquid thermal carrier was invented. Analysis of result data shows that measured accuracy of figure of merit is +/- 2%.

References

[1] Rowe D.M.: *Thermoelectrics Handbook – Macro to Nano*, edited by D.M.Rowe, Ph.d., D.Sc., 2006.
[2] Rasit Ahiska: *New Method for Investigation of Dynamic Parameters of Thermoelectric Modules*, Turk J Elec Engin 15 no1, 2007.
[3] *Greber G*., *Erk S*., Grigull U.: *Principles of Heat Exchange*, Translation from the German edited by Prof. A. A. Gukhman 1958.
[4] Chirkin V.S.: *Thermal Conductivity of Industrial Materials*, Fd.2 (in Russian), Mashgiz, Moscow,1962.

Methods and optoelectronic means for human eye retina metabolism estimation

**A.I. Kubarko[1), S.A. Lisenko[2), A.A. Skobliakov[2), V.A. Firago[2),
M.M. Kugeiko[2), O. Hotra[3)**

[1) *Belarusian State Medical University, Minsk, Belarus, E-mail: kubarko@bsmu.by*
[2) *Belarusian State University, Minsk, Belarus*
[3) *Lublin University of Technology, Lublin, Poland*

Human eye plays role of a key for functional state of the different human organism systems estimation. In particular, in accordance to the system arterioles pathology hypothesis, system hemodynamic disruption accompanying large number of modern diseases, leads to the blood flow characteristical parameters change not only in the problematic organ but in every nexus of the blood net, including retina vessels. Malfunction of the nutrients supply system leads to the incorrect retina functioning. This is a premise for the way of discovering retina metabolism disruption with the help of special equipment on preclinical or early clinical stages of vessel system diseases by studying visual system performance. That is why the task of creation of new generation diagnostic complex for diagnosis starting signs of vessels pathologies or inclinations to them is very actual. This complex will also help to qualitatively and quantitatively estimate treatment efficiency.

In our report the method for eye retina metabolism estimation and structure of the complex is discussed in details. Most difficulties are associated with necessity to construct blood oxygenation map of the retina, because it is practically impossible to compare measured values of SaO_2 with true one without direct invasive intervention. Therefore we are forced to use indirect optical methods for SaO_2 estimation studying spectral composition of the reflected from retina light. This method is approbated for well distinguished large retinal vessels but to construct 2D hemoglobin oxygenation map in small capillary vessels we need adequate optical model for incoming light distribution in optical mediums of the retina. Here we consider multispectral method for light registration and processing on three wavelengths where absorption coefficients of the two forms of hemoglobin (oxygenated and not oxygenated) are equal and maximally differ and on some additional wavelength to take into account individual retina features. Concrete values of additional wavelength, their optimal number and requirements to the backscattered light measurement accuracy we propose to chose with help of the numerous regression method and multilayered retina model with varied geometrical and biophysical layers parameters. We used four layered structure for retina optical model construction and transmittance, absorption and scattering coefficients for these layers were taken into consideration. It was demonstrated that modeled with the help of our model retina reflection spectrums are very close to ones registered experimentally. This model gives an opportunity to specify and correct parameters, which will be helpful on the stage of experimental research to determine polynomial coefficients, which link SaO_2 with values of backscattered light $R(\lambda_i)$ on selected wavelengths λ_i. The errors estimation was performed by biophysical parameters and retina layers thicknesses variation and showed that optimal wavelength selection leads to relative errors of hemoglobin concentration determination at about 7% and 2 - 3% for SaO_2.

Oculographic means for human eye retina functional state estimation

A.A. Skobliakov[1], A.I. Kubarko[2], V.A. Firago[1], I.S. Gurski[2], O. Hotra[3]
[1] *Belarusian State University, Minsk, Belarus, E-mail: firago@bsu.by*
[2] *Belarusian State Medical University, Minsk, Belarus*
[3] *Lublin University of Technology, Lublin, Poland*

Electrooculography and electroretinography are widely used by ophthalmologists for human retina functional state estimation. Electrooculography is used for resting potential (RP) registration which is formed on the cornea and retina boundary due to biochemical processes in cells. This potential is an integral characteristic of retina pigment epithelium and photoreceptors functioning and directly depends upon maintenance of retina energetical needs as one of the most metabolically active organs of human being. The absolute RP value registered by electrodes varies with eye ball movement and with retina metabolic mechanism malfunction.

To answer the question what is the cause for RP variation an electrooculography method with video fixation is proposed by the authors. The idea of method is in synchronous electrooculogram and videooculogram registration with the help of IR video camera with 125 Hz frame frequency and resolution 640x480 pixels. When video recording is performed eyes are illuminated by low intensity IR source to enhance pupil contrast. Video sequence is used to insure whether variation in electrooculographic trend was caused by eye movement or not. This method is also well suited for pupil diameter variation estimation during tests.

When registering saccadic eye movements potentials acquired by electrodes resemble idealized square pulses with sharp fronts. Their amplitudes lies in the range between 250 µV and 1000 µV and RP values is about 70 µV. This sets some requirements to the electronics for their acquisition. To eliminate transition processes inherent to general electrooculographs with input filters which doesn't pass DC component of the biopotentials we've developed digital electrooculograph with extended dynamical range of registered signals on the base of 4 channel 24-bit sigma-delta ADC. The ability to capture potentials in the range from tenth microvolts to hundreds millivolts gives a possibility to acquire signals keeping DC component. Slow base line drift due to electrode polarization and movements is corrected by using sliding window and parabolic permanent component interpolation in the window involving signals lying next to the window borders. Digital electrooculograph has better frequency characteristic and resolution in comparison to currently used.

The absolute value of RP as integral indicator of retina functional statement does not answer the question what is the cause of its deviation from norm. The key for understanding this lies in investigation of correlation between retina cells functioning and biochemical processes proceeding in them which are maintained by local retina blood system. The necessity to find out correlations between integral characteristics of the retina functional state and metabolism provision mechanism is obvious for us and requires complex approach.

Ways of increasing the distance range of the portable laser rangefinders in the range of 1.5 microns

V.A. Firago[1),]I.P. Petrovich[2),]A.S. Buiko[2),]W. Wojcik[3),]D.V. Shumak[1)]
[1)]*Belarusian State University, Minsk, Belarus, E-mail: firago@bsu.by*
[2)]*LEMT Scientific and Technical Centre of the BelOMO, Minsk, Belarus*
[3)]*Lublin University of Technology, Lublin, Poland*

In recent years, producers of laser rangefinders pay much attention to the spectral range of 1.5 microns, which is safe for the organs of sight. There appeared compact rangefinders, which use pulse semiconductor injection lasers with peak power 200 W, pulse duration 40 ns and repetition rate of 100 Hz. The usage of digital signal accumulation for approximately 100 ms enables to measure the distance to objects remote on 2 - 3 km. The tasks of increasing the repetition rate and power of the emitted pulses and improving the threshold sensitivity of the photo detector channel of the rangefinder are topical problems for the increasing the distance range of pulse rangefinders.

Increasing power of the emitted pulses while saving size of the rangefinder is possible due to using solid-state light emitters pumped with laser diode. The investigation of the prototypes of a miniature pulse erbium glass lasers with diode pumping and a passive switch based on a crystal of magnesium-aluminum spinel doped with divalent cobalt, $Co: MgAl_2O_4$ (developed by the LEMT Scientific and Technical Centre of the BelOMO), has shown the possibility of their use in compact rangefinders. In the Q-switched mode when changing the concentration of the activator (trivalent erbium) from $0.25 \cdot 10^{20}$ cm^{-3} to $1.3 \cdot 10^{20}$ cm^{-3} the following parameters were obtained: generation wavelength – 1.534 microns, pulse energy – from 5 to 45 µJ; pulse duration – from 5 to 15 ns at a repetition rate from 1.0 to 7.5 kHz, and peak power – from 0.25 to 3 kW. The pumping was provided with the input of the laser diode radiation with the wavelength of 970 nm and power of 6 W into the active element.

The second direction is to increase the threshold sensitivity of the photo detector channel of a rangefinder. The report considers the schemes of photo detecting units of the pulse rangefinders, the characteristics of modern avalanche photodiodes based on InGaAS and estimates the achievable threshold sensitivity of the photo detecting channel.The advantages and disadvantages of using the dynamic high-frequency biasing of operating point of the avalanche photodiode are analyzed.

It is shown that for providing the distance range of the rangefinder more than 3 km it is necessary to use the digital accumulation of the recorded reflected signals within 100 milliseconds and the digital filtering consistent with the shape of the emitted pulse. A functional scheme of photo detecting channel and the results of the modeling of the distance measurement process using a standard reflective object (in view of the photo detecting channel noises and atmospheric transmission) are presented. Possible schemes and the effectiveness of applying a temporary automatic control of the amplification of the photo detector channel, as well as the ways of synchronization of the samplings produced by high-speed analog-to-digital converter with the moments of the formation of laser pulses are analyzed.

Photometric methods of estimation visual system light sensitivity and its variations under hemodynamic dysfunctions

**A.I. Kubarko[1], N.P. Kubarko[1], O. Hotra[2], D.A. Aleksandrov[1],
U.A. Kubarko[1], I.S. Gurski[1]**
[1] Belarusian State Medical University, Minsk, Belarus, E-mail: kubarko@bsmu.by
[2] Lublin University of Technology, Lublin, Poland

For blood flow estimation in retina vessels the methods of doplerography, fluorescent angiography, optical coherent tomography, photoregistering are used. They give to physician valuable information about arterias, arteriols, venuls and veins state but don't allow to estimate whether blood flow in microcirculatory bed vessels is sufficient or not for visual functions support. It's known that retina and others structures of the visual system are among ones most metabolically active in organism and light sensitivity depends on blood flow.

Taking into account this dependency we studied an opportunity to use parameters of threshold and contrast-color sensitivity (CCS) as markers of the blood flow state in the visual system vessels. Estimation of these parameters was performed by modified computer perimetry method. Light stimulus with gradually increasing intensity from minimum to maximum during 6 s was formed on the computer display in front of which a patient was sitting.

For photopic cones CCS investigation a visual object as small red square with 2x2 mm dimensions was formed on the dark-gray display background (about 0.1 kd/m^2). At his minimal intensity value illumination on the patient's face was about $1.1 \cdot 10^{-6}$ lux and at maximal – about $4.1 \cdot 10^{-5}$ lux. For rods threshold light sensitivity (TLS) investigation the same white colored visual object was formed on the display at minimal intensity of which face illumination was about $1 \cdot 10^{-7}$ lux and at maximal - $5 \cdot 10^{-7}$ lux. Before measurements subjects were dark adapted.

It was discovered that visual system CCS of the healthy young people (18-30 years old) was in the range of $0.78 \pm 0.09 \cdot 10^{-5}$ lux and decreased with age. CCS of the 30 young people the same age rank with increased arterial blood pressure (1 - 2 arterial hypertension stage) was greatly decreased comparing to healthy subjects and lied in the range $0.9 \pm 0.18 \cdot 10^{-5}$ lux. Investigation of bulbar conjunctiva state of this group by means of digital video recording with post analysis found out vasospasm predisposition signs presence and positive correlation between CCS and parameters of the eye microcirculatory vessels state. TLS was about $2.4 \pm 0.3 \cdot 10^{-7}$ lux at healthy subject group and there was a moderate positive correlation between its value and diastolic arterial pressure.

Outstanding CCS decrease was discovered in 45 patients with ischemic optical neuropathy characterized by hemodynamics disruption in optical nerve and retina vessels caused by atherosclerosis, increased arterial pressure, vasculitis, vasospasm. The degree of CCS was maximal at strong optical neuropathies, sensitivity had not recovered to normal degree after treatment and was one of the cause of patients life quality reduction.

Light estimation using light probe devices

Przemysław Mazurek
West Pomerania University of Technology, Szczecin, Department of Signal Processing and Multimedia Engineering, 10 26. Kwietnia Str., 71-126 Szczecin, Poland
E-mail: przemyslaw.mazurek@zut.edu.pl

Light measurements are very important for the modeling of objects' illumination in computer graphics. There are different techniques of light modeling. The light sources modeling technique is usually used. This technique is not sufficient for realistic scenarios and complex configuration. Another technique is based on the measurement of incident light in real environment [1]. Such measurement allows lighting of objects using measurements only by the application of the light sphere. This sphere is a light filter used for modification of light rays emitted from the sphere to the centre of sphere. Light probe measurements are obtained using spherical or hemispherical panorama acquisition techniques. The multiple image stitching (panoramic technique) and single image (light probe based) techniques are used typically. The light probe device is spherical or hemispherical mirror placed in the measurement point. The camera is used for acquisition of the reflected hemispherical light from this mirror. Conversion of the circular area to the spherical image projection is necessary for application in computer graphic software.

The light probe measurements are limited to the selected point only. Multiple light probe acquisitions for large objects and different position of objects are necessary. Automatic light probe extraction from the large image set is necessary. Finding of the circular flange of the light probe is possible using the Hough Transform (HT) [2], that is proposed in [3].

The circular HT is time consuming algorithm and processing of the single frame takes tens of minutes, so faster processing technique is necessary. Implementation of HT using more optimal code and processing platform would be used for processing time reduction. Another approach, based on modeling of the motion of the light probe, is proposed in this paper. The first two frames are processed completely, but next frames are processed only in selected area (due to motion estimation) and in selected diameter range (due to estimation of distance changes between the camera and the light probe device).

Different tracking techniques, based on motion estimators for reduction of computation time, are compared in this paper. It is necessary for application of the light probe measurements for objects rendering. Light probe technique is also valuable for complex light configuration and reduces rendering time.

References
[1] Debevec P.: *Rendering Synthetic Objects into Real Scenes: Bridging Traditional and Image-based Graphics with Global Illumination and High Dynamic Range Photography*, SIGGRAPH 98, 1998, p. 189-198.
[2] Hough P.V.C., Arbor A.: *Method and Means for Recognizing Complex Patterns*, US Patent no.3, 1962, 069,654.
[3] Mazurek P.: *Estimation of position of the light probe device for photorealistic computer animation purposes*, Elektronika – konstrukcje, technologie, zastosowania, R. LII no1, 2011.

Pyrometric methods of measuring the true temperature of heated metals

V.A. Firago[1), A.G. Sencov[2), W. Wojcik[3), Y.V. Chorba[1)

[1) *Belarussian State University, Minsk, Belarus, E-mail: firago@bsu.by*
[2) *Belarussian State Agrarian Technical University, Minsk, Belarus*
[3) *Lublin University of Technology, Lublin, Poland*

To provide the quality of production of the machine building enterprises it is required a permanent control of the temperature of metals in technological processes of furnace hardening, pressing, forging, etc. Usually to measure the temperature they use brightness pyrometers (the partial radiation pyrometers) or the spectral ratio pyrometers. To measure metal's true temperature T by pyrometers of these types one needs to know and to enter down into the pyrometer the value of the emissivity (emittance coefficient) of the controlled surface or the ratio of emissivities in the two spectral bands. The emissivity value depends on many factors so its precise measuring is often impossible in working conditions at the machine building plant. Besides, the list of produced lots of metal details is often quite long, but the lot sizes are small. Therefore is very actual today the task of finding out the new ways of measuring metals' true temperature that would be invariant to changes and non-uniformity of the emissivity and wouldn't complicate significantly the construction of pyrometers.

There are several types of pyrometers that allow determining the true temperature of the body by registering thermal radiation of the heated surface in three narrow spectral bands (at three wavelengths). But their construction is rather complex as there are used rotating interference filters for spectral selection of the registered radiation, besides, they aren't able to eliminate the influence of non-uniform distribution of the emissivity across the controlled surface. To overcome these drawbacks there is suggested in this paper to use pyrometers based on commercially produced three spectral multi-element matrices of photo detectors on Si.

In the paper are discussed in details the drawbacks of the known poly-chromatic methods of pyrometry. There is shown that the carry-over factor between the errors of measuring the radiation flows and the error of measuring the temperature increases with the increase of the number of wavelengths used for registering the body's thermal radiation. If the additional a priory assumptions about the emissivity are used, for example, if the spectral distribution of emissivity is assumed to depend linearly on wavelength, then it is necessary to register thermal radiation at just three wavelengths. But the linear dependence of metals' spectral emissivity on wavelength is usually observed in quite narrow spectral region. That restricts the choice of intervals $\Delta\lambda$ between spectral bands used in pyrometer and leads by-turn to increase of the temperature measurement error. To overcome this contradiction in the paper are analyzed possible ways of determining the true temperature by using three spectral bands with their central wavelengths closely situated to each other one at the intervals of $\Delta\lambda \approx 100$ nm between. There is shown that at such spectral intervals between the used spectral bands one can competently assume linear approximation of the spectral dependence of the emissivity $\varepsilon(\lambda)$. There are suggested methods of determining the temperature providing the measurement ratio error of 0.01 without any a priory information about the metal's emissivity. There are also described ways of determining the true temperature at non-linear approximation of spectral emissivity $\varepsilon(\lambda)=a+d/\lambda$. There are specified the limitations of applying proposed methods for permanent control of metals' temperature in working conditions at the machine building plant.

Quasi-chemical modeling of point defects in iodine-doped cadmium telluride

U. Pysklynets

Ivano-Frankivsk National Medical University, 2 Galitska Str., 76018 Ivano-Frankivsk, Ukraine, E-mail: pysklynets@pu.if.ua

Cadmium telluride crystals have long been the subject of extensive studies owing to their special physicochemical properties, which make CdTe attractive material for high-efficiency optoelectronic devices and nuclear radiation detectors. An important issue is to study the physicochemical properties of halogen-doped CdTe crystals.

The influence of high-temperature processing conditions on the defect structure and physicochemical properties of iodine-doped cadmium telluride has been analyzed in terms of quasi-chemical defect reactions and equilibria in a heterogeneous system comprising an imperfect doped crystal and vapor.

To analyze the defect state of CdTe<I>, we examined two models:

- a model that included I_{Te}^+ substitutional defects and their complexes with native point defects, $(V_{Cd}^{2-}I_{Te}^+)^-$ and $(V_{Cd}^{2-}2I_{Te}^+)^0$, and

- a model that, in addition, took into account the formation of DX^- centers.

Without allowance for DX^- centers, there was unsatisfactory agreement between the calculated carrier concentration and the high-temperature Hall measurement results.

Both models took into account the formation of electrically inactive precipitates: some of the iodine atoms were thought to be aggregated.

The results suggest that the role of the iodine dopant in CdTe crystals is connected with the I_{Te}^+, substitutional defects; their complexes with native point defects, $(V_{Cd}^{2-}I_{Te}^+)^-$ and $(V_{Cd}^{2-}2I_{Te}^+)^0$ and the DX^- center.

The formation of the $(V_{Cd}^{2-}I_{Te}^+)^-$ complex and DX^- center can be represented by the quasi-chemical reactions

$$I_{Te}^+ + V_{Cd}^{2-} \Leftrightarrow (I_{Te}^+ V_{Cd}^{2-})^- \equiv A^- , \quad K_{A^-} = \frac{[(I_{Te}^+ V_{Cd}^{2-})^-]}{[I_{Te}^+][V_{Cd}^{2-}]} ;$$

$$I_{Te}^+ + 2e^- \Leftrightarrow DX^- , \quad K_{DX^-} = \frac{[DX^-]}{[I_{Te}^+]n^2} .$$
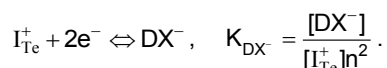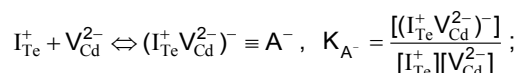
The mass-balance constraint has the form

$$I_{tot} = [I_{Te}^+] + [A^-] + [DX^-] .$$

The electroneutrality condition is given by

$$n + [V_{Cd}^-] + 2[V_{Cd}^{2-}] + [Te_i^-] + [A^-] + [DX^-] = p + 2[Cd_i^{2+}] + 2[V_{Te}^{2+}] + [I_{Te}^+].$$

The concentrations of native point defects, impurities, their complexes, and charge carriers have been determined as functions of two-temperature annealing parameters (annealing temperature and cadmium vapor partial pressure).

The equilibrium constants of formation of the $(V_{Cd}^{2-}I_{Te}^+)^-$ acceptor complex $K_{A^-} = 2 \cdot 10^{-29} \exp(-2.5/kT)$ and DX^- center $K_{DX^-} = 2 \cdot 10^{-40} \exp(-1.0/kT)$ have been evaluated.

Application of thin films based on indium and tin oxides as functional elements of electronic devices

Valery Luhin[1), Vitaly Zarapin[2), Ivan Zharsky[1), Tomasz N. Kołtunowicz[3)
[1) *Belarusian State University of Technology,13A Sverdlova Str., 220006 Minsk, Belarus,*
E-mail: Luhin_Valery@mail.ru
[2) *Belarusian State University of Economics, 7 Sverdlova Str., 220050 Minsk, Belarus*
[3) *Lublin University of Technology, Department of Electrical Devices*
and H.V. Technology, 38a Nadbystrzycka Str., 20-618 Lublin, Poland

Over the last decades, the use of transparent conducting oxide coating has increased exponentially for many applications due to its low sheet resistance and the high optical transparency. The most important transparent conducting materials are indium and tin oxides and their dopped composition. At the present time the thin indium and tin oxides thin films are widely applied to creation of transparent spending coverings, heterogeneous catalysts, IR-reflectors, monochromators, solar cells, photoelectrochemical electrodes, MOS-structures, heterojunction, etc.

In this work we cover the main tendencies in the development of the technologies of transparent semiconducting thin films based on indium and tin oxides and their composition using for various types functional elements of electronic devices. The special attention is devoted to the transparent conductive indium and tin oxides thin films materials that are used for liquid displays, organic light emitted diodes and displays, solar cells and thin-films transistors.

We also present results to use of indium oxide and tin oxides films as a gas sensitive material. In view with an opportunity of increase of the gas sensitivity and selectivity by modification their chemical composition and structure [1, 2].

As shown from the different methods of deposition indium and tin oxides layers the most perspective are vacuum methods which allow ensuring high purity, reproducibility, compatibility with microelectronic technologies.

References

[1] Luhin V., Zarapin V., Zharsky I.M., Zukovski P., Kolasik M., Kozak C.: *Zastosowanie sensorów termoelektrycznych do analizy gazów,* Elektronika 6/2008, 2008, p. 262-264.
[2] Лугин В.Г., Жарский И.М., Жуковски П.: *Получение газочувствительных структур на основе тонких пленок оксида индия и их физико-химические свойства*, Przegląd Elektrotechniczny 7/2010, 2010, p. 272-275.

The electrophysical properties of thin nanocrystalline tin dioxide films obtained by thermal oxidation

Vitaly Zarapin[2], Valery Luhin[1], Ivan Zharsky[1], Pawel Zhukowski[3]

[1] *Belarusian State University of Technology,13A Sverdlova Str., 220006 Minsk, Belarus,*
E-mail: Luhin_Valery@mail.ru
[2] *Belarusian State University of Economics, 7 Sverdlova Str., 220050 Minsk, Belarus*
[3] *Lublin University of Technology, Department of Electrical Devices*
and H.V. Technology, 38a Nadbystrzycka Str., 20-618 Lublin, Poland

In this work laws of change of structural and electrophysical parameters semiconductor nanocrystalline tin dioxide films with thickness 30 - 50 nanometers obtained by thermal oxidation of thin tin films, received by a DC magnetron sputtering method in argon.

The purpose of the work is determining optimum modes of thermal oxidation of tin films for formation tin dioxide films with stabile electrophysical properties. The use of various conditions and temperature modes of oxidation allows operating structure, stoichiometry and composition of films and, as consequence, its electrophysical and sensor properties.

Structure, phase structure, morphology of a surface and a chemical composition of received films have been investigated by methods of electron diffraction, TEM, SEM, AES, ESCA, SIMS. The temperature dependence of conductivity and thermal-EMF with study of physical properties was measured.

It was found that the semiconductor tin dioxide films continuous nanocrystalline structure whis advanced surface and non-uniform distribution of element on thinckness. For the description of phisical properties of films is the barrier model of electrocarry whis the mechanism under of tunnelingmost acceptable. the dasis parameters of the barriers are established.

The obtained results may be used to create highly sensitive and selective sensors for detecting gas mixtures containing CO, NO_2 and NH_3 [1, 2].

References
[1] Luhin V., Zarapin V., Zharsky I.M., Zukovski P., Kolasik M., Kozak C.: *Zastosowanie sensorów termoelektrycznych do analizy gazów*, Elektronika 6/2008, 2008, p 262-264.
[2] Лугин В.Г., Жарский И.М., Жуковски П., Партыка Я.: *Использование термоэлектрических эффектов тонких полупроводниковых пленок для создания химических газовых сенсоров*, Przegląd Elektrotechniczny 3/2008, 2008, p. 174-177.

Structure and electrical properties of the layered single crystals TlGaSe$_2$ and TlInS$_2$

A.K. Fedotov[1], M.I. Tarasik[1], T.G. Mammadov[2], I.A. Svito[1], P.W. Zhukowski[3], T.N. Kołtunowicz[3], K. Nowacki[3], M.Yu. Seyidov[4], R.A. Suleymanov[5], V. Grivickas[5], V. Bicbaevas[5]

[1] *Belarusian State University, 220030 Minsk, Belarus, E-mail: fedotov@bsu.by*
[2] *Institute of Physics of Azerbaijan National Academy of Science, Baku, Azerbaijan*
[3] *Lublin University of Technology, Lublin, Poland*
[4] *Gebze Institute of Technology, Gebze, Turkey*
[5] *Vilnius University, Vilnius, Lithuania*

The ternary compounds $A^3B^3C^6_2$ belong to the group of chalcogenide semiconductor crystals with layered structure. At room temperature these crystals have a space symmetry group of *C2/c* [1]. It has been established [1] that, on cooling, some of these crystals exhibit a sequence of structural phase transitions which accompanied by peculiarities on temperature dependencies of different properies – dielectric, elastic, etc.

This paper is devoted to the study of the surface structure and some electrical properties of TlGaSe$_2$ and TlInS$_2$ crystals. The single crystals were grown and doped with Ag, B, Tb, Er and Al impurities in evacuated quartz tubes by using the modified Bridgman method. The samples, which were in rectangular form, were oriented along the polar axis which lies in the cleavage plane (the morphology of crystals permits cleavage to plane parallel plates with mirror-like surfaces). For electrical measurements the plates were gently polished, cleaned and covered with silver paste for the formation of the electrical probes for electric and photoconductance measurements.

SEM investigations of the grown single crystals have shown that surfaces of their normally-spaced faces displayed layered-like structure either with smooth or piramid-like terraces.

The study of inequilibrium carriers life times τ using photoconductance drop kinetics and microwave probed photoconductivity transient technique displayed that it is 5 - 7 µs for 77 K and 10 - 15 µs at 295 K for the undoped crystals. There were observed that $\tau \sim n^2$ (when concentration of inequilibrium carriers n is higher than $2 \cdot 10^{16}$ cm^{-3}) that is feature of Auger recombination. For the doped crystals τ was between 1 and 10 ns depending on type of doping impurity.

For the doped crystals frequency dependence of real part of impedance *G(f)* at 300 K in the range of 100 Hz $< f <$ 30 MHz revealed power-like dependence $G \sim f^\alpha$, where α values are strongly dependent on the frequency range changing from 0.18 to 1.8 that is characteristic for AC hopping conductance for the model described in [2].

In the crystals TlGaSe$_2$ and TlInS$_2$, using method of temperature dependencies of DC resistivity in the temperature range of 77 - 300 K, the phase transitions at the temperatures of the order of 240 K and 105 - 120 K were observed.

References
[1] Panich A.M.. *Electronic properties and phase transitions in low-dimensional semiconductors*, J. Phys.: Condens. Matter, 20, 2008, p. 3-31.
[2] Żukowski P., Kołtunowich T., Partyka J., Węgierek P., Kolasik M., Larkin A., Fedotova J., Fedotov A., Komarov F., Vlasukova L.: *Model przewodności skokowej i jego weryfikacja dla nanostruktur wytwarzanych technikami jonowymi*, Przegląd Elektrotechniczny 84, 3/2008, 2008, p. 247-249.

Study properties of thin film ZnO by (CVD) before and after annealing

**A.D. Pogrebnyak[1), N.Y. Jamll[2), G.A-K.M. Mommed[3), J. Partyka[4)

[1) *Ukraine Sumy Institute for Surface Modification, P.O.Box 163, 40030 Sumy, Ukraine,*
E-mail: apogrebnjak@simp.sumy.ua
[2) *University of Mosul, Mosul, Set Culture, Iraq, E-mail: nawfaljamil@yahoo.com*
[3) *Sumy State University, 2 Rimsky-Korsakov Str., 40002 Sumy, Ukraine,*
E-mail:kareem1959@yahoo.co.uk
[4) *Lublin University of Technology, Lublin, Poland*

Zinc oxide ZnO is an n-type semiconductor with a wide direct band gap of 3.2 eV at room temperature belong to II-VI compound group [1]. Thin films of ZnO has many application in term of radioactive binaries and in solar cells, so that the thin films ZnO has achieved a great success at recent years as transparent conductor oxide (TCO) on what it has processed of a good optical and electrical properties with wide gap energy [2] ZnO is considered one of the Zn compounds well-known and not being dissolved by water but easily dissolves by acid to produce solution with positive ion ,and with acids it produces negative hydrocrcozonat ,also when heated ZnO it turns to yellow and turns white by cooling it [3], Several deposition techniques have been used in preparing ZnO thin films including chemical vapor deposition(CVD), spraying, sol-gel, pulsed laser deposition,chemical bath deposition.

In this paper we will prepared thin films from transparent conductive oxide(TCO) ZnO pure by (CVD) with different temperature (400, 450, 500) ,the results from the X-ray diffraction show that all the pure ZnO thin films had that the crystal structure of the deposited thin film are multi – crystalline ,also there are many peaks with higher intensity value from the rest at level (0 0 2) and with diffraction angles: ZnO 1,($2\theta = 34.76$), ZnO 2, ($2\theta = 34.34$), ZnO 3, ($2\theta = 34.74$), this indicates the preferred direction for the growth was (0 0 2)). The optical measurements have shown spectrum of transmittance as a function of wave length, the decrease of wave length , as its value very high at the wave length which is located with in optical spectrum and infra – red radiation, which indicates that these films have large energy gap to allow most of the visible light to pass and the transmittance value increases by increasing substrate heat degree, which leads to improve the crystal structure. Optical Microscopic test has been used to test the regularity and homogeneity of the prepared films in addition to study the affect of annealing on them and we have reached that the annealing process has increased the area and size of the prepared ZnO grains and increase the distance between them.

References
[1] Shan F.K., Yu Y.S.: *Band gap energy of pure and Al-doped ZnO thin films*, Journal of the European Ceramic Society 24, 2004, p. 1869-1872.
[2] Young-Sung Kim, Weon-Pil Tai, Su-Jeong Shu: *Effect of preheating temperature on structural and optical properties of ZnO thin films by sol-gel process*, Thin Solid Films 491, 2005, p. 54-60.
[3] De Merchant J., Cocivera M.: *Preparation and doping of zinc oxide using spray pyrolysis*, Chemistry of Materials 7 №9, 1995, p. 1742-1749.

Formation of micro- and nanostructured phases in the coatings based on Ni-Cr and Co-Cr, their structure and properties

M.V. Il'yashenko[1), 2)], V.M. Rogoz[1), 2)], A.V. Pshyk[1), 2)], D.L. Alontseva[3)], N. Prohorenkova[3)]

[1)] *Sumy Institute for Surface Modification, Sumy, Ukraine*
[2)] *Sumy State University, Sumy, Ukraine, E-mail: aleksandrpshik@rambler.ru*
[3)] *East-Kazakstan State Technical University, Ust-Kamenogorsk, Kazakstan*

Applying a layer of protective coating on a steel can make it highly resistant to impact, rust, and scratches, and can allow it to withstand high temperatures.

Difference in phase composition and mechanical properties of this coatings before and after duplex processing have been established. After duplex processing coatings have high nano- and microhardness, wear resistance and corrosion resistance in sea water. The improvement properties of coatings after duplex processing attain through phase conversion, smoothing coating roughness and its homogenization upon melting by plasma jet.

For the coating applied in 2 passes of the plasma jet, characterized by the formation of surface oxides of chromium and cobalt. Chromium content decreases with depth from the surface. Cobalt in the coating forms a solid solution with iron, with a primitive cubic lattice. The iron content in the coating is locally increased in comparison with the original powder coating. Observed X-ray amorphous structure of the upper layers of the coating and the transition to a substrate layer, which indicates the formation of these layers of nanoscale components. In general, the methods of X-ray diffraction and scanning electron microscopy with energy dispersive analysis revealed layer by layer structure of AN-35 coating deposited by plasma detonation. On the surface coating a thin layer containing oxides, carbides and nitrides of Co and Cr, as well as carbon and compounds with Ni (Cr_7Ni_3, $Ni Cr_2 O_4$, NiFe). The middle layer coating contains high content of elements of Co and Cr and phases based on them, mostly in compounds with iron. The basis of the coating is a solid solution CoFe with a primitive cubic lattice. Despite the low weight. Fe content in the coating composition, the compounds and solid solutions based on it dominate the coverage. Characteristically, the peaks of Co with the hcp lattice in this coverage do not. Adjacent to the substrate, the coating consists mainly of solid solution of CoFe with a primitive cubic lattice, but the phases containing Cr, it does not contain.
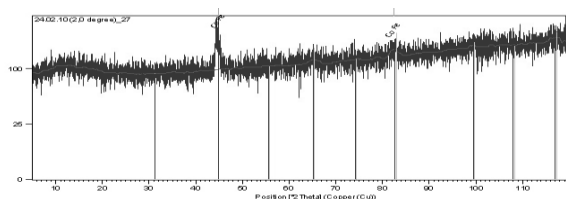
Fig. 1. X-ray diffraction pattern of the coating layer of AN-35, adjacent to the substrate, taken at a small angle of 2°

References
[1] Celik E., Ozdemir I., Avci E. et al.*: Corrosion behavior of plasma sprayed coatings*, Surface and Coatings Technology 193 №1-3, 2005, p. 297-302.
[2] Pogrebnjak A.D., Alontseva D.L. et al.: *The Effect of Electron beam Fusion on the Structure and Properties of Plasma Jet Sprayed Nickel Alloy Coating*, Technical Physics Letters 30 №2, 2004, p. 164-167.

Structure and properties of Co-Cr coatings
after a pulsed jet treatment

S.N. Bratushka

Sumy State University, 2 Rimsky-Korsakov Str., 40007 Sumy, Ukraine,
E-mail: s_bratushka@mail.ru

Goal of this work was to study the structure and properties of powder materials on Co-Cr base deposited using the high-velocity plasma-detonation jet on (321 stainless steel with Mo) the stainless steel substrate before and after this plasma jet treatment applying also coating surface layer melting.

Obtained coating structure was mainly composed of α-fcp- and β-fcc-cobalt. Selected temperature interval for coating formation, according to XRD analysis, allowed us to form inter-metalloid compounds of Co_xCr_y-type cobalt with chromium. Subsequent melting of a surface layer by a plasma jet resulted to doping of the coating surface by Mo atoms (compounds) from doping electrodes. It was demonstrated that essential improvement of servicing characteristics was due phase transformations induced by high-temperature plasma flux, Mo doping, redistribution of elements in the coating, and appearance of micro- and nano-grained structure, as well as decreasing porosity due to repeated melting [1].

It is assumed that this change in the element and phase composition (appearance of molybdenum oxide films in the surface), the decrease in porosity and surface relief occurred in the process of thermal treatment by high-velocity pulsed plasma treatment resulted in increased nano- and microhardness, as well as higher coating wear resistance and their long life in aggressive media [2].

References

[1] Pogrebnjak A.D., Bratushka S.N., Beresnev V.M. et al.: *Structures and properties of Ti alloys after double implantation*, Vacuum 83, Suppl.1, 2009.
[2] Pogrebnjak A.D., Tyurin Yu.N.: *Modification of material properties and coating deposition*, Physics Uspekhi 48 (5), 2005, p. 487-514.

The analysis of properties and structure of the oxide coatings Al$_2$O$_3$, obtained by vacuum arc method with HF

A.D. Pogrebnjak[1], V.M. Beresnev[2], A.Sh. Kaverina[1], N.A. Makhmudov[3], I.V. Yakushchenko[1], R.Yu. Tkachenko

[1] *Sumy State University, Sumy, Ukraine, E-mail: mixifox@mail.ru*
[2] *Kharkov National University, Kharkov, Ukraine*
[3] *Samarkand Branch of Tashkent State University of Information, Samarkand, Uzbekistan*

The Al$_2$O$_3$ oxide films are among the most promising materials. Their excellent mechanical and chemical properties allow these films to be the best protective coatings. They are heat resistant and have good wear resistance. Al$_2$O$_3$ films can be obtained by different methods, like magnetron sputtering, thermal and electron beam evaporation. Method of magnetron sputtering allows a good control over strength, elastic modulus, adhesion and physical properties of the coating [1].

Coatings based on aluminum oxides were prepared by magnetron sputtering. Coatings deposited on steel specimens (12X18H10T, $\varnothing$20 mm, δ = 4 mm), as well as witness-samples (glass substrate). Evaporating material is aluminum A999. Before coating the metal specimens were grounded, polished, and then together with witness-samples were processed in ultrasonic bath for 100 seconds with output power of 50 watts.

Quality of preparation of the coating surface was investigated profilometer. The results of processing profilograms indicate that the average surface roughness R_a = 0.088 microns. After coating Al$_2$O$_3$ surface roughness decreased significantly.

The results of the phase composition research of Al$_2$O$_3$ coatings show that α-phase is forming.

The results of hardness (H) and elastic modulus (E) measurements show that the hardness of coatings Al$_2$O$_3$, deposited on steel substrate, was H = 11.05 GPa, and Young's modulus E = 193 GPa. The results of hardness measuring of Al$_2$O$_3$, deposited on steel substrate, which was attended by hard-surfaced titanium nitride (TiN), showed an increase in the hardness and Young's modulus: H = 26.07 GPa, E = 294.4 GPa.

One of the parameters characterizing the structural state of materials is the criterion of viscoplasticity. The values of H/E^* for the Al$_2$O$_3$ coating was 0.057, which characterizes the state of the material as a fine-grained, and coating Al$_2$O$_3$, deposited on a substrate with an intermediate layer of titanium nitride, H/E^* was 0.08, as nanocrystalline.

The process of destruction and the strength of adhesion to the substrate of formed coating were analyzed by scratch-test method. Analysis of scratch coating Al$_2$O$_3$ shows that the load P = 6.19 H does not provide any explicit cracks on the coatings surface. With increasing load at P = 10.83 H the surface becomes chipped. Then, the load P = 16,65 H provides the destruction of coating.

References

[1] Portinha A., Teixeira V., Carneiro J.: *Mechanical properties of ZrO$_2$-Al$_2$O$_3$ nanostructured PVD coatings evaluated by nanoindentation,* Reviews on advanced materials science 5, 2003, p. 311-318.

Physical and mechanical properties, effect of thermal annealing in vacuum and in air on nanograin sizes in hard and superhard coatings Zr-Ti-Si-N

A.D. Pogrebnjak[1], A.A. Demianenko[1], V.S. Baidak[1], V.M. Beresnev[2], A.P. Shypylenko[1], V.V. Grudnitskii[2]
[1] Sumy State University, Sumy Institute for Surface Modification, 2 Rimsky-Korsakov Str., 40007 Sumy, Ukraine, E-mail: alexp@i.ua
[2] Kharkov National University, Kharkov, Ukraine

Hard and super hard coatings of Zr-Ti-Si-N of from 2.8 to 3.5 μm thickness were fabricated using vacuum arc source with (HF) stimulation. Six series of samples with various Zr and Ti content were studied. The samples were annealed in vacuum and in air at 1200°C. It was found that films with a high Zr and Ti content were thermally stable up to 1180°C. At the same time, a thin oxide layer of 180 to 240 nm was found in the surfaces, which protected the sample from destruction.

XRD-diffraction patterns demonstrate 17% volume fraction of quasi-amorphous α-Si$_3$N$_4$ phase, 54% of nano-composite nano-structured phases, and the rest was α-Fe from samples substrates. A size of grains of a substitution solid solution (Zr, Ti)N varied from 10 - 12 nm to 25 nm, but Ti concentration in the solid solution increased. In the process of annealing, hardness of the best series of samples increased from 41.6 ± 1.4 GPa to 55.6 GPa, which seemed to indicate that a spinodal segregation along grain interfaces was finished. The relative intensities of peaks indicate amorphous β-Si$_3$N$_4$, α-Fe phase crystallites and metallic sublattice of (Zr, Ti)N solid solution. Elastic modulus $E \approx 400$GPa, deformation value corresponded to that occurring under action of compressing stresses $\zeta c \approx$ -8.5 GPa. Was determined scratch properties: normal force, acoustic emission, penetration depth. Hardness, which was increased in the process of annealing, seems to be related to incomplete spinodal phase segregation at grain boundaries resulting from deposition of Zr-Ti-Si-N-(nanocomposite). Annealing stimulated spinodal phase segregation, forming more stable modulated film structures with alternating in volume concentration of phase components (ZrN; (Zr, Ti)N; Si$_3$N$_4$). Tribotechnical characteristics of coatings were measured for various contents of basic elements Zr, Ti, and Si.

Tribological and physical–mechanical properties of protective coatings from Ni–Cr–B–Si–Fe/WC–Co–Cr before and after fission with a plasma jet

M.V. Il'yashenko[1), 2)], A.V. Pshyk[1), 2)], V.N. Rogoz[1), 2)], D.L. Alontseva[3)],
N. Prohorenkova[3)]

[1)] *Sumy Institute for Surface Modification, Sumy, Ukraine*
[2)] *Sumy State University, Sumy, Ukraine, E-mail: aleksandrpshik@rambler.ru*
[3)] *East-Kazakstan State Technical University, Ust-Kamenogorsk, Kazakstan*

The use of protective coatings to improve the mechanical and physical–chemical properties of metals and alloys is a promising trend in materials science.

The aim of the work is to study the structure and physical-mechanical and tribological properties of coatings deposited from a mixture of two alloys Ni–Cr–B–Si–Fe/WC–Co by a high speed plasma jet involving the detonation and plasma detonation methods.

A new type of coating is developed, which is a mechanical mixture of two different powders, namely, Ni–Cr–B–Si–Fe (PG-19N-01) and WC–Co (hard alloy). As shown in [1 - 3], alloys based on Ni–Cr (Mo, Fe, Cu, and others) possess good anticorrosion properties, particularly in solutions of the acids HCl, H_2SO_4, HNO_3+HF_4, and others, at room and elevated temperatures. It is also reported in [1 - 3] that chrome in nickel alloys and molybdenum in nickel–molybdenum alloys hamper the active dissolution of their nickel base; chrome favors the passivity of the base, while molybdenum impedes it. These properties give Ni–Cr(Mo) alloys stability in acid media and it is for this reason that they are promising for protection of metals against wear and corrosion.

After the coatings from this mixture are deposited, their surface layer is fused with a plasma jet using an eroding electrode made of W. The additional treatment of the coatings with the plasma jet yields new phases and causes the redistribution of elements in the layer 45 - 60 μm deep; the percentage ratio of the phases WC, A-CoCr, Co, and Ni, as well as $Cr_3Ni_2+\gamma$-(Fe, Ni) appearing during coating deposition also changes. The redistribution of elements occurs in the upper coating layer owing to fusion with the plasma jet. These processes yield variations in the physical-mechanical properties of the coatings, such as the hardness and elastic modulus; the coating wear rate decreases severalfold. It is found that with increasing load applied to the Berkovich pyramid the elastic modulus of the coating drops from 240 (at an indentation depth of 50 nm) to 175 GPa (at 150 nm). The elastic modulus of the substrate rises from 25 to 42 GPa. The coating hardness calculated from the loading-unloading curves is 15.3 to 10.6 GPa under increased load applied to the indentor. Specimens covered with the coating fused with the plasma jet in three passes demonstrate the lowest material wear.

References
[1] Svistunova T.V.: *Corrosion–Resistant Alloys for Very Highly Corrosive Media*, Metal. Term. Obrab. Met. 8, 2005, p. 36-42 [Metal Sci. Heat Treat. (Engl.Transl.) 47 no.7-8, p. 383-389.
[2] Friend W.Z.: *Corrosion of Nickel and Alloys*, New York: Wiley, 1980.
[3] Shiemiev A.P., Svistunova G.V.: *Korrozionnostoikie, zharostoikie i vysokoprochnye stali i splavy: Spravochnik (Corrosion–Resistant, Heat–Resistant and High–Strength Steels and Alloys: Handbook)*, Moscow: Internet inzhiniring, 2000.

Ternary semiconductor thin films for solar cells application

V.V. Kosyak[1), A.S. Opanasyuk[1), Yu.P. Gnatenko[2), P. Koval[1)
[1) Sumy State University, Sumy, Ukraine, E-mail: v_kosyak@ukr.net
[2) Institute of Physics NAS of Ukraine, Ukraine

The $Cd_{1-x}Mn_xTe$ semiconductor compound is a promising material for hetero-junction thin films solar cells application [1]. But physical properties (optical, structural and electrophysical) of polycrystalline $Cd_{1-x}Mn_xTe$ thin films are not studied well. However these properties have strong effect on thin films performance. Therefore the main task of this research is to study the main physical properties of $Cd_{1-x}Mn_xTe$ thin films obtained at different growth condition.

The polycrystalline $Cd_{1-x}Mn_xTe$ ($x = 0\text{-}10\%$) thin films were obtained by the close-spaced vacuum sublimation technique [2] on cleaned glass substrate at different growth conditions. The surface morphology and structural properties of films were investigated by the scanning electron microscopy (SEM) and X-ray diffraction methods (XRD). It is allowed as to determined influence of growth conditions on main structural parameters of the thin films, namely: texture, lattice parameter, grain size and concentration of microdeformation. Joint analyze of the chemical composition used energy dispersive X-ray analysis (EDX) and X-ray induced luminescence with structural study by the X-ray diffraction method provide investigation of the effect of chemical composition change on structural properties of the thin films.

The investigation of the optical characteristics of the layers was performed by the spectrophotometric analysis method near the ‚red boundary' of the semiconductor photoactivity. As a result, the reflection, transmission, absorption and refraction coefficients of the thin films deposited at different temperatures as well as the band-gap energy of the compound were determined. The values of the band-gap energy were used for determination of manganese concentrations in the films depending on the growth condition. In order to investigate band-gap deep levels and estimate concentration of point and extended defects in thin films the low-temperature photoluminescence was also used

References

[1] Rohatgi A., Ringel S.A.: *Investigation of polycrystalline CdZnTe, CdMnTe and CdTe films for photovoltaic applications,* Solar Cells 27, 1989, p. 219-230.
[2] Kosyak V.V., Opanasyuk A.S., Gnatenko Yu.P.: *Study of the structural and photoluminescence properties of CdTe polycrystalline films deposited by close-spaced vacuum sublimation*, Crystal Growth 312, 2010, p. 1726-1730.

Gigantic magnetoresistive effect in n-Si/SiO$_2$/Ni nanostructures fabricated by the template-assisted electrochemical deposition

Julia Fedotova[1], Dmitry Ivanou[2], Yulia Ivanova[2], Alexander Fedotov[2], Alexander Mazanik[2], Ivan Svito[2], Eugen Streltsov[2], Anis Saad[3], Serguey Tyutyunnikov[4], Tomasz N. Koltunowicz[5]

[1] *National Center of Particles and High Energy Physics of BSU, 153 Bogdanovich Str., 220040 Minsk, Belarus*
[2] *Belarusian State University, 4 Independence av., 220030 Minsk, Belarus, E-mail: fedotov@bsu.by*
[3] *Al-Balqa Applied University, P.O. Box 2041, Amman 11953, Salt, Jordan*
[4] *Joint Institute for Nuclear Research, 6 Joliot-Curie Str., 141980 Dubna, Russia*
[5] *Lublin University of Technology, 38a Nadbystrzycka Str., 20-618 Lublin, Poland*

At the present time a special interest is the development of the methods to create arrays nanostructures exploiting the giant (GMR) or tunneling (TMR) magnetoresistive effects [1]. Much of such nanoarrays of magnetic sensors and related nanodevices are based on porous templates (SiO$_2$, Al$_2$O$_3$, etc.), where nanopores are filled with different nanostructured substances (see, references in [2]). One of the approaches to the template-assisted fabrication of nanostructured arrays is based on the Nuclear Ion Track Etch Method (NITEM) where selective etching of the latent ion tracks leads to the creation of channels (pores) to form porous templates for further array growth [2, 3].

In this work we study the temperature (2 - 300 K) and magnetic fields (up to 8 T, normal or parallel to the template plane) dependencies of carrier transport properties in the bundles of Ni nanorods embedded into the n-Si/SiO$_2$ porous template created by selective etching of swift heavy ion tracks in a SiO$_2$ layer and the following filling of the pores with Ni nanoparticles.

The n-Si/SiO$_2$/Ni nanostructure, being electrically similar to two Si/Ni Schottky diodes switched-on opposite to each other, displayed 3 contributions to the temperature dependences of resistance: the carrier transport by Si substrate at T > 250 K; impurity conductance by the phosphorus-doped Si substrate at 20 K < T < 200 K when the zone-zone transitions of electrons are freezed-out and electrons move along the interface n-Si/SiO$_2$ over the electrons-enriched layer due to the band bending; and hopping conductance by the localized states at temperatures lower than 20 K.

In n-Si/SiO$_2$/Ni nanostructures at the temperatures ranging 15 - 40 K, where impurity conductance by the phosphorus-doped Si substrate is predominant, a gigantic positive contribution (up to 1200%) to the magnetoresistive (MR) effect was observed, that may be attributed to the impurity avalanche mechanism in Si/Ni Schottky barriers and the influence of 2D electronic gas at the interface n-Si/SiO$_2$ formed between two Si/Ni Schottky diodes.

References
[1] Imry Y.: in *Nanostructures and Mesoscopic Systems*, ed. by W. P. Kirk and M. A. Reed, *Academic, New York*, 1992, p. 11.
[2] Fink D., Petrov A.V., Hoppe K., Fahrner W.R. et al., *Nucl. Instr. Meth.* B 218, 2004, p. 355.
[3] Fink D., Sinha D., Opitz-Coutureau J., Petrov A.V., Demyanov S.E., Fahrner W.R., Hoppe K., Fedotov A.K., Chadderton L.T., Berdinsky A.S.: Nanotechnology with ion track - tailored media, *Physics, Chemistry and Application of Nanostructures (Materials of the "Nanomeeting – 2005", Minsk, Belarus)*, 2005, p. 474.

Magnetotransport in nanostructured Ni films

**Julia Fedotova[1), Dmitry Ivanou[2), Yulia Ivanova[2), Alexander Fedotov[2),
Alexander Mazanik[2), Ivan Svito[2), Eugen Streltsov[2), Anis Saad[3),
Serguey Tyutyunnikov[4), Tomasz N. Koltunowicz[5)**

[1) *National Center of Particles and High Energy Physics of BSU, 153 Bogdanovich Str.,
220040 Minsk, Belarus*
[2) *Belarusian State University, 4 Independence av., 220030 Minsk, Belarus,
E-mail: fedotov@bsu.by*
[3) *Al-Balqa Applied University, P.O. Box 2041, Amman 11953, Salt, Jordan*
[4) *Joint Institute for Nuclear Research, 6 Joliot-Curie Str., 141980 Dubna, Russia*
[5) *Lublin University of Technology, 38a Nadbystrzycka Str., 20-618 Lublin, Poland*

In perfect crystalline transition metals such as Ni, Fe or Co, according to the conventional Boltzmann transport theory that relies on weak scattering, the scattering parametr $k_F l$ >> 1 (here k_F is the Fermi wavevector and l is the mean free path). In strongly disordered metals the $k_F l$ value is strongly lowered (they are called "bad metals") leading to significant changes in the electrical transport properties [1] because the Boltzmann theory of transport is not self-consistent [2] and ceases to work.

We have studied electrochemically deposited nanogranular Ni films, which can be prepared to mimic a bad metal. The procedure of Ni electrodeposition were presented in our previous paper [3]. A thickness of the films was close to 500 nm. The structure of Ni films was studied using SEM LEO-1455VP, AFM SolverPro, and X-Ray analysis. SEM pictures for Ni films at the earliest and final stages of electrodeposition point to their granular structure with the particle dimensions of about 10 - 20 nm at the initial stages of deposition. With increase of the deposition times the films displayed a dense homogeneous coating with 30 - 70 nm grains having the face-centered cubic structure, the lattice parameter found from XRD being equal to a = 0.352 nm.

The study of the temperature dependences of the resistivity $\rho(T)$ and magnetoresistivity MR$(T) = \Delta\rho/\rho(0) = [\rho(B) - \rho(0)]/\rho(0)$ (where $\rho(B)$ and $\rho(0)$ are film resistivity with and without a magnetic field, respectively) in granular Ni films was performed over the temperature range 2 - 310 K and at the magnetic field induction up to 8 T. The I-V characteristics of Ni films revealed a linear behavior at low bias voltages (up to 5 V) over the whole temperature range 2 - 310 K. The observed $\rho(T)$ curves were characterized by a typical metallic behavior, showing a residual resistivity lower than 20 K and a power-like growth of the resistivity with temperature increase due to phonon scattering of the electrons.

Our experiments demonstrated that the magnetic field and temperature dependences of the MR effect in Ni films observed two main differencies: (1) dependencies on the orientation of B relative to the film (substrate) plane; (2) two contributions to the magnetoresistive effect – negative anisotropic MR (predominant at high temperatures and in weak magnetic fields) and positive Lorentz-like MR (predominant at low temperatures and in high magnetic fields).

References
[1] Okram G.S., Soni A., Rawat R., Nanotechnology 19, 2008, p. 1.
[2] Allen P.B., Beaulac T.P., Khan F.S., Butler W.H., Pinski F.J., Swihart J.C., Phys. Rev. B 34 1986, p. 4331.
[3] Ivanova Yu.A., Ivanou D.K., Fedotov A.K., Streltsov E.A., Demyanov S.E., Petrov A.V., Kaniukov E.Yu., Fink D., J. Mater. Sci. 42, 2007, p. 9163.

Effect of absorbing layer thickness on efficiency of solar cells based on Cu(In,Ga)(S,Se)$_2$

M.S. Tivanov[1], L.E. Astashenok[1], A.K. Fedotov[1], M.I. Tarasik[1], P. Węgierek[2]
[1] *Belarusian State University, 4 Nezavisimosti av., 220030 Minsk, Belarus,*
E-mail: tivanov@bsu.by
[2] *Lublin University of Technology, Lublin, Poland*

One of the problems for the development of solar power is the high cost of solar cells, mainly due to the price of the absorbing material. Also, when using solar cells in space, it is important for power-to-weight ratio. Therefore, the priority is the development of thin film solar cells. Semiconductor solid solutions Cu(In,Ga)(S,Se)$_2$ (hereinafter referred to as CIGSS) are a promising materials for thin-film solar cells due to unique combination of their properties: high values of optical absorption index and radiation resistance, stability of operating parameters, a large range of possible values of the band gap. But the reduction of the CIGSS-based absorbing layer thickness results also in the solar cells efficiency decrease.

In this work we present the results on computer simulation of the effect of absorber thickness on the photocurrent density in CIGSS solar cell. The photocurrent density is a key parameter which shows the collection efficiency of photogenerated charge carriers. The one-dimensional model of a solar cell was used. The following assumptions are accepted: the reflection of charge carriers from back contact is absent, window and buffer layers are transparent, the recombination losses at the metallurgical p-n-junction interface are low. The dependence of the photocurrent on the thickness of the absorbing layer for various ratios of solid solution components (S/Se and In/Ga) for lighting conditions AM0 and AM1.5 were obtained.

It was established that required thickness of the absorbing layer of CIGSS solar cell is determined by diffusion length and width of the space charge region. In accordance with the simulation results, for typical terrestrial and space CIGSS-based solar cells the optimal thickness represents 1.5 microns.

Microcontroller kit for training and control characteristics of LED-drivers

I.A. Karpovich[1], V.B. Odzhaev[1], G.N. Prosolovich[2]

[1] *Belarussian State University, Minsk, Belarus, E-mail: odzaev@bsu.by*
[2] *National Education Institute, Minsk, Belarus*

The software and circuit solution for the simulation of LED-drivers in the real conditions and test their parameters are created. The results are displayed in graphical form for the visualization and subsequent computer analysis.

There is well known large family of LED drivers for use in devices for different purposes on the world market. High-brightness LEDs began to displace the halogen lamps and bulbs. For the design of portable equipment some problems are solved: the organization of the power circuit of a single LED (for example, indicator), groups of LEDs (light keyboard) or OLED-panel (LCD displays). However, the LED is a device, which is very sensitive to the quality of the supply voltage. That is why it is necessary to create high current stabilizing power supply, because may decrease the life of the device or even a failure of the system. In addition, the widespread introduction of energy-saving technologies requires providing high efficiency power circuit. Obviously, the creation of an optimum power supply system of LEDs is an actual circuit design problem nowadays.

Some LED-drivers are designed for use in harsh operating conditions, such as in automotive applications. For optimal circuit solution the debug layout, which produce a simulation of the driver in conditions of increased noise in the onboard network and perform measurement parameters of the chip and their subsequent visualization have to be performed.

Layout is designed to study the parameters of chip LED driver in real-time simulation of external impulse noise in a wide range of supply voltages. It provides measurement and visualization of the electrical characteristics of the chip drivers with a peak output current of 0.8 and 1.5 A. Layout is based on the AVR microcontroller. Microcontroller of the measuring unit is used to synchronize the processes of measurement, control real-time timers of measuring signals, measuring the amplitude of the signals and transfer the data into the computer.

There are 6 channels for the measurement of analog signals. Timer control allows to select the scale and a number of accumulations in the measuring channel. In addition, there are 2 discrete channels to simulate the impulse noise-board network.

The analog-digital converter (ADC) has 12-bit resolution and sampling time signal 13 µs. Knot simulating noise-board network is made on the MOSFET transistor, and provides the supply of high-voltage pulses in the power circuit of the chip through a current limiting resistor. The duration of pulse noise is controlled by a microcontroller.

This device can be used for training students.

Nanoscale surface analysis of rapidly solidified Al-Fe alloys

Iya Tashlykova-Bushkevich[1)], Czesław Kozak[2)]

[1)] *Belarusian State University of Informatics and Radioelectronics, Minsk, Belarus,*
E-mail: iya_itb@gmail.com
[2)] *Lublin University of Technology, Lublin, Poland*

Rapid solidification processing (RSP) is an advanced technique that results in alloys with significant beneficial modifications of microstructure and properties compared with conventionally processed counterparts [1, 2]. At present, Al based alloys modified through RSP have received significant attention as versatile electrical engineering materials. In fact, RSP defined as cooling from the liquid to the solid at exceptionally high cooling rates is capable of producing grain refinement, increases in the equilibrium solid solubilities of solute elements and inducing one or more of the metastable effects. It should be highlighted that along with the continued advances in microstructure analysis, attention to the surface microstructure of the rapidly solidified (RS) Al alloys foils is considered to be essential in understanding of solidification mechanisms, taking place during rapid solidification. Nevertheless, as far as we are concerned, there is a lack of information on dope depth distribution in the RS foils of Al alloys. Only few studies have thus far addressed such microscale phenomenon and are scattered in the literature.

The present work focuses on effect of rapid solidification on composition and microstructure of Al-Fe alloys foils produced through centrifugal melt quenching. A feature of this paper is the application of ion beam analysis (IBA) techniques with nanoscale precision. The Rutherford backscattering spectroscopy (RBS) was used to study evolution of the microstructure through the foil depth to investigate solute redistribution and trapping during the solidification process. On the other hand, in order to nondestructively obtain depth profiles of light elements in the foils we employed elastic recoil detection (ERD) spectroscopy and qualified content of hydrogen and its depth distribution in the RS alloys. Atomic force microscopy experiments were performed to monitor surface morphology and topography of the foils.

The RBS experiments show nonuniform dope depth distribution below the foil surface up to a depth of 1.2 μm. Effects of cooling rate and thermal annealing on layer-by-layer composition are revealed, regarding the enrichment of the thin foil surface layer by dope as well as hydrogen depth distribution behaviour. The role of lattice defects on solute/microstructure interactions is discussed in detail. Original results demonstrate that RBS technique combined with ERD analysis provides a useful tool for the nanoscale structural study of elemental distribution in RS materials produced under nonequilibrium conditions.

References
[1] Asta M., Beckermann C., Karma A., Kurz W., Napolitano R., Plapp M., Purdy G., Rappaz M., Trivedi R*.: Solidification microstructures and solid-state parallels: Recent developments, future directions*, Acta Mater 57, 2009, p. 941-971.
[2] Jones H.: *Some effects of solidification kinetics on microstructure formation in aluminium-base alloys*, Materials Science and Engineering A 413-414, 2005, p. 165-173.

NEET
2011

Effect of electrodynamic and climatic loads on flexible busbar of high-voltage open switchgear

I.I. Sergey[1), Y.G. Panamarenka[1), P.I. Klimkovich[1), J. Partyka[2)
[1) Belarusian National Technical University, Minsk, Belarus, E-mail: power.st@mail.ru
[2) Lublin University of Technology, Lublin, Poland

For flexible conductors of open switchgear applied static loads of wind and ice and electrodynamic load short-circuit (SC). In the Republic of Belarus and in the Russian Federation estimated short-circuit currents on the side of 110 - 220 kV up to 40 - 50 kA (according to design organizations), so that electrodynamic effects of high currents and static loads is becoming a key factor when choosing a current-carrying and supporting structures with flexible conductors.

In Belarusian National Technical University (BNTU) made mathematical models, algorithms and software, allowing to fully evaluate the mechanical strength and withstand of the open switchgear elements [1]. A distinctive feature of BNTU developments is the choice and validation of various design solutions aimed at improving the electrodynamic stability of flexible conductors. This may be the installation of interphase spacers, using conductors of large cross section, change the initial sag and suspension points of conductors, and other solutions.

Calculation of wires movement under the action of electrodynamic loads made in several standard climatic conditions. An important task is the selection of design combinations of climatic conditions (wind speed and direction, temperature, thickness of ice) and short-circuit parameters (type, duration, phase inclusions), at which observed the closest approach of flexible conductors and having the maximum tension and loads on the supporting structures and apparatus. Studies conducted in BNTU have shown that the occurrence of an unacceptable rapprochement of wires most likely in conditions with a maximum wind velocity, and when the conductors have the highest temperature. The highest static and dynamic loads occur during the formation of ice on the busbar, or at a minimum temperature in areas with moderate severity of icing. In a typical open switchgears calculations of electrodynamic stability should be made for a two-phase short-circuit with the highest estimated duration.

To reduce the rapprochement of the conductors at short-circuit can be applied interphase spacers. BNTU computer programs allow us to determine the optimal number and the spacers installation place. Calculations for spans of 220 kV Cherepetsk power plant showed that in such cases only one set of spacers in the middle of the span is enough. But the installation of two sets of spacers in each third of the span can also be reduced the dynamic tension by 30 - 40 % by limiting the movements of the conductors. Compressive forces on the interphase spacers due to substantial conductors flexibility is not exceeded 1500 N.

BNTU Developments in this area have been applied at the design of current-carrying structures with flexible conductors in the Republic of Belarus and the Russian Federation.

References

[1] Сергей И.И., Стрелюк М.И.: *Динамика проводов электроустановок энергосистем при коротких замыканиях: теория и вычислительный эксперимент*, М.: ВУЗ-ЮНИТИ, 1999.

Fabrication and electrical properties of nickel and nickel oxide nanoclusters

V.K. Ksenevich[1), V.B. Odzhaev[1), I.A. Bashmakov[2), A.D. Wieck[3)
[1) *Physics Department, Belarusian State University, Minsk, Belarus,*
E-mail: ksenevich@bsu.by
[2) *Research Institute for Chemical Problems, Belarusian State University, Minsk, Belarus*
[3) *Department of Physics and Astronomy, Bochum Ruhr-University, Bochum, Germany*

The interest toward investigation of magnetic nanostructured materials are caused by their unusual properties and possibility of application in magnetoelectronics and information storage devices. Ferromagnetic nickel/antiferromagnetic nickel oxide systems are prospective materials for the observation of -exchange bias" phenomena that can be used in magnetoresistive devices [1].

Different techniques are developed for the preparation of magnetic nanoparticles. For the fabrication of Ni nanoparticles arrays embedded in carbon matrix we applied method based on the thermolysis of thin polymer films with the following treatment in nickel developer [2]. For the transformation of ferromagnetic nickel nanoclusters array into antiferromagnetic nickel oxide we used heat treatment processes in the temperature range 400 - 700°C in the air atmosphere.

Temperature dependences of the resistance of the nickel and nickel oxide nanoclusters arrays were measured using standard four-probe dc-technique in the temperature range 4.2 - 300 K. Electrical contacts on the top of the layers were produced by thermal evaporation of Al. It was found that in dependence of the sizes of particles and their density in carbon matrix Ni nanoclusters can vary their electrical properties from insulating to metallic ones. Weak localization and electron-electron interaction phenomena were observed in the arrays of nickel nanoparticles in the vicinity of metal-insulator transition. Effect of magnetic ordering was observed on the temperature dependencies of the resistance of nickel oxide nanoclusters arrays below temperature of about 100 K.

References

[1] Seto I., Akinaga H., Takano F., Koga K., Orii T., Hirasawa M.: *Magnetic properties of Monodispersed Ni/NiO Core-Shell Nanoparticles*, The journal of physical chemistry B letters 109, 2005, p. 13403-13405.
[2] Bashmakov I.A., Dorosinets V.A., Ksenevich V.K., Melnikov A.A., Kaputskii F.N.: *Formation of thin carbon films containing metal nanoparticles by thermolysis of a Polymer Precursor*, Russian Journal of Applied Chemistry 80 No2, 2007, p. 285-289.

Production of doubly charged ions in an arc discharge ion source with an evaporator

Marcin Turek, Andrzej Droździel, Krzysztof Pyszniak
Institute of Physics, Maria Curie-Skłodowska University, Lublin, Poland

Ion implantation is one of the most important methods enabling modification of metals and semiconductors: improving their tribolgical properties, preparing new light sources, tailoring magnetic properties of implanted target and many others. In many cases, especially when the large depth and width of the dopand profile is required, the maximal energy of accelerated beam in a typical implanter (several hundreds of keVs) could be a severe restriction. The easiest way to overcome this difficulty is using a beam of multiply charged ions produced in a hollow cathode [1], rf-powered [2], or other type of ion source, as ion energy E_n rises as $E_n = nE_1$, where n is a charge state of an ion.

In the paper we present studies of doubly charged ions production using an arc discharge ion source with an internal evaporator, which construction was described in details in [3, 4]. The evaporator enables using solids as a feeding material. Test wee done for several substances, including Al, Sb, As, Ga, Bi, Mn, Te and others. Typicaly, ion currents in the range 2-15 μA were obtained, which enables moderate dose implantations (up to 10^{15} ions/cm^2) with ion energies up to 550 keV with a standard implanter used in Institute of Physics, Lublin. In order to find optimal working parameters for doubly charged ion production we measured basic characteristics of the ion source, namely the dependeces of ion current and anode voltage on discharge current I_a, cathode current I_c and magnetic field flux density. Some results for arsenic are presented below (squares – ion current, circles – anode voltage).
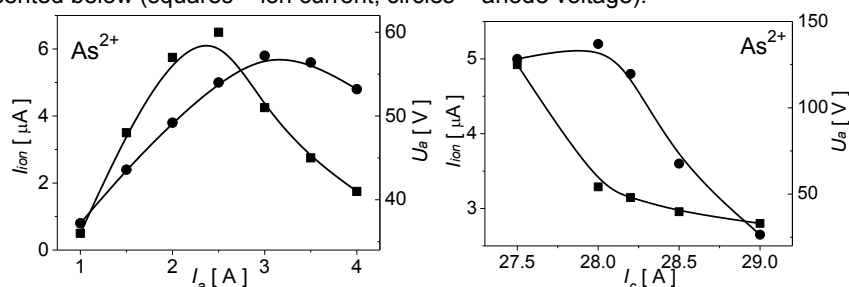
A simple theoretical model based on splitting of ionization process into many intermediate stages is also presented in the paper. It describes production and extraction of ions in charge states +1 and +2 making use of experimental electron impact ionization cross-section data. Results provided by that model are compared to experimental data in order to enrich discussion.

References
[1] Maczka D., Kiszczak K., Drozdziel A., Pyszniak K.: *Multiple ionization in plasma ion source of electromagnetic isotope separator*, Vacuum 58 2000, p. 536-542.
[2] Le Roux H.F., Lutsch A.G.K., Lacquet B.M.: *Source for doubly charged ions*, Nucl. Instrum. Meth. B 6 1985, p. 133-134.
[3] Turek M., Prucnal S., Drozdziel A., Pyszniak K.: *Arc discharge ion source for europium and other refractory metals implantation*. Rev. Sci. Instr. 8 No 4, 2009, p. 043304.
[4] Turek M., Prucnal S., Drozdziel A.., Pyszniak K.: *Versatile plasma ion source with an internal evaporator.* Nucl. Instrum. Meth. B 269, 2011, p. 700-707.

Modeling processes of doping redistribution during oxidization processes

Volodymyr Berezhansky

The Precarpathian National University, 57 T. Shevchenko Str., 76025 Ivano-Frankivsk, Ukraine, E-mail: berezhansky@mail.ru

Redistribution of doping during diffusive -oxidizing processes is simulated. The optimal technological conditions of diffusive -oxidizing processes is determined. Modeling conducted by the finite-difference schemes on an occasional grid, enabling more likely to conduct evaluation of various factors processes.

The increase of integration degree not only in horizontal but also in a vertical direction is a priority direction in microelectronics that results in reduction of the minimal topological size of an element, and also quantity of diffusive processes, which are realized at high concentration of an impurity (formation of emitter and the drain-source areas), a problem of development of two and three-dimensional models of diffusive – oxidizing processes is appears.

Diffusion at high concentration of an impurity is quasilinear process and it is necessary to use numerical methods for its modeling. Diffusivity depends on a ratio of current carrier concentration and own concentration ni: $D=f(n/n_i)$, and also not all atoms of an impurity are active through the phenomenon of precipitation and clusterization of impurity. Thus, models of technological processes should consider the $N=f(C)$ dependence (where N – active impurity, C – the entered ones). Hence, problems of redistribution of alloying impurity near interphase border and problems of modeling of these phenomena remaining actual now.

The received result testifies to reduction of diffusive stream of a base impurity into area of strong doping by an emitter one and leads to the dip formation at the front of diffusive distributions of emitter impurity.

It is enough interesting to model the given effect at different stages of oxidation. It will find out influence of segregation on redistribution process, as the interphase border moves to depth of the sample during oxidation. The volume change of silicon is the consequence of it. The Deale-Grove's model is used for modeling of oxide growth, which is approximated for a two-dimensional case by modeling diffusion of an oxidizer in growing oxide (mechanical stress in oxide and near nitride masks are not considered for simplification of computing process, and is accepted that growing oxide behaves at oxidation temperature as not compressing substance).

The modeling distribution of concentration profiles are realized for a case of the inert environment and at local oxidation.

Interference is shown, and redistribution of concentration profiles is modeling quantitatively at consecutive diffusion both for a case of the inert environment and for local oxidation.

The results of the given mathematical modeling of these technological processes can be used as entrance parameters for models of electrophysical functioning of instrument structures of integrated circuits.

Detection of high resistive ground faults in MV mining networks basing on a phase relationship of selected current harmonics

B. Miedziński[1), D. Pyda[1), W. Dzierżanowski[1), H. Nouri[2), S. Khariu[3)

[1) Wroclaw University of Technology, Wroclaw, Poland,
E-mail: bogdan.miedzinski@pwr.wroc.pl
[2) University of the West of England, Bristol, United Kingdom
[3) Kazakh-British Technical University, Almaty, Kazakhstan

In spite of variety of ground fault protection offered in the market it is difficult to fulfil requirements if about effective detection and clearing of high resistive ground faults, particularly in open-cast MV mining networks. We have found that use of a phase relationship of selected current harmonics can overcame this problem. Therefore, a new detection method has been developed in which a phase correlation between injected (at selected short time intervals) even current harmonics and basic current harmonics is considered as ground fault indication factor.

In the paper the investigation results using ATP-EMTP package are presented and discussed. The simulations have been performed for MV (6 kV) mining networks operating as isolated as well as with ineffectively grounded neutral point. The phase correlation between the second and basic current harmonic for healthy and faulty line have indicated that the high resistive ground faults are able to be effectively detected up to about 100 kΩ. On the basis of the results the conclusions on proper development of the effective ground fault protection have been specified.

Influence of sludge on electric processes in paper-oil insulation

Marek Zenker, Andrzej Mrozik
West Pomeranian University of Technology, Szczecin, Poland,
E-mail: marek.zenker@zut.edu.pl

The paper presents measurements of relaxation phenomena of sludge layer on the paper in the model of transformer oil gap with PDC and FDS (Polarization Depolarization Current, Frequency Domain Spectroscopy). The measurements have been taken at 22°C for various thickness of sludge on a cellulose [1]. The analysis of PDC characteristics showed presence of two relaxation phenomena [2]. For both values of time constants have been estimated. The research showed that after exceeding given value of surface resistivity there is significant change of time constant τ_1 value connected to interface paper-sludge-oil relaxation. The influence of sludge on the paper surface on the relaxation phenomena has been measured also with FDS method for a model of OIP bushing. In such insulating system the sludge may appear as the result of pressboard and oil degradation process under the influence of partial discharges. The sludge can significantly change a shape of dielectric response of OIP bushing model (Fig. 1). These changes appear mainly in the frequency range from 1 Hz to 5 kHz and reflect quite fast relaxation processes in the interface paper-sludge. In specific cases this effect may influence correctness of moisture level assessment in paper-oil insulation. The analysis results of relaxation processes of pressboard barrier with sludge presence show that depending on the moisture level in pressboard and thickness and resistivity of sludge, the presence of sludge shall be taken into consideration e.g. as moisture equivalent. This statement results from a fact that in PDC and FDS easurements it is difficult to distinguish sludge relaxation from interface relaxation with higher moisture level [3]. It is worth mentioning that treating sludge as additional moisture and ageing equivalent is proposed in the paper of G. Csepes about RVM measurement interpretation [4].

Fig. 1. FDS characteristics of the model of OIP bushing without sludge (a) and with sludge presence (b)

References
[1] Lisowski M.: *Pomiary rezystywności i przenikalności elektrycznej dielektryków stałych*, Oficyna Wydawnicza Politechniki Wrocławskiej, Wrocław 2004.
[2] Zenker M.: *Spektroskopia dielektryczna układu papier-olej z osadami na celulozie*, Przegląd Elektrotechniczny 11b, 2010, p. 82-85.
[2] Zenker M.: *Wpływ struktury oleju i papieru na relaksację dielektryczną kanałów olejowych Transformatorów energetycznych*, Rozprawa doktorska 2011, p. 76-94.
[4] Subocz J. (red.): *Transformatory w eksploatacji*, Wydawnictwo Energo-Complex, 2008.

In-situ method of diagnose of thermocouples

Tomasz Zyska
Department of Electronics, Lublin University of Technology,
38a Nadbystrzycka Str., 20-618 Lublin, Poland, E-mail: t.zyska@pollub.pl

The main applied thermocouple diagnostic method consists in comparison of a thermocouple parameters with ones of the model sensor on a specially designed laboratory stand. The method, however, requires a thermocouple to be dissembled from a device, which in most cases means interruption of a technological processes.

The method to diagnose a thermoelectric sensor just where it is assembled was developed. It enables avoiding technical and economical problems. The method is based on measurement of output voltage of the sensor modified by the Peltier effect that occurs in a joint when the thermocouple is controlled by direct current of alternating polarization. Measurement of such signals requires proper measurement strategy to be followed.

The paper presents the method algorithm based on analysis of thermal state that allows determining properties of a thermocouple in situ with a sufficient accuracy. Some effects associated with heating a thermocouple by DC are represented by simulation results.

Final equations consolidate material parameters, which describe the thermocouple. Preliminary research results are also presented.

References
[1] Borowik L.: *Pozyskiwanie wiedzy do celów diagnostyki wybranych urządzeń elektrotermicznych w eksperymentach biernych*, Wydawnictwa Politechniki Częstochowskiej, Częstochowa, 2003.
[2] Лозбін В., Столярчук В.: *Перевірка термопар за допомогою ефекту Пельтьэ*, Вимірювальна техніка та метрологія 62, 2003, p. 48-50.
[3] Лозбін В., Столярчук В., Гук А.: *Вивчення властивостей термоелектричних перетворювачів з використанням ефекту Пельтьэ*, Вимірювальна техніка та метрологія 65, 2005, p. 100-109
[4] Лозбін В., Яцук В., Столярчук В., Зиска Т.: *Розроблення теоретичних підстав для експериментального тестування термопар за допомогою нагріву струмом*, Автоматика вимірювання та керування 551, 2006, p. 26-32.
[5] Carslaw H.S.: *Introduction to the mathematical theory of the conduction of heat in solids*, DOVFR Publications, New York, 1945.
[6] Lozbin V., Zyska T.: *Analiza możliwości stosowania efektów termoelektrycznych do badań termoogniw*, Przegląd Elektrotechniczny 84 3/2008, 2008, p. 255-258.

Numerical algorithms and practical implementations in Electrical Impedance Tomography

Tomasz Rymarczyk

NET-ART, 3 Lotnicza Str., 20-322 Lublin, E-mail: tomasz@rymarczyk.com

The image reconstruction in Electrical Impedance Tomography (EIT) is a highly ill-posed inverse problem. In this paper was proposed several of numerical techniques with different advantages to solve the inverse problem. The conductivity values in different regions are determined by the finite element method. The representation of the boundary shape and its evolution during an iterative reconstruction process is achieved by the level set method [2, 3]. The shape derivatives of this problem involve the normal derivative of the potential along the unknown boundary. Numerical algorithm is a combination of the level set method and Chan-Vese model [1] for following the evolving step edges, and the finite element method for computing the velocity. The idea is merely to define a smooth function ϕ, that represents the interface. The motion of the interface is analyzed by the convection the ϕ values (levels) with the velocity field v. The Hamilton-Jacobi equation is describing this process:

$$\frac{\partial \phi}{\partial t} + \mathbf{v} \cdot \nabla \phi = 0$$

The following steps are used in numerical algorithm:
- From the level set function $\phi(\mathrm{x},\mathrm{y})$ (initial) at a time level t
- Calculate the electric potential (solving the Laplace equation)
- Compute the difference of the computed solution with the observed data
- Solve the adjoint equation
- Find the normal velocity of the level set function
- Calculate the velocity
- Update the level set function
- Reinitialize the level set function.

The Fig. 1 presents the image reconstructions in EIT.
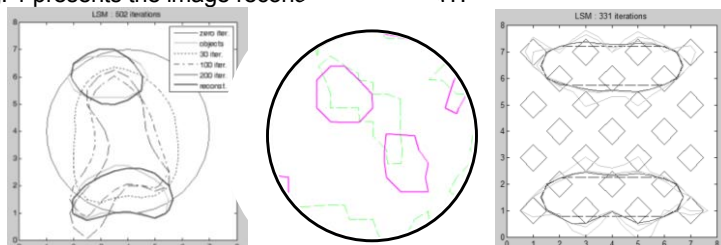
Fig. 1. The image reconstructions

References
[1] Chan T., Vese L.: *Active contours without edges*, IEEE Transactions on Image Processing 10, 2001, p. 266-277.
[2] Ito K., Kunish K., Li Z.: *The Level-Set Function Approach to an Inverse Interface Problem, Inverse Problems* 17 No5, 2001, p. 1225-1242.
[3] Osher S., Sethian J.A.: *Fronts Propagating with Curvature Dependent Speed: Algorithms Based on Hamilton-Jacobi Formulations*, Journal of Computational Physics 79, 1988, p.12-49.

Acoustic environment recognition system

Eugeniusz Kornatowski
West Pomeranian University of Technology, Faculty of Electrical Engineering,
Department of Signal Processing and Multimedia Engineering, Szczecin, Poland,
E-mail: eugeniusz.kornatowski@zut.edu.pl

In the robotics and artificial intelligence fields, the most popular sensory modality to be incorporated in systems is vision; until very recently hearing has not played much of a role in the intelligent systems research. Few attempts have been made to incorporate sound processing in a self-contained robot [1-4]. However, sound provides a rich source of information: many animals rely on localization and other auditory perceptual tasks to survive; speech and hearing are the primary means of communication for human beings. In some ways audition on a robot is more subtle and difficult than vision. Unlike the eyes, the ears do not directly receive spatial information from the surroundings. The auditory system thus relies much more heavily on the processing of raw sensory data to extract acoustic cues and indirectly derive spatial information.

The paper offers a system for determination of sound source direction with a use of the microphone array. This solution may be useful in design of robots, e.g. as one of the components for a recognition of surroundings.

The experimental testing was conducted in a 5 x 6 x 3 m room, with a reverb time RT60 equal to 0.8 s. The microphone array was located at about 1.5 m above the floor. A loudspeaker playing signal obtained from a pink noise test tone generator was used as a sound source. Distance to speaker from the microphone was set at around 1.5 m. Signals were registered using a digital Zaxcom DEVA 5.8 recorder. The 10 s duration time samples were recorded with sampling frequency of 96 kHz and 24 bit resolution for various sound source locations.

During the first phase of experiment the sound source was immobilized, and next – the sound source change location. Signals from each microphone of the array were divided into 250 ms duration time frames. The elevation angle and azimuth was calculated for each set of these frames, and subsequently the results were averaged for a total time of recording (10 s).

Obtained results of simulation tests are very encouraging. The errors (maximum 6°) prove that the system is able to localize the sound source direction as well as human ear. Based on sense of hearing, a human being is able to determine the azimuth and elevation within accuracy of 6° to 10°.

References
[1] Brandstein M., Silverman H.: *A practical methodology for speech source localization with microphone arrays*. Comput., Speech Ing. 11 no.2, 1997, p. 91-126.
[2] Martinson E., Arkin R.C.: *Noise Maps for Acoustically Sensitive Navigation*. Proceedings of SPIE 5609, 2004.
[3] Li H., Yoshiara T., Zhao Q., Watanabe T., Huang J.: *A spatial sound localization system for mobile robots*. IEEE Volume, Issue, Trans. Instrum. and Meas., 2007, p. 1-6.
[4] Ghose K., Zotkin D., Duraiswami R., Moss C.F.: *Multimodal localization of a flying bat*. Proceedings of International Conference of Acoustic, Speech and Signal Processing, ICASSP 2001, Salt Lake City.

N_{EE}T
2011

Image and video quality assessment
with the use of various verification databases

Krzysztof Okarma
West Pomeranian University of Technology,Szczecin, Faculty of Electrical Engineering,
Department of Signal Processing and Multimedia Engineering, Szczecin, Poland,
E-mail: okarma@zut.edu.pl

Automatic image and video quality assessment methods may be divided into three main categories depending on the knowledge of the original (reference) image which is not affected by any distortions. The first group is called ―blind" or no-reference quality assessment, since such methods do not require the use of the original image. Nevertheless, they are usually specialised and sensitive only to one or two chosen types of distortions. Another group of metrics know as reduced-reference methods require only the partial knowledge of the original image.

The most universal approach is the application of the full-reference metrics, which compare the distorted image with the original one. Such metrics are usually sensitive to many types of various distortions, such as noise, compression artifacts, transmission errors, blur and many more, and well correlated with subjective evaluations.

In recent years the rapid progress in this field has taken place and many new full-reference metrics have been provided starting from the Universal Image Quality Index proposed in 2002. All recently proposed metrics, e.g, based on the SVD decomposition [1] are much better than traditionally used Mean Squared Error and similar metrics, such as e.g. PSNR, but their verification is usually performed using arbitrarily chosen database of images. A reliable comparison of the properties of some modern image and video quality metrics requires the use of several verification databases which contain the images or video files with many distortion types together with subjective quality scores.

Currently, several image quality assessment databes are available, but some of them are limited to only two or three types of distortions applied for small number of images. Another disadvantage of some of them is small number of human observers assessing the quality of images, what leads to relatively low reliability of delivered Mean Opinion Scores (MOS) or Differential MOS (DMOS) values. The two largest image quality assessment databases are LIVE Database delivered by Laboratory for Image and Video Engineering (LIVE) from Texas University at Austin and Tampere Image Database (TID2009) containing 1700 images with 17 types of distortions.

The verification of the video quality assessment metrics is more troublesome, since only two databases are currently available, both delivered by LIVE (one of them has only four types of distortions specific for wireless transmission of compressed video data.

In the paper the verification results obtained for the most of state-of-the-art image and video (using frame-by-frame approach) metrics, together with combined ones [2], using currently avaliable databases are presented. Obtained values of the metrics have been compared to MOS and DMOS values and the linear correlation coefficients have been used for the verification of the usefulness of metrics for each type of distortions.

References
[1] Mansouri A., Mahmoudi-Aznaveh A., Torkamani-Azar F., Jahanshahi J.A.: *Image quality assessment using the Singular Value Decomposition theorem*, Optical Review 16 no. 2, 2009, p. 49-53.
[2] Okarma K.: *Combined full-reference image quality metric linearly correlated with subjective assessment*, Lecture Notes in Artificial Intelligence, 6113, Springer-Verlag, 2010, p. 539-546.

Fuzzy logic controller dedicated for dc motors

Marek Poplawski, Michal Bialko
Department of Electronics and Computer Science, Koszalin University of Technology,
2 Sniadeckich Str., 75-453 Koszalin, Poland

The objective of this work is a presentation of practical implementation of a digital fuzzy logic controller dedicated for permanent magnet dc motors, which could be used for steering of electric wheelchair for unable persons [1]. The electric wheelchair is usually driven by two dc motors, which are supplied from the battery [2]. Steering of the wheelchair is based on differential control of electric motors driving back wheels of the wheelchair, allowing driving the wheelchair in left/ right and onward/ back directions. The task of proposed fuzzy system is a generation of output signals, steering two electric motors based on input signals (left/right, front/back), created by the operator using joystick; additionally a feedback signal (Δv) is used to cancel a difference of rotations of electric motors, while driving straight on. The knowledge, based on which steering signals are generated is included in fuzzy rules and terms of linguistic variables [3].

The propossed fuzzy system is based on classical Mamdani model in which one can distinguish the blocks: fuzzification, inference and defuzzification. The fuzzification process changes input signal value from the fields of real numbers to the value of membership function $\mu(x)$ of the fuzzy sets. In the proposed fuzzy system the fuzzification process is performed by reading out from system's memory the values of membership function of activated sets and also codes of these sets. In hardware realization of fuzzy systems only 2^n rules from L^n rules existing in the rule base are activated (where L – number of input fuzzy sets, n – number of input linguistic variables) [4]. The utilization of technique of addressing in fuzzy systems allows to process only active rules [5]. Elimination of verification of degree of activation of all fuzzy rules allows to limit occupied equipment stocks (memory). In the proposed system a technique of addressing is applied, which is implemented in inference process. The creation of the address of the conclusion is based on the codes of activated fuzzy sets. Proposed digital fuzzy system assigned for steering electric wheelchair was realized in FPGA circuit – Spartan3.

References:
[1] Popławski M., Białko M.: *Implementation of dedicated digital fuzzy controller in microcontroller circuit,* Zakopane Neet 2009.
[2] Kalus M., Skoczkowski T.: *Sterowanie napędami asynchronicznymi i prądu stałego*, Gliwice 2003.
[3] Yager R.R., Filev D.P., Filev; Wiley J. and Sons: *Essentials of fuzzy modeling and control*, New York, USA 1994.
[4] Patyra M.J., Grantner J.L.: *Hardware implementaions of digital fuzzy logic controller*, Elesiver Information Science 113, 1999, p. 19-54.
[5] Falchieri D., Gabrielli A., Gandolfi E., Masetti M.: *Very fast VLSI fuzzy processor: 2 inputs 1output*, Fuzzy Sets & Systems, November 2002, Volume/Issue 132/2 p. 261-272.

Application of self-organizing neural network to the interpretation of gases dissolved in transformer oil

Tomasz Piotrowski

Institute of Electrical Power Engineering, Technical University of Lodz, Lodz, Poland,
E-mail: tomasz.piotrowski@p.lodz.pl

Power transformers, because of the important role they play in power systems, are usually a subject of special inspections during service. Among many diagnostic methods one of the most important is the analysis of gases dissolved in oil (DGA).

There are several DGA schemes, mainly based on gas ratios, exist. Attempts are also made to utilize artificial intelligence tools in order to improve faults recognition achieved by the application of traditional DGA methods. The most popular of such tools are fuzzy logic and neural networks. In the latter case are typically used feedforward neural network and sometimes radial basis function network or probabilistic neural networks.

In this paper the self-organizing neural network is presented. This kind of artificial neural network is trained using unsupervised learning. The network can be trained using an learning algorithm WTA (Winner Takes All) or WTM (Winner Takes Most).

During the learning process were used tens sets of measured concentrations of 5 typical gases (hydrogen - H_2, methane - CH_4, acetylene - C_2H_2, ethylene - C_2H_4 and ethane - C_2H_6). Gases were taken from transformers of a known defect.

The values of gas concentrations before fetched to the input of the network were subjected to a process of normalization according to the formula:

$$x_i^{'} = \frac{x_i}{\sqrt{\sum_i x_i^2}}$$

After completion of training phase the network was able to recognize the three types of defects: PD – partial discharges, D – discharges and T – thermal faults.

In order to verify the correct operation of the trained network several sets of concentrations of gases from the transformer of known defect were used. Obtained results are presented in the table below.

	% of correctly identified defects	
	Ratios methods	Self-organizing neural network with WTA learning algorithm
Partial discharges	71,4	85,7
Discharges	84,6	92,3
Thermal faults	80,7	88,5

The self-organizing network can better identify faults then traditional DGA ratios methods. The difference ranges from a few to several percent depending on the type of defect.

Since the network under consideration does not give correct results in all cases it can be used as a complement to traditional methods of DGA.

Dielectric Response of OIP Bushings with various insulation defects

Andrzej Mrozik, Marek Zenker, Jan Subocz
West Pomeranian University of Technology, Szczecin, Poland,
E-mail: amrozik@zut.edu.pl

The paper presents the influence of various insulation defects on dielectric response of models of transformer OIP bushings. The first model represents OIP 145 kV bushing in natural scale, while the second one was prepared as a sample on the base of real paper-oil insulation from OIP bushing. The paper-oil insulation of 145 kV bushing model had subsequently added gases, to simulate gas products of oil degradation during partial discharges. The dielectric response has been measured with two methods: Frequency Domain Spectroscopy (FDS) in a frequency range 10^{-4} - $5 \cdot 10^3$ Hz and with Step Voltage Measurement (SVM) at temperature $T = 23°C$. After performing preliminary measurements there was simulated partial failure of the insulation by the core due to partial discharges. It was based on point injection into paper-oil insulation products of oil and cellulose deterioration, which was dissolved in the mineral oil sludge. It was taken from the real insulation, operated for several dozens years and consisted mainly from smut, cellulose fibres and acid products of oil deterioration. These products were injected into several layers between screens close to the core in the way that other structure of insulation system remained unchanged. In addition into the insulation between steering screens there were air bubbles inserted. In this way one of partial discharges development stages was simulated, which did not influence significantly on the electric strength of the bushing.

The analysis of dielectric response showed that gases contents in insulation influences mainly tgδ characteristics in frequency range 10^{-3} - 10^0 Hz. On the other hand deterioration products without gas phase change this response mainly in frequency range 10^0 - $5 \cdot 10^4$ Hz. They cause also an increase of polarization index K_a.

The research showed that dynamic measurements of polarization phenomena performed at relatively low measuring voltage, combined with analysis of phenomena physics can be more effective diagnostic method of paper-oil insulation than standard interpretation of tgδ_{50Hz} value.

References
[1] Walczak K., Gielniak J., Graczkowski A., Morańda H.: *Analiza FDS w ocenia zawilgocenia izolacji transformatorów*, Pomiary Automatyka Kontrola 10, 2008.
[2] Subocz J.: *Transformatory w eksploatacji*, Wydawnictwo Energo – Complex, kwiecień 2007.
[3] Kaźmierski M., Szymański Z.: *Przyczynek do diagnostyki stanu technicznego izolatorów przepustowych transformatorów*, Międzynarodowa konferencja transformatorowa, Transformator 2009, p. 99-111.
[4] Zenker M.: *Spektroskopia dielektryczna układu papier – olej z osadami na celulozie*, Przegląd Elektrotechniczny 11b, 2010, p. 82-85.
[5] Mrozik A.: *Odpowiedź dielektryczna modelu przepustu wysokiego napięcia*, Przegląd Elektrotechniczny 11b, 2010, p. 59-62.

Split-complex numbers in neural cryptography

M. Płonkowski, P. Urbanovich
John Paul II Catholic University of Lublin, Lublin, Poland,
E-mail: marcin.plonkowski@kul.pl

A new field of research on neural networks, which uses neural network methods in cryptographic solutions is known as neural cryptography. One of its most important aspects is the application of the TPM (Tree Parity Machine) architectures in the key exchange protocol [1]. However, unlike the well known Diffie-Hellman key exchange protocol, it does not use the number theory and it is not based on the factoring problem.

Nevertheless, the classic TPM model turned out to be susceptible to the cryptographic attacks (genetic, geometric and probabilistic attacks). The geometric attack considered as the most dangerous one threatened the security of the key exchange protocol based on the TPM architecture. That is why, new solutions have been found in order to guarantee a higher level of security and greater resistance to the known attack patterns [2]. One of these solutions is the application of the complex numbers in the TPCM (Tree Parity Complex Machine) architecture. Thanks to the use of a more advanced, complex transfer function, the key exchange protocol based on the TPCM architecture turned out to be resistant to the geometric attack. Other solutions based on the extension of the real number system have been found (quaternions - TPQM and octonions – TPOM). However, apart from ensuring a higher level of security, these solutions proved to have lower time efficiency [3].

This article describes the TPSCM (Tree Parity Split–Complex Machine) architecture based on the algebraic structure of the split-complex numbers and is founded on the classic TPM model. Nonetheless, the use of the new algebraic structure will require a change to the transfer function and a modification to the training algorithm.

In addition, proposals of other algebraic structures which could be used in the TPM architecture's modification will be presented. One of the chief assets of the solutions proposed herein is greater flexibility in the choice of the TPSCM architecture's parameters (e.g. the choice of the set restricting the weight vector).

The higher level of security of the TPSCM architecture as compared to the classic TPM model are confirmed by mathematical analyses and real simulations. Finally, the proposed solutions' results will be presented in terms of their efficiency and security level as compared to similar TPM architecture's modifications (TPCM, TPQM, TPOM).

References

[1] Kanter I., Kinzel W., Vanstone S.A.: *Secure exchange of information by synchronization of neural networks*, Europhys. Lett. 57, 2002, p. 141-147.
[2] Klimov A., Mityaguine A., Shamir A.: *Analysis of Neural Cryptography*, Advances in Cryptology, ASIACRYPT, 2002, p. 823-828.
[3] Płonkowski M., Urbanowicz P.: *Криптографическое преобразование информации на основе нейросетевых технологии*, Труды БГТУ. Серия VI. Минск: БГТУ, 2005, p. 161-164.

The use of steganographic techniques for protection of intellectual property rights

N. Urbanovich, V. Plaskovitsky

Belarusian State Technological University, Minsk, Belarus, E-mail: nadya_ur@rambler.ru

It is known that copyright is an important part of universal human rights system. Digital technology can solve this problem on new, higher level [1]. One of such technology based on the use of steganographic methods.

Steganography — the science of secure communication by means of conservation of a secret of the fact of the transfer. Steganography, using text containers, is called as text steganography. The fact of existence information is secret [2, 3].

The color of each character is represented in a certain color model. We investigated the effectiveness of embedding secret information (relating to copyright marks) in the text using the color of the symbol. The work was carried out using the capabilities of word processor MS Word 2007.

Such technique is widely used in graphic methods of steganography, and called Least Significant Bit (LSB). In its implementation insertion is made in the last 1-2 bits of color image pixel. In adapting the above algorithm to the text insertion can be done in the last 3-5 bits of the color of the symbol. Increasing the number of used bits of color in the text, as compared with the graphics comes from the fact that the image will usually contain gradations and transitions from one color to another. Text is monotonic and reproduces in most cases, a single color, so it becomes possible to increase used to embed the color range.

For example, it is necessary to introduce a secret message "101" in the text-container "A" using a word processor. In this processor, the color of the symbols represented in the RGB c 8 bits per channel (each of 3 standard colors is represented by 8 bits – a number from 0 to 255). Embedding secret messages will produce in a lower bits of color symbols. The result will be obtained by color: (00000001, 00000000, 00000001).

In carrying out this work the authors developed a new method of text steganography to protect intellectual property rights, based on the use color and size attributes, fonts, and performed studies to assess the effectiveness of the proposed method.

References

[1] Пласковицкий В.А.: *Методы защиты программного обеспечения от несанкционированного использования и модификации*, Сборник науных работ 61-й НТК студентов и магистрантов. Минск:БГТУ, 2010, с.156-158.

[2] Ярмолик В. Н.: *Криптография, стеганография и охрана авторского права*, В. Н.Ярмолик, С. С. Портянко, С. В. Ярмолик, Минск: Изд.центр БГУ, 2007, 240 с.

[3] Urbanovich P. , Urbanovich N. , Chourikov K. , Rimorev A.: *Niektóre aspekty zastosowania metod steganograficznych do przechowywania powiadomień tekstowych*, Przeglad elektrotechniczny 7/2010, 2010, s. 95-97.

A comprehensive assessment of product quality in the relation to anthropogenic impacts on the environment

A.I. Brakovich[1), V.L. Kolesnikov[1), P.P. Urbanovich[1), 2)
[1) *Belarusian State Technological University, Minsk, Belarus,*
E-mail: brakovich@yandex.ru
[2) *Catholic University of Lublin, Lublin, Poland*

Product quality is most often achieved by changing the operating parameters of the process. This, in turn, can lead to an increase in anthropogenic impact on the environment. In this regard, especially relevant is an integrated environmental assessment. Based on the experience of environmental practices to a comprehensive environmental assessment have been developed a number of requirements. Some of the most important requirements are the following:

- integrated environmental assessment must be united and be a certain way formed mathematical expression that takes into account the partial evaluation of individual factors;
- methodology for conducting private evaluations (evaluations of individual factors) should be focused on being independent, and at the same time, be part of an integrated environmental assessment;
- formation of an integrated environmental assessment must be simple enough, allowing its use in the units guarding the environment.

In a real situation enterprises assessment is based on more than a dozen criteria: performance, cost to profitability, air and water pollution, etc. We live and work in multicriteria world where goals are often conflicting. For example, productivity and profitability to maximize, and the production cost and pollution – to minimize [1, 2].

For integrated environmental assessment different mathematical methods are used: the linear estimates, component and factor analysis, cluster analysis, etc., which are limited in their usage because of several shortcomings [1].

A new method of multicriteria evaluation of the enterprise activity on production, economic, environmental and consumer indicators is proposed, where the synthesis assessment criterion performs a complex function of desirability. It allows to convert an array of output values of large-scale to a single-column generalized observations.

Mathematical foundations of complex function desirability set out in the well-known expression [1-3].

The example of calculation for the company, which produces printing paper is given. It shows that the proposed method of multicriteria evaluation of the enterprise activity, where as the synthesis assessment criterion performs a complex function. It allows to evaluate the desirability of such activities on industrial, economic, environmental and consumer indicators.

References
[1] Kolesnikov V.L., Zharsky I.M., Urbanovich P.P.: *Computer modeling and optimization of chemical and technological systems*, Minsk BSTU, 2004, 532 p.
[2] Kolesnikov V.L.: *The mathematical basses of computer modeling of chemical and technical systems*, Minsk BSTU, 2003, 312 p.
[3] Kolesnikov V., Romantsevich A., Urbanovich P., Brakovich A., Zarski I.: *Modeling and the process analysis in engineering ecology*, Przegląd Elektrotechniczny, 3/2008, 2008, p. 155-157.

W-cyclic method interleaving of the data for communication systems

Yu. Gorbunova[1)], P. Urbanovich[1), 2)]
[1)] *Belarussian State Technological University, Minsk, Belarus, E-mail: mailuli@mail.ru*
[2)] *Catholic University of Lublin, Lublin, Poland*

Currently communication systems require high speed transmission and transformation of information with ensuring the required level of reliability. But the influence of noise leads to appearance module errors [1]. Therefore, for reliable information processing in many communication channels are used scheme, based on correcting codes and interleavers.

Interleaving procedure reduces the correlation between adjacent symbols, which allows to convert a module errors to single. The most famous interleavers are the block, s-random and cyclic interleavers [2]. The advantage of cyclic interleaver is a small time bit interleaving.

The function of the cyclic interleaving is as follows:

$$\pi(i) = i \cdot a \bmod N, \tag{1}$$

where $a < \lfloor \sqrt{2 \cdot N} \rfloor$ – the step, that determines the distance between two neighboring bits after interleaving. Besides parameters values of *a* and N must be coprime.

The investigation showed that due to different step values cyclic interleaver has different properties. As shown in Fig. 1, with step size $a = 31$ cyclic interleaver can spread errors high multiplicity to the relatively small distance, with $a = 251$ cyclic interleaver shows excellent results at a low multiplicity of errors, but at a higher multiplicity of the depth of errors diversity is low.
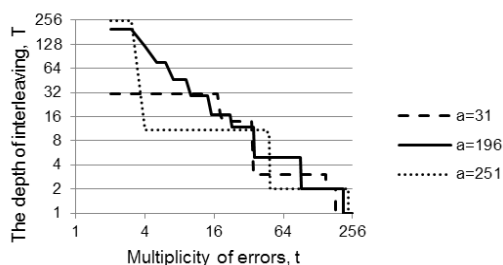
Fig. 1. The curves of minimum separation distances errors by cyclic interleaver with different values of the step at $N = 512$

Therefore, it is expedient to improve the cyclic interleaver with the aim of separation to long distances errors of high multiplicity and low multiplicity ($a = 196$ for $N = 512$). It is proposed to use the following function, as a modification of cyclic interleaver:

$$\pi(i) = i \cdot W \bmod (N + 1), \tag{2}$$

where W – is an integer number, prime to (*N+1*). Experimentally established that the with step $W = \lfloor 0{,}382 \cdot N \rfloor$ (where 0.382 – Fibonacci ratio) interleaver carries errors of any multiplicity very well.

References
[1] Lyapa N. N. *Analysis of methods for improving the reliability of transmitted data*, N.N. Lyapa, V.N. Lysenko. Herald Sum DU. A series of technical sciences № 2, 2009, p. 41-46.
[2] Shloma A.M.: *New algorithms for signal generation and processing in mobile systems*, A. M. Shloma, Moscow: Hot line - Telecom, 2008, 344 p.

Conductivity of (FeCoZr)$_x$(CaF$_2$)$_{1-x}$ nanocomposites

Tomasz N. Kołtunowicz[1)], Paweł Zhukowski[1)], Paweł Michna[1)],
Jakub Paciorkowski[1)], Vera V. Fedotova[2)], Andrey V. Larkin[3)]
[1)] Lublin University of Technology, Department of Electrical Devices
and H.V. Technology, 38a Nadbystrzycka Str., 20-618 Lublin, Poland,
E-mail: t.koltunowicz@pollub.pl
[2)] SSPA, Scientific-Practical Materials Research Center of NAS of Belarus,
19 P. Brovka Str., 220072 Minsk, Belarus
[3)] Belarusian State University, 4 Independence av., 220030 Minsk, Belarus

Investigation into temperature (77 K – 300 K) and frequency dependences of (FeCoZr)$_x$(CaF$_2$)$_{1-x}$ nanocomposite conductivity has been presented. The nanocomposites have been produced by ion sputtering of two targets made of the Fe$_{0.45}$Co$_{0.45}$Zr$_{0.10}$ alloy and the CaF$_2$ dielectric. Atoms that are ejected from the targets get deposited onto a substrate where a nanocomposite forms – metallic-phase grains of the 2-10 nm diameter fused into a dielectric matrix. Two sample series have been produced. They have differed from each other by chemical composition of the beam that has been applied for the sputtering purposes. The series I has been produced with the use of pure argon beam while for the series II a mixture of argon and oxygen has been applied.
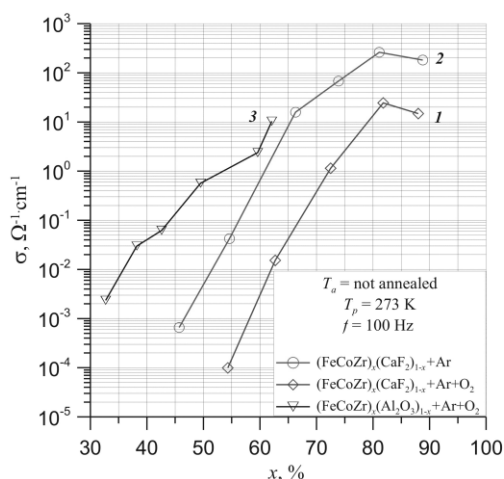
Fig. Dependence of $\zeta(x)$ measured at the frequency 100 Hz and T = 273 K for (FeCoZr)$_x$(CaF$_2$)$_{1-x}$ – curves *1* i *2* and (FeCoZr)$_x$(Al$_2$O$_3$)$_{1-x}$ – curve *3*.
Ion sputtering of Ar ions – *1* and Ar+O$_2$ ions – *2* i *3*

Fig. 1 shows dependences of conductivity measured at the 100 Hz frequency and T = 273 K on the metallic phase content x. The $\zeta(x)$ characteristic can be divided into two sections. Within the first one, at lower x values, a rapid increase of conductivity can be observed, while in the other one little decrease of conductivity occurs. As can be seen in the figure, the Ar+O$_2$ mixture application brings about a shift of the $\zeta(x)$ characteristic into the area of higher values of the metallic-phase content x as well as a decrease of conductivity at the highest values of the metallic-phase content x.

In order to establish the effect of a dielectric matrix composition the results have been compared to the $\zeta(x)$ characteristic obtained for (FeCoZr)$_x$(Al$_2$O$_3$)$_{1-x}$ nanocomposites produced by sputtering with a beam of Ar+O$_2$ [1].

References

[1] T.N. Kołtunowicz, P. Zhukowski, V.V. Fedotova, A.M. Saad, A.K. Fedotov: *Hopping Conductance in Nanocomposites (Fe$_{0.45}$Co$_{0.45}$Zr$_{0.10}$)$_x$(Al$_2$O$_3$)$_{1-x}$ Manufactured by Ion-Beam Sputtering of Complex Target in Ar+O$_2$ Ambient*, Acta Physica Polonica A 120, 2011, p. 39-42.

The appearance of conflict by using the chaos function to calculate the hash code

P. Urbanovich[1), 2)], M. Plonkowski[2)], K. Churikau[1)]
[1)] *Belarussian State Technological University, Minsk, Belarus,*
E-mail: chkv85@gmail.com
[2)] *Lublin Catholic University, Lublin, Poland*

The use of artificial neural networks (ANN) for modeling cryptographic information transfer systems is a new, promising trend in the field of information security.

There are three basic learning algorithms of ANN: with teacher, without a teacher, with reinforcement.

ANN interaction model of "learning without a teacher" has the following properties: mutual learning, self-learning, stochastic behavior, low sensitivity to noise, inaccuracies (data distortion, weights weighting coefficients, program errors). These properties can be used to solve the crypto-conversion problems in systems with a public key, for key distribution, for hash messages and for generation of pseudorandom numbers.

In [1] a neural network architecture for hashing messages is proposed. In [2] this idea was developed through the use of complex numbers algebra. In this case, the neural network model suggests to use the dependencies known from chaos theory as a transition functions.

They are:

totality of the Julia set - a set of chaotic dynamics:

$$z_{n+1} = z_n^2 + c;$$

equation of Duffing oscillator:

$$\begin{cases} x_{n+1} = x_n + y_n, \\ y_{n+1} = y_n - x_n^3 + ax_n - by_n; \end{cases}$$

equation of Hanon:

$$\begin{cases} x_{n+1} = y_n + 1 + ax^2, \\ y_{n+1} = bx. \end{cases}$$

An important aspect of these functions is their resistance to conflict, which affects the security of the entire neural network as a hash function. This concerns the question of the existence of two different input vectors, generating a single output value. The analysis showed that the emergence of collisions in the equation describing the Julia set arise 3 times less than in the equation of Duffing oscillator, and they arise 4 times more often in the Hénon equation: if you take the emergence of collisions in the equation of the Duffing oscillator for the average value of 1, then the equation describes the conflicts of the Julia set is equal to 0.33, while in the Henon equation is equal to 4.

References
[1] Kinzel W., Kanter I.: *Interacting neural networks and cryptography*, Advances in Solid State Physics 42 Springer, 2002, p. 383-392.
[2] Plonkowski M.: *Analiza funkcji chaosu w funkcjach skrótu opartych na sieciach neuronowych*, Przegląd Elektrotechniczny 3/2008, 2008, p. 102-104.

Multithreshold majority decoding of LDP-codes

P.P. Urbanovich[1), 2)], D.M. Romanenko[1)], D.V. Shiman[1)]
[1)] *Belorussian State Technological University, Minsk, Belarus,*
E-mail: upp@rambler.ru, rdm@tut.by
[2)] *Lublin Catholic University, Lublin, Poland*

Observed sharp increase of informational flows and tightening requirements for transmitted and treated information aggravated the problem of secure storage and transmission of Binary Data. Using redundant codes can solve the described problems. There are many different codes with high-correcting capabilities (for example BCH-codes, Reed-Solomon, low-density and other's). But at the same time the main role in the process of error correcting plays the decoder. So, the purpose of this work is studying of multithreshold majority decoding of Low-Density Parity Codes (LDPC).

The progressive development of iterative codes led to the emergence of three-dimensional versions, which can be attributed to LDPC-codes thanks to the low-density units in the generator matrix (in rows – not more than $\sqrt[3]{k}$; units). Expedient to use not more 9 linearly independent parities in LDPC-code. With length increasing of the information sequence for the considered low-density code rate parameter increases and for k = 4096 bits reaches 0.76.

To study the correction of multiple batch and independent errors multithreshold decoder and three-dimensional iterative code was developed a software model that simulates the process of coding, the appearance and correction errors.

The results of the modeling process of majority multithreshold decoding (threshold values were $T1$ = 5, $T2 \geq 4$, $T3 \geq 3$) the different types of triple independent errors for the information sequence length k = 64 bits and three-dimensional iterative code with 5 linearly independent parities are represented in table 1.

Tab. 1. The results of the modeling of the correction errors process

Error type	Quantity of corrected errors, %	Quantity of errors after decoding, %			
		Single	Double	Triple	Quadruple and more
Single	100	0	0	0	0
Double	100	0	0	0	0
Triple	99	0,6	0,6	0	0,2
Quadruple	97	0,7	0,7	0	1,6

Simulation of the communications model of a radiological laboratory, based on the model prepared by the IHE organization

Dariusz Gutek

Lublin University of Technology, Lublin, Poland, E-mail: darekg@cs.pollub.pl

The article presents a radiology lab management application, which organizes the operations performed by the peripheral systems of the laboratory. The prerequisite for its operation is its correct communication with the other systems used in the laboratory as well as the IT system of the hospital. The purpose of this application is to improve the operation of an institution handling a large number of patients and requiring quick data handling within the laboratory.

The work on development of the structure of the reports involved a large emphasis being placed on the adherence to IHE recommendations, as presented in [1, 2]. The model put forward assumes a multiple sending process for the very same information in order to maintain synchronization. Those decisions were important from the point of view of programming the report handling procedures. The exact project of data exchange improves the process of application programming. The use of XML format for coding the information allows the data exchange to be traced with use of a sniffer. The communication mechanics adopted by us allows for efficient exchange of information.

There are more than a dozen commercially available HL7 protocol interfaces [4]. The lack of availability of a specification and the ambiguous mechanics of data organization, used within Polish hospital applications has led us to use of our own protocol. The working solution utilizes only a few communicates based on HL7. The work puts a higher emphasis on the informational content of those communicates. Our own protocol is also used to code DICOM communicate equivalents, which convey text messages or serve as event reminders.

Both of those protocols convey information that has to be conjoined while performing the tasks of the laboratory. The appropriate organization of spreadsheet data in database allows for a quick connection to be made between data originating from different sources. The examination order information is connected with the information coming from acquisition apparatus, and, later on, the performed report. The relational structure of the database offers a proper solution to the problem of connecting different information. The Hibernate technology allowed for a quick acquisition of complex structures with just a few instructions of Java programming language, replacing the need to type complex SQL formulas.

Producing software, that can be applied to production environment requires a well-developed testing process. In case of medical institutions that process is even longer. The application is continuously developed. The next step will be the preparation of communication interfaces for the HL7 and DICOM protocols [3]. It will allow to conduct tests with the use of software simulating events with the use of those protocols, and will form the next stage of application tests leading to its introduction in an actual radiological laboratory.

References
[1] IHE Radiology Technical Framework Volume II Transactions Revision 9.0. Final Text June 27, 2008, http://www.ihe.net/Technical_Framework/upload/ihe_tf_rev9-0ft_vol2_2008-06-26.pdf.
[2] IHE Radiology Technical Framework Volume III Transactions (Continued) Revision 9.0. Final Text June 27, 2008, http://www.ihe.net/Technical_Framework/upload/ihe_tf_rev9-0ft_vol3_2008-06-26.pdf.
[3] Pianykh O.S.: *Digital Imaging and Communications in Medicine (DICOM)*: A Practical Introduction and Survival Guide, Springer, 2008.
[4] Piętka E.: *Zintegrowany system informatyczny w pracy szpitala*, PWN, Warszawa, 2004.

Resource security in the cloud computing structures

Sławomir Przyłucki, Daniel Sawicki
Department of Electronics, Lublin University of Technology,
38a Nadbystrzycka Str., 20-618 Lublin, Poland, E-mail: sawi@politechnika.lublin.pl

Cloud computing has become nowadays a buzzword among IT and industry engineers. The cloud phenomenon is quickly growing towards becoming the de facto standard of computing, storage and hosting, both in industry and Internet.

Cloud computing is typically divided into three levels of service styles: Software as a Service (SaaS), Platform as a Service (PaaS), and Infrastructure as a service (IaaS). The article covers the bottom level of a cloud structure, the IaaS level. We concentrate on the security aspects of the IaaS delivering hardware (server, storage and network), and associated software (usually virtualization technology, distributed file system) [2]. When categorizing cloud service offerings one often refer to clouds in terms of "service style" depending on the portion of the software stack delivered as a service. Other words, it refers to the nature of access and control with respect to use and provisioning of virtual and physical resources [1]. From that point of view, there are three cloud types: public, private and hybrid [4]. The security issues are to extremely important in case of the last two types of cloud structures. Simultaneously, private and hybrid cloud are most popular in industry and require deep security considerations. Thus, the article presents studies on the resources security mechanisms in the private cloud.

Private clouds give users immediate access to computing resources hosted within an organization's infrastructure. Users self-provision and scale collections of resources drawn from the private cloud, typically via web service interface, just as with a public cloud. However, because it is deployed within the organization's existing data center, and in most cases behind the organization's firewall, a private cloud is subject to the organization's security regulations and thus offers a higher degree of security over sensitive code and data. Presented results cover the resource security aspects in the area of deployment of variety of physical network infrastructures [3]. The investigating features are: *security groups*, the sets of networking rules applied to all virtual machines instances associated with a group; e*lastic IPs. a way to* gain control over a set of Public IP addresses to allow users to run well-known services within the private cloud; m*etadata service,* the mechanism provides access to useful information from inside a running virtual machine; *virtual machines isolation,* mechanism to enforce isolation of network traffic between different security groups.

All mechanism and tests presented in the article base on Eucalyptus cloud structure [3] and give a detailed vie on process of securing the resources inside private IaaS cloud structure.

References

[1] Vaquero L.M., Rodero-Merino L., Caceres J., Linder M.: *A Break in the Clouds: Towards a Cloud Definition*, ACM SIGCOMM Computer Communication Review 39 No.1, 2009, p. 50-55.
[2] Foster I., Zhao Y., Raicu I., Lu S.: *Cloud Computing and Grid Computing 360-Degree Compared*, Grid Computing Environments Workshop, 2008, p. 1-10.
[3] Johnson D., Murari K., Raju M., Suseendran R.B., Girikumar Y.: *Eucalyptus Beginner's Guide – UEC Edition*, CSS Corp. 2010, http://www.csscorp.com/eucauecbook, June 2010.

Viedo encoding in multiview monitoring systems

Sławomir Przyłucki
Department of Electronics, Lublin University of Technology,
38a Nadbystrzycka Str., 20-618 Lublin, Poland, E-mail: spg@politechnika.lublin.pl

Encoding and transmitting video data, such as 3D and incorporating multiple views, a new challenge to the existing network of transmission systems and industrial monitoring installation. The video from one camera can be efficiently compressed by the similarity between the particulary frames located within time and space. In the case of two or more cameras in addition, there are similarities between frames from the same time but from different cameras [1]. This occurs when multiview monitoring systems, as they represent the same scenę scene from slightly different perspectives. Coding standard with presented above properties multiview is H.264/AVC MPEG-4 Part 10 [2] and its extension called MVC (Multiview Video Coding). For video material from multiple cameras and then compressed and used in the monitoring of any service,it must be converted it into a data stream. The way this transformation can be formed due to the requirements of the transmission network and the expected quality of the image used in monitoring.

Research, described in the article, are based on reference software for Multiview Video Coding standard developed by the Fraunhofer HHI. The software is called JMVC (Joint Multiview Video Coding) allows encoding and decoding video streams from multiple cameras. It is therefore a promising solution for all applications for monitoring objects, both in 3D technique and multiview. Based on this encoding algorithm was tested methods of predicting the impact of the bitrate of the multiview output signal and the index of the PSNR (Peak Signal English-to-Noise Ratio), describing the image quality [3]. Based on the tests conclusions were reached about the effectiveness of video compression based on the H.264/AVC standard MVC in the context of monitoring systems.

The experiments include several typical scenarios multiview prediction that can be used in monitoring systems. Coding system was examined in the absence of prediction of another view for B-frames, without multiview prediction for all frames and the impact of selection and number of views of reference for compression multiview prediction.

Based on the results cited in the article, conclusions as to the choice of encoding parameters MVC monitoring systems. Pointed out the manner and conditions to minimize the resulting bandwidth video stream, while the discussion of these methods affect the image quality provided by the multiple monitoring system.

References

[1] Chen Y., Wang Y., Ugur K., Hannuksela M., Lainema J., Gabbouj M.: *The Emerging MVC Standard for 3D Video Services*, Hindawi Publishing Corporation, 2009.
[2] ISO/IEC 14496-10:2008. *Information technology - Coding of audio -visual objects: Part 10 Advanced Video Coding*, ISO Standard, 2009.
[3] Vetro A.: *Representation and Coding Formats for Stereo and Multiview Video*, Seria: Intelligent Multimedia Communication: Techniques and Application, Springer, 2010.

Combustion process monitoring in a stoker fired boiler using endoscope and thermo-visual camera

Waldemar Wójcik, Piotr Popiel, Andrzej Kotyra
Faculty of Electronics, Lublin University of Technology, Lublin, Poland,
E-mail: p.popiel@pollub.pl

This article presents the results of experiments carried out on stoker fired boiler EKM50 using a thermo-visual camera and an endoscope prepared to work at high temperatures. The aim of these experiments was determining both combustion spatial homogeneity and influence of boiler load as well as slag temperature on amount of underburn loss. The experiments were done at lower levels of boiler efficiency, 31 t/h and 26 t/h respectively. Additional problem was connected with variable properties of fuel that had negative influence on combustion rate. It causes simultaneous formation of holes in a combusted fuel layer, that causes improper primary air distribution within area being considered.

Flame images were captured by placing endoscope inside a combustion chamber, a few meters above the grate. Considerable differences of the burning fuel temperature have pointed out to lower efficiency of the combustion process.

A sieve analysis of coal was carried out as well as determination of basic fuel parameters such as: colorific value, ash content, amount of both volatile and combustible contents. The analysis determined extent of the required rebuild and modernization activities. Moreover, it have pointed to the improper primary air distribution within the grate and revealed the need of grate seal exchange.

References

[1] Pronobis M.: *Modernizacja kotłów energetycznych*, WNT, Warszawa 2002.
[2] Wójcik W., Cięszczyk S., Komada P., Popiel P.: *Optyczna metoda oznaczania węgla całkowitego w popiele lotnym przy współspalaniu biomasy z pyłem węglowym,* Elektronika 6/2010, 2010, p. 105-107.
[3] Wójcik W., Kotyra A., Popiel P.: *Wykorzystanie spektrofotometru światłowodowego do pomiaru widm emisyjnych płomienia,* Przegląd Elektrotechniczny 7/2010, 2010, p. 264-266.
[4] Ściążko M., Zuwała J., Pronobis M.: *Zalety i wady współspalania biomasy w kotłach energetycznych na tle doświadczeń eksploatacyjnych pierwszego roku współspalania biomasy na skalę przemysł*ową, Energetyka 3/2006, 2006, p. 207-220.
[5] Zamorowski K.: *Współspalanie biomasy w kotle rusztowym (na przykładzie badanego obiektu),* Energetyka 1/2006, 2006, p. 41-46.

The device for cold-junction temperature compensation of thermoelectric transducers with temperature-dependent voltage source

Oleksandra Hotra
Lublin University of Technology, Department of Electronics, Lublin, Poland,
E-mail: o.hotra@pollub.pl

The accuracy of the temperature measurement and control is relevant for the quality of production and the operating safety of many power installations. On these objects, primary thermoelectric transducers are widely used for temperature measurement and control [1]. In industrial conditions, for the correction of the temperature measurement error due to cold-junction temperature change, some automatic devices for measurement error self-correction (e.g. temperature-dependent resistor bridge circuits) are employed [2]. To increase the accuracy of compensation of the influence of cold-junction temperature change, a temperature-dependent voltage source for driving the temperature-dependent resistive bridge circuit can be applied [3].

The improvement of compensation circuits with temperature dependent voltage source, especially in low temperature range measurements, is an important task of thermometry. For designing a compensation device supplied with a temperature dependent voltage source, different temperature-dependent elements can be used. In this paper, a design of the temperature-dependent voltage source which performs required output characteristics, based on operational amplifier and thermoresistor is proposed.

The thermocouples of L-type (chrome l- copel), K-type (chromel - alumel), S-type (90% platinum - 10% platinorhodium) and R-type (87% platinum - 13% platinorhodium) were investigated.

The analysis of the relationship between the absolute compensation error value and the cold junction temperature has shown that the circuit in question provides good reproducibility of thermo-emf for cold junction compensation of various thermocouple types. The compensation error is less than 0,01°C for thermocouples of L-type, 0,05°C for thermocouples of K-type, 0,1°C for thermocouples of R-type, and 0,2°C for thermocouples of S-type. The lower accuracy of the reproducibility of the thermo-emf for cold junction compensation for thermocouples of R-type and S-type is caused by the error of reproducibility of nominal characteristics of these thermocouples; the mean value of this error equals 0,18°C for thermocouples of R-type, and 0,17°C for thermocouples of S-type, according to IEC 584-1.

The design of the supply source based on operational amplifier and temperature-dependent resistor allows setting the optimum value of the supply voltage, and the temperature changes of the output voltage, at which the values of thermo-emf of cold junction of the thermocouple are reproduced with higher accuracy. Experimental investigations of the described compensation circuit have confirmed the results of theoretical calculations.

References

[1] Готра О.З.: *Мікроелектронні елементи та пристрої для термометрії,* Львів: Ліга-Прес, 2001, 487с.
[2] Поліщук Є.С., Дорожовець М.М., Яцук В.О. та ін.:*Метрологія та вимірювальна техніка*, Львів: Бескид Біт, 2003, 544 с.
[3] Hotra O.: *Cold-junction temperature compensation of thermoelectric transducers*, Przegląd Electrotechniczny 10/2010, 2010, p. 24-26.

Problems with estimation of the conversion error in a slotted line with a frequency data carrier

Piotr Warda

*Lublin University of Technology, Department of Automatics and Metrology,
Lublin, Poland, E-mail: p.warda@pollub.pl*

The slotted line with a frequency data carrier is more and more often using in order to conversion and sending information about measurement quantities. Frequency signals have more advantages: the easily long distance sending, easily mathematical operations direct to signal and the resistance to interference.

The "physical quantity-to-frequency" (X/f) converters are using in many domains of everyday life, for example: a temperature measurement, a voltage measurement, a heart rate measurement, and a radar technology. In order to measure instantaneous value of a physical quantity in dynamic states is essential to obtain the instantaneous value of frequency of the frequency signal. In this condition, is very convenient to use the "frequency-to-code" (fDC) conversion based on the use of an "on the fly" counter. The metrological analysis of a slotted line composed of a fDC converter shown that the accuracy of the slotted line is determined by the construction-depending error of the X/f converter, fDC converter errors and approximation error [2].

The paper presents select problems in estimation of the conversion error in the slotted line with a frequency data carrier. The estimation influence of component errors on the total error can be carrying out by theoretical and experimental ways.

The theoretical way is presented in [1]. Author presented formulas describing a static work fDC converter. An output value in case, when frequency is changing causes a constantly increasing phase shift between consecutive output values, because of finite accuracy of a mathematical calculation in the computer. Obtained results are little useful to estimate the total error in a dynamic work converter.

The experimental way of estimation the total error is presented in [2]. In order to evaluation obtained theoretical formulas was done experiment. The problem is displayed in the phase increasing between a testing signal and obtained from a slotted line signal [3]. A source of the testing signal – a generator with a frequency modulation caused problem by its inaccuracy of signal generation. In order to minimise influence of the phase shift was worked out a special application, which analysed differences between a maximum and a minimum of the testing signal and the obtained signal and decreases the phase shift to minimum value.

Presented solution is making possible to compare the testing signal and obtained from the slotted line signal. The results confirmed that the shift phase decrease process was carrying out correctly. Showed problems and considerations present, that estimation of total errors in the slotted line with the frequency carrier of information requires a further research.

References

[1] Świsulski D.: *Koncepcja cyfrowego przetwornika napięcie-częstotliwość*, Pomiary, Automatyka, Kontrola 4/2007, 2007, s. 91-93.
[2] Warda P.: *Programowe odtwarzanie dynamicznych wielkości wejściowych czujników z wyjściem częstotliwościowym*, Rozprawa doktorska (19.03.2008), Politechnika Lubelska, Wydział Elektrotechniki i Informatyki.
[3] Warda P.: *Generator z modulacją częstotliwości jako źródło sygnału testującego dla toru pomiarowego z częstotliwościowym nośnikiem informacji*, Przegląd Elektrotechniczny 86 8/2010, 2010.

The cogeneration of energy in house building

Piotr Filipek
Lublin University of Technology, Lublin, Poland, E-mail: piotr.filipek@pollub.pl

The article presents the analysis of a cogenerating system with a gas boiler which both produces thermal energy for house and water heating and generates electrical energy to supplement grid supply [1, 2].

In order to evaluate the efficiency of the system operation a few models were developed: the model thermal absorptivity model of the house, hot water requirement and climate conditions of chosen country region. The computer simulations were carried out for a typical detached house built according to the latest technology [3] and of 120 m^2 useable floor area and 350 m^3 cubature. As a result, a characteristic estimation of house demanded heat energy in function of external ambient temperature was prepared. The amount of thermal energy needed to heat water was calculated for an average four-person Polish family. The data mentioned above was used to choose the gas boiler.

The boiler in question has built-in Stirling engine powered by heat energy produced during gas combustion in specially constructed gas burners [4]. This engine drives a generator producing power, the amount of which depends on the boiler operating mode. Additionally, the produced heat energy is directed to heat exchanger which allows house heating and producing hot running water.

The model of the considered system was developed in MATLAB-SIMULINK. The parameters of the cogeneration boiler are as follows: output nominal thermal power 8 kW, maximum thermal power 12 kW, output electrical power up to 1.2 kW, average total efficiency 90%, and self consumption energy 30 W in stand-by and 110 W during an operation [5].

Taking into account the amount of the demanded heat energy, the required gas cubature and the quantity of the generated electrical energy during every month of a year was calculated. On this basis, an economic balance involving additional investment and exploitation costs was made and the savings due to the energy cogeneration were estimated [6]. The results helped to calculate a payout time of the system implementation and to evaluate the point of using the system.

References
[1] Twidell J., Weir T.: *Renewable Energy Resources*, CRC Press Taylor and Francis Group, second edition, 2007.
[2] Kalina J.: *Small-scale cogeneration in Poland. 2003 market report*, Politechnika Śląska 2003.
[3] Strategie redukcji emisji gazów cieplarnianych w Polsce do roku 2020, Ministerstwo środowiska, Marzec 2003.
[4] Drobniak S.: *Energetyka i Ekologia*, Politechnika Częstochowska 2007.
[5] PPS24-ACLG5 – Operating Manual, http://www.whispertech.co.nz, Whispergen 2009.
[6] Klugmann-Radziemska E.: *Odnawialne źródła energii. Przykłady obliczeniowe*, Gdańsk 2009.

HID Lamp System with electronic balast controled
with ZigBee Network

Bohdan Borowik[1], Miroslav Woznak[2], Barbara Borowik[3]

[1] *University of Bielsko-Biala Electrical Engineering and Automation Dept., Bielsko-Biala, Poland, E-mail: bborowik@ath.bielsko.pl*
[2] *VSB-Technical University of Ostrava, Telecommunicatons Dept., Ostrava, Czech Republic*
[3] *Cracow University of Technology, Physics, Mathematics and Computer Science Dept. Crakow, Poland*

The paper discusses advanced driving system for an HID (High Intensity Discharge) lamp with the electronic ballast. Electronic switch unit driven by ZigBee system controls illumination of lamps in network. RF ZigBee transceivers are employed to turn the HID lamps on and off and to control illumination through wireless remote communications. Thereby are achieved considerable energy saving. Also operational status of the ballast and HID lamp can be controlled by the sensors and all failures will be automatically detected and notified to users.

References

[1] Borowik B., Wojnarowski J.: *Applying the Zigbee technology for the enhancing the remote objects control*, 80 Annual Meeting International Association of Applied Mathematics and Mechanics (GAMM2009) Gdansk University of Technology, February 9-13, 2009.
[2] www.zigbee.org.
[3] PIC24HJXXXGPX06A/X08A/ X10A High-Performance 16-bit Microcontrollers Data Sheet, 2009 Microchip Technology Inc., DS70592B.
[4] Xbee®/Xbee-PRO® ZB RF Modules, Digi International, 2010.
[5] Borowik B. et al.: *Meandry języka C/C++*, PWN, Warszawa 2006.
[6] Borowik B., *Interfacing PIC Microcontrollers to Peripheral Devices*, Springer Science + Business Media B.V. 2011.

Design and simulation of a vibration-based energy harvesting system for a bicycle

Andrzej Kociubiński, Jakub Kazubek, Katarzyna Sobańska
Lublin University of Technology, Lublin, Poland, E-mail: akociub@semiconductor.pl

Energy harvesting devices based on the piezoelectric effect that converts ambient energy to electric energy are becoming a very attractive alternative energy sources nowadays. These are clean and vast energy sources and it is possible to scavenge enough energy to power micro devices. These sources are applied in many engineering applications and are used for manufacturing of sensors and actuators [1].

This paper reports design and simulation of a piezoelectric device that harvests mechanical energy from low frequency range vibrations of a moving bicycle. The first peak in the bicycle vibrations spectrum corresponds to the natural frequency of bike + cyclist. The interesting frequency band to harvest energy, where 80% of the energy of the vibrations is concentrated, lies approximately between 10 Hz and 30 Hz [2]. The energy harvesting system consists of a cantilever beam with a piezoelectric material, the energy receiver (Light-Emitting Diode) and a simple power interface circuit used to control system [3].

A moving bicycle vibrates and the mechanical energy of the vibrations can be converted into electrical energy by using electromechanical transducers, such as piezoelectric materials. The electrical energy produced this way can be used to power a rear lamp of the bicycle. This system is a clean power source that could be an alternative to a dynamo and lengthen battery lifetime.

The influence of the proof mass, beam shape and damping on the harvester performance are modeled to provide a design guideline for maximum output power harvested from vibrations available on a bicycle. The main part of the energy harvester, its piezoelectric element, is designed and evaluated in CoventorWare®. Suggested power conditioning circuit for the scavenging device is also designed and analyzed. The power converter circuit is simulated in SPICE. The results of these simulations, like generated electrical power and others, are reported and commented herewith.
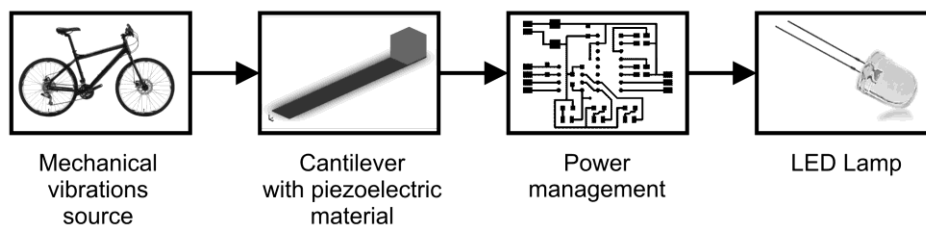
Fig. 1. General diagram of a device based on vibrations energy harvesting

References
[1] Saadon S., Sidek O.: *A review of vibration-based MEMS piezoelectric energy harvesters,* Energy Conversion and Management 52, 2011, p. 500-504.
[2] Minazara E., Vasic D., Costa F.: *Piezoelectric Generator Harvesting Bike Vibrations Energy to Supply Portable Devices.* International Conference on Renewable Energies and Power Quality ICREPQ'08, 12-14 March 2008.
[3] Qiu J., Jiang H., Ji H., Zhu K.: *Comparison between four piezoelectric energy harvesting circuits,* Front. Mech. Eng. China 4 No 2, 2009, p. 153-159.

Universal acceleration measurement unit for energy harvesting sources

Jakub Kazubek, Andrzej Kociubiński
Lublin University of Technology, Lublin, Poland, E-mail: kazubek@pollub.pl

This article describes a universal acceleration measurement unit designed for measuring parameters of vibrations of different objects and using the results especially to allow modeling energy harvesters for them. The paper presents the design of the unit, the prototype and example measurements taken with the use of the prototype.

Energy harvesters allow to regain energy from heat, lights or vibrations and convert it to electrical energy. Systems which use energy harvesters as their only power supply can work as long as mechanical or other form of energy is generated by the main system. Energy harvesters can be used, for example in wireless sensor networks installed in hazardous environment on vibrating elements like pumps, generators. The knowledge of the character of vibrations produced by these elements is crucial in the phase of modeling and prototyping energy harvesters. Knowledge of the vibrations' frequencies allows to tune the resonance frequency of the piezoelectric energy converter to maximize its output power. Knowledge of acceleration amplitude in each axis allows to estimate the value of maximum output power and the optimal direction in which the circuit should be installed.

Presented measurement unit consists of a 3 axis acceleration sensor, microcontroller and communication interface. The unit has its own battery supply and optional wireless communication interface. The accelerometer is a Freescale MEMS sensor with integrated analog front end and digital circuitry. The main task of the microcontroller is to acquire 3 axis acceleration values from the sensor, perform scaling of the values and providing them to the input of the communication interface. The communication interface uses a USB link or a wireless Bluetooth connection with a computer. Wireless connection and battery supply allow to conduct measurements on moving objects. The system's structure is presented in Fig. 1.

In the last part of the article example measurement results taken with designed measurement unit are presented. The measurement results show that the designed unit allows to measure vibrations' parameters and next use them in modeling of a specific energy harvester.

Fig. 1. Structure of the acceleration measurement unit

References
[1] Erturk A.: *Electromechanical Modeling of Piezoelectric Energy Harvesters*, Virginia Polytechnic Institute and State University, 2009.
[2] Roundy S., Wright K.P., Rabaey J.: *A study of low level vibrations as a power source for wireless sensor nodes*, Computer Communications 26, p. 1131-1144.
[3] Kimberly T.: *Frequency Analysis in the Industrial Market Using Accelerometer Sensors*, Freescale Semiconductor AN3751, rev 0, 2008.

Integration of supervision alarm system with the control and management systems in the electric equipment applied at buildings

Marcin Buczaj

*Lublin University of Technology, Department of Computer and Electrical Engineering,
Lublin, Poland, E-mail: mbuczaj@pollub.pl*

Actually the tasks to be performed by the modern electric installations installed in the buildings are not limited only to the reliable supply of electric energy with required parameters. The specialized systems are expected to exercise the control over the object status and to control the operation of the devices installed in this system. The purpose of these systems is to perform assumed tasks associated with the operation of the lighting, heating and ventilation in the object; to perform the role of processes control systems and to enable the permanent supervision over the processes occurring in specified rooms for the user.

The are two principal kinds of the systems performing the control and management functions in the electric equipment applied at buildings:

- island system – the system based upon autonomous systems with one of the systems performing precisely assigned tasks only (e.g. controlling the building heating of performing the alarm system functions only);
- integrated system – the system based upon information exchange, sharing of individual systems infrastructure or upon centralized management system.

The integration of the autonomous systems can be performed in the following manner:

- through information exchange between the autonomous systems;
- through the detection and decision making elements sharing by the systems;
- through the performance of the functions assigned to individual systems by the same control system.

The system wholly integrated in hardware and functional scope is illustrated in Fig. 1.
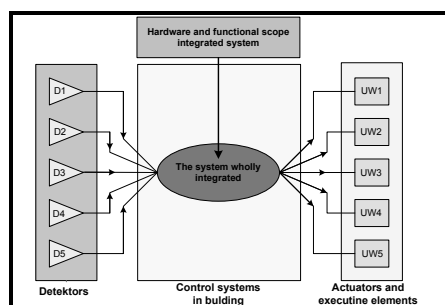
Fig. 1. The system wholly integrated in hardware and functional scope

References

[1] PN-EN 50131-1 – *Systemy alarmowe. Systemy sygnalizacji włamania i napadu. Część 1: Wymagania systemowe*. PKN, Warszawa 2009.

[2] Buczaj M., Sumorek A.: *Wirtualny system nadzoru sterujący pracą systemu sygnalizacji włamania i napadu*, Motrol – Motoryzacja i Energetyka Rolnictwa 12, 2010, s. 46-53.

[3] Petykiweicz P.: *Nowoczesna instalacja elektryczna w inteligentnym budynku*, Wydawnictwo COSiW SEP, Warszawa 2001.

Microscopic methods of examining the state of metal and alloy surfaces

Piotr Budzyński, Piotr Tarkowski
Lublin University of Technology, 36 Nadbystrzycka Str., Lublin, Poland,
E-mail: p.budzynski@pollub.pl

Depending on the type of changes appearing on the surface of metals and their alloys and on the size of the area where they were found, various methods of microscopic analysis were applied. The examination of resistance to erosion and corrosion was carried out with the use of optical microscopes (MO) or electron microscopes (ME). Alteration of the state of the surface after ion implantation and changes caused by the exploitation process were documented with the help of electron microscopes, atomic force microscopes (AFM) and scanning tunnel microscopes (STM). Local analysis of the content of elements inside the wear tracks of mating surfaces was carried out with the help of an X-ray microprobe (EDX) and with the use of the method of photoemission electron spectroscopy. The depth of wear tracks on tested samples and their shapes were examined with the help of a profile measurement gauge.

Protective coatings based on Zr-Ti-Si-N and Al-Ti-N/Ti-N/Al$_2$O$_3$, their physical and mechanical properties and phase composition

G.V. Kirik
Sumy State University, St.R-Korsakov 2, 40007 Sumy, Ukraine
Concern "UkrRosMetal", Av. Kurskii 6, 40012 Sumy, Ukraine

A short review of results obtained by the author on formation and studies of superhard and hard nanostructured coatings based on Zr-Ti-Si-N and Al-Ti-N/Ti-N/Al$_2$O$_3$ is presented. The coatings based on Zr-Ti-Si-N demonstrated high thermal stability up to 1180°C, high elastic modulus, good adhesion characteristics. However, their hardness values varied within a very wide interval between 33.7 GPa to 48.6 GPa. A size of *nc*-(Ti, Zr/N) nanograins increased from 10-12 nm to 25 nm in the process of annealing at 1200°C temperature. As for combined nano- and microstructured coatings, which were composed of three different layers Al-Ti-N/Ti-N/Al$_2$O$_3$, they demonstrated higher protective functions. However, their thermal stability was low. The coatings owned a high adhesion and a high corrosion resistance in NaCl and HCl media, and a very low friction coefficient.

The above coatings can be successfully employed in chemistry and machine-building industry. Their stoichiometry, thickness, as well as production conditions can be oriented on the goals and objectives of their future applications.

Lift car doors drive system with hi-efficient BLDC drive

Krzysztof Kolano
Lublin University of Technology, Lublin, Poland, E-mail: krzysiekkolano@wp.pl

The basic structure of modern drive of lift car doors consists of a permanent magnet DC motor and one-stage planetary gearbox. To reduce the maintenance to the minimum permanent magnet DC motors are often replaced by PM BLDC motors. Although this structure is much more sophisticated it still needs planetary gearbox to reduce rotary speed. In small drive systems (less than 500 Watts) one-stage planetary gearbox has mechanical efficiency less than 70 %, so that it affects negatively on energy consumption of the whole drive system. To reduce main disadvantages of most popular drive systems widely used in lift car doors, the new drive structure based on slow speed gearless BLDC motor has been presented. In this paper basic problems with speed control feedback have been described. To simplify the drive structure rotary encoder was eliminated from the motor speed feedback and replaced by the rotor position signals and special routine, that calculates the actual speed as a function of the rotation time.

The paper presents construction of gearless driver for lift door. Driver consists of DC brushless motor and electronic controlling circuit. Basic constructing assumptions were low turning velocity, high nominal and starting torque and low cogging torque. Motor control was realized by microcontroller MB91F267 fitted with u-DSP core. Working conditions required the application of algorithms of speed feedback with assumed trajectory of door movement. Cost reduction forced the authors to give up the module of continuous measurement of speed and utilize existing rotor's position sensors. Presented solution was successfully tested in real object.

Application of a fuzzy controller in regulation of active composite structure with varying parameters

Wojciech Jarzyna[1), Michał Augustyniak[2), Adam Wójcik[3)
[1) *Electrical Drive Systems and Electrical Machines Department, Lublin University of Technology, Lublin, Poland, E-mail: w.jarzyna@pollub.pl*
[2) *INDUSTER Sp. z o.o. Lublin, Poland, PhD student of Lublin University of Technology*
[3) *MSc student of Lublin University of Technology, Lublin, Poland*

The paper presents the results of the application of fuzzy controllers in control systems of active piezoelectric composite structure. These elements belong to a group of actuators, which can be used either in position control or oscillation reduction of vibrating elements. Such systems require operation run in a closed loop control systems. This control selection plays key role in obtaining the required accuracy and operational speed. For systems with fixed parameters, good results can be achieved using linear PID controllers. However, in real systems, due to possible mass changes, e.g. in stiffness or damping coefficients, linear PID controllers are not suitable for use. One of these alternatives is the application of fuzzy controllers.

This paper shows a fuzzy controller based on Mamdani and Takagi-Sugeno models design. Results for different μ membership functions having various triangle bases and gamma characteristics of membership function, are presented for a model with variable parameters. The results of the work give possibility to evaluate the usefulness of fuzzy control systems for active regulation of piezoelectric composite systems.

References
[1] Bocheński M., Warmiński J.: *Badania doświadczalne drgań autoparametrycznego układu belkowego*, Przegląd Mechaniczny 12, 2006, p. 32-34.
[2] Filipek P., Augustyniak M., Bocheński M.: *Control of active piezoelectric beam system applying DSP – based controller,* Przegląd Elektrotechniczny 7/2010, 2010, p. 323-325.
[3] Jarzyna W., Augustyniak M., Warmiński J., Bocheński M.: *Characteristics and Implementation of Piezoelectric. Structures in Active Composite Systems*, Przegląd Elektrotechniczny 7/2010, 2010, p. 320-322.
[4] Karami-Mohammadi A., Sadr A.: *An active vibration control of beam by piezo electric with Fuzzy approach*, Int. Journal of Signal System Control and Engineering Application 2 Issue 1, 2009, p.1-7.

Development of supercapacitors for hybrid energy safety systems

Liudvikas Pranevičius, Juozas Augutis
Vytautas Magnus University, 8 Vileikos Str., LT-44404 Kaunas, Lithuania,
E-mail: l.pranevicius@gmf.vdu.lt

There is a need for a rechargeable energy source that can provide high power, can be recharged quickly, has a high cycle life and is environmetally benign for a myriad of applications including defense, consumer goods, and electric vehicles. Recently developed low inertial high-power uninterruptable power supply systems start using new kinds of power sources: hybrid of battery-capacitor and supercapacitor (also known as ultracapacitor').

A variety of porous forms of carbon are currently preferred as the supercapacitor electrode materials because they have exceptionally high surface areas, relatively high electronic conductivity, and acceptable cost. Since only the electrolyte-wetted surface-area contributes to capacitance, the nanoscale carbon processing is required to form surface topographies that promote carbon wettability with electrolyte.

The purpose of this research paper is focused on the surface modification of carbon electrodes using plasma techniques, so as to control the increase in surface roughness in order to improve the capacity of supercapacitors. In this study, the surfaces of the carbon electrodes were chemically and physically modified using low-pressure plasma in oxygen. The treated and untreated (as-received) surfaces of the carbon electrodes were subjected to detailed characterization. The chemical and physical aspects of the surfaces were examined by scanning electron microscopy (SEM), atomic force microscopy (AFM) and Raman spectroscopy.

The surface topography has been optimized considering interaction between carbon electrode and electrolyte for supercapacitor. High capacity of supercapacitor is obtained due to fabrication of porous electrodes with surface topography accessible for electrolyte to form double charge layer. The carbon etching in plasma is accompanied by nanoscale changes of the surface geometry. The oxygen plasma treatments caused ablation of the carbon electrode surface, removing carbon atoms such as CO and CO_2 molecules. Carbon electrodes treated in oxygen plasma sor 1-3 min significantly (2.6 times) increases the capacity of supercapacitor. This effect is amplified in the case of plasma etching during deposition of Ni atoms. Deposited Ni atoms are transformed into NiO in oxygen plasma. The erosion rate of NiO in oxygen plasma may be neglected. The etching of C takes place through the windows unprotected by NiO. In that case the NiO film fulfils the role of mask through which C is etched.

The conclusion is made that the modification of surface topography of carbon electrodes by oxygen plasma is a suitable technique for the improvements of the electrical properties of supercapacitors.

Self ion-assisted treatment steel cord surface

A.V. Ksperovich[1), I.S. Tashlykov[2), V.V. Miadzelets[1), V.G. Luhin[1), O.G. Bobrovich[1)
[1) *Belorusian State Technological University, Minsk, Belarus,*
E-mail: kasperovich@bstu.unibel.by
[2) *Belorusian State Pedagogical University, Minsk, Belarus, E-mail: tashl@bspu.unibel.by*

As is known, deformations in the field of carcass and belt tyre lead to destruction rubber-cord systems. Therefore an actual direction is search of methods of updating of a surface steel cord for increase in adhesion between rubber and a cord. We are applied of ion-beam assisted deposition (IBAD) metal coatings deposition on steel cord.

Me-based coatings (Me = Ti, Mo) deposited on steel cord by means of self-ion assisted deposition (SIAD) technique exhibit some advanced properties such as improved adhesion stability, hardness and other. Metal layers were deposited on steel cord from resonance arc vacuum ion source (RVAS) [1].

(RVAS) with titanium or molybdenum electrodes was used to produce a mixture of Ti and Ti^+ ions or Mo and Mo^+ ions species. The ion-beam assisted energy was 10 keV. The IBAD system was pumped by a conventional diffusion pump charged with silicon oil and attains, during film deposition, a base pressure of 10^{-2} Pa.

Deposited films were investigated using Scanning Electron Microscopy by scanning electron microscope JSM-5610 LV with energy dispersive X-ray spectrometer JED-2201 JEOL.

References

[1] Tashlykov I.S., Belyi I.M.: *Method of coatings deposition* – Patent of Republic of Belarus №2324 (in Russian).

Investigation of electrochemically produced black silicon with silver nanoparticles

R. Jarimaviciute-Zvalioniene[1], Z. Kaminskiene[1], I. Prosycevas[1], S. Lapinskas[2]
[1] *Institute of Materials Science, Kaunas University of Technology, 271 Savanoriu Str., Kaunas, Lithuania*
[2] *Institute of Applied Research, Vilnius University, 10 Sauletekio Str., Kaunas, Lithuania*

Porous silicon is very known material and is useful for many applications, such as for the light emitting diodes, lasers, gases sensors, solar cells and etc. Black porous silicon is new material, which was performed in 2006, using femtosecondary laser. It can by produced too using reactive ion etching (RIE), electrochemical and chemical etching methods. Using electrochemically performed black porous silicon we can produce cheaper solar cells with higher efficiency, what is important economically today. To increase efficiency of solar cells *it's can be expected too using nanoparticles with* inherent plasmonic resonance, such as gold, silver, platinum and copper. Black silicon with precipitated plasmonic nanoparticles (such as silver) can revolutionary change the market of solar cells.

In this work the porous black silicon were prepared electrochemically in n-type (100) silicon wafers at room temperature in $HF:H_2O:C_2H_5OH$ solution by ratio 2:1:1, using ultrasound excitation 4.4 mW. The silver nanoparticles were precipitated from silver nitrate and sodium citrate solution.

The structures of porous silicon and porous silicon with silver nanoparticles were investigated by SEM and reflectance of samples was detected. The size of Ag nanoparticles has varied from 30 to 70 nm. Silver on porous silicon surface was detected by SEM-EDX.

Ionoluminescence of SiC bombarded by H+ and H2+ ion beams

Jerzy Zuk, Krzysztof Pyszniak, Andrzej Droździel, Marcin Turek
Institute of Physics, Maria Curie-Skłodowska University, Lublin, Poland

Silicon carbide is a wide band-gap semiconductor that attracts attention of scientists due to its possible applications in high-power, high-frequency devices [1, 2]. Another advantage of this material is its resistance to high temperature and harsh environment.

In the paper we present studies of the ionoluminescence of silicon carbide induced by the bombardment by protons and H_2^+ molecular ions. Ion beam energy varied in the range of 120 - 240 keV provided by ion implanter (UNIMAS-79 at Institute of Physics, Lublin). Schematic view of the experimental set-up is shown in the figure below.
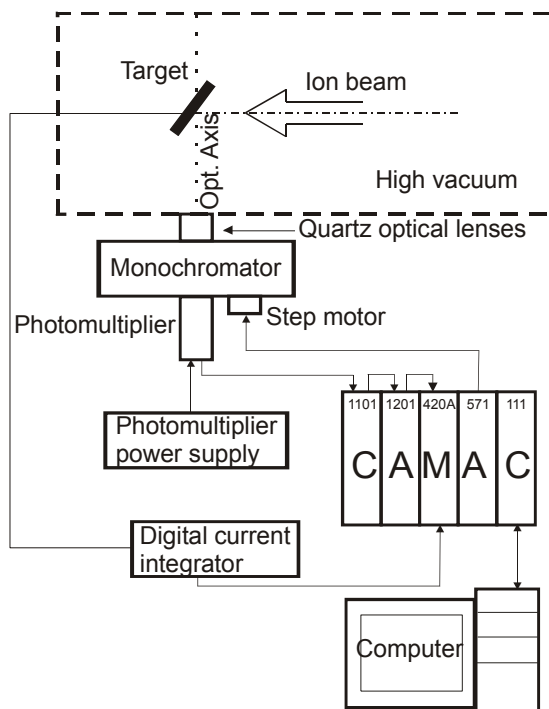

Fig. 1. Schematic view of the experimental set-up used for ionoluminescence studies

References
[1] Poggi A., Moscatelli F., Solmi S., Armigliato A., Belsito L., Nipoti R., J. Appl. Phys. 107, 2010, p. 044506.
[2] Zhang H.H., Zhang C.H., Li B.S., Han L.H., Zhang Y., Nucl. Instrum. Methods Phys. Res. B 268, 2010, p. 2318.

Structural properties of nanocrystalline TiN film

A.D. Pogrebnjak[1)], A.M. Mahmood[2)]

[1)] *Ukraine Sumy Institute for Surface Modification, P.O.Box 163, 40030 Sumy, Ukraine,*
E-mail: apogrebnjak@simp.sumy.ua.
[2)] *Sumy State University, 2 Rimsky-Korsakov Str., 40002 Sumy, Ukraine, E-mail:*
Amm19802007@yahoo.com

A rapid development in recent years has been seen in the field of nanotechnology due to the existing and/or potential applications of nanomaterials in a wide variety of technological areas such as electronics, catalysis, ceramics, magnetic data storage and structural components. With reduction in size, the materials exhibit peculiar and interesting mechanical and physical properties, e.g. increased mechanical strength, enhanced diffusivity, higher specific heat and electrical resistivity, compared to the conventional coarse grained counterparts. Nanomaterials include sintered materials with an ultrafine grain structure, loosely aggregated nanoparticles and nanocrystalline thin films [1-3]. One of the wear-resistant surfaces which are of a great interest for machine building, electronics and microelectronics, is the surface on the basis of titanium nitride. They are widely used as the firm wear-resistant surfaces for cutting instruments, diffusion barriers in electronics, decorative and corrosion resisting surfaces etc, because titanium nitride has high solidity, wear resistance and modulus of elasticity and it is chemically stable. At present time such surfaces are obtained in various types of vacuum systems, such as ‚Bulat', ‚Plasma copper', ‚Ang-1', etc. All these units differ by the amount and location of cathode packs, volume of vacuum chambers, force characteristics and heating methods of substrates, also by the deposition methods (vacuum-arched, ion-plasma, condensation with ion bombardment, magnetron sputtering, high-frequency discharge. Therefore it is necessary to study the structure and functional properties of surfaces obtained not only in different units, but also in different modes.

The aim of the work is to carry out the complex investigation of tribological properties, structural-phase composition and morphology of surfaces and their comparison with TiN surfaces obtained in conditions of continuous deposition or ion-plasma implantation.

By the means of scanning electron microscopy and X-ray diffraction analysis there were studied the structure and phase composition of nitride-titanic surfaces obtained in conditions of continuous deposition and ion-plasma implantation. It was shown that surfaces, got during ion-plasma implantation, have higher wear resistance and lesser friction coefficient. There was investigated the influence of pores and particles of drop fraction on the surface's characteristics. A physical mechanism describing such an influence was suggested.

References

[1] Major B., Ebner R., Wierzcho´n T., Mroz W., Waldhauser W., Major R., Wozniak M.: *Thin layers of TiN fabricated on metallic titanium and polyurethane by pulsed laser deposition*, Annals of Transplantation 9 (1A) (Suppl.), 2004.
[2] Chrisey D.B., Hubler G.K.: *Pulsed Laser Deposition of Thin Films*, John Wiley & Sons, 1994.
[3] Major B.: *Ablation and Deposition with a Pulsed Laser*, Wydawnictwo Naukowe Akapit, Kraków, 2002, (in Polish).

Stainless steel surface modification
induced by argon and krypton ion beam irradiation

Zbigniew W. Kowalski

Wrocław University of Technology, 27 Wybrzeże Wyspiańskiego Str.,
50-370 Wrocław, Poland

In many areas of science and technology various processes, such as: machining, chemical and ion etching, electron beam or photon flux bombardment, etc. (for example [1-4]) are used for surface modification of materials. Morphological properties of the surface depends on the type of process used. This paper presents the studies results of the basic aspects of the surface morphology of stainless steel modified in the process of ion etching, using perpendicular and oblique ($\Theta = 80° - 87°$) ion beam. In the experiments argon and krypton ion beams from GD ion source with hollow anode (beam diameter of about 1 mm, energy up to 6 keV and ion beam density up to 0,5 mAcm^{-2}) were utilized.

a)   b)   c)
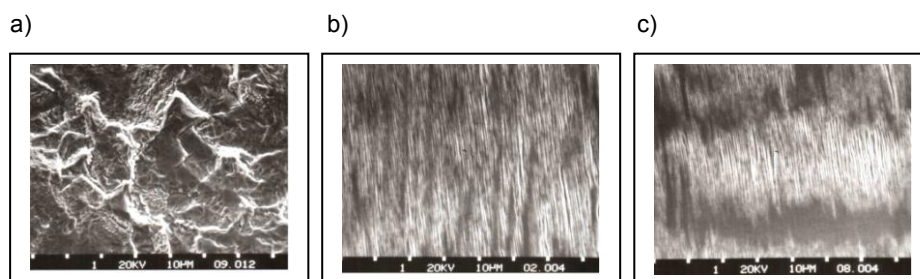
Fig. 1. *Ex situ* SEM photomicrographs of stainless steel surface topography induced by neutralized argon ion beam: a) at normal incidence, b) at quasi-tangential incidence, parallel to surface polishing direction, c) at quasi-tangential incidence, perpendicular to surface polishing direction

References
[1] Shinonaga Y., Arita K.: *Surface modification of stainless steel by plasma-based fluorine and silver dual ion implantation and deposition*, Dental Materials Journal 28 No6, 2009, p. 735-742.
[2] Chikararakara Evans, Naher Sumsun, Brabazon Dermot: *Process mapping of laser surface modification of AISI 316L stainless steel for biomedical applications,* Applied Physics A: Materials Science & Processing 101 No2, 2010, p. 367-371.
[3] Wang H., Teeter G., Turner J. A.: *Modifying a stainless steel via electrochemical nitridation*, J. Mater. Chem. 21, 2011, p. 2064-2066.
[4] Akira Okada, Yoshivuki Uno, Hiroaki Watanabe, Kunihiko Fujiwara, Kenji Doi: *Surface modification of stainless steel for surgical tool by EB-Polishing*, Key Engineering Materials 407-408, 2009, p. 339-342.

Thermal comparison of new electromagnetic switches to used ones

Mirosław Pawłot

Department of Electrical Devices and HV Technology, Lublin University of Technology, Lublin, Poland, E-mail: m.pawlot@pollub.pl

Among electrical switches there is a large group of electromagnetically driven switches with electromagnetic contactors in that number. The range of contactor applications is wide. Their operation reliability to a considerable extent depends on service conditions, adequate selection and proper operational use. When basic rules of proper operational use such as adequate selection of rated values and of installation locations as well as routine inspections are not observed permanent damages can occur.

Thermal parameters of brand new switches and of the ones that have been operated for many years have been compared in the paper. The testing included measurements of temperature at switch contacts and voltage drop at contact junction. The testing have shown that operation processes bring about changes in contact resistance and heat-transfer conditions defined by the shape of heating curves. Heating time constant of a used contactor has changed as compared to the corresponding value of a brand new contactor. Contact temperature increase is related not only to the growing transition resistance but also to changes in physical and chemical parameters that are responsible for heat transfer to the environment.

Consequently, continuous load capacity decreases with not exceeding of allowable temperatures for switches taken into account.

Analysis of the possibility of using ultraviolet radiation in the diagnosis of high voltage insulators

Tomasz Boczar, Paweł Frącz
Opole University of Technology, 5 Mikołajczyka Str., 45-271 Opole, Poland,
E-mail: t.boczar@po.opole.pl

The scope of this paper considers possibility determination and application area indication of a camera for ultraviolet radiation recording in diagnosis of linear insulators. Measurements results of ultraviolet radiation emitted by partial discharges (PDs) generated on a post insulator mounted in the air are presented in the paper. Recording was performed by use of a professional UVollé camera by the firm OFIL which enables for ultraviolet radiation measurement in the range from 250 nm to 280 nm. The main aim of works, performed under laboratory conditions, was to estimate the influence of supply voltage value changes in the range from 0 to 0.99 Up (breakdown voltage) on the counting quantity of PDs occurring on the surface of the ceramic bushing isolator. Moreover, the measurements and analyses performed enclosed influence estimation of the duration time of voltage apply to high tension electrodes on the optical phenomena progress connected with PDs generation. In the scope of works executed also the influence analyses of the distance between electrodes as well parameters of camera applied (sensitivity, amplification and size of the counting window) on the achieved results were investigated [1, 2].
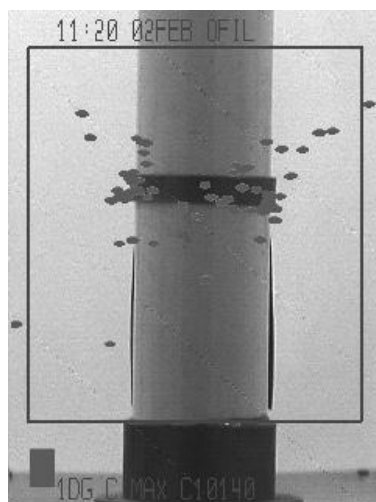
Fig. 1. SPDs generated on the model of bushing isolator by voltage equal to 0.99 U_b (breakdown voltage) distance between electrodes – 10 cm, and relative sensitivity – 100

References
[1] Frącz P.: *Analysis of camera application possibility for measurement of ultraviolet radiation emitted by partial discharges generated on a bushing isolator model*, Pomiary Automatyka Kontrola 59 No.4, 2011, p. 387-390 (in Polish).
[2] Frącz P.: *Use of the optical radiation signals emitted by electric discharges in the diagnosis of isolators*, SiM z. 285, Of. Wyd. PO, Opole, 2011 (in Polish).

Analysis of measurement uncertainty of acoustic cavitation intensity in mineral insulating oil

Marek Szmechta, Tomasz Boczar, Dariusz Zmarzły, Paweł Aksamit
Opole University of Technology, ul. Mikołajczyka 5, 45-271 Opole, Poland,
E-mail: m.szmechta@po.opole.pl

The subject area taken in this article is a result of a cycle of research work concerning the analysis of ultrasonic cavitation phenomenon in mineral insulating oils [1]. The article includes an analysis of the impact of long measurement time for an acoustic emission signal generated during cavitation phenomenon. The study focuses on spectral analysis of acoustic emission signal and changes in the spectra of recorded signals. We investigated the acoustic emission of cavitation accompanying the forced signal frequencies ranging from 100 kHz to 140 kHz and rms values range from 0 V to 1000 V [2]. The paper introduces a method of evaluation of measurement uncertainty of acoustic emission spectra by the statistical analysis of series of observations. The drawn probability density functions of used cavitation intensity factor values at different generated source signal parameters show the differences of its uncertainty. The obtained standard deviation of cavitation intensity P_{CAV} was in the range between 0.06 dB and 1.64 dB. At acoustic cavitation generation in insulating oil using signal rms value of 800 V and frequency of 115 kHz the highest uncertainty of P_{CAV} measurements was observed (Fig. 1).
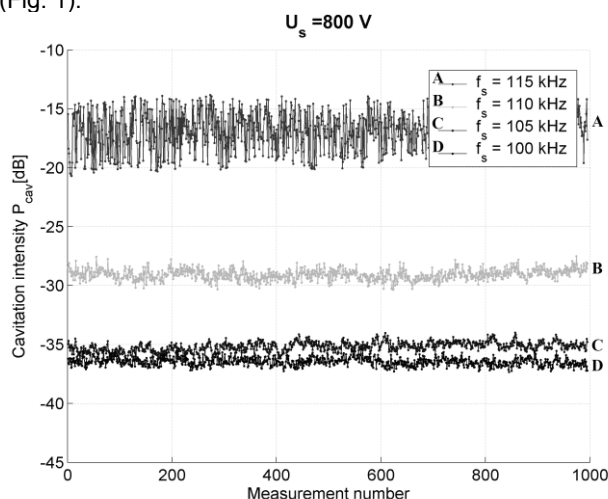
Fig. 1. The changes of cavitation intensity factor values (P_{CAV}) at the rms value of generated signal of 800 V

References
[1] Szmechta M.: *Analiza zjawisk kawitacyjnych w olejach izolacyjnych*, Rozprawa doktorska, Politechnika Opolska, 12/2009.
[2] Zmarzły D., Szmechta M.: *Investigation of acoustic emission generated by cavitation in insulating oils*, Pomiary Automatyka Kontrola 54 2/2008, s. 64-66.

The use of photographic technique in the diagnosis of electrical insulators

Paweł Frącz

Opole University of Technology, 5 Mikołajczyka Str., 45-271 Opole, Poland,
E-mail: p.fracz@po.opole.pl

The subject area of the paper concerns determination of possibility and application scope suggestion for the photographic technique in the linear isolators diagnosis. Measurements results of the optical radiation emitted by partial discharges (PDs) generated on a model of the bushing isolator, which was placed in the air, are presented in the paper. Pictures were taken using a professional camera which allowed the optical spectra of registration of optical radiation in the range of 420 to 780 nm. The main aim of laboratory research works performed was to estimate the influence of the supply voltage value changes in range from 0 to 0.99 U_b (breakdown voltage) on the intensity and character of the optical radiation spectrum emitted by PDs occurring on the ceramic insulating surface of the bushing isolator. In the scope of research works analysis of voltage value changes influence on the gathered spectra was performed while its accretion and decrease was investigated. Furthermore, the measurements and analysis performed enclose the influence estimation of the time, when the voltage was attached to the high voltage electrode, on the proceeding of the optical phenomena connected with generation of PDs.
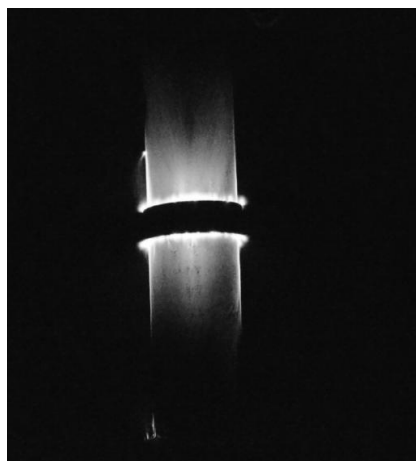
Fig. 1. Photo of PDs generated on a model of the bushing isolator

References
[1] Frącz P.: *Analysis of camera application possibility for measurement of ultraviolet radiation emitted by partial discharges generated on a bushing isolator model*, Pomiary Automatyka Kontrola 59 No.4, 2011, p. 387-390 (in Polish).
[2] Frącz P.: *Voltage value influence estimation on the measurement results for the optical radiation generated by surface partial discharges in stand-off isolator*, Pomiary Automatyka Kontrola 59 No.4, 2011, p. 383-386 (in Polish).
[3] Frącz P.: *Use of the optical radiation signals emitted by electric discharges in the diagnosis of isolators*, SiM z. 285, Of. Wyd. PO, Opole, 2011 (in Polish).

Use of stochastic test approach for simulation of nano-structural changes in metals

N.F. Denissova

*D. Serikbaev East Kazakhstan State Technical University, Ust-Kamenogorsk,
Kazakhstan, E-mail: nata69_07@mail.ru*

The industrial application of a new class of materials called intermetallics is currently increasing. Intermetallics have complex crystalline structure which accounts for their unique physic-mechanical properties. A special part in development of materials with predefined properties is played by diffusive processes. Research of diffusive processes at microscopic level in real-life experiments is not always probable and effective. Computer simulation allows to investigate at an atomic scale the dynamics of both fast and prolonged processes.

The purpose of this work is construction of a computer model on the basis of Monte-Carlo method, which allows to simulate structure-energy changes in metals and alloys.

The object of research is a system consisting of Grade A and B atoms which are located in the knots of a rigid hexagonal crystalline lattice. Periodic boundary conditions are imposed on the system.

The energy of atom pair bonding $\theta^i_{\alpha\beta}$ depends on the coordination sphere radius and the variety state of considered atoms (α, β can take the value A, B and V). The energy of bonding $\theta^i_{\alpha V}$ and $\theta^i_{\beta V}$ are set equal to zero, as vacancy-atom energy is usually 10 times less than the one between atoms.

Probability Q of one of the atoms located next to a vacant knot at the moment of time t_k will take its place:

$$Q = \exp\left(-\frac{E^V}{kT}\right), \tag{1}$$

where T is alloy annealing temperature, E_V – activation energy of a vacancy jump, k – Boltzmann constant. Probability Q can be also written down through probabilities p_{kl} of jump of k atom located on coordination sphere l:

$$Q = \sum_{k=1}^{6}\sum_{l=1}^{n} p_{kl} \tag{2}$$

The prospective value of released energy E_{kl} is estimated for each atom that surrounds a vacancy:

$$E_i = -\left(N_{AA}\varphi_{AA} + N_{BB}\varphi_{BB} + N_{AB}\varphi_{AB}\right), \tag{3}$$

where θAA, θBB, θAB – energy of interaction of atom pairs AA, BB, AB; NAA, NBB, NAB – numbers of atom pairs AA, BB, AB.

$$N_{AA} = \frac{1}{2}\left(zN_A - N_{AB}\right), \qquad N_{BB} = \frac{1}{2}\left(zN_B - N_{AB}\right) \tag{4}$$

where z – coordination number. The maximum value is received from all E_{kl}. For the description of interatomic interactions we used pair potential Morse functions.

We have developed an algorithm for simulating structure-energy changes in metals. It provides the basis for development of an application which allows to conduct a computer experiment and to visualize: atomic displacement situations, location of atoms in a crystalline lattice, changes of diffusion factors.

References

[1] Heerman D.V.: Methods of Computer Experiment in Theoretical Physics, M: Science, 1990, p.176.

Investigation of hydrogenation of Ti films under ion irradiation using water vapour plasma

Liudas Pranevičius, Simona Tuckute

Vytautas Magnus University, 8 Vileikos St., LT-44404 Kaunas, Lithuania,
E-mail: l.pranevicius@gmf.vdu.lt

Hydrogen storage in solids is one of the most promising and safe solutions for sustainable use. Different techniques are used for the hydrogen loading. However, the loading kinetics of equilibrium molecular hydrogen for metals and alloys is extremely low in comparison with that of the non-equilibrium hydrogen. It is known that hydrogen particles with energy (kinetic or internal) exceeding ~1 eV are accommodated in the metal lattice or just stick to its surface with a probability close to 1, independent either on the temperature or the atomic composition of the metal. Paper aims to show that plasma implantation technique is capable of splitting water molecules into their constituent atoms and storing of implanted hydrogen in the bulk of nanocrystalline Ti.

The 0.5 μm thick Ti films were deposited on different (stainless steel, silicon and melted quartz) substrates employing sputter deposition in vacuum technique. Plasma implantation was performed at 10 Pa pressure of water vapour using vacuum system PVD–75. Flow of water vapour was continuously controlled by mass flow controller. The plasma was generated using DC and RF energy sources. The dissipated power in plasma was verified in the range 100 – 300 W. Three irradiation regimes were realized in dependence of ion current density extracted from water vapour plasma and directed to the sample: (i) case A – (5 – 10) μA/cm^2, (ii) case B – (1 – 2) mA/cm^2 in, and (iii) case C – about 10 mA/cm^2.

The microstructure of the samples was characterized by X-ray diffraction (XRD) method using Bruker diffractometer (Bruker D8). The measurements were performed with 2θ angle in the range 20° – 70° using Cu Kα radiation in steps of 0.01°. The identification of peaks has been done using Search – Match software. The thickness and surface topography of Ti films were measured using the nanoprofilometer (AMBIOS XP 200). The surface views before and after hydrogenation were investigated by a scanning electron microscopy (SEM, JEOL JSM – 5600). The elemental composition of plasma treated films was analyzed by energy dispersive X-ray spectroscopy (EDX, Bruker Quad 5040). The distribution profiles of oxygen in Ti films after hydrogenation were measured by Auger Electron Emission spectroscopy (AES, PHI 700XI AUGER NANOPROBE) and the distribution profiles of hydrogen – by glow discharge optical emission spectroscopy (GDOES, Spectruma Analytic GMBH). Topographic AFM studies were carried out to reveal crystallite boundaries and surface morphology. The spatial resolution was several nanometers.

Results of the present study show that energetic water molecules are disintegrated into their constituent atoms during irradiation of Ti film by ions extracted from plasma in water vapour. The broken H and O atoms form chemical compounds with Ti atoms in the near-surface region within 40 nm and diffuse into the bulk along the entire thickness of Ti film presumably by diffusion along grain boundaries of nanocrystalline Ti.

Characteristics of an ion source for short-lived nuclide production

**M. Turek[1), D. Maczka[2), B. Słowiński[2), Yu. Vaganov[3), Yu. Yushkevich[3),
J. Zubrzycki[4)**
1) Institute of Physics, Maria Curie-Skłodowska University, Lublin, Poland
2) Institute of Atomic Energy POLATOM, Swierk-Otwock, Poland
3) Joint Institute for Nuclear Research, Dubna, Russia
4) Lublin University of Technology, Lublin, Poland

Efficiency of an ion source is a crucial point in nuclear spectroscopy of short-lived radioactive isotopes using ISOL facilities (Isotope Separation On Line) [1]. An electron beam generated plasma ion source [2] for nuclear spectroscopy purposes at YASNAPP isotope separation on-line facility is presented. Working conditions both in on- and off-line mode are presented and discussed. Formation of the potential trap inside the discharge chamber is an advantage of the presented construction, allowing obtaining relatively high ionization efficiences (2 - 5%) even for hard-to-ionize elements like Be, Ti, V, Zr, Nb, Mo, Tc, Ru, Rd, Hf, Ta, W, Re, Os, Ir, Pt. The papers presents estimation of critical working parameters of the ion source that enable the ion trap formation and high efficiency of ionization. The optimal temperature of the discharge chamber and cathode walls is found to be in the range 2600 - 2800 K.
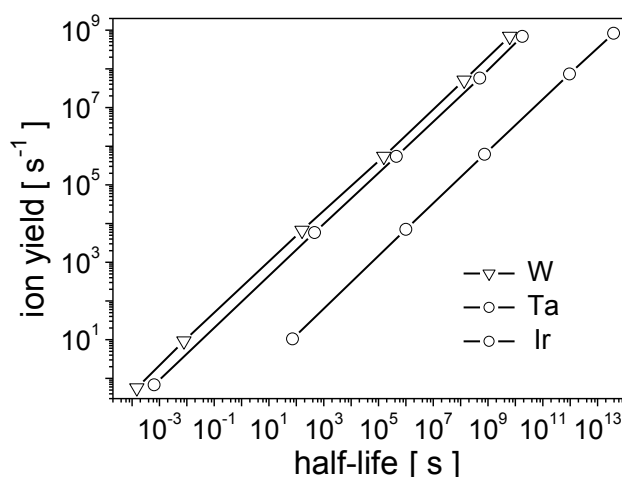
Calculations of the output rates of nuclides produced in the on-line mode are also presented (see the figure above) as well as the constraints on the half-life time of produced efficiently in the ion source imposed by construction details like the target material and its thickness

References
[1] Shmor P.W. Rev. Sci. Instrum. 73, 2002, p. 707.
[2] Nitschke J. M., Nucl. Instr. Meth. in Phys. Res. A 236, 1985, p. 1.

PLS CADD™ and TOWER™ as a tool for determining air gap clearances within towers in large scale voltage upgrading

K. Kupisz[1), S. Berlijn[2)
[1) *Stri AB, Ludvika, Sweden, E-mail:* konrad.kupisz@stri.se
[2) *Statnett SF, Oslo, Norway*

Many countries have experienced a small but steady increase in the power consumption. To be able to meet extension of transmission capacity in Norway Statnett is busy upgrading 300 kV network to 420 kV [1].

The important problem during voltage upgrading is insulation coordination and so that follows to determine the actual air gap clearance within towers.

PLS-CADD™ and TOWER™ from Power Lines Systems Inc. have been selected for the modelling of OHL and for calculations of the air clearances.

The upgrading process starts with line scanning of the existing line. All geometries of towers and the insulators are modelled in TOWER™. After that completely computer model is created in PLS-CADD™. With the help of pictures and drawings the old documentation is updated. The line model looks as line is built at present.

Then the existing 14 or 15 units insulator strings need to be extend in TOWER™ software to 17 units to withstand the higher service voltage under pollution or different weather loads. Clearances for the line with extended insulator are examined for four weather loads. This is no wind condition with max. temperature and max. ice load for lightning overvoltage, the three year return time wind condition for switching overvoltage and the 50 year return time wind condition for service voltage [2].

In case of critical clearances between conductor bundle and tower legs or guy wires different insulator solutions are checked. Critical towers are identified in PLS-CADD™ and one by one investigated until clearance problem has been solved.

This paper will focus on how PLS-CADD™ and TOWER™ are used for determining air gap clearance. Usability of both software will be also discussed.

References
[1] Berlijn S., Olsen A., Muhr M., Judendorfer T., Hinteregger M., Runde M.: *Voltage upgrading of overhead lines – an insulation coordination challenge,* ISH 2011, Hanover, Germany.
[2] Berlijn S., Halsan K., Jonsdottir R.I., Lundquist J., Gutman I., Kupisz K.: *Voltage Uprating of Statnet's 300 kV Transmission Lines to 420 kV,* To be published CIGRE SC B2, PS1, Paris 2012.

Dielectric response of OIP bushings with various insulation defects

Andrzej Mrozik, Marek Zenker, Jan Subocz
*West Pomeranian University of Technology, Department of Electrotechnology
and Diagnostics, Szczecin, Poland, E-mail: amrozik@zut.edu.pl*

The paper presents measurements of dielectric response of two OIP busing models with various types of insulation defects. The response has been examined in a frequency domain (FDS) in the range 10^{-4} - $5 \cdot 10^3$ Hz and in a time domain (Step Voltage Method). In a paper-oil insulation of bushing there were two defects simulated resulting from long term partial discharge activity. In the first case there was presence of solid products of oil and paper decomposition simulated. In this purpose between steering screens of bushing core there was natural sludge taken from long operated transformer injected. The second case modeled gas products of oil decomposition with injection of air bubbles into the insulation. In this way given stage of partial discharge development was achieved, which has not influenced significantly dielectric strength of the whole bushing.

The FDS measurements showed that dielectric response of the insulation is dependent on amount and type of dielectric material. When solid decomposition products are present there is additional relaxation process observed for frequency higher than 10 Hz, which time constant depended on volume concentration of contaminants. On the other hand gases amount in the insulation influences mainly $\mathrm{tg}\delta$ characteristics in the range $(10^{-3}$ - $10^0)$ Hz as fuzzy relaxation phenomena with wide spectrum of time constants. It was also found that solid products of paper and oil decomposition lead to increase of polarization index Ka obtained from SVM test. It was noted that the insulation temperature has insignificant influence on Ka values.

The research showed that dynamical measurements of polarization processes performed even with relatively low measuring voltage, combined with analysis of phenomena physics can be more effective diagnostic method of paper-oil insulation than standard $\mathrm{tg}\delta_{50Hz}$ value interpretation.

References

[1] Walczak K., Gielniak J., Graczkowski A., Morańda H.: *Analiza FDS w ocenia zawilgocenia izolacji transformatorów*, Pomiary Automatyka Kontrola 10, 2008.
[2] Subocz J.: *Transformatory w eksploatacji*, Wydawnictwo Energo – Complex, kwiecień 2007.
[3] Kaźmierski M., Szymański Z.: *Przyczynek do diagnostyki stanu technicznego izolatorów przepustowych transformatorów*, Międzynarodowa konferencja transformatorowa, Transformator 2009, p. 99-111.
[4] Zenker M.: *Spektroskopia dielektryczna układu papier – olej z osadami na celulozie*, Przegląd Elektrotechniczny 11b, 2010, p. 82-85.
[5] Mrozik A.: *Odpowiedź dielektryczna modelu przepustu wysokiego napięcia*, Przegląd Elektrotechniczny 11b, 2010, p. 59-62.

Medium-Voltage transformer PPN20

Janusz Ropa[1], Czesław Karwat[2]
[1] *Elektromontaż-Lublin Sp. z o.o., 1 Diamentowa Str., 20-447 Lublin, Poland*
[2] *Lublin University of Technology, Department of Electrical Devices*
and H.V. Technology, 38a Nadbystrzycka Str., 20-618 Lublin, Poland,
E-mail: c.karwat@pollub.pl

Further investigations have been performer on a PPN20 transformer in order to obtain optimal and stable parameters of a capacitive voltage divider cooperating with an electronic amplifier and to determine its practical applications. Stable parameters of the divider have been obtained by the selection of adequate materials and circuit arrangements for its individual elements. Full stability of the capacitive divider parameters ensures its advantageous use for the measurements of electrical energy at the MV side and makes also possible to analyze higher harmonics and thereby evaluate the electric energy quality. The analysis of higher harmonics has been possible up to the frequency of 10 kHz.

The proposal of an electronic control unit
for fuel injection system in aircraft prototype piston engine

P. Jaklinski[1], T. Zyska[2]

[1] *Department of Thermodynamics, Fluid Mechanics and Aircraft Propulsion,*
Lublin University of Technology, 36 Nadbystrzycka Str., 20-618 Lublin, Poland
[2] *Department of Electronics, Lublin University of Technology*
38a Nadbystrzycka Str., 20-618 Lublin, Poland, E-mail: t.zyska@pollub.pl

In the era of aviation the market of light and ultralight aircraft is becoming increasingly important. The basic requirements of such market are the low price of the engine, ease of maintenance and the possibility to use commonly available fuels (e.g. E95 which available at any petrol station).

The design of a new aircraft piston engine is the result of collaboration between Lublin University of Technology and WSK —PZŁKalisz". The power unit was based on Subaru's commercial 2 liters engine block.

The paper presents the idea and implementation of such engine control unit that considers the specificity of the strict requirements imposed by the aviation market.

Preliminary results of experimental studies of the designed electronic control unit are also presented.

The diagnostic method to verify of properties of LPG/CNG injectors

J. Czarnigowski[1)], T. Zyska[2)]
[1)] *Department of Machine Design, Lublin University of Technology,*
36 Nadbystrzycka Str., 20-61 Lublin, Poland, E-mail: j.czarnigowski@pollub.pl
[2)] *Department of Electronics, Lublin University of Technology, 38a Nadbystrzycka Str.,*
20-618 Lublin, Poland, E-mail: t.zyska@pollub.pl

One of the many markets, formed under the influence of economics and ecology is the automotive market. Manufacturers are constantly looking for components: cheaper, more reliable and with green badge attached, certifying environmental performance.

One of the important vehicle components are fuel injectors. These components are expected to dose precise amount of fuel along whole long lifetime. Therefore, new constructions of injectors are constantly being placed on the market, including those designed for alternative fuels such as LPG and CNG for example. New designs result in necessity reprogram the engine controllers for specific types of injectors.

This paper presents a method of operation analysis of selected types of gas injectors based on observation of deformation of current flowing through the injector. For the purposes of verification of the method the test rig was fitted with the properly oriented vibration sensors, as well as pressure sensors monitoring the injector outlet.

The article shows preliminary results of research made using specially designed test rig.

References

[1] Małek A., Wendeker M., Czarnigowski J., Grabowski Ł., Jakliński P., Barański G., Sochaczewski R., Podleśny M.: *Stanowisko do badań prehomologacyjnych dla pojazdów wyposażonych w układ sekwencyjnego wtrysku gazu LPG*, PTNSS CONGRESS-2007 P07-C148, Silniki Spalinowe PTNSS-2007-SC2.

[2] Regulamin nr 83 Europejskiej Komisji Gospodarczej Organizacji Narodów Zjednoczonych (EKG ONZ) — Jednolite przepisy dotyczące homologacji pojazdów w zakresie emisji zanieczyszczeń w zależności od paliwa zasilającego silnik" Dziennik Urzędowy Unii Europejskiej L(legislacja) nr. 119 z 6.5.2008, s. 1-181.

Electron hopping and DC conductivity of dampness-soaked paper-oil insulation of HV transformers

Pawel Zhukowski[1),]Marek Szrot[2),]Jan Subocz[3)]
*[1)]Lublin University of Technology, Department of Electrical Devices
and H.V. Technology, 38a Nadbystrzycka Str., 20-618 Lublin, Poland,
E-mail: pawel@elektron.pol.lublin.pl*
[2)]Energo-Complex Sp. z o.o., 9 Lotników Str., 41-949 Piekary Śląskie, Poland
*[3)]West Pomeranian University of Technology, Department of Electrotechnology
and Diagnostics, Szczecin, Poland*

Quality of paper-oil insulation to a great extent is determined by the water content in the paper. It has to be noted that most of the water concentrates in the paper while the water content in the insulation oil is by 1,000 times lower than in the paper [1]. According to the effective US standard it is assumed that a dampness-level increase in the insulation by a double causes a two-times decrease of its service life [2] and an increase of the dampness level by over 2.5% brings about a hazard of accelerated excessive degradation of the insulation. Hence the need for accurate and unambiguous determination of a dampness level in the paper component of a HV transformer insulation. The elaboration of a method (methods) for the dampness level determination should be based on physical phenomena as: first – they actually occur in a damp paper, secondly – they are sufficiently sensitive to the water content and thirdly – they are not sensitive (or only insignificantly sensitive) to other changes that structurally occur in cellulose and on its surface as a result of ageing processes.

The article presents investigations into dependences of direct-current conductivity of dampness-soaked pressboard on the dampness level and temperature of the samples. Conductivity activation energy has been determined. It has been found that the conductivity is realized by hopping exchange of electrons between potential wells formed by water molecules in the amorphous cellulose structure. On that basis, theoretical dependences have been determined. They accurately describe the experimentally obtained dependences on the water content and temperature. Based on the testing results location radius of the water-molecule valence electron that is concordant with the O^{2-} ion radius has been determined.

Information system for environmental monitoring

Iurii Krak, Oleg Stelia, Igor Stelia
Taras Shevchenko National University of Kyiv, Kyiv, Ukraine,
E-mail: oleg.stelia@gmail.com

The developed software and accumulated information allows to create an Information System for water quality monitoring in transboundary rivers.

The Information System aims at:
- development of the monitoring system and follow-up strategy for water quality in the trans-border rivers,
- application of European directives on water quality in the basins of this rivers,
- definition and promotion of analysis and technical monitoring procedures in accordance with the terms and conditions of these directives,
- proposing of possible changes in these directives according to the obtained results.

The Information System will be based on:
- collection of the existing quality data from automatic sensors,
- identification of the main point sources of pollution,
- assessment of dispersed sources of pollution,
- standardization of procedures in the member countries.

Generalization and analysis of various data collected at the national and international levels will become a tool for standardized, coordinated, and sustained computer water quality monitoring system for pollution management.

The system will make it possible to:
- facilitate the collection and processing of water quality data,
- develop the national information system in the Ukraine,
- use the data sharing procedures at international level between member countries.

As a result the computer system will be created, which will consist of:
- database containing information on water quality in basins of the rivers under study;
- mapping unit for processing and visualization of various spatial data on the map;

This Information System can be applied to the Western Bug River, which flows from central Ukraine to the west, forming part of the boundary between Ukraine and Poland, passes along the Polish-Belarusian border and into Poland, and empties into the Narew river near Serock. It also can be applied to the San River, a tributary of the Vistula River which arises in the Carpathian Mountains near the village of Sianky, exactly on the Polish-Ukrainian border and forms the border between Poland and Ukraine for approximately its first 50 km.

The effect of direct voltage polarity on the value of electric arc burning on the W-10 switch contacts

Czesław Kozak

*Lublin University of Technology, Department of Electrical Devices
and H.V. Technology, 38a Nadbystrzycka Str., 20-618 Lublin, Poland
E-mail: mario@elektron.pol.lublin.pl*

The paper presents results of changing energy values of W-10 switches for various design solutions of their contacts.

The experiments have been performed on a computer-supported testing stand described in [1].

The testing cycle consisted in recording characteristics of current, voltage drop and temperature of a normally-closed fixed contact as well as the real-time arc energy values for each switching cycle at direct voltage and for every 20th cycle at alternating voltage. The measurements have been performed at the voltage of 120 V in order to avoid incessant burning of the arc at direct voltage.

In the process of performing measurements for direct voltage an automatic change of polarity has been applied at starting of each subsequent switching cycle.

It follows from the obtained measurement results [2] that at positive polarity of the fixed contact the mean arc energy value has been higher than in the case of negative polarity.

Therefore, at positive polarity a higher value of arc energy can cause accelerated wear of switch contacts.

Switch operation at alternating voltage involves a lower mean value of arc energy than it is in the case of direct voltage. It follows from different conditions of arc interruption. Switch operation at direct voltage with the polarity change applied to each subsequent switching cycle has resulted in the arc energy decrease, reduction of the contact wear and in the increase of wear quality and reliability of switches.

References

[1] Zukowski P., Kozak C.: *Badanie energii łuku prądu stałego w zależności od biegunowości podłączenia styków łącznika*, Mechanizacja i Automatyzacja Górnictwa 7 (473), 2010, s. 137-140.

[2] Zukowski P., Kozak C.: *Symulacja komputerowa zjawisk cieplnych w szczelinie międzystykowej łącznika spowodowanych łukiem elektrycznym*, Mechanizacja i Automatyzacja Górnictwa 7-8 (450) 2008, s. 96-100.

# Research on jump mechanism of electric charge transfer probability in gallium arsenide irradiated with H+ ions

Paweł Węgierek, Piotr Billewicz
Department of Electrical Devices and High Voltage Technology,
Lublin University of Technology, Lublin, Poland, E-mail: p.wegierek@pollub.pl

A model of jump mechanism of electric charge transfer has been presented in the article [1].

Described model introduces an assumption that an electron jump takes place between neutral potential wells, what causes dipole formation. Electron would be able to participate in direct current if only it makes another jump from negative potential well in direction opposite to electric field vector. However electric field of positively charged potential well which first jump has been made from withstands succeeding jumps. The one of basic parameters of described model is probability of second electron's jump p. Probability that electron will return to the first potential well equals $1 - p$ and defines conductivity for high frequencies.

The figure above presents dependence of probability p value on inverted temperature plotted for gallium arsenide sample exposed to polyenergy implantation with H+ ions [2] and annealed in temperatures $T_a \leq 663$ K. As it could be seen after analyzing presented graph, plots $p(1000/T_p)$ for annealing temperature lower than $T_a = 473$ K consists of two curve segments which differ from each other in decreasing rate. For $T_a = 533$ K and higher rapid change of plots $p(1000/T_p)$ proceeds, precisely increase of $p(1000/T_p)$ is observed.
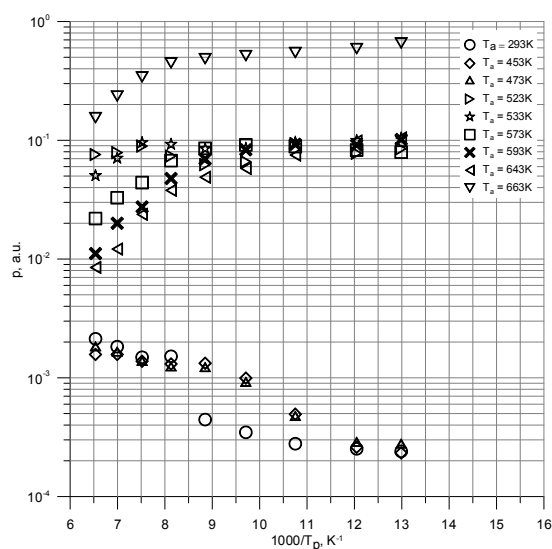
References

[1] Żukowski P., Kołtunowicz T., Partyka J., Węgierek P., Komarov F.F., Mironov A.M., Butkievith N., Freik D.: *Dielectric properties and model of hopping conductivity of GaAs irradiated by H+ ions,* Vacuum 81, 2007, p. 1137.

[2] Kowalski M., Partyka J., Węgierek P., Żukowski P., Komarov F.F., Jurchenko A.V., Freik D.: *Frequency-dependent annealing characteristics of the implant-isolated GaAs layers*, Vacuum, 78, 2005, p. 311.

Durability of protective coatings on contact surfaces

Mariusz Kolasik
Department of Electrical Devices and High Voltage Technology,
Lublin University of Technology, Lublin, Poland, E-mail: m.kolasik@pollub.pl

During the operation of apparatus switches on the surfaces of their contacts electrochemical phenomena occur. The phenomena bring about deterioration of electrical parameters of those devices. The hitherto elaborated and applied methods for contact modification have significantly contributed to the enhancement of switching apparatus reliability.

However, the performed testing indicates insufficient wearing quality of protective coatings deposited on the contacts which is easily noticeable over longer operation periods. That disadvantage can be compensated by selecting adequate layer thickness for a protective coating to be deposited.

Within the presented research work electrical parameter measurements have been performed for apparatus switches of contacts coated with silver layers of varied thickness that have been their protective coatings. The contacts operated within an AC circuit of the current intensity I = 10 A and voltage U = 230 V. Based on the obtained results characteristics of voltage drop and temperature variations have been determined for each switching cycle over the whole service life of a switch. It has been found that protective layers of standard thickness undergo total degradation in a period of ca thousand cycles. The testing has been repeated for switch contacts of non-standard coating thickness and specifically – for a three times thicker coating. The assumption concerning the effect of coating thickness on electrical parameters has been proved valid as the period characterized by a very low voltage-drop value has been prolonged by about five times.

Durability of a deposited protective layer also depends on the conditions of the electric circuit where a given switching apparatus operates. The above discussed measurements have been also performed for various load current values, which has made it possible to plot the protective coating wear rate as a function of load with the initial coating thickness taken into account.

The obtained results can make a basis for optimal selection of coating thickness, which can contribute to the enhancement of the switch service parameters over its whole service life.

An effect of contact shape on protective coating properties

Mariusz Kolasik
Department of Electrical Devices and High Voltage Technology,
Lublin University of Technology, Lublin, Poland, E-mail: m.kolasik@pollub.pl

Deposition of protective coatings onto contact surfaces is a popular method for enhancing electrical parameters of apparatus switches. When such metals as silver or tungsten that are more resistant to the action of electric arc than copper are applied for that purpose a reduction of tarnish layer formation and degradation of the surface can be obtained and thereby lower voltage drop at the contacts and lower emission of thermal energy there.

Apparatus switches of the normally-closed type include a flat fixed contact and the moving one of a near-spherical surface. The different shapes can be the reason for non-uniform wear of protective layers on the contacts.

Two sets of switches with protective coatings on their contacts have been tested. In the first set protective layer thickness on the fixed contact has been of 6 μm and on the moving one – of 18 μm, while in the other set the arrangement has been reversed: the 18 μm layer – on the fixed contact and the 6 μm layer – on the moving one. Measurements have been recorded for switches operating in an AC circuit of the current intensity of I = 10 A and nominal voltage of U = 230 V over the period of ca 10,000 switching cycles.

The obtain results illustrate the effect of the thickness of protective layers on switch contacts on their service parameters depending on the service time. The application of various coatings onto moving and fixed contacts has made it also possible to determine the effect of a contact shape on its service life.

Puncture of a protective layer causes rapid increase of temperature and voltage drop at the contacts. It proceeds the faster the thinner is the layer. The performed testing on the content proportions of individual element components of the layer has shown that in the case of the moving (spherical) contact the protective coating wear has occurred much faster than on the fixed flat contact where some of the coating has remained. It indicates the need for considering the shape of a contact when selecting thickness for protective coatings to be deposited.

Cu-Ni thin film solid solutions obtained on the basis of Ni nanoparticle arrays

V. Zlenko, S. Protsenko

Sumy State University, Sumy, Ukraine, E-mail: serhiy.protsenko@elit.sumdu.edu.ua

Arrays of nickel nanoparticles were formed on polyimide substrates by dispersing of thin metal films with different initial effective thicknesses during annealing in vacuum [1]. Cu - Ni thin film solid solutions were formed during the subsequent deposition of copper layer with an effective thickness of 5.5 nm, their thermoresistive properties were studied.

Polyiimide films were fabricated from polyamic acid solution on copper microscopic grids and Al_2O_3 plates. The PI precursor was thermally imidized under vacuum at 420 K for 40 min. Nickel thin films obtained on polyimide substrates by thermal evaporation of material in vacuum (residual gas pressure of 10^{-3} Pa). Effective thickness of the metal films in course of deposition process was controlled by quartz resonator method and was 1.5-3.5 nm. The samples were annealed in vacuum at different temperatures (700-850 K). TEM studying of structural-phase state showed that all samples had the fcc-nickel structure. Decreasing of the initial effective thickness of metal films from 3.5 to 1.5 nm under selected annealing process conditions leads to the transition from film to island structure and array of nanoparticles (average size of 3-3.5 nm) with a uniform distribution over the substrate surface. The increase of annealing temperature leads to a slight increase in the average size of the nanoparticles.

Obtained after annealing at T = 800 K Ni/PI samples used as the substrate for deposition of Cu (in single cycle). The effective thickness of the copper layer measured was 5.5 nm. As known from phase diagrams, Ni and Cu can form a solid solution throughout all period of component concentrations and size of the lattice parameter varies according to the Vehard`s rule. Experimental data, received from TEM studying of samples shows forming of Ni-Cu solid solution and change of lattice parameter size from 0.3594 to 0.3587 nm when calculated Ni concentration changes from 23 to 41 % what corresponds to the information from works of other authors [2, 3]. Also we noted Cu_2O phase present with lattice parameter size of 0.4238-0.4254 nm. TEM plan view images shows quite structured morphology of obtained Cu_xNi_{100-x}/PI thin film samples.

Thermoresistive properties of Cu_xNi_{100-x}/PI/Al_2O_3 were studied during annealing process of samples (3 cycles, T=750 K) in vacuum. Experimental results show that all samples after first annealing cycle have resistivity in range from $4\text{-}8 \cdot 10^{-6}$ Ohm∘m and negative coefficient of thermal resistance what is typical to island metal films or semiconductors. The explanation is probably structured morphology of the samples and presence of oxide phase.

References
[1] Zlenko V., Protsenko S.: *Fabrication of Cu and Ni small particles by dispersing method*, Metalophyzika Noveishie Technologii 33 No 5, 2011, p. 495-501.
[2] Lee B.-J., Shim J.-H.: *Amodified embedded atom method interatomic potential for the Cu–Ni system*, Computer Coupling of Phase Diagrams and Thermochemistry 28, 2004, p. 125-132.
[3] van Ingen R.P., Fastenau R.H.J., Mittemeijer E.J.: *Laser ablation deposition of Cu-Ni and Ag-Ni films: Nonconservation of alloy composition and film microstructure*, Journal of Applied Physic 76, 1995, p. 1871-1883.

The investigation of magnetoresistive properties in spin-valve structures based on Co and Cu or Au in FIP and FPP geometries

M. Demydenko, S. Protsenko, D. Kostyuk

Sumy State University, Sumy, Ukraine, E-mail: protsenko@aph.sumdu.edu.ua

The effect of giant magnetoresistance (GMR) was detail studied on the base of different thin film systems (Fe/Cr, Co/Cu, Co/Au, Co/Ag, Co/Ru, Ni/Cu etc.). The research of GMR in spin-valves systems is the most serious science interest [1, 2]. The value of angle of magnetic field direction is the most important influence on magnetoresistive properties of multilayer thin film systems. There are two geometry of magnetic field direction: FIP (the lines of magnetic induction have a parallel direction relatively to the sample plane) and FPP (the lines of magnetic induction have a perpendicular direction relatively to the sample plane).

Due to theoretical aspects the aim of this work was the research of changes magnetoresistance (MR) from FPP to FIP geometry.

Presented work was devoted to investigation of spin-valve structures obtained by vacuum deposition under residual gas pressure of 10^{-7} Pa. The thickness of the layers in the course of deposition process was studied by quartz resonator method. The materials were deposited by electron beam deposition method on Si wafers with oxide layer. The magnetoresistance was measured at a temperature of 300 K with using developed hardware/software complex, described in work [3]. The possibility of automation MR measurement of thin film systems in different geometries of magnetic field direction in angle range of ±180° with minimal step of 1° was the principal feature of developed system.

The research of changes magnetoresistance was provided on base of next spin-valve systems with CIP geometry of current flowing: Au(1)/Co(**3**)/**Au**(6)/Co(**20**)/SiO$_2$/Si; Au(1)/Co(**3**)/**Cu**(6)/Co(**20**)/SiO$_2$/Si; Au(1)/Co(**20**)/**Au**(6)/Co(**3**)/SiO$_2$/Si; Au(1)/Co(**20**)/**Cu**(6)/Co(**3**)/SiO$_2$/Si, where in brackets the layer thickness in nm is showed. The main feature of investigated spin-valve systems was the difference between the material of non magnetic midlayer (Cu or Au) and thickness of Co layers.

In the result of experimental researches the dependences of MR from magnetic field value and geometry were built. The values of MR are:

1,90% and 1,60% for Au(1)/Co(**3**)/**Au**(6)/Co(**20**)/SiO$_2$/Si;

1,18% and 0,70% for Au(1)/Co(**3**)/**Cu**(6)/Co(**20**)/SiO$_2$/Si;

0,60% and 0,50% for Au(1)/Co(**20**)/**Au**(6)/Co(**3**)/SiO$_2$/Si;

0,50% and 0,35% for Au(1)/Co(**20**)/**Cu**(6)/Co(**3**)/SiO$_2$/Si for FIP and FPP geometry respectively. However, the most significant change of MR value and coercitive force were in the angle range from 90° to 80°.

References

[1] Anwarzai B., Ac V., Luby S., Majkova E., Senderak R.: *Pseudo spin-valve on plastic substrateas sensing elements of mechanical strain*, Vacuum 84, 2010, p. 108-110.

[2] Katranas G.S., Meydan T., Ovaria A., et al.: *Simulation and measurement of bilayer sensor characteristics*, Sens. Actuators A 129, 2006, p. 43-46.

[3] Demydenko M., Protsenko S., Siffalovic P.: *The feature of magnetoresistance in spin-valve structures based on Au/Co/Cu/Co/Au/SiO$_2$*, Metalophyzika Noveishie Technologii 33 No 5, 2011, p. 621-628.

N_{EET}
2011

Influence of thin copper coating on electrophysical properties of silver films

H.V. Fedchenko, S.I. Protsenko
Sumy State University, Sumy, Ukraine, E-mail: serhiy.protsenko@gmail.com

The presence of coating on the film could lead to changes in its electro physical properties due to grain boundary diffusion or variation of surface reflection coefficient. The main goal of this paper was to define how deposition of thin copper layer (up to 3 nm) influences on Ag film.

To solve this problem we measured such parameters as coefficient of longitudinal strain sensitivity, temperature coefficient of electrical resistance of Ag films at different thickness and of Ag films with copper coating (0.5-3 nm). We investigated the microstructure, diffraction patterns of given samples and the dependency of mean crystallite dimensions on Ag film thickness [1].

For example we obtain such results: for Ag(27)/Sub film the coefficient of longitudinal strain sensitivity (γ) is 1.57 units, for Cu(0.5)/Ag(27)/Sub – 1.62; for Ag(42)/Sub γ – 0.6 and for Cu(1)/Ag(42)/Sub – 0.9 units. Accordingly we can see that the presence of coating influence on film resistance [2].

Decoding of obtained electron diffraction indicates that there is no phase formation in this system during coating deposition because only Ag (FCC), Cu (FCC) and CuO phases occur. The lattice parameters do not significantly vary from given in the tables: $a_m(Ag) = 0.410$, $a_0(Ag) = 0.408$ and $a_m(Cu) = 0,362$, $a_0(Cu) = 0.361$. The absence of phase formation indicates that variation of strain sensitivity coefficient could be caused by the different grain boundary transparency or surface reflectivity for pure films and films with coating [3].

To evaluate the influence of grain boundary diffusion the electron transfer parameters were computed: λ_0 – mean electron free path; p – film reflectivity coefficient and R – carriers' dissipation factor on crystallite boundaries. Since the definition of dependency of mean grain dimensions (L) on Ag film thickness showed that L $\geq$ d we can use linearized relation of Tellier C.R., Tosser A.J., C.R. Pichard in computation. The results of modeling showed that parameters λ_0 = 50 nm and p = 0,2 are the same for sample with and without coating but R is different and its value for Ag film with copper coating is 0.19 and 0.16 for pure silver film. Since this technique has some inaccuracy in calculations it was decided to use isotropic scattering model in addition to it to define the electron transfer parameters more accurate. For this purpose we measured the temperature coefficient of resistance (TCR) for Ag films at different thicknesses with and without coating.

The mean values of TCR for Ag(40)/Sub and Cu(3)/Ag(40)/Sub are : $\beta \cong 2$ and $\beta \cong 1$ respectively.

References
[1] Misjak F., Barna P.B., Toth A.L., Uivari T.: *Structure and mechanical properties of Cu–Ag nanocomposite films*, Thin Solid Films 516, 2008, p. 3931-3934.
[2] Choi Y., Suresh S.: *Size effects on the mechanical properties of thin polycrystalline metal films on substrates*, Acta Materialia 50, 2002, p. 1881-1893.
[3] Chornous A.M., Dekhtyaruk L.V., Govorun T.P., Stepanenko A.O.: *Influence of Diffusing Impurities on the Electrical Conductivity of Single-Crystal and Polycrystalline Metal Films*, Metallofiz. Noveishie Tekhnol. 29, 2007, p. 249-266.

Energy parameters of drive system with induction motor and three-level voltage inverter

Leszek Pawlaczyk[1), Vitezslav Styskala[2)

[1) *Wroclaw University of Technology, Institute of Electrical Machines, Drives and Measurements, Wroclaw, Poland, E-mail: leszek.pawlaczyk@pwr.wroc.pl*
[2) *VŠB - Technical University of Ostrava, Faculty of Electrical Engineering and Computer Science, Department of Electrical Engineering, Ostrava, Czech Republic*

For many years intensive R&D work on drive systems with induction motors supplied with power from frequency converters has concentrated on new topologies of converter power circuits [1-3] and new types of control systems, mainly vector control systems and direct motor electromagnetic moment control systems [4]. The focus has also been on sensorless drive control systems which do not include mechanical tachometric relays or motor rotor position sensors.

The majority of the squirrel-cage induction motors used in such systems have a typical general purpose design. Modifications, consisting mainly in improving the electric insulation of the stator windings and incorporating structures reducing the flow of bearing currents, are sometimes introduced in the case of motors supplied from pulse-width modulation (PWM) inverters. Also foreign ventilation, ensuring the proper cooling of the motor at angular velocities below the rated one, is often added.

As regards their electromagnetic and electromechanical specifications, induction motors still offer significant advantages. These are connected with their principle of operation and normal operating conditions, i.e. when being supplied directly from the mains they show high resistance to surge currents of short (relative to the rated current) duration and to the corresponding surge moments arising in transient states. For example, during counter switching braking and in the unattenuated motor field at a speed close to synchronous, surge currents and moments may reach very high values: $i_{s(max)}/i_{s,n} \cong (15 - 20)$ $m_{max}/m_n \cong (10 - 12)$ [5].

In the case of power supply from a frequency converter and fully controllable high moment overloads, by exploiting the above properties of induction motors one can built low- and medium-power drive systems (based on mass-produced or slightly modified asynchronous machines), having dynamic properties similar to those of the state-of-the-art servomechanism systems, equipped with special AC motors.

The main static and dynamic losses in a drive system with a frequency-controlled induction motor with extreme electromagnetic moments have been determined. A mathematical model and simulations results for a 2.2 kW drive system are presented.

References

[1] Bin Wu: *High-Power Converters and AC Drives*. IEEE Press, Jon Wiley & Sons, Inc., Hoboken,, New Jersy, 2006.
[2] Holmes D.G., Lipo T.A.*: Pulse Width Modulation For Power Converters*, IEEE Press, Jon Wiley & Sons, Inc., Hoboken, 2003.
[3] Monmasson E.: Power *electronics converters, PWM Strategies and Current Control Techniques*, Jon Wiley & Sons, Inc., Hoboken, 2011.
[4] Sikorski A.: *Bezpośrednia regulacja momentu i strumienia maszyny indukcyjnej.* Oficyna Wydawnicza Politechniki Białostockiej, Białystok, 2009.
[5] Фираго Б.И., Павлячик Л.Б.: *Теория электропривода* – Мниск.: ЗАО "Техноперспектива", 2004.

Nonlinear regulators of three-level voltage inverter neutral point voltage

Leszek Pawlaczyk

Wroclaw University of Technology, Institute of Electrical Machines, Drives and Measurements, Wroclaw, Poland, E-mail: leszek.pawlaczyk@pwr.wroc.pl

Present-day electromechanical systems are based on frequency-controlled electric drive systems with induction motors. Autonomous voltage inverters with pulse-width modulation (PWM) are typically used to supply the induction motor with power [1].

Multilevel voltage inverters are used in high-power drive systems and to improve the quality of the voltage supplying the motor. In comparison with two-level inverters, multilevel inverters offer such advantages as: reduced voltage on the inverter semiconductor devices, a larger number of inverter output voltage levels, a lower higher harmonic content in the output voltage, a lower derivative of induction motor stator voltage pulse edges and reduced induction motor current and electromagnetic moment ripples. The main disadvantage of such inverters is the larger number of power semiconductor devices and the more complicated control of the inverter [2].

In practice, three-level inverters with a neutral point (obtained on the capacitor voltage divider of the input capacitor filter) in the DC circuit, referred to as neutral-point-clamped (NPC) inverters, are most commonly used. In order to ensure faultless inverter operation it is necessary to maintain the neutral point potential constant, which is a major challenge. The unbalance of voltages on the filter capacitors intensifies when asynchronous inverter output voltage modulation methods, such as nonlinear inverter voltage and current control methods, are used [3].

The paper describes the operation of an inverter input filter capacitor neutral potential control system. The system works in tandem with a nonlinear vector modulator controlling the spatial motor stator current vector. The synthesis of the control system was based on elements of the theory of variable structure systems operating in the slip mode [4, 5]

A mathematical model of the system, simulation results and selected bench test results for a three-level voltage inverter supplying a 2.2 kW induction motor are presented.

References
[1] Kazmierkowski M.P., Krishnan R., Blajjberg F.: *Control in Power Electronics, Selected Problems*. Academic Press, San Diego, 2002.
[2] Bin Wu: *High-Power Converters and AC Drives*. IEEE Press, Jon Wiley & Sons, Inc., Hoboken,, New Jersey, 2006.
[3] Holmes D.G., Lipo T.A.*: Pulse Width Modulation For Power Converters*, IEEE Press, Jon Wiley & Sons, Inc., Hoboken, 2003.
[4] Monmasson E.: Power electronics converters, PWM STRATEGIES AND Current Control Tecniques, Jon Wiley & Sons, Inc., Hoboken, 2011.
[5] Utkin V.: *Skoziasceie rezimy i ich primienienie v sistiemach pieriemiennoj struktury*. Nauka, Moskwa 1980.

Operation of power transformers using the TrafoGrade system

Marek Szrot, Janusz Płowucha
Energo-Complex Sp. z o.o., 9 Lotników Str., 41-949 Piekary Śląskie, Poland,
E-mail: marek.szrot@energo-complex.pl

The paper presents the TrafoGrade system which has been developed to support decisions to be taken in respect of power transformer operation. The system has been composed in four parts. The multi parametrical evaluation of the transformer's technical condition is the most important element of the system. Evaluation of the importance index of a unit in the power system is additional information that complements the project. It is based on analysis of such factors as ease of transformer exchange or repair and reliability or safety of the power supply. Another step is to determine perspectives of further operation of each unit separately taking into consideration technical-economical aspects. Finally, results of analysis are put into a computer based management system which supports decisions to be taken in respect of transformer operation. The paper presents an example of the system implemented in one of the distribution companies in Poland.